

SCOUR AND SCOUR PROTECTION AT BRIDGE ABUTMENTS

Ş. YURDAGÜL KAYATÜRK

JANUARY 2005

SCOUR AND SCOUR PROTECTION AT BRIDGE ABUTMENTS

A THESIS SUBMITTED TO
THE GRADUATE SCHOOL OF NATURAL AND APPLIED SCIENCES
OF
MIDDLE EAST TECHNICAL UNIVERSITY

BY

Ş. YURDAGÜL KAYATÜRK

IN PARTIAL FULFILLMENT OF THE REQUIREMENTS
FOR
THE DEGREE OF DOCTOR OF PHILOSOPHY
IN
CIVIL ENGINEERING

JANUARY 2005

Approval of the Graduate School of Natural and Applied Sciences

Prof. Dr. Canan ÖZGEN
Director

I certify that this thesis satisfies all the requirements as a thesis for the degree of Doctor of Philosophy.

Prof. Dr. Erdal ÇOKÇA
Head of Department

This is to certify that we have read this thesis and that in our opinion it is fully adequate, in scope and quality, as a thesis for the degree of Doctor of Philosophy.

Dr. M. Ali KÖKPINAR
Co-Supervisor

Prof. Dr. Mustafa GÖĞÜŞ
Supervisor

Examining Committee Members

Prof. Dr. Mustafa GÖĞÜŞ (METU, CE)

Prof. Dr. Nevzat YILDIRIM (GAZİ Univ., CE)

Prof. Dr. Melih YANMAZ (METU, CE)

Assoc. Prof. Dr. İsmail AYDIN (METU, CE)

Dr. Şahnaz TİĞREK (METU, CE)

I hereby declare that all information in this document has been obtained and presented in accordance with academic rules and ethical conduct. I also declare that, as required by these rules and conduct, I have fully cited and referenced all material and results that are not original to this work.

Name, Last name : Ş. Yurdagül KAYATÜRK

Signature :

ABSTRACT

SCOUR AND SCOUR PROTECTION AT BRIDGE ABUTMENTS

Kayatürk, Şerife Yurdagül

Ph. D., Department of Civil Engineering

Supervisor: Prof. Dr. Mustafa Göğüş

Co-Supervisor: Dr. Mehmet Ali Kökpınar

January 2005, 213 pages

Bridge failures are mainly caused by scouring the bed material around bridge foundations during flood. In this study, scour phenomenon around bridge abutments is experimentally studied.

Effect of abutment size, location and size of the collars placed around the abutments, time evaluation of scour hole around the abutment, scour characteristics of abutment and pier interaction were experimentally investigated. Scour measurements were conducted in a rectangular channel of 30 m long and 1.5 m wide filled with erodable uniform sediment.

In the first part of the study, in order to investigate the size effect of the abutment on the maximum scour depth, abutments of nine different sizes were tested for three different water depths. It was found that the length of the abutment is more important parameter than the width of it. Secondly, efficiency of various sizes of collars, which are used to reduce the local scour depth, located at different elevations around the abutments was determined. It was noticed that when the collar width was increased and placed at or below the bed level, the reduction in scour depth increases considerably. Some tests for partial-collar arrangements around the abutments were conducted and it was shown that instead of full-collar one can use partial-collar arrangements around the abutments to achieve the same efficiency as the full-collar.

Time development of scour holes around the abutments with and without collar cases were recorded. It was observed considerable reductions in scour depths around the abutments can be obtained with collars compared to the cases in which there are no collars over the same time period.

Finally, a series of experiments were carried out to investigate the interaction between bridge abutments and piers related to the local scour around them. Based on the experiments conducted with two different abutment lengths and pier diameters varying the lateral distances between them it was observed that scour depth reduction capacities of collars vary significantly while comparing a single abutment or pier.

Keywords: Scour, Bridges, Abutments, Piers, Collar, Time Scale, Abutment-Pier Interaction

ÖZ

KÖPRÜ YAN AYAKLARINDA OYULMA VE OYULMAYA KARŞI

KORUMA

Kayatürk, Şerife Yurdagül

Doktora Çalışması, İnşaat Mühendisliği Bölümü

Tez Yöneticisi: Prof. Dr. Mustafa Göğüş

Ortak Tez Yöneticisi: Dr. Mehmet Ali Kökpınar

Ocak 2005, 213 sayfa

Köprü yıkılmalarının en yaygın nedeni, köprü temelleri etrafındaki yatak malzemesinin taşkınlarla aşınması ve oyulmasıdır. Bu çalışmada, köprü yan ayakları etrafındaki oyulmalar deneysel olarak çalışılmıştır.

Köprü yan ayağının boyutları, köprü yan ayağının etrafına yerleştirilen plakaların boyutları ve yerleri, köprü yan ayağı etrafında oluşan oyulma çukurunun zamanla değişimi ve köprü yan ayağı ile köprü orta ayağın birbirini etkilediği durumlardaki oyulma çukurunun özellikleri deneysel olarak araştırılmıştır. Oyulma deneyleri boyu 30 m ve genişliği 1.5 m olan üniform yatak malzemesi ile doldurulmuş bir kanalda yapılmıştır.

Çalışmanın ilk kısmında, köprü yan ayağı boyutlarının yersel oyulma üzerindeki etkisini araştırmak için, dokuz adet değişik yan ayak şekli, üç farklı su derinliğinde test edilmiştir. Köprü yan ayak boyunun, eninden daha önemli bir parametre olduğu bulunmuştur. İkinci olarak, yersel oyulma derinliğini azaltmak amacı ile köprü yan ayağının etrafına farklı derinliklere yerleştirilen değişik boyutlardaki plakaların etkileri araştırılmıştır. Plakanın genişliğinin artması halinde ve plakanın kum seviyesine veya kum seviyesinin altına yerleştirilmesi durumunda, oyulma derinliğindeki azalmanın arttığı dikkat çekmiştir. Köprü yan ayakları etrafına yerleştirilen plakaların kesilmesi ile elde edilen kısmi-plaka çalışmaları da yapılmış ve kısmi-plakaların bazı durumlarda tam plaka kullanıldığı zaman elde edilen etkiye sahip olduğu gösterilmiştir.

Köprü yan ayaklarının etrafında, meydana gelen oyulmaların zamanla değişimi plakalı ve plakasız durumları için incelenmiş ve plakaların kullanılması durumunda aynı zaman periyodunda plakasız duruma göre oyulma derinliğinde dikkate değer bir azalma olduğu görülmüştür.

Son olarak, köprü yan ayağı ve köprü orta ayaklarının hidrolik olarak etkileşimlerinin araştırılması amacı ile bir seri deneyler yapılmıştır. İki farklı uzunluktaki yan ayak ile iki farklı çaptaki orta ayağın kullanıldığı bu deneylerde yan ayak ile orta ayak arasındaki mesafenin değiştirilmesi ile oyulma çukurundaki etkileşimleri araştırılmıştır. Plakaların, yan ayak ve orta ayağın birlikte olduğu çalışmalarda gösterdiği davranışın, yan ayak ile orta ayak tek başlarıyken etraflarına yerleştirildiği zaman elde edilen davranıştan çok farklı olduğu gözlenmiştir.

Anahtar Kelimeler: Oyulma, Köprüler, Köprü Yan Ayakları, Köprü Orta Ayakları, Zamanla Değişim, Etkileşim

TO MY PARENTS

ACKNOWLEDGMENTS

This study was suggested and has been completed under the supervision of Prof. Dr. Mustafa GÖĞÜŞ in the State Hydraulic Works at the Technical Research and Quality Control Department in Ankara, Turkey.

I would like to express my sincere thanks to my supervisor Prof. Dr. Mustafa GÖĞÜŞ and my co-supervisor Dr. M. Ali KÖKPINAR for their invaluable guidance, continued interest, patient and encouragement throughout this enjoyable study.

I would like to extend my thankful feelings to State Hydraulic Works for its encouragements and offering its all possibilities without any reciprocal throughout the study.

I am indebted to my colleague, H. Çetin Çelik for his support and patience for my frequent disturbances.

I am grateful to Ahmet GÜVENÇ and Abidin TEKE for their help in the laboratory.

Finally, I would like to thank my husband Uğur KAYATÜRK for understanding my absences and also his encouragement and patience, which gave me the inspiration to complete this study.

TABLE OF CONTENTS

ABSTRACT.....	IV
ÖZ.....	VI
DEDICATION.....	IX
ACKNOWLEDGEMENTS.....	X
TABLE OF CONTENTS.....	XII
LIST OF TABLES	XV
LIST OF FIGURES	XVII
LIST OF SYMBOLS.....	XXIII
CHAPTERS	
1. INTRODUCTION.....	1
1.1 GENERAL.....	1
2. SCOUR TYPES AND PARAMETERS AFFECTING THE SCOUR.....	4
2.1 SCOUR TYPES.....	4
2.1.1 General Scour.....	4
2.1.2 Contraction Scour.....	4
2.1.3 Local Scour.....	5
2.2 SCOUR PROCESS AROUND BRIDGE PIERS AND ABUTMENTS.....	5
2.3 PROTECTION OF STRUCTURES FROM LOCAL SCOUR.....	8
2.4 PARAMETERS AFFECTING SCOUR AROUND BRIDGE STRUCTURES.....	9
2.5 LOCAL SCOUR CONDITIONS.....	9
3. EFFECT OF ABUTMENT SIZE ON LOCAL SCOUR AT BRIDGE ABUTMENTS.....	11
3.1 GENERAL.....	11

3.2 LITERATURE REIVIEW.....	11
3.3 DIMENSIONAL ANALYSIS.....	16
3.4 EXPERIMENTAL PROCEDURE.....	17
3.5 DISCUSSION OF RESULTS.....	23
3.5.1 Effect of Abutment Length.....	23
3.5.2 Effect of Abutment Width.....	25
3.5.3 A dimensionless Scour Depth Relation for Vertical Wall Abutments.....	26
3.5.4 Comparison of Experimental Results with Garde's (1961) Equation.....	27
3.6 CONCLUSIONS.....	27
4. APPLICATION OF COLLAR TO CONTROL SCOURING AROUND ABUTMENTS.....	29
4.1 GENERAL.....	29
4.2 LITERATURE REVIEW.....	29
4.3 DIMENSIONAL ANALYSIS.....	31
4.4 EXPERIMENTAL PROCEDURE.....	32
4.5 SCOUR MECHANISM.....	36
4.6 DISCUSSION OF RESULTS.....	36
4.6.1 Scour Profiles Around the Abutment with and without Collar.....	36
4.6.2 Maximum Scour Reductions Around the Abutments with Collars.....	66
4.6.3 Effect of Flow Depth on the Maximum Scour Depth at Bridge Abutment.....	80
4.6.4 Effect of Flow Depth on the Formation of Scour Hole Around the Bridge abutment.....	92
4.7 PARTIAL-COLLAR ARRANGEMENTS.....	96
4.8 CONCLUSIONS.....	97
5. TIME DEVELOPMENT OF SCOUR AROUND ABUTMENTS.....	98
5.1 GENERAL.....	98
5.2 LITERATURE REVIEW.....	98
5.3 EXPERIMENTAL SETUP.....	103

5.4 ANALYSIS OF RESULTS.....	103
5.5 TIME DEVELOPMENT OF d_s FOR LONG DURATION (12-HOURS) TESTS.....	118
5.6 STUDIES ON EQUILIBRIUM SCOUR DEPTH AROUND THE ABUTMENTS.....	120
5.6.1 Comparison of Experimental Results with Coleman et. al.'s (2003) Equation.....	121
5.6.2 Comparison of Experimental Results with Oliveto and Hager' s (2002) Equation.....	123
5.7 CONCLUSIONS.....	125
6 INTERACTION BETWEEN THE ABUTMENT AND THE PIER.....	126
6.1 GENERAL.....	126
6.2 LITERATURE REVIEW.....	126
6.3 DIMENSIONAL ANALYSIS.....	127
6.4 EXPERIMENTAL PROCEDURE.....	128
6.5 DISCUSSION OF RESULTS.....	130
6.5.1 Interaction Cases.....	130
6.5.2 Comparisons of Interaction Cases 1, 2, 3, 4.....	130
6.5.3 Comparisons of Interaction Cases 5, 6, 7, 8.....	136
6.5.4 Comparisons of Interaction Cases 9, 10, 11, 12.....	142
6.5.5 Comparisons of Interaction Cases 13, 14, 15, 16.....	147
6.5.6 Comparisons of Interaction Case 17.....	151
6.6 CONCLUSIONS and RECOMMENDATIONS.....	155
7 SUMMARY AND CONCLUSIONS.....	156
REFERENCES.....	158
APPENDICES	
APPENDIX A.....	166
APPENDIX B.....	183
APPENDIX C.....	199
APPENDIX D.....	200
APPENDIX E.....	205
VITA.....	213

LIST OF TABLES

TABLE

Table 3.1	Experimental series for abutment length and width effect.....	20
Table 4.1	Abutment and collar sizes used in the tests.....	35
Table 4.2	Experimental conditions for $Q=0.05 \text{ m}^3/\text{s}$ and $y=10 \text{ cm}$ and $B_a=10 \text{ cm}$	68
Table 4.3	Optimum design parameters of an abutment-collar arrangement.....	73
Table 4.4	Experimental data for various flow depths at threshold condition of sediment motion.....	83
Table 4.5	Optimum design parameters of an abutment-collar arrangement for various flow depths corresponding to threshold conditions of sediment motion.....	87
Table 4.6	Experimental data for various Q and L_a values tested	94
Table 4.7	Optimisation of collar shape.....	96
Table 5.1	Parameters used in calculation of equilibrium scour depth.....	122
Table 6.1	Schematic view and results of the interaction Case 1.....	132
Table 6.2	Schematic view and results of the interaction Case 2.....	132
Table 6.3	Schematic view and results of the interaction Case 3.....	134
Table 6.4	Schematic view and results of the interaction Case 4.....	134
Table 6.5	Schematic view and results of the interaction Case 5.....	138
Table 6.6	Schematic view and results of the interaction Case 6.....	138
Table 6.7	Schematic view and results of the interaction Case 7.....	140
Table 6.8	Schematic view and results of the interaction Case 8.....	140
Table 6.9	Schematic view and results of the interaction Case 9.....	143
Table 6.10	Schematic view and results of the interaction Case 10.....	143

Table 6.11	Schematic view and results of the interaction Case 11.....	145
Table 6.12	Schematic view and results of the interaction Case 12.....	145
Table 6.13	Schematic view and results of the interaction Case 13.....	148
Table 6.14	Schematic view and results of the interaction Case 14.....	148
Table 6.15	Schematic view and results of the interaction Case 15.....	149
Table 6.16	Schematic view and results of the interaction Case 16.....	149
Table 6.17	Schematic view and results of the interaction Case 17.....	153
Table A.1	Cross-sections of the scour holes for $L_a=7.5$ cm.....	166
Table A.2	Cross-sections of the scour holes for $L_a=15$ cm.....	168
Table A.3	Cross-sections of the scour holes for $L_a=20$ cm.....	171
Table A.4	Cross-sections of the scour holes for $L_a=25$ cm.....	175
Table A.5	Cross-sections of the scour holes for $L_a=35$ cm.....	179
Table B.1	Time variation of scour depth around the abutment for $L_a=7.5$ cm.....	183
Table B.2	Time variation of scour depth around the abutment for $L_a=15$ cm.....	187
Table B.3	Time variation of scour depth around the abutment for $L_a=20$ cm.....	191
Table B.4	Time variation of scour depth around the abutment for $L_a=25$ cm.....	195
Table C.1	Time development of 12-hours tests for $L_a=20$ cm.....	199

LIST OF FIGURES

FIGURE

Figure 2.1	General view of pier the scour.....	6
Figure 2.2	General view of the abutment scour.....	7
Figure 2.3	Change of the scour depth with respect to flow velocity and time (after Graf, 1996).....	10
Figure 3.1	General view of the experimental installation.....	18
Figure 3.2	Upstream view of the scour hole ($L_a=20$ cm, $B_a=20$ cm, $y=10$ cm)....	21
Figure 3.3	Downstream view of the scour hole ($L_a=20$ cm, $B_a=20$ cm, $y=10$ cm).....	21
Figure 3.4	Top view of the scour hole ($L_a=20$ cm, $B_a=5$ cm, $y=14$ cm)..<	22
Figure 3.5	Side view of the scour hole ($L_a=20$ cm, $B_a=5$ cm, $y=14$ cm)..<	22
Figure 3.6	Influence of abutment length on scour depth.....	24
Figure 3.7	Influence of flow depth on scour depth.....	24
Figure 3.8	Variation of maximum scour depth with abutment width.....	25
Figure 3.9	Variation of $(d_s)_{\max}/y$ with related dimensionless terms.....	26
Figure 3.10	Comparison of present data with Garde's (1961) equation....	27
Figure 4.1	Definition sketch of collar-abutment arrangement.....	33
Figure 4.2	A General view of scour hole when a collar is used (R69, $L_a=25$ cm, $B_c=5$ cm, $Z_c=+2.5$ cm).....	34
Figure 4.3	Bed profiles around the bridge abutment of $L_a=7.5$ cm with and without collars.....	38
	a) $L_a/B_c=0.75$	38
	b) $L_a/B_c=1.0$	39
	c) $L_a/B_c=1.5$	40

	d) $L_a/B_c=3.0$	41
Figure 4.4	Bed profiles around the bridge abutment of $L_a=15$ cm with and without collar.....	43
	a) $L_a/B_c=1.5$	43
	b) $L_a/B_c=2.0$	44
	c) $L_a/B_c=3.0$	45
	d) $L_a/B_c=6.0$	46
Figure 4.5	Bed profiles around the bridge abutment of $L_a=20$ cm with and without collar.....	48
	a) $L_a/B_c=2.0$	48
	b) $L_a/B_c=2.67$	49
	c) $L_a/B_c=4.0$	50
	d) $L_a/B_c=8.0$	51
Figure 4.6	Bed profiles around the bridge abutment of $L_a=25$ cm with and without collar	53
	a) $L_a/B_c=2.5$	53
	b) $L_a/B_c=3.33$	54
	c) $L_a/B_c=5$	55
	d) $L_a/B_c=10$	56
Figure 4.7	Bed profiles around the bridge abutment of $L_a=25$ cm with and without collar.....	58
	a) $L_a/B_c=3.5$	58
	b) $L_a/B_c=4.67$	59
	c) $L_a/B_c=7.0$	60
	d) $L_a/B_c=14$	61
Figure 4.8	Abutment-collar arrangement and scour hole ($L_a=20$ cm, $Z_c=+5$ cm, $B_c=10$)	62
	a) Upstream view.....	62
	b) Top view.....	62
Figure 4.9	Abutment-collar arrangement and scour hole ($L_a=20$ cm, $Z_c=-5$ cm, $B_c=10$).....	63

	a) Upstream view.....	63
	b) Top view.....	63
Figure 4.10	Abutment-collar arrangement and scour hole ($L_a=25$ cm, $Z_c=\pm 0.0$ cm, $B_c=5$ cm).....	64
	a) Upstream view.....	64
	b) Top view.....	64
Figure 4.11	Abutment-collar arrangement and scour hole ($L_a=35$ cm, $Z_c=\pm 0.0$ cm, $B_c=10$ cm).....	65
	a) Upstream view.....	65
	b) Top view.....	65
Figure 4.12	Effect of collar size and elevation on the maximum scour depth around the abutments of various lengths ($Q=0.05$ m ³ /s,	72
Figure 4.13	Variation of $[(d_s)_{\max}/y]_{\text{opt}}$ with θ	74
Figure 4.14	Variation of $[(d_s)_{\max}/y]_{\text{opt}}$ with $\theta^{0.5}(L_a/B_c)^{0.5}$	76
Figure 4.15	Variation of $[Z_c/y]_{\text{opt}}$ with L_a/B_c	77
Figure 4.16	Variation of [% Reduction] _{opt} with L_a/B_c	79
Figure 4.17	Variation of percent reduction in maximum scour depth with Z_c/y for $B_c=10$ cm and $B_c=5$ cm for various discharges.....	81
Figure 4.18	Variation of % reduction of maximum scour depth with Z_c/y .	88
Figure 4.19	Variation of $[(d_s)_{\max}/y]_{\text{opt}}$ with θ for various discharges.....	89
Figure 4.20	Variation of $[Z_c/y]_{\text{opt}}$ with L_a/B_c for various discharges.....	90
Figure 4.21	Variation of [% Reduction] _{opt} with L_a/B_c for various discharges.....	91
Figure 4.22	Definition Sketch for ξ	93
Figure 4.23	Upstream view of the eroded bed around the abutment ($Q=0.055$ m ³ /s, $y=9.6$ cm, $U/U_c=0.98$, $Z_c=-5$ cm, $B_c=10$ cm).	93
Figure 4.24	Location of $(d_s)_{\max_c}$ far from the abutment face	95
Figure 5.1	Time development of maximum scour depth around the abutment for various values of Z_c	105
	a) $L_a=7.5$ cm and $B_c=10$ cm.....	105

	b) $L_a=7.5$ cm and $B_c=7.5$ cm.....	105
	c) $L_a=7.5$ cm and $B_c=5$ cm.....	106
	d) $L_a=7.5$ cm and $B_c=2.5$ cm.....	106
Figure 5.2	Time development of maximum scour depth around the abutment for various values of Z_c	109
	a) $L_a=15$ cm and $B_c=10$ cm.....	109
	b) $L_a=15$ cm and $B_c=7.5$ cm.....	109
	c) $L_a=15$ cm and $B_c=5$ cm.....	110
	d) $L_a=15$ cm and $B_c=2.5$ cm.....	110
Figure 5.3	Time development of maximum scour depth around the abutment for various values of Z_c	112
	a) $L_a=20$ cm and $B_c=10$ cm.....	112
	b) $L_a=20$ cm and $B_c=7.5$ cm.....	112
	c) $L_a=20$ cm and $B_c=5$ cm.....	113
	d) $L_a=20$ cm and $B_c=2.5$ cm.....	113
Figure 5.4	Time development of maximum scour depth around the abutment for various values of Z_c	116
	a) $L_a=35$ cm and $B_c=10$ cm.....	116
	b) $L_a=35$ cm and $B_c=7.5$ cm.....	116
	c) $L_a=35$ cm and $B_c=5$ cm.....	117
	d) $L_a=35$ cm and $B_c=2.5$ cm.....	117
Figure 5.5	Time development of scouring around the abutment for $L_a=20$ cm and $B_c=10$ cm for various values of Z_c (T=12 hour)	119
Figure 5.6	Comparison of present data with Oliveto and Hager' s (2002)	124
Figure 6.1	Variation of maximum scour depth around the abutment and pier in the interaction cases of 1, 2, 3, and 4	135
Figure 6.2	Variation of maximum scour depth around the abutment and pier in the interaction cases of 5, 6, 7, and 8.....	141
Figure 6.3	Variation of maximum scour depth around the abutment and pier in the interaction cases of 9, 10, 11, and 12.....	146

Figure 6.4	Variation of maximum scour depth around the abutment and pier in the interaction cases of 13, 14, 15, and 16.....	150
Figure 6.5	Variation of % reduction in maximum scour depth with dimensionless collar location for pier in case 17.....	154
Figure 6.6	Variation of % reduction in maximum scour depth with dimensionless collar location for abutment in Case 17.....	154
Figure D.1	Abutment-collar arrangement and scour hole ($Q=0.035 \text{ m}^3/\text{s}$, $y=6.45 \text{ cm}$, $Z_c=-5 \text{ cm}$, $B_c=5 \text{ cm}$, $L_a=25 \text{ cm}$)..	200
	a) Downstream view.....	200
	b).Upstream view.....	200
Figure D.2	Abutment-collar arrangement and scour hole ($Q=0.040 \text{ m}^3/\text{s}$, $y=7.15 \text{ cm}$, $Z_c=-5 \text{ cm}$, $B_c=5 \text{ cm}$, $L_a=25 \text{ cm}$)..	201
	a) Downstream view.....	201
	b)Upstream view.....	201
Figure D.3	Abutment-collar arrangement and scour hole ($Q=0.045 \text{ m}^3/\text{s}$, $y=7.95 \text{ cm}$, $Z_c=-5 \text{ cm}$, $B_c=5 \text{ cm}$, $L_a=25 \text{ cm}$) ..	202
	a) Downstream view.....	202
	b)Upstream view.....	202
Figure D.4	Abutment-collar arrangement and scour hole ($Q=0.050 \text{ m}^3/\text{s}$, $y=8.85 \text{ cm}$, $Z_c=-5 \text{ cm}$, $B_c=5 \text{ cm}$, $L_a=25 \text{ cm}$)...	203
	a) Downstream view.....	203
	b) Upstream view.....	203
Figure D.5	Abutment-collar arrangement and scour hole ($Q=0.055 \text{ m}^3/\text{s}$, $y=9.60 \text{ cm}$, $Z_c=-5 \text{ cm}$, $B_c=5 \text{ cm}$, $L_a=25 \text{ cm}$)..	204
	a) Downstream view.....	204
	b) Upstream view.....	204
Figure E.1	Scour hole around the pier ($Q=0.055 \text{ m}^3/\text{s}$, $y=9.60 \text{ cm}$, $D=10 \text{ cm}$).....	205
	a) Upstream view.....	205
	b) Top view.....	205

Figure E.2	Pier-collar arrangement and scour hole ($Q=0.055 \text{ m}^3/\text{s}$, $y=9.60 \text{ cm}$, $D=10 \text{ cm}$, $Z_{cp}=\pm 0.0 \text{ cm}$).....	206
	a) Upstream view.....	206
	b) Downstream view.....	206
Figure E.3	Scour hole around the abutment ($Q=0.055 \text{ m}^3/\text{s}$, $y=9.60 \text{ cm}$, $L_a=25 \text{ cm}$)	207
	a) Upstream	207
	b) Top view	207
Figure E.4	Scour hole around the abutment ($Q=0.055 \text{ m}^3/\text{s}$, $y=9.60 \text{ cm}$, $L_a=25 \text{ cm}$, $Z_c=-5 \text{ cm}$)	208
	a) Top view.....	208
	b) Upstream view	208
Figure E.5	Interaction between abutment and pier ($Q=0.055 \text{ m}^3/\text{s}$, $y=9.60 \text{ cm}$, $D=10 \text{ cm}$, $\lambda=37.5 \text{ cm}$)	209
	a) Top view.....	209
	b) Upstream view.....	209
Figure E.6	Abutment and pier arrangement for $Q=0.055 \text{ m}^3/\text{s}$ and $\lambda=37.5 \text{ cm}$ ($L_a=25 \text{ cm}$, $Z_c=-5 \text{ cm}$ for abutment and $D=10 \text{ cm}$)	210
	a) Top view.....	210
	b) Upstream view.....	210
Figure E.7	Abutment and pier arrangement for $Q=0.055 \text{ m}^3/\text{s}$ and $\lambda=37.5 \text{ cm}$ ($L_a=25 \text{ cm}$, $Z_c=-5 \text{ cm}$ for abutment and $D=10 \text{ cm}$, $Z_{cp}=\pm 0.0 \text{ cm}$ for pier)	211
	a) Downstream view.....	211
	b) Upstream view.....	211
Figure E.8	Abutment and pier arrangement for $Q=0.055 \text{ m}^3/\text{s}$ and $\lambda=37.5 \text{ cm}$ ($L_a=25 \text{ cm}$, $Z_c=-5 \text{ cm}$ for abutment and $D=10 \text{ cm}$, $Z_{cp}=-5 \text{ cm}$ for pier)	212
	a) Downstream view.....	212
	b) Upstream view.....	212

LIST OF SYMBOLS

A_{total}	Total area of the abutment with collar
A_{abutment}	Abutment area on the horizontal plane
B	Channel width
B_a	Abutment width
B_c	Collar width around the abutment
B_{cp}	Collar width around the pier
B_t	Total width of the abutment width and collar width on horizontal
D	Pier Diameter
d_s	Scour depth at the abutment at any time
$(d_s)_{\text{max}}$	Maximum scour depth at the abutment at the end of the given time duration
d_{se}	Equilibrium scour depth at the abutment
$[(d_s)_{\text{max}}]_{\text{int.}}$	Maximum scour depth around the abutment or pier, interacting each other
$(d_s)_{\text{max}_c}$	Maximum scour depth at the abutment with collar
$[(d_s)_{\text{max}}]_{\text{or.}}$	Maximum scour depth around the abutment or pier corresponding to the experiments conducted with only pier or abutment
d_{50}	Median size of sediment
d_{84}	Sediment size for which 84 % of the sediment finer
d_{16}	Sediment size for which 16 % of the sediment finer
F_o, F_d	Densimetric Froude number

F_r	Froude number of flow
F_{rc}	Critical Froude number
g	Gravitational acceleration
g'	Reduced gravitational acceleration
K_d	Sediment size factor
K_G	Approach channel geometry factor
K_I	Flow intensity factor
K_s	Shape factor
K_{yw}	Flow depth-abutment size factor
K_θ	Foundation alignment factor
L_a	Projecting length of abutment, perpendicular to the flow
L_R	Dimensionless definition of geometrical dimensions of abutment
r^2	Correlation coefficient
N	Shape number for pier structures
Q	Discharge of the flow
S	Slope of the channel
T	Dimensionless time of scour
T_c	Collar thickness
t	Scouring time
t_e	Time required to reach equilibrium scour depth
t^*	Dimensionless scouring time
U	Mean approach flow velocity
U_c	Threshold approach velocity for sediment
U_{cr}	Critical velocity for incipient motion of sediment

U_*	Shear velocity of the approach flow
U_{*c}	The value of the U_* at the threshold of grain motion
x	Axis in the direction of flow
y	Approach flow depth
w	Sediment fall velocity
z	Axis in the vertical direction to the flow
Z	Dimensionless scour depth
Z_c	Collar level on the abutment with reference to bed level
Z_{cp}	Collar level on the pier with reference to bed level
α	Channel contraction ratio = $\frac{B - L_a}{B}$
λ	Distance between the abutment and the pier
θ	Ratio of total area of the abutment and collar to the abutment area on horizontal plane
θ_c	Shield's entrainment factor
ξ	The angle describing the location of the maximum scour depth
σ_g	Standart deviation of particle-size distribution
ϕ	Some combination of the non-dimensional shear stress
ρ	Fluid density
ρ_s	Sediment density
μ	Dynamic viscosity of fluid

CHAPTER 1

INTRODUCTION

1.1 GENERAL

Flow in an open channel with a mobile bed is usually accompanied by transport of sediments (Raudkivi, 1967). Scour may occur as a result of natural changes of flow in the channel or as a result of man-made activities, such as construction of structures in the channel or dredging of material from the bed. Although it may be greatly affected by the presence of structures encroaching on the channel, scour is a natural phenomenon caused by the flow of water over an erodable boundary (Breusers et. al., 1977; Jansen, 1979; Kwan and Melville, 1994; Graf, 1996; Balachandar and Kells, 1997; Lim, 1997; Kouchakzadeh and Townsend, 1997; Lim and Cheng, 1998; Cardoso and Bettess, 1999; Ballio and Orsi, 2001; Kothyari and Ranga Raju, 2001; Chaurasia and Lal, 2002; Kuhnle et. al., 2002, Breusers and Raudkivi, 1991).

During the last decades, statistical studies have shown that the most common cause of bridge failures have resulted from the removal of bed material around bridge foundations. In 1973 Federal Highway Administration of USA studied about 383 bridge failures, which were resulted from catastrophic floods (Federal Highway Administration, 2001). The research showed that 25% of the failures involved pier damage while 75% of it included abutment scour. Federal Highway Administration

of USA stated that during the spring floods of 1987, 17 bridges in New York and New England were damaged or destroyed by scour. In 1985, 73 bridges were destroyed by floods in Pennsylvania, Virginia and West Virginia. In 1993, 23 bridge failures, 14 from abutment scour and 2 from pier scour, resulted from floods caused to damage of \$15 million in the upper Mississippi basin. In 1994 in Georgia, flooding from storm, causing approximately \$130 million, damaged over 50 bridges (Federal Highway Administration, 2001).

Shutherland compiled all major flood hazards in New Zealand during the period of 1960-1984. Among the 108-recorded failures, 29 were attributed to abutment scour. In the United States, Brice reported that damage to bridges and highways from floods in 1964 and 1972 amounted to about USA \$100,000,000 per event. In 1990, Macky reported on a survey of reading expenditure in New Zealand as the result of damage due to scour. The survey showed that about 50% of total expenditure for bridges, and of this abutments and approaches comprised more than 70% (see Melville, 1992).

Kandasamy and Melville (1998) found that 6 of 10 bridge failures that occurred in New Zeland during Cyclone Bola were related to abutment and approach scour.

There have been a lot of floods, which lead to bridge failures in Turkey during last decades. Some of these floods occurred in Trabzon (1990), Malatya (1991), Bartın (1998), Hatay (2001), and Mersin (2001) (Yanmaz, 2002).

The collapsed bridges are very important with respect to goods and life losses, repair expenditure, and also traffic problems arised from damages. In order to remove these

damages, the existing bridges must be checked and then strengthened if it is necessary. But the main problem is the difficulty of solving and calculating flow mechanism. Since 1950, it has been studied but a universal model, which has included all conditions about flow type, bridge structure, and river characteristics, has not been developed yet.

The aim of this study is to investigate the effect of collars to be placed around abutments on the development of local scour at the base of abutments. For this reason, a series of experiments were conducted at the laboratory under clear-water flow conditions with vertical abutments and collars of various sizes using almost uniform sand of $d_{50}=1.48$ mm. In Chapter II, scour types and parameters affecting the scour are given. Chapter III describes the effect of abutment size on local scour at bridge abutments. Application of collar-plates to control scouring around abutments are presented in Chapter IV. Chapter 5 presents the development of scour around the abutments with time. Finally, in Chapter 6 the problem of the interaction between abutment and pier concerning the local scours around them is studied and the effect of the collar-plate on interaction cases is illustrated.

CHAPTER 2

SCOUR TYPES AND PARAMETERS AFFECTING THE SCOUR

2.1 SCOUR TYPES

Scour types can be classified into three groups:

- a) General scour
- b) Contraction scour
- c) Local scour

2.1.1 General Scour

General scour involves the removal of material from the bed and banks across all or most of the width of a channel. This type of scour may be natural or man induced causes and needs both sediment and geomorphologic analysis.

2.1.2 Contraction Scour

Contraction scour results from the acceleration of the flow due to either a natural or bridge contraction. With a decrease in flow area there is an increase in average velocity and bed shear stress. Because of the increase in velocity and shear stress, more bed material is transported through the contracted reach than the reaches have no contraction.

2.1.3 Local Scour

The basic mechanism causing local scour at bridge piers and abutments is the formation of vortices at their base (Fig. 2.1 and Fig. 2.2). The vortex removes bed material from the base of the obstruction. As the sediment transport rate, which is outgoing from the scour hole is higher than that coming into, a scour hole develops. As the depth of the scour increases, the strength of the vortices is reduced. On the other hand, there are vertical vortices downstream of the structure called wake vortices. The intensity of wake vortices diminishes rapidly as the distance downstream of the structure increases. Generally, depths of local scour are much larger than general or contraction scour depths, often by a factor of ten (Federal Highway Administration, 2001).

2.2 Scour Process Around Bridge Piers and Abutments

Flow pattern and mechanism of scouring around a pier and an abutment is a complex phenomenon resulting from the strong interaction of the three-dimensional turbulent flow field around the bridge foundations and the erodable sediment bed. Piers and abutments are usually considered as similar in case of scour phenomena (Laursen, 1962; Melville, 1997) but in the abutments case the presence of the incoming wall boundary layer generates a more complex flow field than that observed at piers. Moreover, the scour depth at the abutment was found to be less than that at the equivalent pier due to the boundary layer effects induced by the channel wall (Kothyari and Ranga Raju, 2001).

Local scour holes around bridge piers are developed by the down flow and horseshoe vortex (Fig. 2.1). Principal vortex, which is analogous to the horseshoe vortex around

bridge piers, is primarily responsible for scour hole development around bridge abutments as shown in Fig. 2.2. For abutments, scour always starts just downstream of the corner region protruding into the upstream flow, whereas the initial movement is on both sides of the piers, at about 70° downstream from the channel axis (Oliveto and Hager, 2002). Scour in the channel axis for piers, or at the channel sidewall for abutments, always starts late as compared to the temporal origin. The maximum scour depth migrates from the element side to the pier axis or to the channel wall with time, respectively.

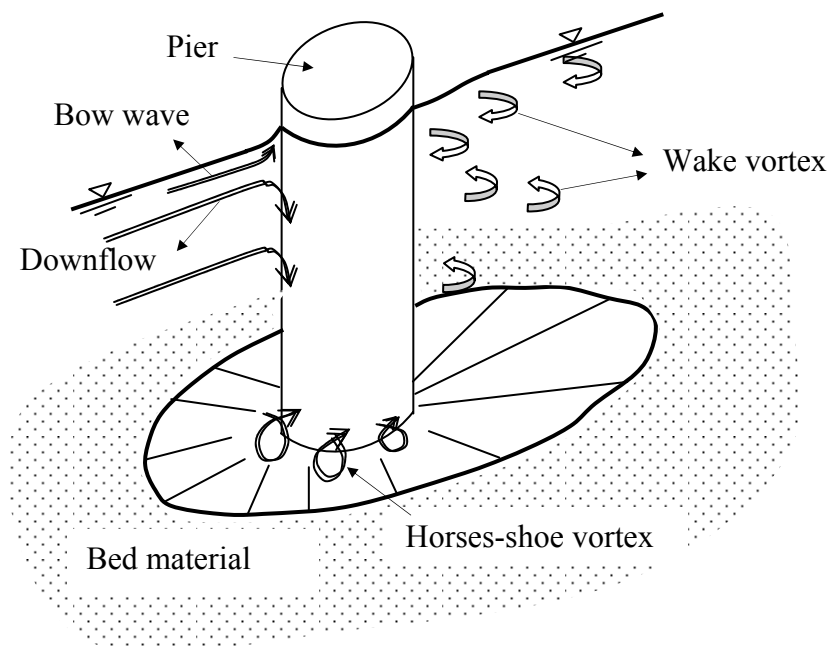


Figure 2.1. General view of pier the scour (after Graf, 1996)

The vortex system and the down flow, along with the turbulence, are the principal causes of the local scour (Kothyari et. al., 1992). At upstream face of the structure, the approach flow velocity goes to zero, called stagnation point. This causes an increase in pressure. Due to this phenomenon the water surface increases in front of the structure and named bow wave. As the flow velocity decreases from surface to

bed, dynamic pressure on the structure face also decreases downwards. Stagnation point will produce a weak pressure gradient along the front of the structure and include a downward flow, namely from high to low velocities.

Once a scour hole is formed, the scouring mechanism is dominated by the vortex system and an associated down flow. The down flow digs a hole in front of the foundation, rolls up and by interaction with the coming flow forms a complex vortex system.

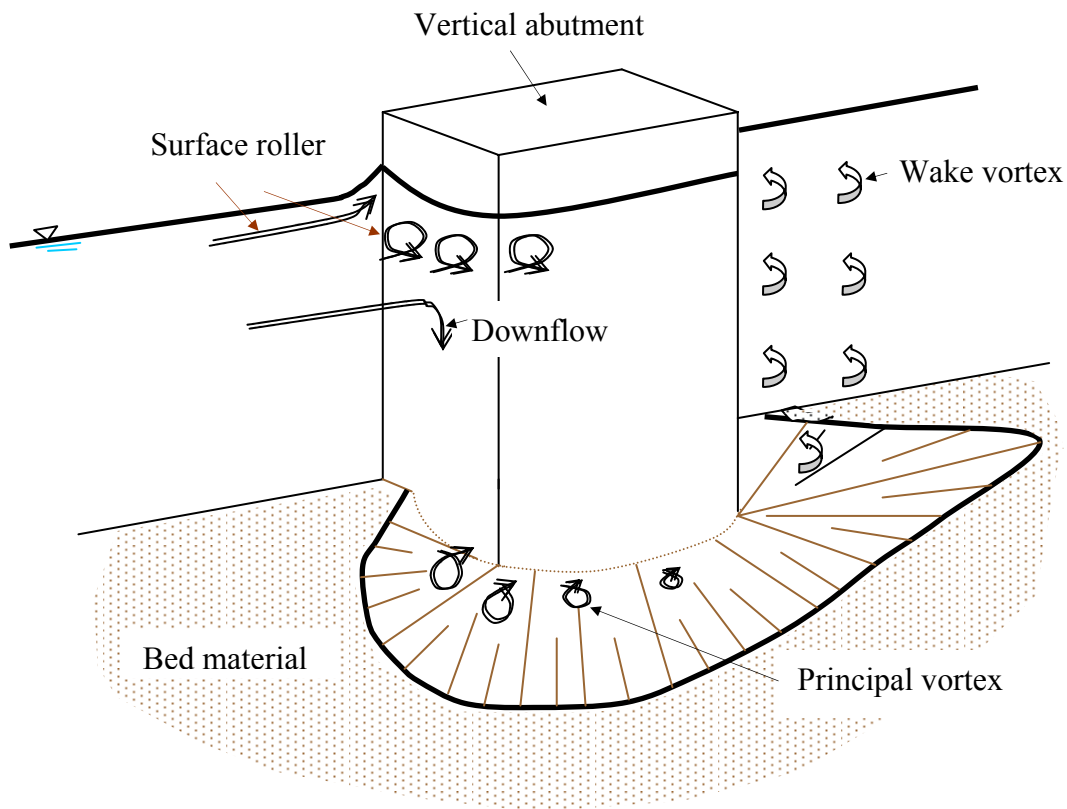


Figure 2.2. General view of the abutment scour (after Graf, 1996)

Since there is also a strong pressure gradient around the bridge structure, the downstream flow will be laterally diverted. If the pressure increase is enough, at the base vortex happens. This vortex loses its strength passing along the structure. At the

rare face of the structure wake vortex system, which scours the downstream sides, is formed.

2.3 Protection of Structures from Local Scour

Three basic methods may be used to protect structures from damage due to local scour (Chiew, 1992 (a); Chiew, 1995; Singh et. al., 1995; Dey, 1997; Duarte and Sainz, 1999; Chiew, 2004). The first is to place the foundations of structures at such depth that the deepest scour hole will not threaten the stability of the structure. The second is to prevent erosive vortices from developing. The third is to provide protection at some level or below the streambed to arrest development of the scour hole.

Riprap piled up around the base of the pier or abutment is a common method of local scour protection. The region of the bed beyond the riprap pile scours and the scour hole is formed, the riprap slides down into the scour hole, eventually armoring the side of the scour hole adjacent to the bridge structure. However, the riprap can be moved downstream during high flows and will not protect the pier or abutment. Therefore excess riprap should be placed and frequent inspections should be made. By frequent inspection, it can be determined whether the size and quantity of riprap used initially is adequate. Where rock mattresses or loose riprap is used, consideration must be given to piping of fine material from underneath of the armor layer. If this occurs, scour depths as deep as those without protection may develop.

2.4 Parameters Affecting Scour Around Bridge Structures

Factors, which affect the magnitude of local scour depth at piers and abutments

are as below:

- a) *Flow velocity*
- b) *Flow depth*: An increase in flow depth can increase scour depth by a factor of 2 or greater for piers. With abutments, the increase is 1.1 to 2.15 depending on the shape of the abutment (Federal Highway Administration, 2001)
- c) *Pier Width and Abutment Length*: As pier width and abutment length increases scour depth increases.
- d) *Bed material size and gradations*: Bed material characteristics such as size, gradation, and cohesion can affect local scour. Sand size range of the bed material has little effect on local scour depth. Likewise, larger size bed material that can be moved by the flow or by the vortices and turbulence created by the pier or abutment will not effect the maximum scour depth, but only the time it takes to attain it (Miller et. al.,1992). Very large particles may armor the scour hole.
- e) *Shape of the pier and abutment*: Streamlining shapes reduce the strength of the horseshoe vortex and leads to smaller scour depths.
- f) *Angle of attack*
- g) *Bed configuration*
- h) *Ice formation or jam and debris*

2.5 Local Scour Conditions

The Shields diagram defines the critical shear velocity U_{*c} for a given d_{50} size of sediment. A corresponding critical mean velocity U_c can be found from the given flow depth. If U is around 50% of U_c , clear-water scour around the bridge structure begins (Graf, 1996; Graf 1971; Simons and Şentürk, 1992). In clear-water scour,

scour depth increases gradually and approaches an asymptotic value, when the capacity of sediment transport out of the scour hole is zero. At this time, obtained scour depth is called as “equilibrium scour depth”. In clear-water conditions, the equilibrium scour depth is usually reached in a long duration. If $U=U_c$, initiation of sediment transport starts. If $U>U_c$, sediment is transported through the scour hole by means of excess shear stress and this scour type is called as “live bed scour”. The scour depth increases rapidly with time, firstly reaches a maximum value and then fluctuates about a mean value known as equilibrium value, when the capacity of sediment transport going out of the scour hole is equal to the one coming into the scour hole.

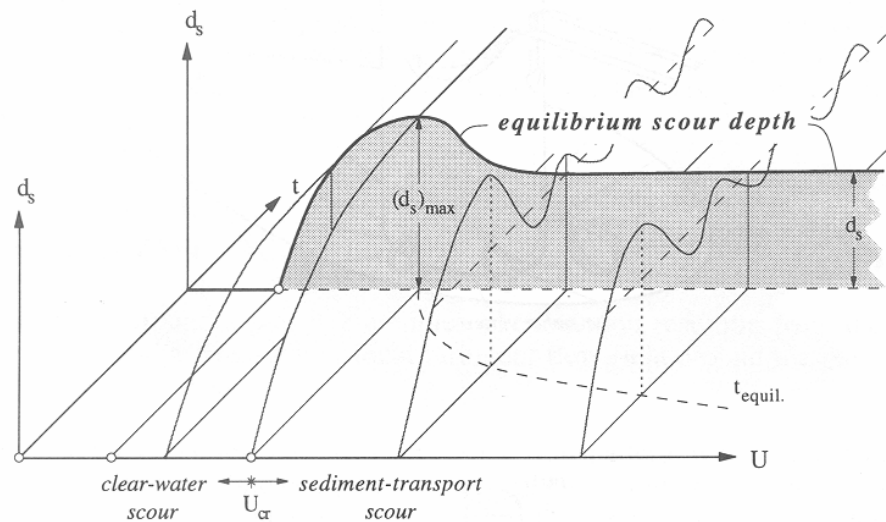


Figure 2.3. Change of the scour depths with respect to flow velocity and time (after Graf, 1996)

This equilibrium condition is reached in a very short time at the live-bed flow condition. This difference is seen in Fig. 2.3 (Graf,1996). Maximum clear-water scour depth is about 10% greater than the equilibrium live-bed scour.

CHAPTER 3

EFFECT OF ABUTMENT SIZE ON LOCAL SCOUR AT BRIDGE

ABUTMENTS

3.1 GENERAL

The length of an abutment has a direct effect on the scour depth. In this study, development of local scour depths at vertical-wall bridge abutments of varying lengths and widths was investigated conducting series of experiments with uniform sediment at clear-water flow conditions. For each flow-abutment combination tested, the maximum local scour depth was recorded and analysed. The obtained results were compared with a number of previous studies related to the local abutment scour. Experimental results show that, the shape of the scour hole resembles an inverted cone around the tip of the structure and the maximum scour occurs at the upstream face of the abutment. The scour depth increases with an increase in the abutment length. On the contrary, the width effect on the scour depth is relatively small with compared to the length effect, and is not needed to account into the abutment scour phenomena.

3.2 LITERATURE REVIEW

An important consideration in designing an abutment is to predict the maximum depth of the scour hole, $(d_s)_{\max}$, which will occur around the abutment so

that the foundation of the structure can be placed deep enough to avoid the possibility of undermining.

Garde et. al. (1961) conducted experiments with four sizes of right angled spur-dikes which have the channe contraction ratio, $\alpha=(B-L_a)/B$, of 0.90, 0.835, 0.667, and 0.530 in a rectangular channel of width $B=0.60$ m where L_a is the abutment length perpendicular to the flow direction. Bed materials of $d_{50}=0.20$ mm, 0.45 mm, 1.00 mm and 2.25 mm having average specific gravity of 2.70 were used to investigate the effect of sediment characteristics. Test duration was varied between 3 to 5 hours. Using dimensional analysis, they arrived the equation given below:

$$\frac{y + (d_s)_{max}}{y} = 4 \frac{1}{\alpha} F_r^{2/3} \quad (3.1)$$

where, y is the approach flow depth and F_r is the approach flow Froude number.

Laursen (1962) studied the effect of geometry of the pier and abutment in a channel having width of $B=3.2$ m. The results of variety sizes of abutments, which were tested in the experiments, were plotted as maximum scour depth versus abutment lengths. All tests were performed under clear-water condition.

Gill (1972) performed the experiments in a rectangular tilting steel flume of 0.67 m wide under threshold flow conditions. Two sizes of sand were used; $d_{50}=0.9$ mm and 1.5 mm. The abutment length was 20 cm and experiments were performed for duration of 6 hours. He suggested that equation (3.2) should be used with no

distinction between clear water and sediment transporting flows.

$$\frac{y + (d_s)_{max}}{y} = 8.375 \left(\frac{d_{50}}{y} \right)^{0.25} \left(\frac{I}{\alpha} \right)^{6/7} \quad (3.2)$$

Melville (1992) identified various zones of dependence of equilibrium scour depth, d_{se} , which is obtained from tests of long duration (days, weeks), on flow depth and the abutment length, L_a . He classified the abutments either short ($L_a/y \leq 1$) or long ($L_a/y \geq 25$) and explained that, at a long abutment, part of the flow approaching the abutment is deflected parallel to upstream abutment face and is therefore ineffective in generating down flow ahead of the abutment. Short abutments experience flow patterns similar to bridge piers, with down-flow along the upstream abutment face, a principal vortex and wake vortices. He collected the previous experimental data of the abutment scour studies of Auckland University and rationalizing the existing laboratory flume data and proposed the following relationships for equilibrium scour depth d_{se} .

$$d_{se} = 10y \quad \text{if } L_a/y \geq 25 \text{ for long abutments} \quad (3.3)$$

$$d_{se} = 2(yL_a)^{0.5} \quad \text{if } 1 < L_a/y < 25 \text{ neither long nor short abutments} \quad (3.4)$$

$$d_{se} = 2L_a \quad \text{if } L_a/y \leq 1 \text{ for short abutments} \quad (3.5)$$

Lim (1997) proposed the equation given below for equilibrium scour depth of vertical-wall abutment under clear-water flow conditions.

$$\frac{d_{se}}{y} = K_s 0.9 \left(\theta_c^{-0.375} F_o^{0.75} \left(\frac{d_{50}}{y} \right)^{0.5} \left[\left(\frac{L_a}{y} \right)^{0.5} 0.9 + I \right] - 2 \right) \quad (3.6)$$

where; K_s is the shape factor, θ_c is Shield's entrainment factor, and F_o is the densimetric Froude number. The experiments were conducted in a tilting rectangular flume, 18 m long, 0.6 m wide, and 0.6 m deep under clear water flow conditions. Experiments lasted between 72 to 193 hours. The uniform sand having $d_{50}=0.94$ mm was used. The abutment model used was the vertical-wall types which were constructed with lengths $L_a=5$ cm, 7.5 cm, 10 cm, 12.5 cm, and 15 cm. He found a good agreement between the computed and measured results.

Kandasamy and Melville (1998) reviewed the scouring mechanism of local scour at piers and wing-wall abutments and highlighted the similarities between them. Experiments were performed to test the effect of abutment length and flow depth on local scour depth near threshold conditions with a uniform sand of median grain size $d_{50}=0.90$ mm. They compiled field data for a wide range of river and flood condition. They investigated that, the field measurements of abutment scour were always less than what they predicted.

Chaurasia and Lal (2002) derived an equation, which gives equilibrium scour depth around the vertical abutment; by using maximum and equilibrium scour depth data reported in the literature. Test durations varied between 38 hrs - 600 hrs under clear-water flow condition. The median grain sizes were $d_{50}=0.56$ mm-1.40 mm. They offered the equation given below for computation of equilibrium scour depth around bridge abutments for both uniformly and non-uniformly graded sediments.

$$\frac{d_{se}}{y} = 2.657\theta_c^{-0.16}F_o^{0.765}\left(\frac{L_a}{y}\right)^{0.245}\left(\frac{d_{50}}{y}\right)^{0.265} - 1 \quad (3.7)$$

Chaurasia and Lal (2002) gave another equilibrium scour depth formula, which was derived by Liu in 1961 for equilibrium scour depth under clear-water flow conditions in their study. Liu's equation was given as:

$$\frac{d_{se}}{y} = 4F_r^{0.33} \quad \text{for} \quad \frac{L_a}{y} \geq 25 \quad (3.8)$$

$$\frac{d_{se}}{y} = 2.15 \left(\frac{L_a}{y} \right)^{0.40} F_r^{0.33} \quad \text{for} \quad \frac{L_a}{y} < 25 \quad (3.9)$$

They also gave Forehlich's equation for non-uniform sediment grain size and clear-water flow conditions as:

$$\frac{d_{se}}{y} = 0.78 K_s K_\theta \left(\frac{L_a}{y} \right)^{0.63} F_r^{1.61} \left(\frac{y}{d_{50}} \right)^{0.43} \sigma_g^{1.87} \quad (3.10)$$

where; K_θ is the coefficient of the angle of embankment to the flow and σ_g is geometric standard deviation of particle size distribution..

Melville (1997) presented an integrated approach to the estimation of the equilibrium scour depth at an abutment:

$$d_{se} = K_I K_{yw} K_d K_s K_\theta K_\sigma \quad (3.11)$$

where; K is an empirical expression accounting for the various influences on scour depth; K_{yw} =flow depth-abutment size factor $\equiv K_{yb}$ for piers and K_{yL} for abutments;

K_I =flow intensity factor, K_d =sediment size factor; K_s =foundation shape factor; K_θ =foundation alignment factor; and K_σ =approach channel geometry factor. K_{yw} and d_{se} have the dimension of length, while the other K factors are dimensionless (estimation methods of these parameters are discussed in Coleman et. al., 2003).

3.3 DIMENSIONAL ANALYSIS

For clear-water approach flow conditions, the maximum scour depth, $(d_s)_{max}$, at an abutment is a function of the following parameters:

$$(d_s)_{max} = f\{L_a, B_a, U, y, S, g, \rho_s, \rho, \mu, d_{50}, \sigma_g, t, B\} \quad (3.12)$$

where, B_a =abutment width, U =mean approach flow velocity, S =slope of the channel, g =gravitational acceleration, ρ_s =density of the sediment, ρ =density of the fluid, μ =dynamic viscosity of fluid, d_{50} =median particle grain size, $\sigma_g=(d_{84}/d_{16})^{0.5}$ =geometric standard deviation of sediment size distribution, d_{84} =sediment size for which 84% of the sediment is finer, d_{16} = sediment size for which 16% of the sediment is finer, and t =scouring time.

In terms of dimensionless parameters equation (3.12) can be written as;

$$\frac{(d_s)_{max}}{y} = f\left\{\frac{L_a}{y}, \frac{B_a}{y}, \frac{\rho_s}{\rho}, \frac{U}{\sqrt{gy}}, \frac{B}{y}, \frac{\mu}{U\rho y}, \frac{Ut}{y}, S, \sigma_g, \frac{d_{50}}{y}\right\} \quad (3.13)$$

Considering that the experiments are conducted with one sediment size, constant; bed slope, channel width and duration of the experiment, and the ignoring of viscous

effects one can simplify Equation (3.13) as:

$$\frac{(d_s)_{max}}{y} = f\left(\frac{L_a}{y}, \frac{U}{\sqrt{gy}}, \frac{L_a}{B_a}, \frac{L_a}{B}\right) \quad (3.14)$$

or

$$\frac{(d_s)_{max}}{L_a} = f\left(\frac{y}{L_a}, \frac{U}{\sqrt{gy}}, \frac{B_a}{L_a}, \frac{B}{L_a}\right) \quad (3.15)$$

where the scour depth is normalized with flow depth and abutment length in equations (3.14) and (3.15), respectively.

3.4 EXPERIMENTAL PROCEDURE

Experimental investigations were performed in a channel at the Hydraulics Laboratory of State Hydraulic Works, Ankara. All tests were conducted under or near the clear water flow conditions at $U/U_c < 1$, where U_c is the shear velocity of the approach flow and U is the value of U_c at the threshold of grain motion. The threshold of bed material motion was found by experiment when the abutment was not installed. Threshold of bed material motion was defined as a condition for which finer materials may move, but the elevation of the bed wouldn't lower more than 1 mm to 2 mm during the test duration. The critical shear velocity, which leads to sediment moving, was calculated from Shield's diagram. A rectangular channel with transparent walls, 30 m long and 1.5 m wide was filled with erodable uniform sediment having a median diameter of $d_{50} = 1.48$ mm with geometric standard

deviation of particle size distribution ratio of $\sigma_g=1.28$ and channel slope of $S=0.001$. The depth and the length of the sand layer in the working reach were 0.50 m and 10 m, respectively. The general view of the channel is shown in Figure 3.1.

The flume had a closed-loop water system and the flow to the flume was supplied from a constant-head water tank by a pump. A gate was mounted at the tail end to adjust flow depths. The flow discharge was measured with a sharp-crested rectangular weir having the width of 1 m and the height of 0.30 m mounted at the

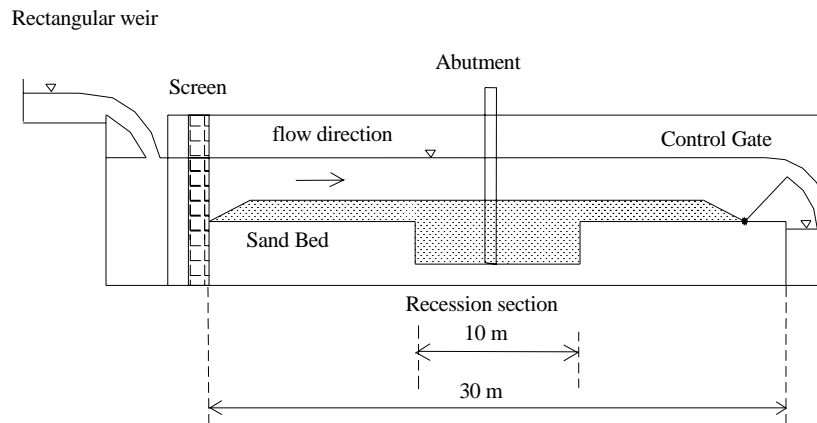


Figure 3.1. General view of the experimental installation

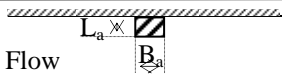

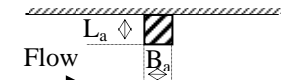
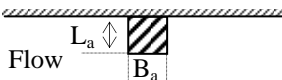
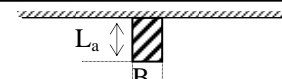
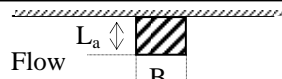

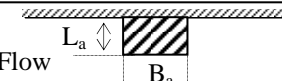
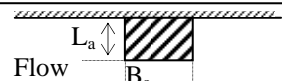
upstream section of the flume. By means of bricks and sheet-iron strainer, which placed between brick-walls, placed at the entrance of the channel as a filter, turbulence of the flow was reduced and the uniform flow conditions were maintained which were required for upstream head measurements. The scour depths were also measured with a pointgage to an accuracy of ± 1 mm. The tip of the gage was painted with white paint and for each measurement the painted tip penetrated the sandy bottom of the scour hole until it could no longer be seen.

The scour hole was obtained by performing a 6-hours continuous run under clear-water conditions and both maximum scour depth and scour formation at the abutment site were investigated. At the end of each experiment, the flume was carefully drained and sand bed level was straightened for the next experiment with a special apparatus, which was made of steel plate welded on a steel frame. This frame could slide from the beginning to the end of the flume over steel rails, which were mounted, on the glass- sidewalls.

The experimental set-up mentioned above forms the main frame of the experimental procedure of all the tests performed during the study. If there is nothing mentioned additional, this procedure will also be followed in the other chapters.

In this study, in order to see the effect of abutment length on the scour depth, abutment lengths of $L_a=10$ cm, 15 cm, 20 cm, and 25 cm, and flow depths of $y=10$ cm, 12 cm and 14 cm were used for the same discharge of $Q=0.050$ m³/s. Corresponding Froude numbers for these flow depths were $F_r=0.34$, 0.26 and 0.20, respectively. Experimental arrangements used in this study and corresponding measured maximum scour depths for each arrangement are tabulated in Table 3.1. Figures 3.2-3.5 show some of the photographs of the abutments tested and scoured channel bed around the abutments.

Table 3.1. Experimental series for abutment length and width effect ($Q=0.05 \text{ m}^3/\text{s}$)

Type	Shape	y (mm)	(d _s) _{max} (cm)	Type	Shape	y (mm)	(d _s) _{max} (cm)
1	 $L_a=10 \text{ cm}, B_a=5 \text{ cm}$	100	9.55	1	 $L_a=25 \text{ cm}, B_a=10 \text{ cm}$	100	16.21
		120	5.18			120	10.04
		140	2.20			140	6.06
2	 $L_a=15 \text{ cm}, B_a=5 \text{ cm}$	100	12.88	2	 $L_a=25 \text{ cm}, B_a=20 \text{ cm}$	100	15.40
		120	7.85			120	8.61
		140	4.03			140	5.48
3	 $L_a=20 \text{ cm}, B_a=5 \text{ cm}$	100	16.40	3	 $L_a=25 \text{ cm}, B_a=30 \text{ cm}$	100	14.88
		120	9.95			120	7.92
		140	6.45			140	5.99
4	 $L_a=25 \text{ cm}, B_a=5 \text{ cm}$	100	18.85	4	 $L_a=25 \text{ cm}, B_a=40 \text{ cm}$	100	15.00
		120	11.55			120	8.17
		140	7.50			140	6.43
				5	 $L_a=25 \text{ cm}, B_a=50 \text{ cm}$	100	14.53
						120	8.45
						140	6.00

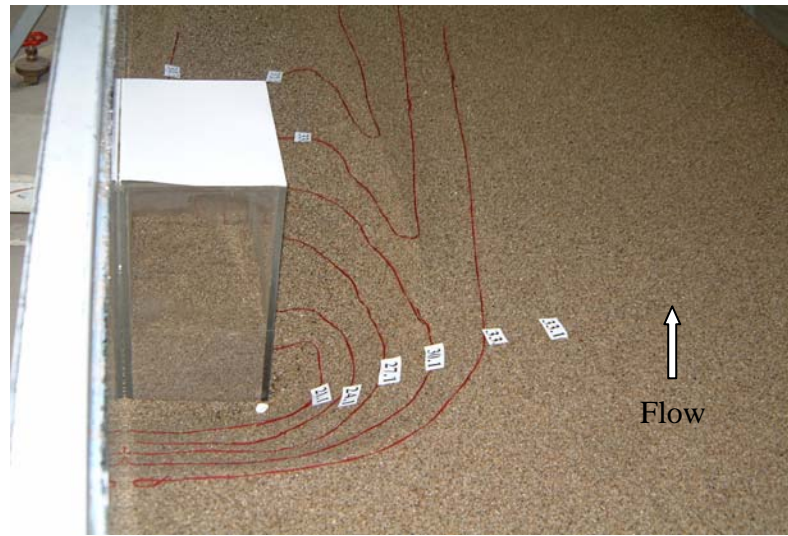


Figure 3.2. Upstream view of the scour hole
 ($L_a=20$ cm, $B_a=20$ cm, $y=10$ cm)

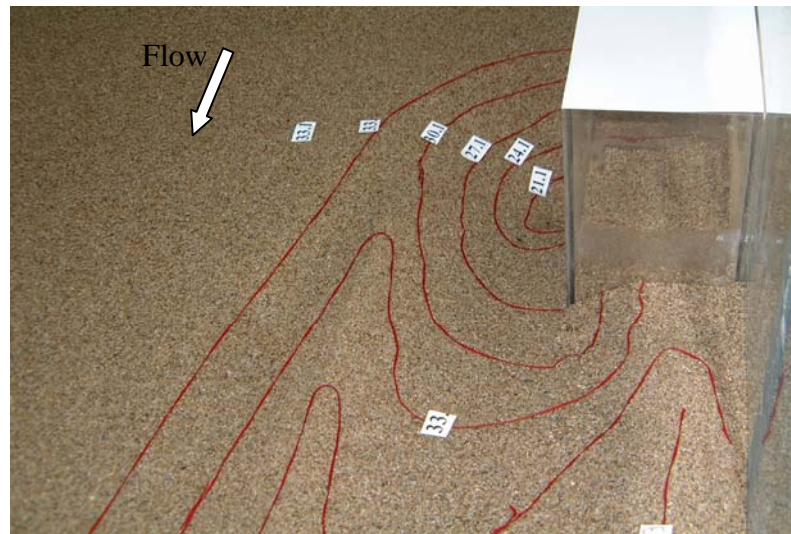


Figure 3.3. Downstream view of the scour hole
 ($L_a=20$ cm, $B_a=20$ cm, $y=10$ cm)

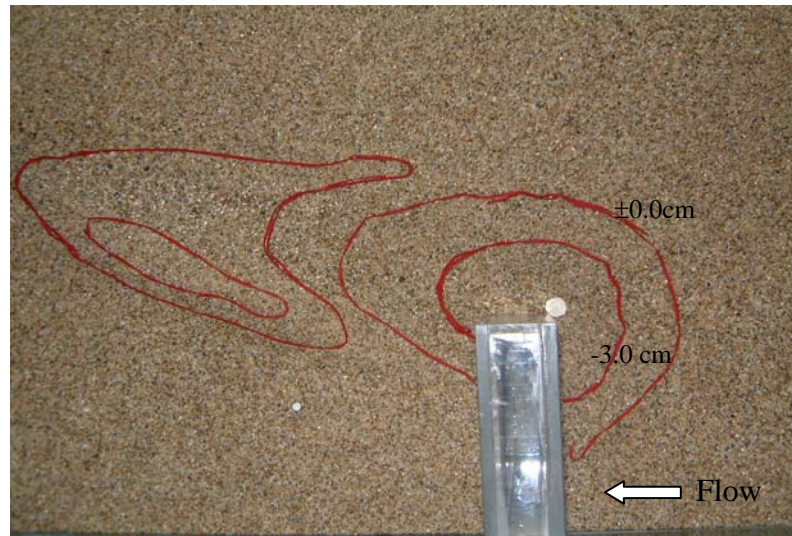


Figure 3.4. Top view of the scour hole
($L_a=20$ cm, $B_a=5$ cm, $y=14$ cm)

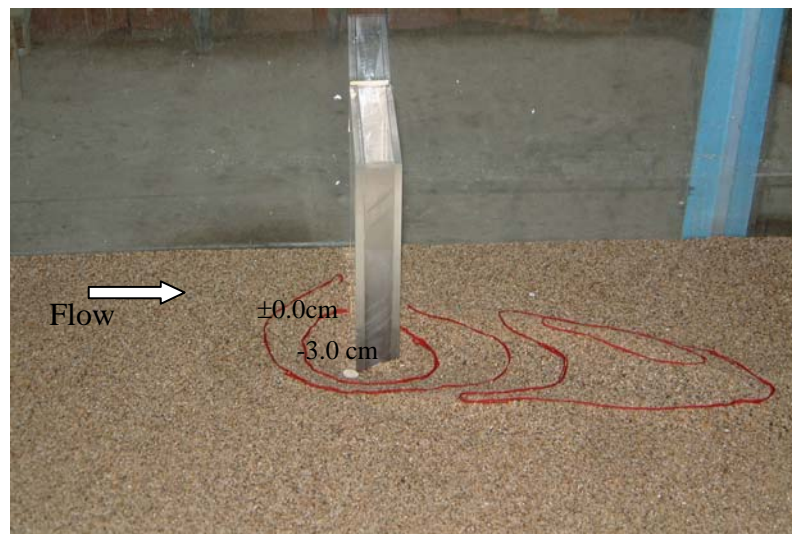


Figure 3.5. Side view of the scour hole
($L_a=20$ cm, $B_a=5$ cm, $y=14$ cm)

3.5 DISCUSSION OF RESULTS

3.5.1 Effect of Abutment Length

Figure 3.6 shows the relationship between dimensionless maximum scour depth, $(d_s)_{\max}/y$, and dimensionless abutment length, L_a/B , which can be expressed in the form of contraction coefficient α , $L_a/B=1-\alpha$, for three different Froude numbers. In this figure the Froude number of 0.34 ($=F_{rc}$) corresponds to the threshold condition of sediment motion in the channel with a flow depth of $y=10$ cm. For other smaller F_r numbers ($F_r < F_{rc}$) the flow depths are $y=12$ cm and 14 cm, respectively, and they both satisfy the condition of clear-water. Referring to the figure one can state that for a given Froude number as the length of the abutment increases, the corresponding maximum scour depth increases.

Figure 3.7 presents the present data along with some other data, which belong to threshold conditions, given in the literature to show the effect of flow depth on the scour depth. Except the data of small Froude numbers; $F_r=0.26$ and 0.20, the data of $F_r=0.34$ follow almost the same trend as those belong to other investigators. In the zone where the present data appear in Fig. 3.7 the value of y/L_a , varies between 0.1 and 1. In this zone the abutments are classified as neither long nor short as defined by Melville (1992).

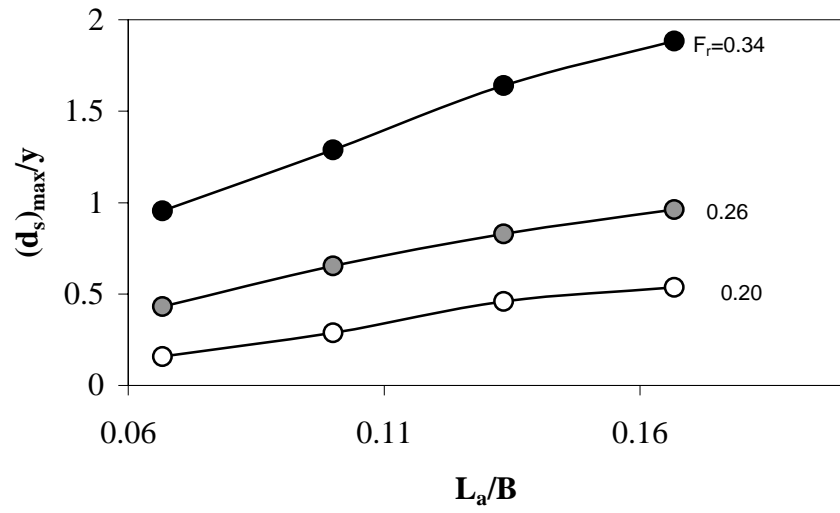


Figure 3.6. Influence of abutment length on scour depth

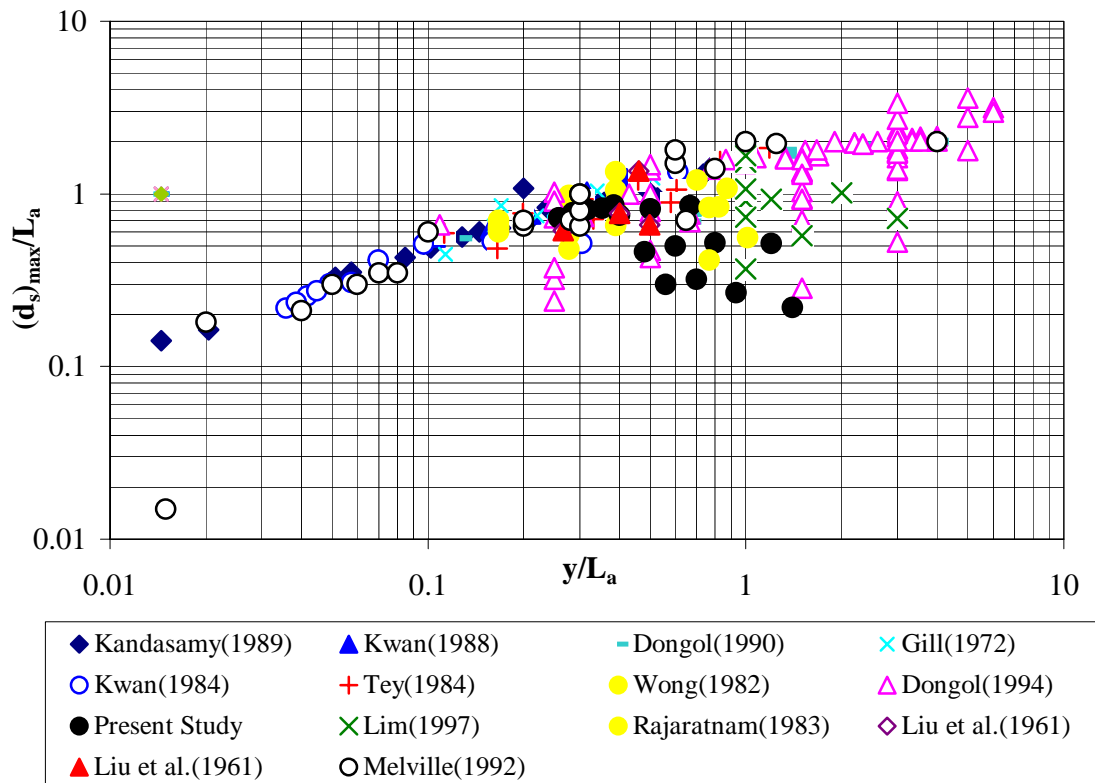


Figure 3.7. Influence of flow depth on scour depth

3.5.2 Effect of Abutment Width

The scour phenomenon usually begins at the upstream tip of the abutment (Figs. 3.2-3.5). The flow accelerates and separates at the upstream face of the abutment as it moves and past the obstacle. As a result, scour always starts just downstream of the corner region protruding into the upstream flow. For sufficiently long scour duration, the maximum scour depth migrates from element side to the channel wall. Fig. 3.8 indicates that, as the abutment width increases, the maximum scour depth does not differ so much and lines belonging to different flow depths are seemed to be parallel to each other. As a conclusion it can be stated that, the effect of the streamwise abutment length on the scour depth is negligible as stated by Oliveto and Hager (2002).

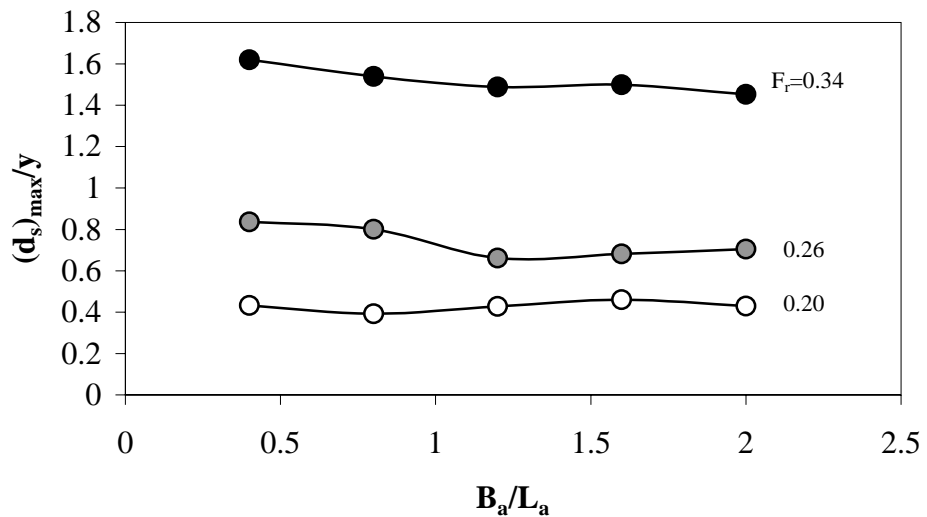


Figure 3.8. Variation of maximum scour depth with abutment width

3.5.3 A Dimensionless Scour Depth Relation for Vertical Wall Abutments

Application of the regression analysis to the dimensionless parameters given in Eqn.(3.14) using the experimental data, results in the following relationship for dimensionless maximum scour depth.

$$\frac{(d_s)_{max}}{y} = \left(\frac{L_a}{y} \right)^{1.4} (F_r)^{1.76} \left(\frac{L_a}{B_a} \right)^{0.12} \left(\frac{L_a}{B} \right)^{-0.66} \quad (r^2=0.99) \quad (3.16)$$

where r^2 is the correlation coefficient. This equation, the plot of which is given in Fig. 3.9, is valid only for the conditions under which the experiments conducted in this study.

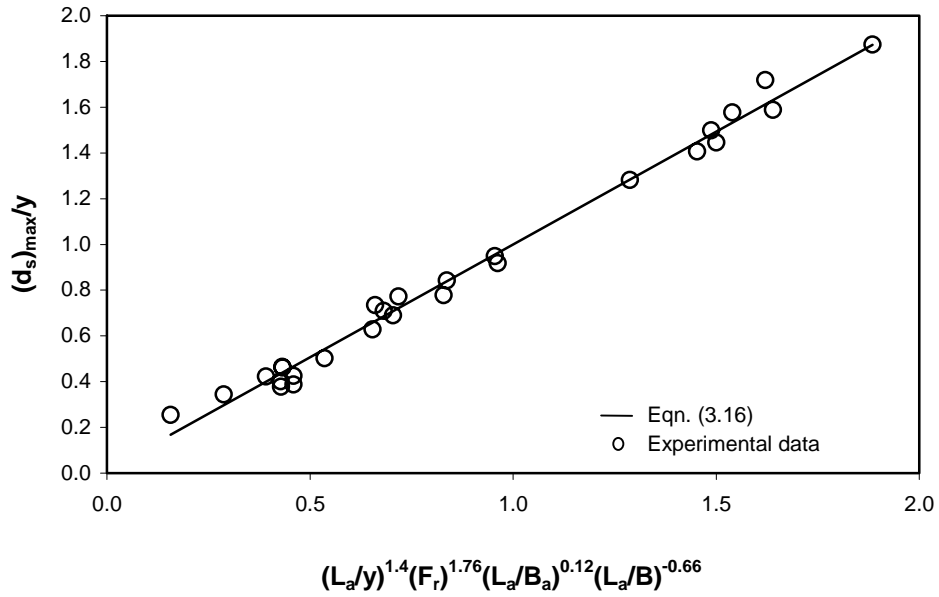


Figure 3.9. Variation of $(d_s)_{max}/y$ with related dimensionless terms

3.5.4 Comparison of Experimental Results with Garde's (1961) Equation

Figure 3.10 presents the experimental data of this study in the form of Eq. (3.1) derived by Garde et.al. (1961). This figure indicates that the general trends of the experimental results are quite consistent with Garde's equation.

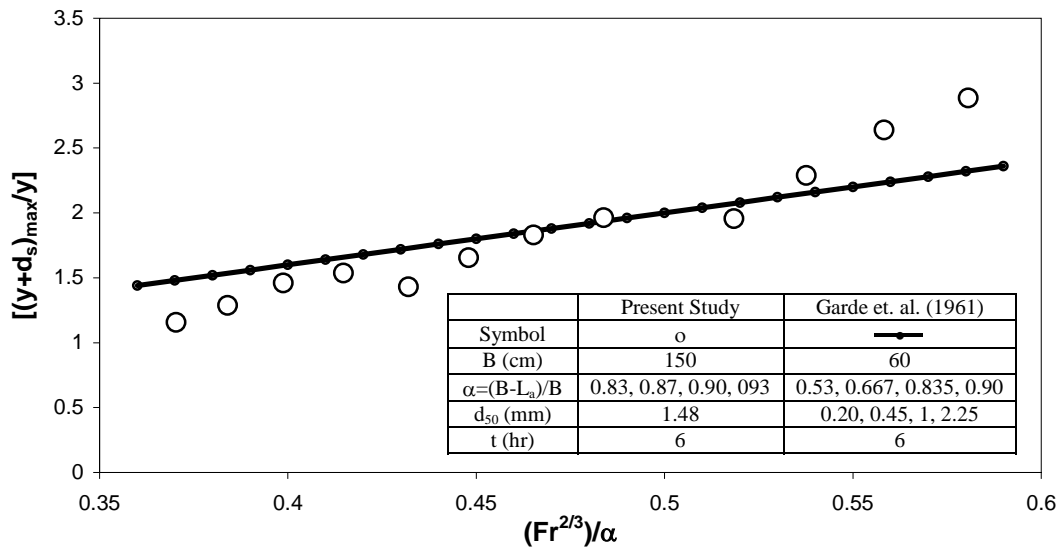


Figure 3.10. Comparison of the present data with Garde's (1961) equation

3.6 CONCLUSIONS

Based on the experimental findings of this study, it can be concluded that the length of the abutment is an important parameter affecting the scour depth. In clear water conditions, the rate of increase of $(d_s)_{\max}/y$ with L_a/B for flows corresponding to the threshold condition of sediment motion ($F_r \cong F_{rc}$) is much greater than those of Froude numbers less than F_{rc} .

The stream wise length of the abutment doesn't affect the maximum scour depth significantly. That is, the abutment's width effect can be dropped while studying abutment scour depth.

CHAPTER 4

APPLICATION OF COLLAR TO CONTROL SCOURING AROUND ABUTMENTS

4.1 GENERAL

The primary objective of the present study is to investigate the effect of collars of different sizes to be placed on bridge abutments at various elevations, on the reduction of the scour around the abutments.

4.2 LITERATURE REVIEW

The primary cause of local scour around a bridge abutment is the presence of vortex flow called the principal vortex. The growth of vortex can be arrested by forming a rigid surface around the abutment with a collar. A literature review shows that placing a collar (thin plate) around a bridge pier can reduce the depth of scour. Dargahi (1990) presented that the collars can effectively reduce the strength of the horse-shoe vortices when placed within the separated boundary layer around the pier. Chiew (1992, (b)) conducted experiments in a 0.30 m wide and 8 m long channel having a cohesionless, uniform sand of a median particle size of 0.33 mm. Chiew used a single cylindrical pier of 3.2 cm-diameter and investigated the effect of a slot, a collar and a combination of both on bridge pier scour. A combination of collar and slot can be an appropriate alternative solution to riprap protection in tackling scour problems at bridge piers.

Kumar et. al. (1997) used a 1-m wide, 30 m long flume having a longitudinal slope of 7.73×10^{-4} and uniform sediments of median diameters 0.78 mm, 1.18 mm and 1.54 mm as bed material. The scour reduction efficacy of slots of two different lengths provided along the height of the pier with a constant width of $0.25D$ was studied, where D is the diameter of the pier. They also developed a predictive equation for scour reduction by the use of collars of different elevations at or above the bed level. For the experiments on collar efficiency, five collar sizes ($1.5D$, $2D$, $2.5D$, $3D$, and $4D$) were used. They presented an equation for predicting the scour depth with collars and concluded that larger diameter collars at or close to the bed were more effective.

Singh et. al. (2001) investigated arresting the growth of the vortex on rigid surface as a collar or by confining it within an enclosure like a sleeve skirting around the pier. Uniform sediment with $d_{50}=0.285$ mm was employed in a 12-m long, 0.6-m wide channel. Model piers of diameters 2.5 cm and 6.2 cm were used. The best location was at $0.1D$ below the average bed level where a collar of a diameter twice of the pier gave a performance potential of 91%. In addition, a collar equal to twice the diameter of the pier was able to reduce scour by 68% when placed at the bed.

Mashahir and Zarrati (2002) studied development of scouring around a rectangular pier with and without a collar. They observed that in addition to reduction of scour depth, collar was very effective in slowing down the development of scouring.

Zarrati et. al. (2004) obtained 35% reduction of scour by using a collar with a width equal to pier width at bed level at the skewed aligned rectangular bridge piers.

This review demonstrates that most of the works toward the understanding of scour evolution were conducted on bridge piers. Therefore, the main objective of the present study is to determine the effect of collars of different sizes and shapes, on the reduction of scour around abutments.

4.3 DIMENSIONAL ANALYSIS

For clear-water approach flow conditions, the maximum scour depth, $(d_s)_{\max}$, at an abutment with a collar is a function of the following parameters:

$$(d_s)_{\max} = f \left\{ L_a, B_a, B_c, Z_c, T_c, U, y, S, g, \rho_s, \rho, \mu, d_{50}, \sigma_g, t, B \right\} \quad (4.1)$$

where, B_c =collar width, Z_c =elevation of the collar with respect to the sand level, and T_c =collar thickness. The definitions of the other parameters are the same as defined in Chapter 3.

Buchingham's π theorem gives the dimensionless terms:

$$\frac{(d_s)_{\max}}{y} = f \left\{ \frac{L_a}{y}, \frac{B_a}{y}, \frac{B_c}{y}, \frac{Z_c}{y}, \frac{T_c}{y}, \frac{\rho_s}{\rho}, \frac{U}{\sqrt{gy}}, \frac{B}{y}, \frac{\mu}{Uy\rho}, \frac{Ut}{y}, S, \sigma_g, \frac{d_{50}}{y} \right\} \quad (4.2)$$

Considering that the experiments are conducted with one sediment size and with constant parameters of bed slope, channel width, collar thickness, abutment width, duration of the experiment, and discharge, one can simplify Equation (4.2) as:

$$\frac{(d_s)_{max_c}}{y} = f\left(\frac{L_a}{B_c}, \frac{Z_c}{y}, \frac{L_a}{B}\right) \quad (4.3)$$

The reduction in the scour depth around the bridge abutments as compared to the case without collar, $(d_s)_{max}$, is

$$\frac{(d_s)_{max} - (d_s)_{max_c}}{(d_s)_{max}} = f\left(\frac{L_a}{B_c}, \frac{Z_c}{y}, \frac{L_a}{B}\right) \quad (4.4)$$

4.4 EXPERIMENTAL PROCEDURE

Figure 4.1 shows a definition sketch with a typical view of a collar-abutment arrangement used in this study. Collars were cut out of 3-mm thick plexi-glass sheet. The locations and the widths of the collars were varied systematically. The abutments used were always rectangular in plan, having lengths of $L_a=7.5$ cm, 15 cm, 20 cm, 25 cm and 35 cm and widths are kept constant at $B_a=10$ cm. According to Oliveto and Hager (2002) and initial findings of this study, the effect of the streamwise abutment length on the development of scour hole is small and may be dropped.

The scour hole was obtained by performing a 6-hours continuous run under clear-water conditions and both maximum scour depth and scour formation at the abutment site were investigated.

Four different collar widths $B_c=2.5$ cm, 5.0 cm, 7.5 cm and 10 cm were used for all abutment types. As the efficiency of the collar is also a function of its vertical location on the abutment, collars of different sizes were placed at different elevations

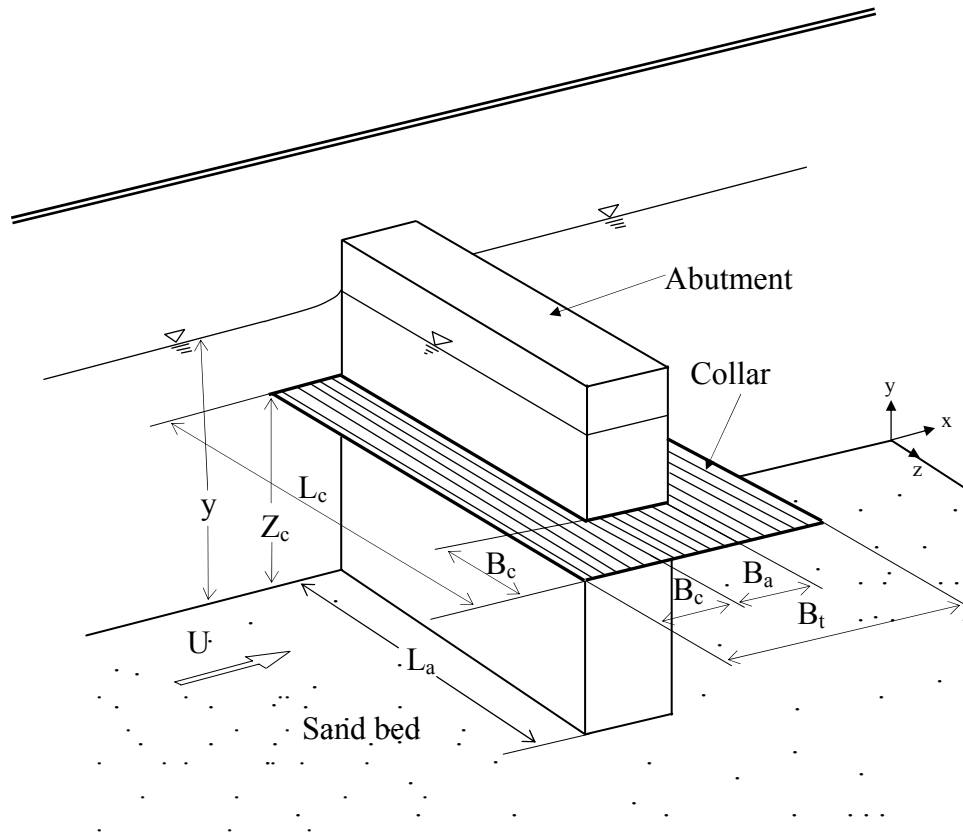


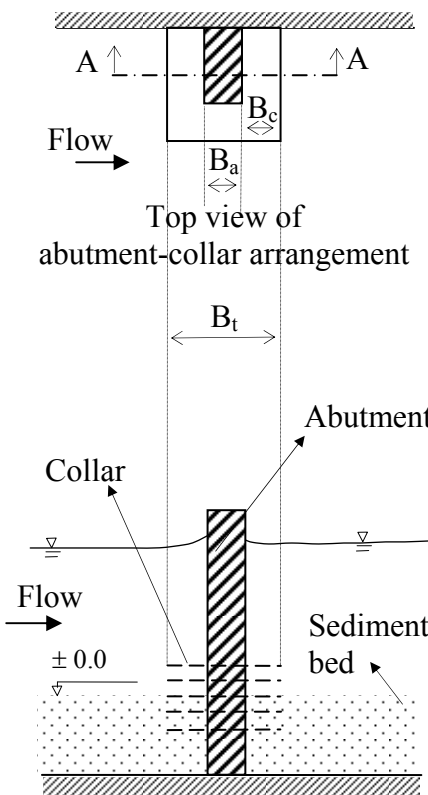
Figure 4.1. Definition sketch of collar-abutment arrangement

on the abutments as; at the bed level, 2.5 cm and 5.0 cm above the bed level and also 2.5 cm and 5.0 cm below the bed level (Fig. 4.2). In Table 4.1, all collars used are classified considering their sizes and also abutment types.



Figure 4.2. A general view of the scour hole when a collar is used
(R69, $L_a=25$ cm, $B_c=5$ cm, $Z_c=+2.5$ cm)

Table 4.1. Abutment and collar sizes used in the tests

Shape	Z_c (cm) = +5.0, +2.5, ± 0.0 , -2.5, -5.0 (with reference to bed material)			
	Type	L_a (cm)	Case	B_c (cm)
 <p>Top view of abutment-collar arrangement</p> <p>Section A - A</p>	1	7.5	a	10.0
			b	7.5
			c	5.0
			d	2.5
	2	15	a	10.0
			b	7.5
			c	5.0
			d	2.5
	3	20	a	10.0
			b	7.5
			c	5.0
			d	2.5
	4	25	a	10.0
			b	7.5
			c	5.0
			d	2.5
	5	35	a	10.0
			b	7.5
			c	5.0
			d	2.5

4.5 SCOUR MECHANISM

Local scour around a solid abutment results from the down flow at the upstream face of the abutment and the subsequent development of principal vortex at the its base. Hence, one way of reducing scour is to weaken and possibly prevent formation of the downflow and the horseshoe vortex.

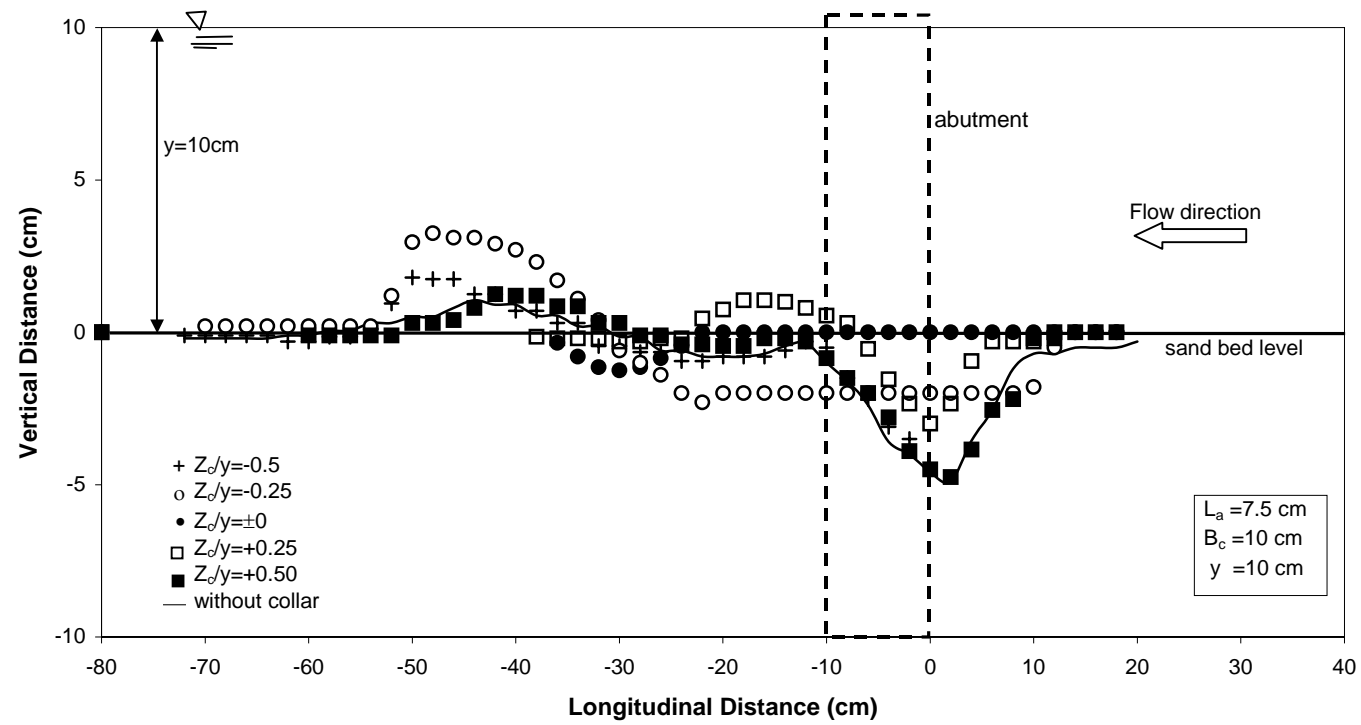
A collar at any level above the bed divides the flow into two regions; i.e. above and below the collar. For the region above the collar, it acts as an obstacle against the downflow in which the downflow loses its strength on impingement at the bed. For the region below the collar, the downflow and the principal vortex are reduced. However, the efficacy of a collar depends on its size and the location on the abutment with respect to the bed.

4.6 DISCUSSION OF RESULTS

4.6.1 Scour Profiles around the Abutment with and without Collar:

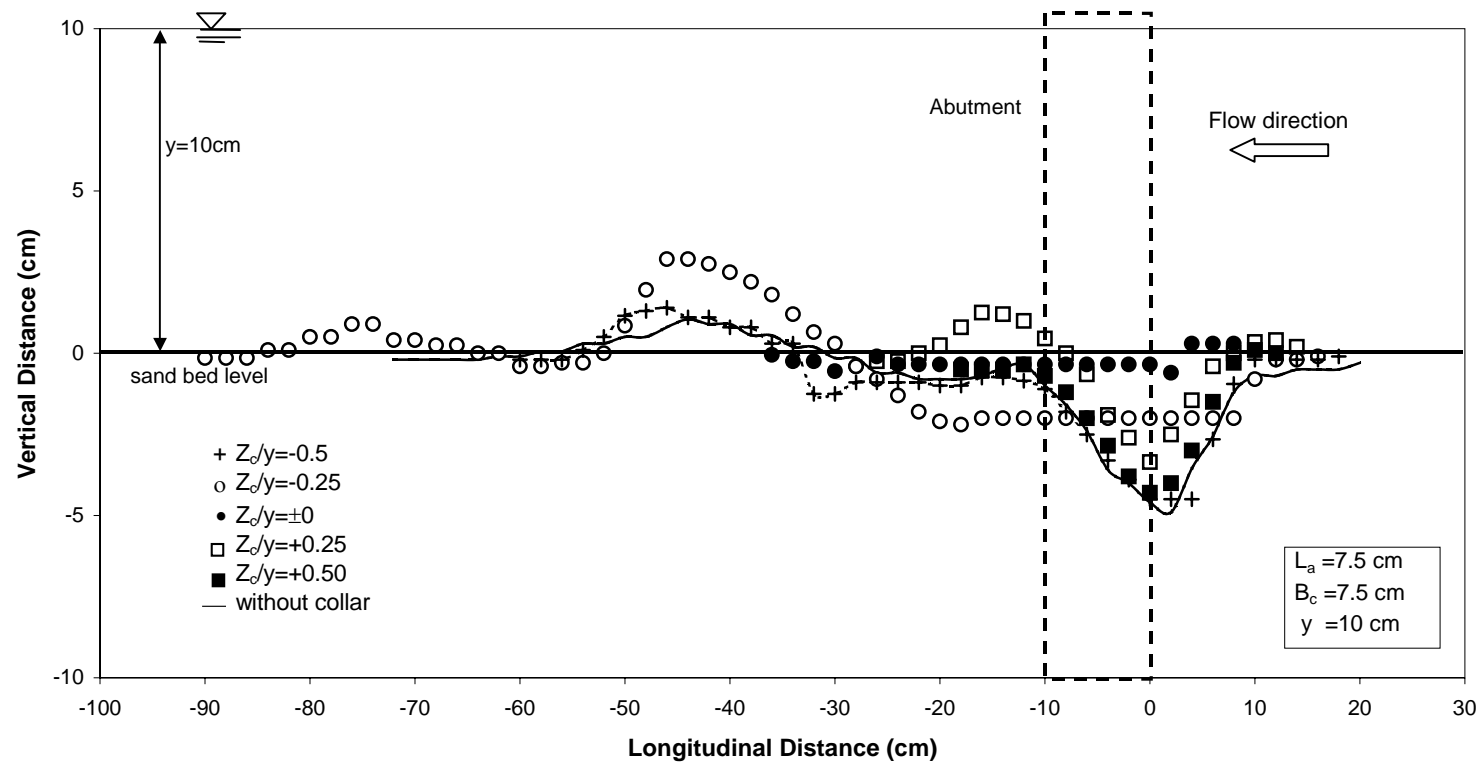
In Figure 4.3, the longitudinal profiles of the channel bed around the abutment of $L_a=7.5$ cm tested without collar and with collars at different elevations are presented. Figure 4.3.(a) shows the case when the largest collar, $B_c=10$ cm is placed around the abutment of $L_a=7.5$ cm. When this collar is placed at an elevation of $Z_c/y=\pm 0.0$, no scour is recorded during the test duration. While the most efficient collar level is observed as $Z_c/y=-0.50$ for the other abutment lengths, it is not so efficient in this arrangement. Even, the one of $Z_c/y=+0.25$ shows higher scour reducing performance than that of $Z_c/y=-0.50$ as the flow usually sweeps away the bed material down to the collar, which are placed below the bed level. As the collar width decreases from $B_c=10$ cm to 7.5 cm, 5 cm and 2.5 cm, as seen from Figs.

4.3.(b)-4.3.(d), the most efficient collar elevation is still $Z_c/y=\pm 0$ although the scour depths resulted from the collar elevation of $Z_c/y=\pm 0$ increases as the collar width decreases.



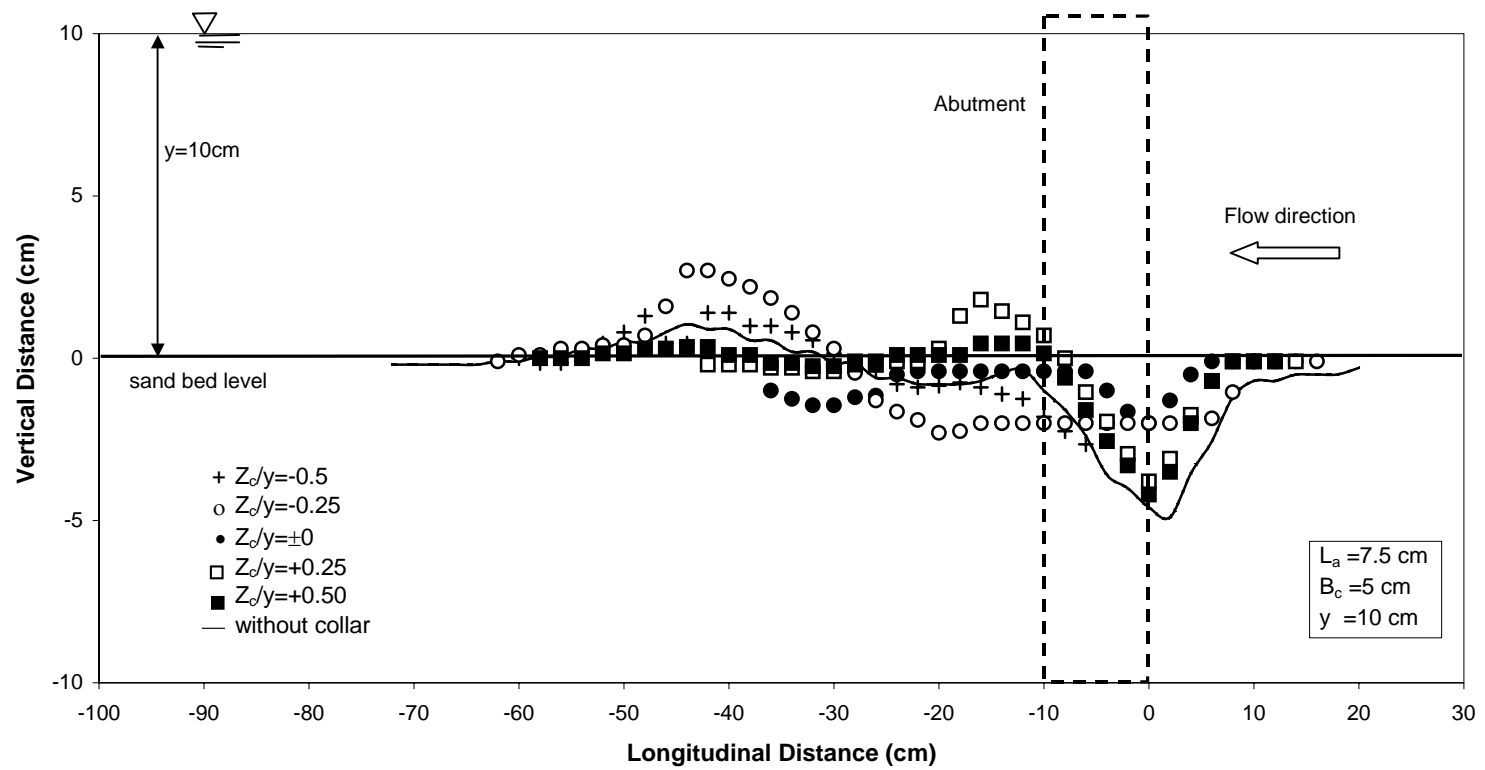
(a) $L_a/B_c = 0.75$

Figure 4.3. Bed profiles around the bridge abutment of $L_a = 7.5$ cm with and without collars



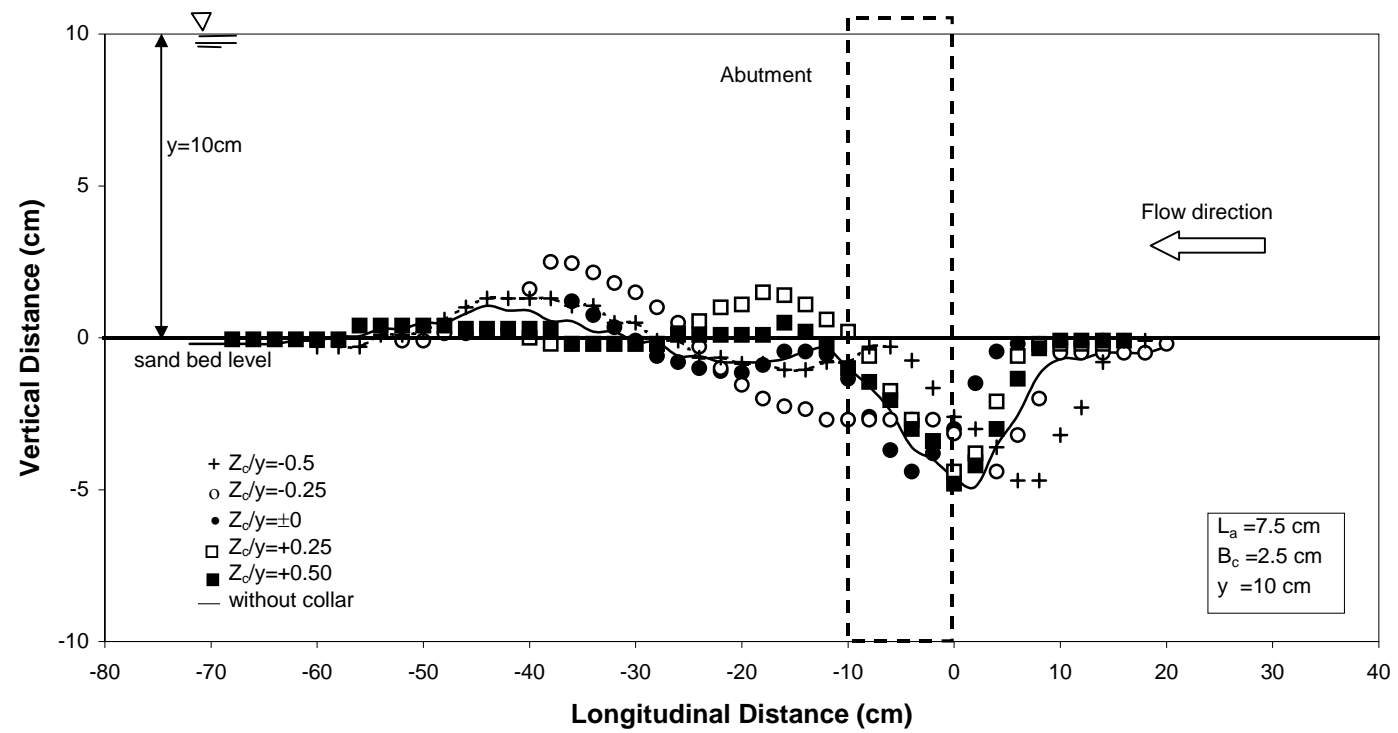
(b) $L_a/B_c = 1.0$

Figure 4.3. Bed profiles around the bridge abutment of $L_a = 7.5 \text{ cm}$ with and without collars



(c) $L_a/B_c=1.5$

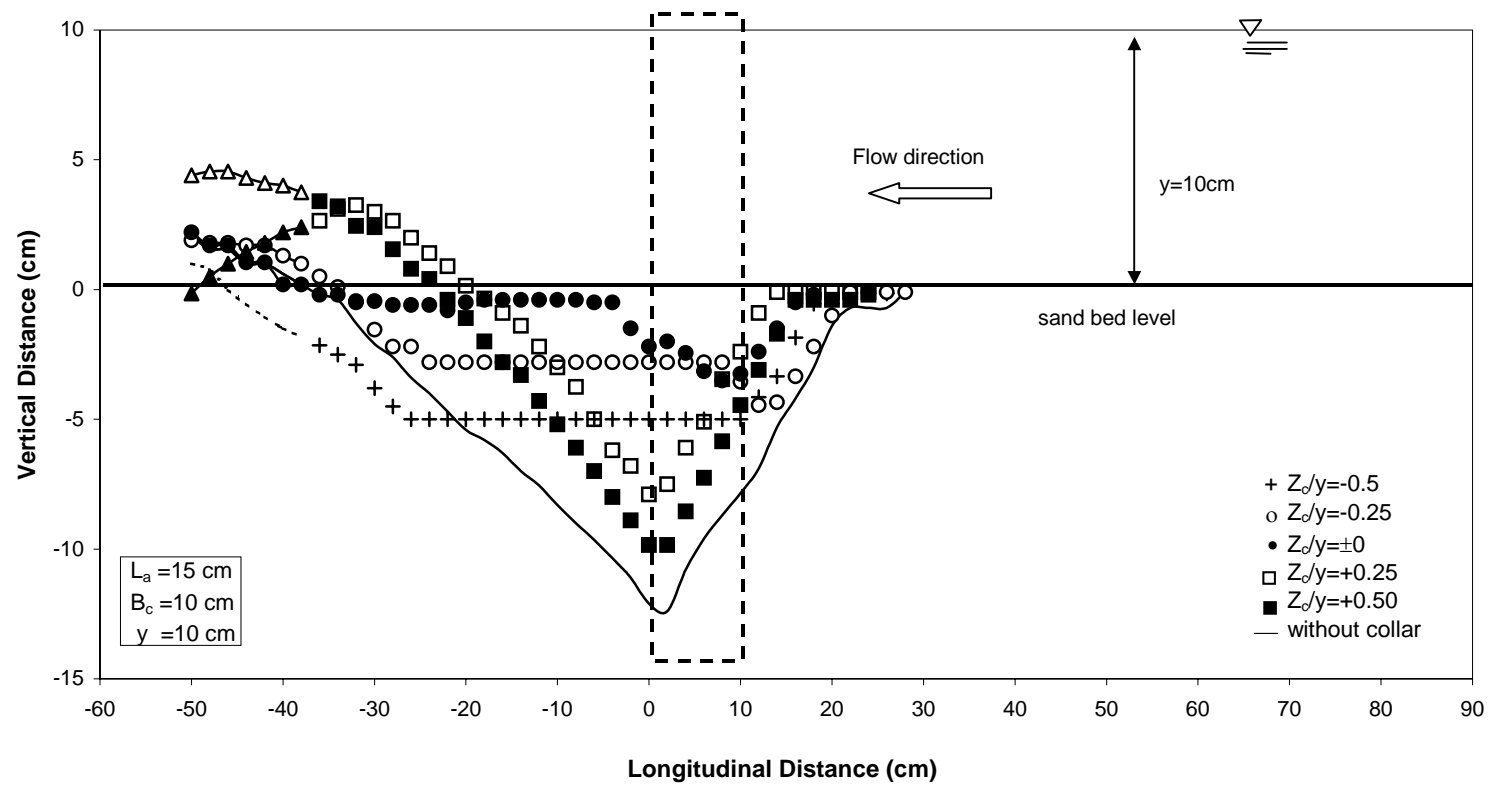
Figure 4.3. Bed profiles around the bridge abutment of $L_a=7.5\text{ cm}$ with and without collars



(d) $L_a/B_c=3.0$

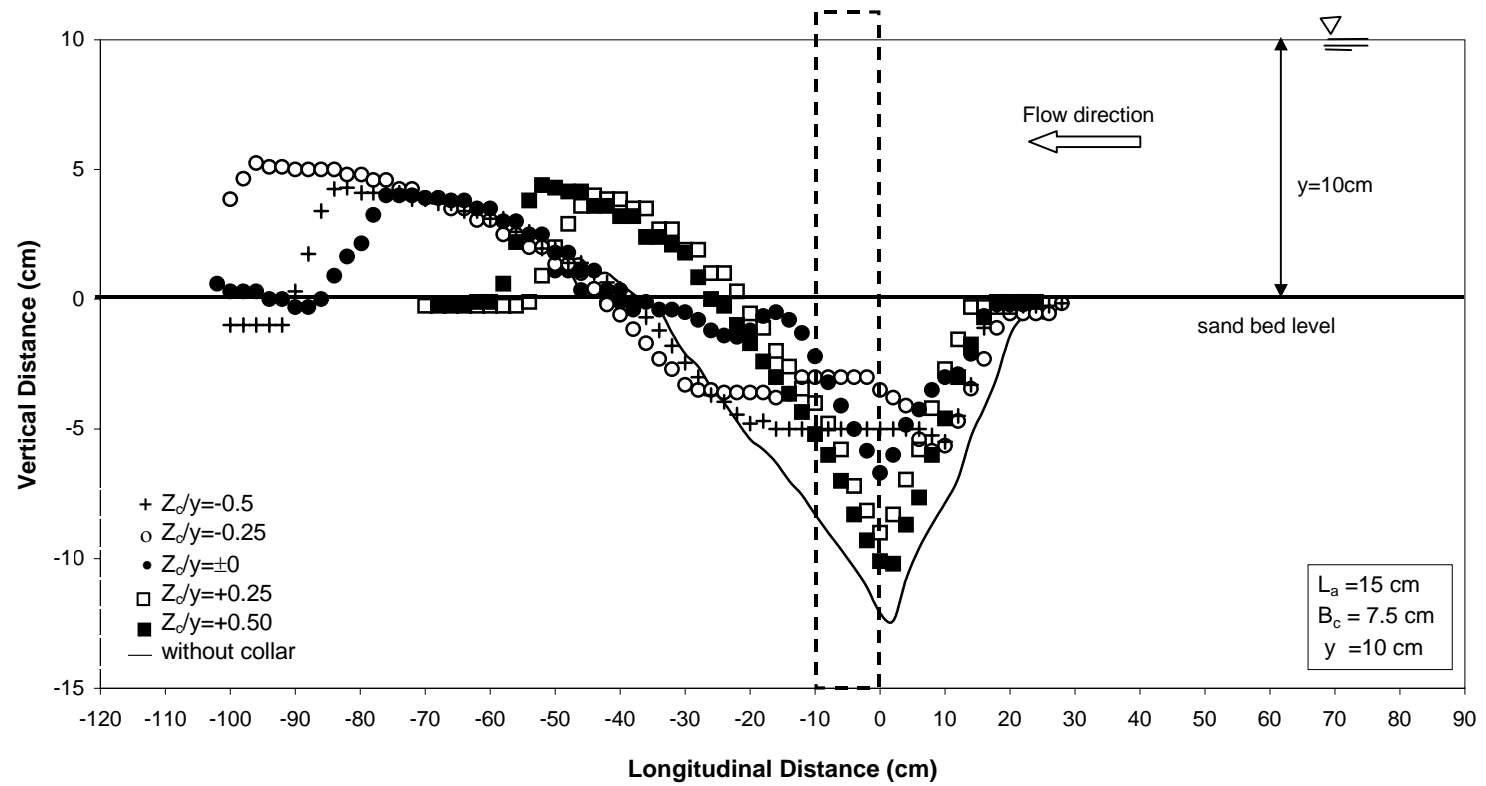
Figure 4.3. Bed profiles around the bridge abutment of $L_a=7.5\text{ cm}$ with and without collars

Figure 4.4.(a) shows the bed profiles at the abutment site for $L_a=15$ cm with $B_c=10$ cm. It can be clearly seen from this figure that, maximum scour depths are in front of the abutment tip and the unprotected case yields the deepest one. At $Z_c/y=-0.50$ and $Z_c/y=-0.25$ mm, bed material are eroded down to the collar levels and scouring process does not continue below the collar levels. When the collar level increases in upward direction, although it still has protecting effect, the maximum scour depth approaches to the value of without-collar case. Eroded sediment deposits at the rear face of the abutment. For the collar of width 7.5 cm, the maximum scour depth is observed below the collar when it is located at $Z_c/y=-0.25$, while no scour occurs below the collar when $Z_c/y=-0.50$ [Fig. 4.4.(b)]. Figs. 4.4.(c) and 4.4.(d) reveal that as the collar width decreases from $B_c=7.5$ cm to 5 cm and than to 2.5 cm, scour penetrates below the collar where ever it is located on the abutment below the bed level.



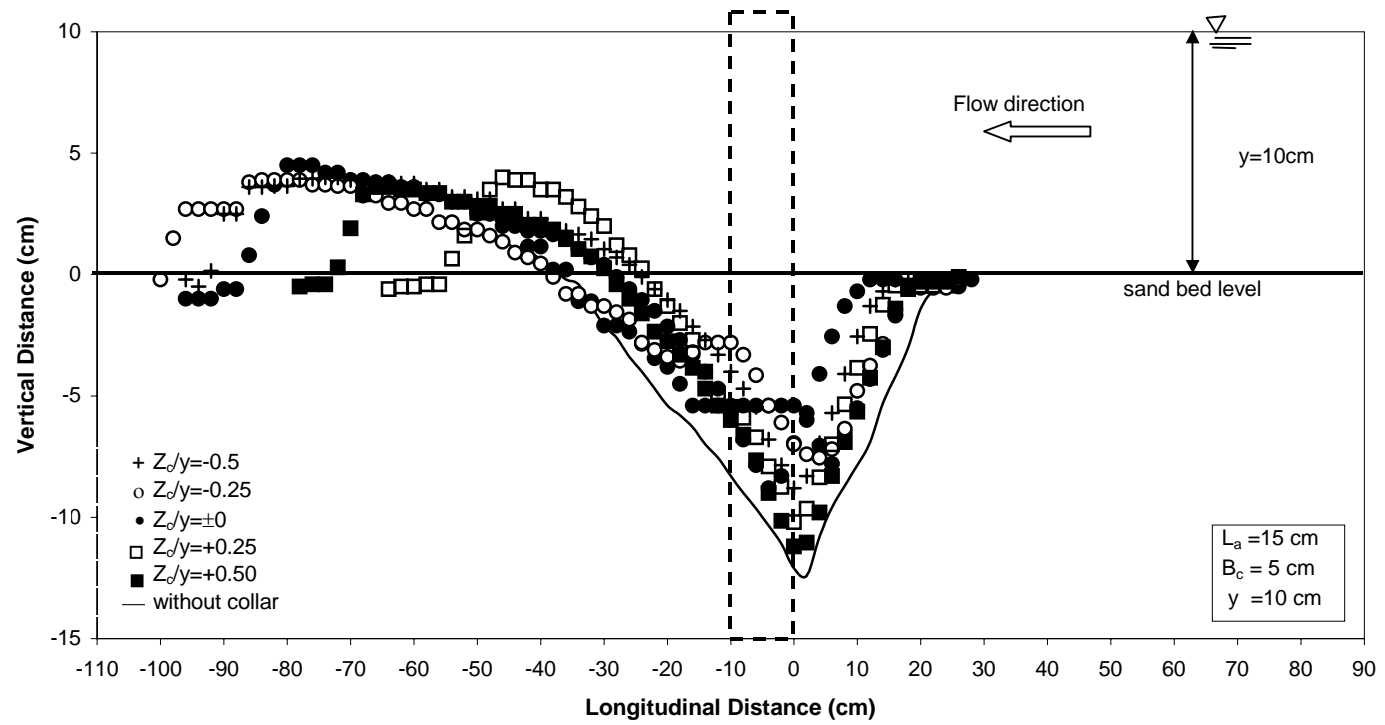
(a) $L_a/B_c = 1.5$

Figure 4.4. Bed profiles around the bridge abutment of $L_a = 15 \text{ cm}$ with and without collars



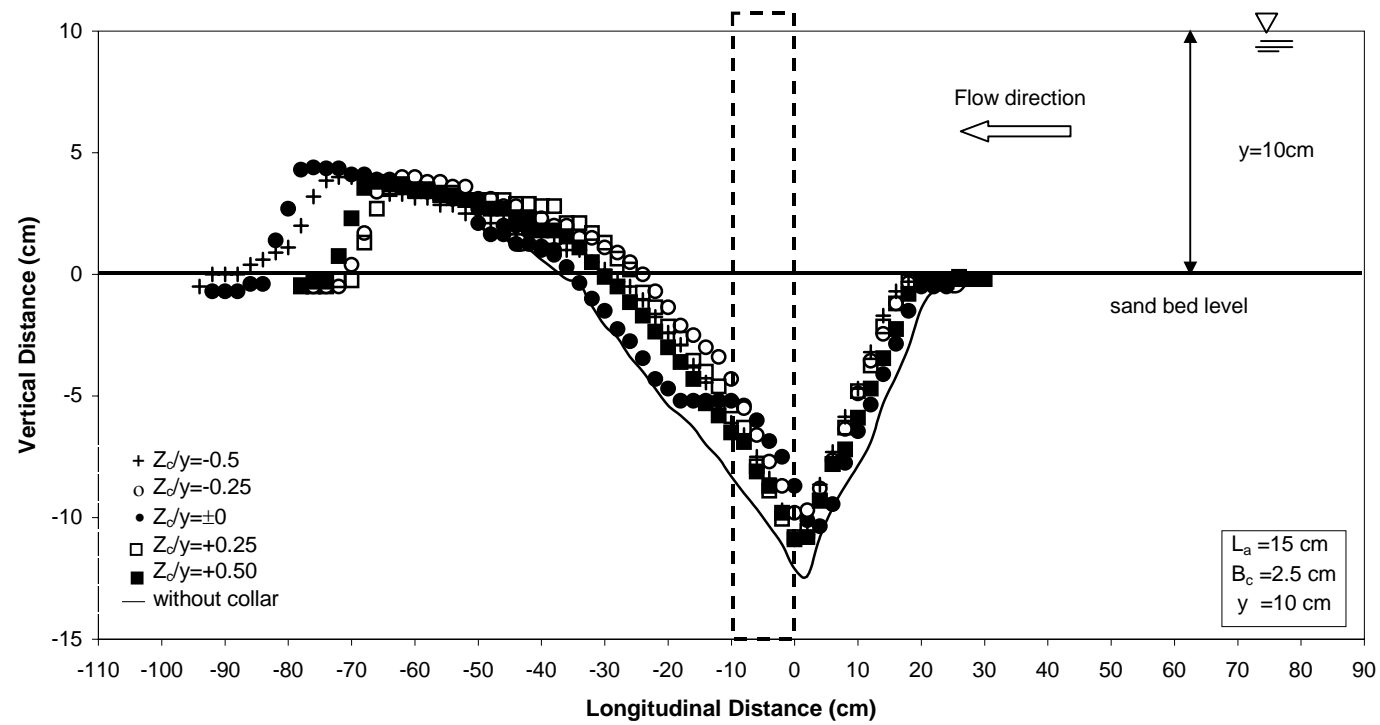
(b) $L_a/B_c = 2.0$

Figure 4.4. Bed profiles around the bridge abutment of $L_a = 15 \text{ cm}$ with and without collars



(c) $L_a/B_c=3.0$

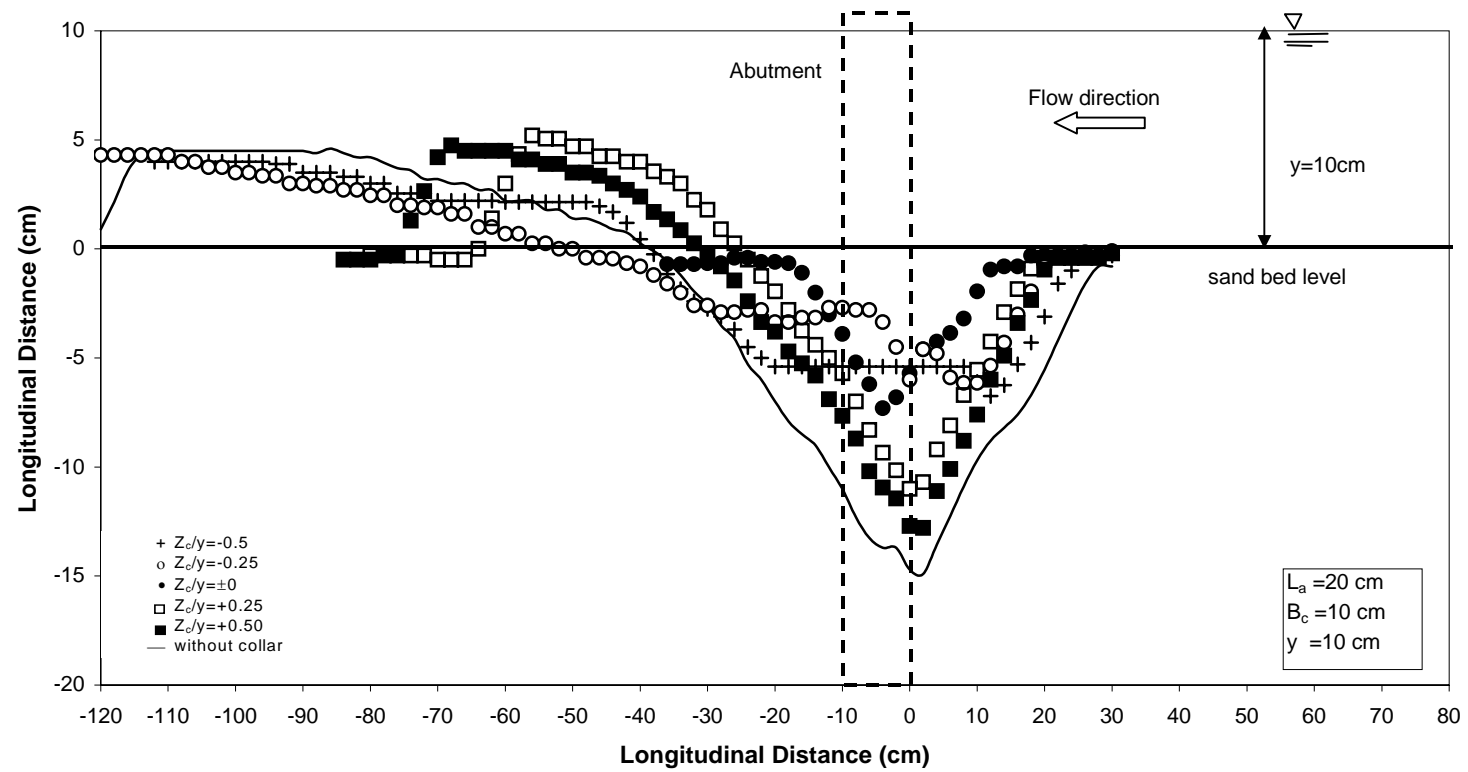
Figure 4.4. Bed profiles around the bridge abutment of $L_a=15\text{ cm}$ with and without collars



(d) $L_a/B_c = 6.0$

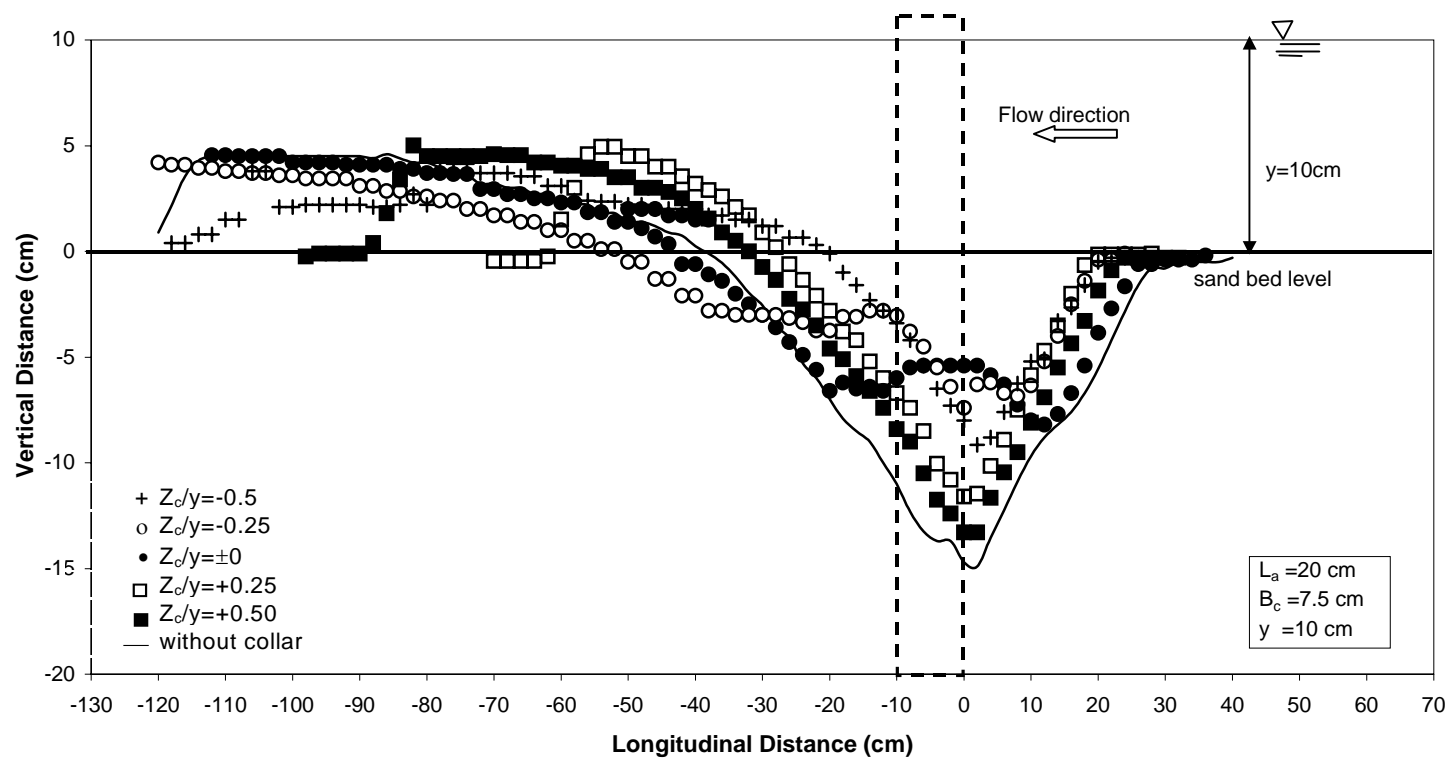
Figure 4.4. Bed profiles around the bridge abutment of $L_a = 15 \text{ cm}$ with and without collars

Bed profiles around the abutment of $L_a=20$ cm without and with collars of different widths, the later located at various elevations are presented in Fig. 4.5. Only for the case of $B_c=10$ cm [Fig. 4.5.(a)], the scour does not penetrate below the collar located at $Z_c/y=-0.50$, which yields the maximum scour reduction among the others compared to the case of no collar. Even though this situation cannot be provided for other collars of B_c less than 10 cm at any of Z_c/y values, maximum scour reduction is attained when the collar is located at $Z_c/y=-0.50$. As the width of the collars decreases, the trend lines of the bed profiles corresponding to Z_c/y values tested get closer to each other.



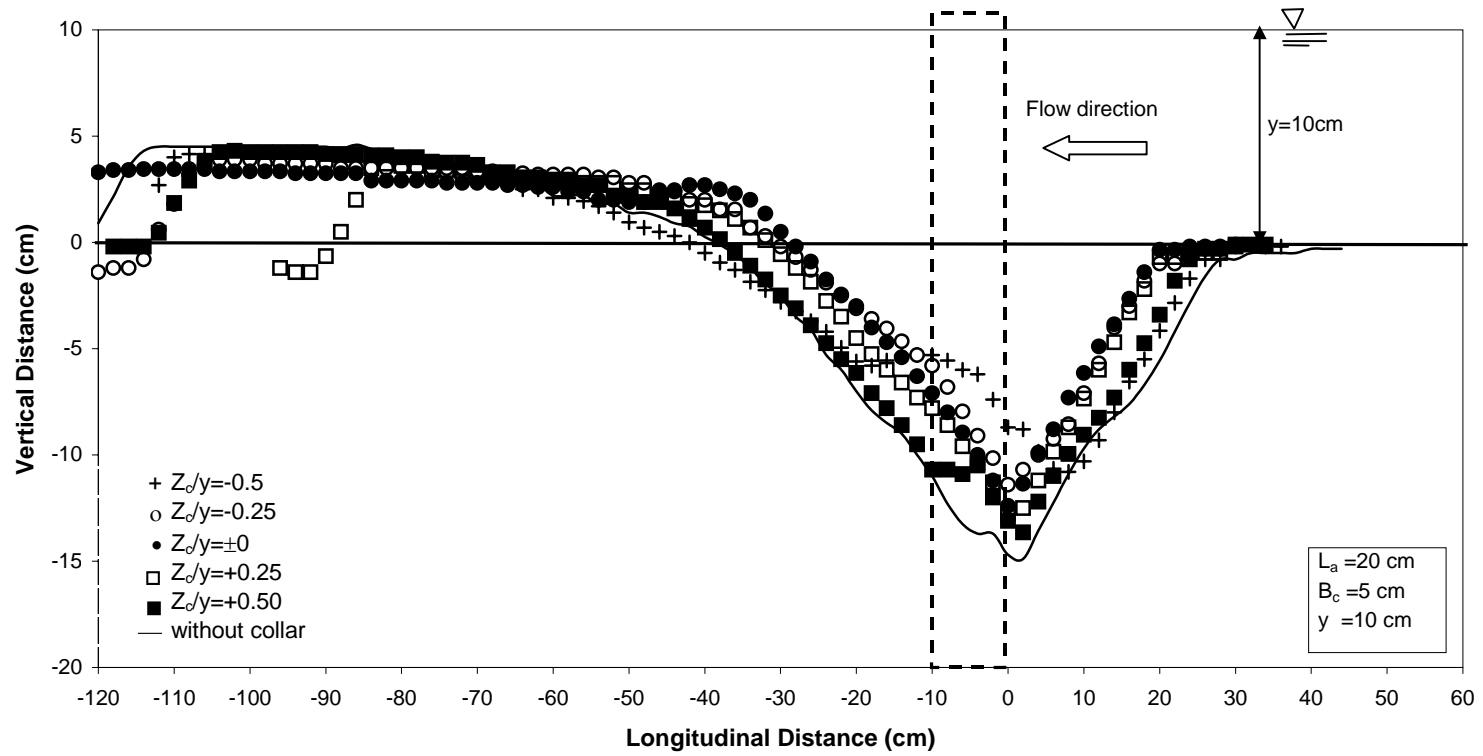
(a) $L_a/B_c=2$

Figure 4.5. Bed profiles around the bridge abutment of $L_a=20 \text{ cm}$ with and without collars



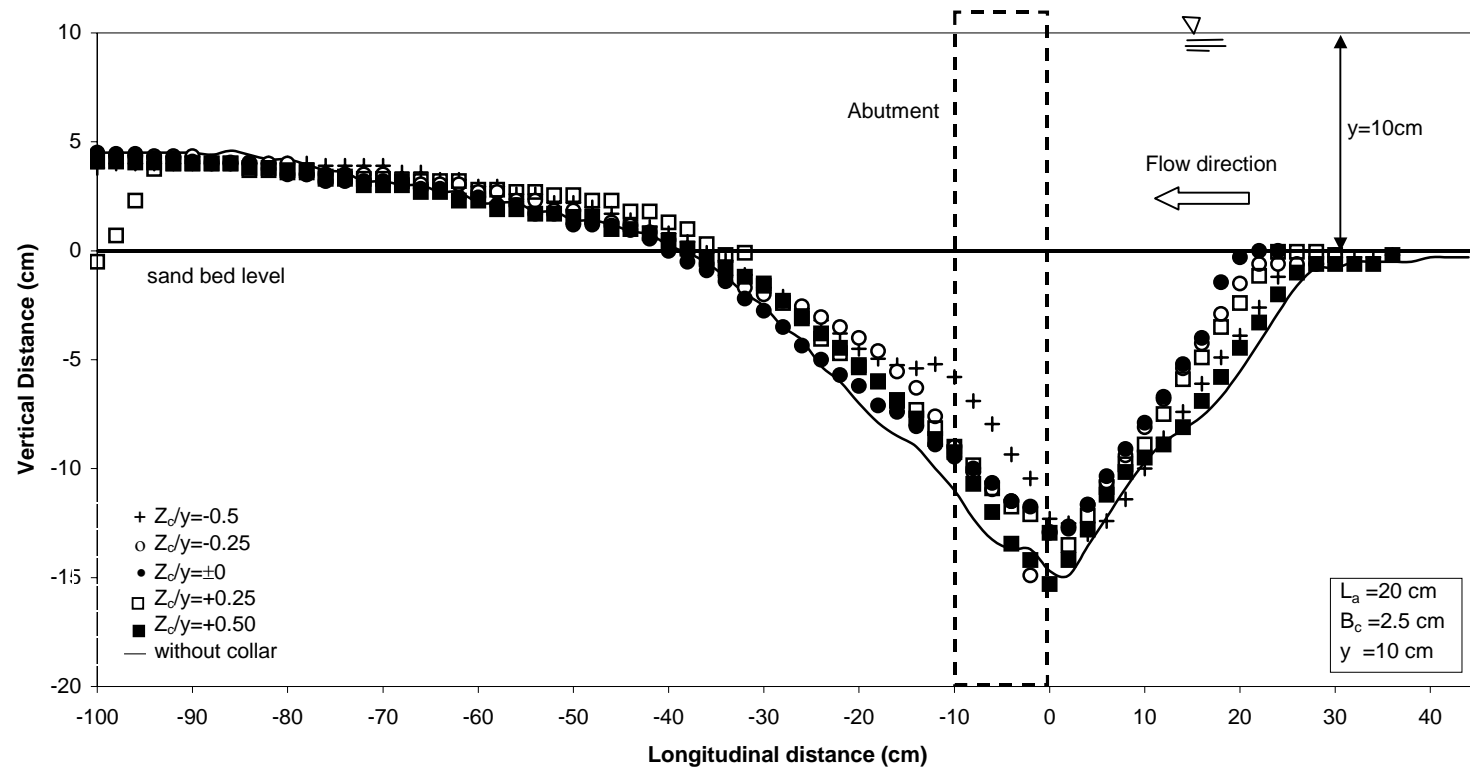
(b) $L_a/B_c = 2.67$

Figure 4.5. Bed profiles around the bridge abutment of $L_a = 20$ cm with and without collars



(c) $L_a/B_c=4.0$

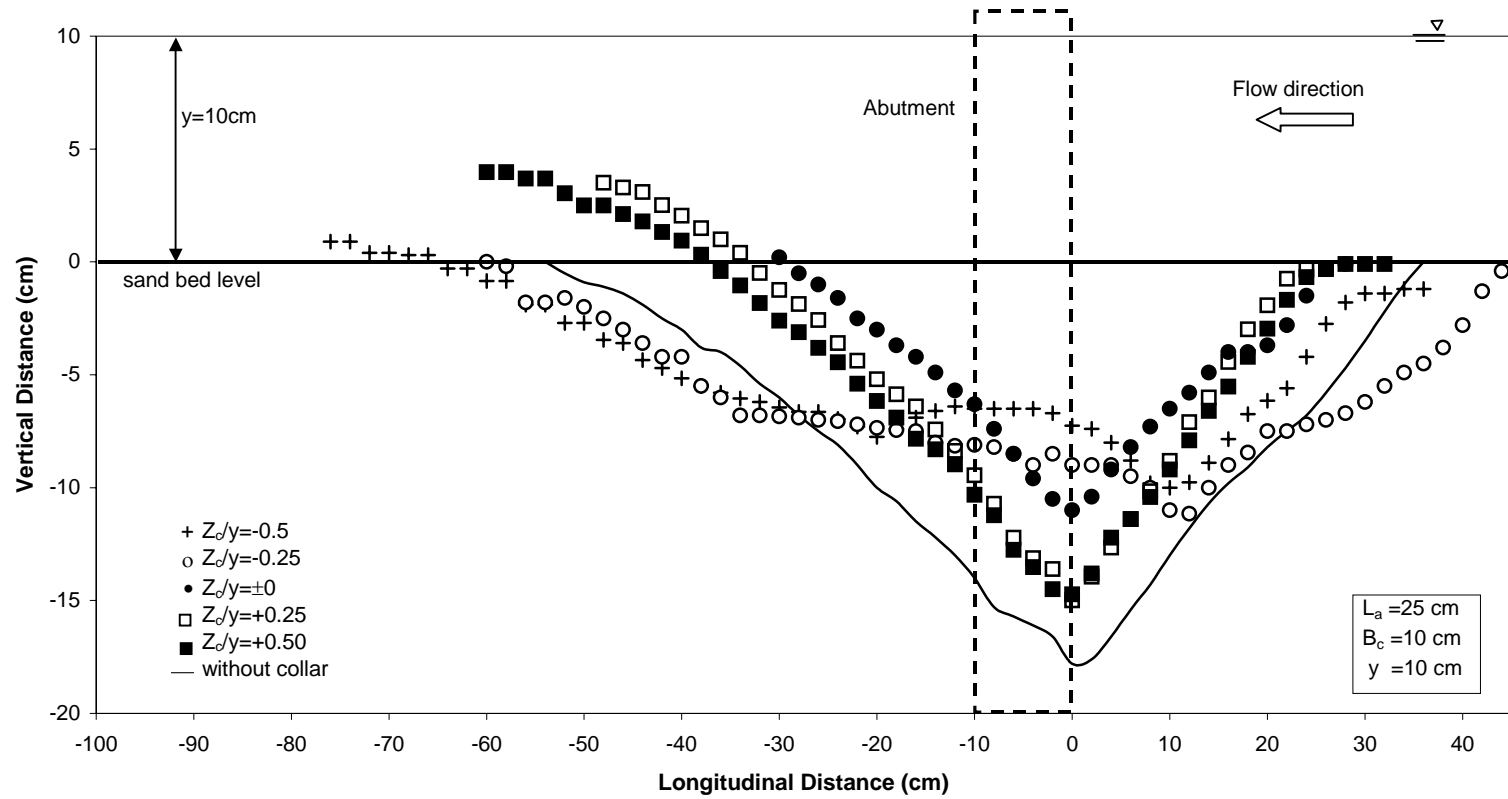
Figure 4.5. Bed profiles around the bridge abutment of $L_a=20\text{ cm}$ with and without collars



(d) $L_a/B_c=8$

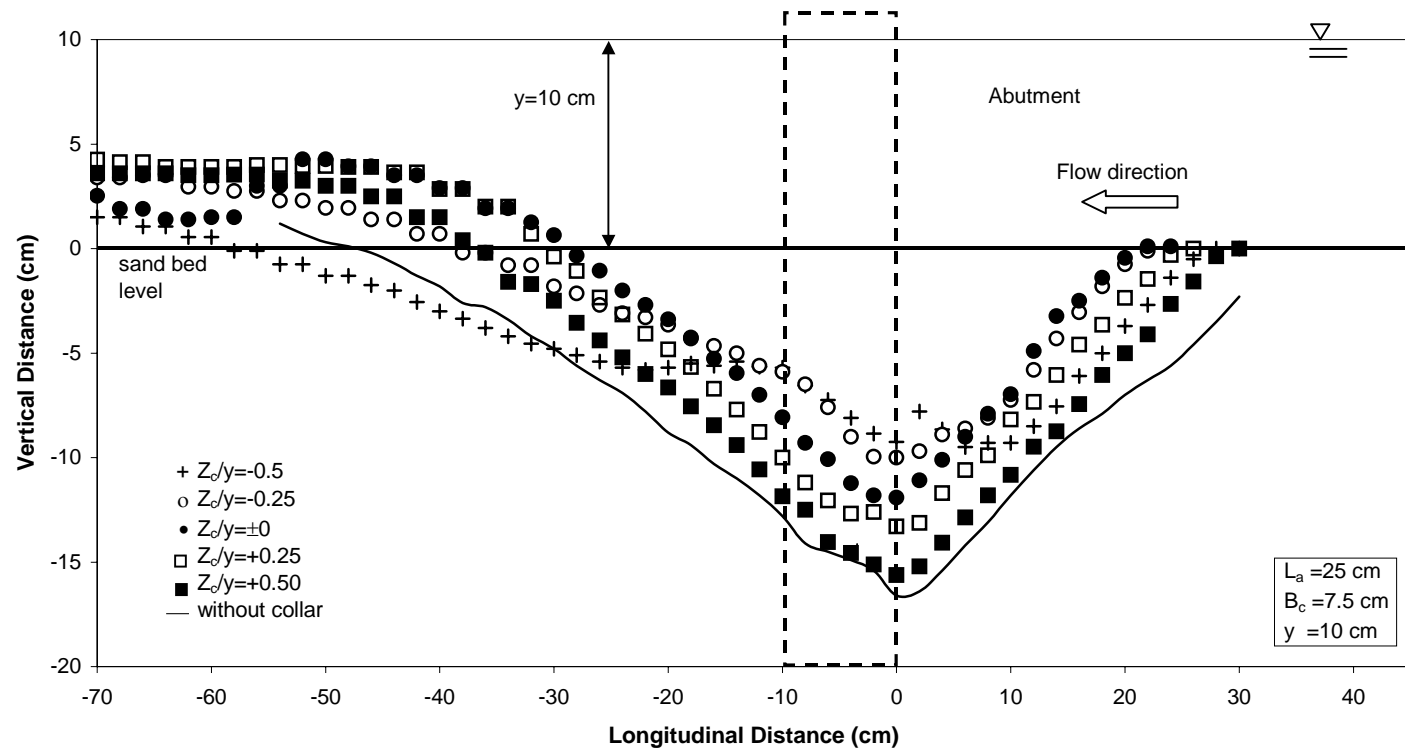
Figure 4.5. Bed profiles around the bridge abutment of $L_a=20\text{ cm}$ with and without collars

Fig. 4.6. shows the bed profiles around the abutment of $L_a=25$ cm with and without collars. When the collar of $B_c=10$ cm is placed around this abutment, the maximum scour reduction of 46 % is obtained for $Z_c/y=-0.50$. This percent value of reduction decreases to about 10% when location of the collar on the abutment increases in upward direction from the bed level. When the collar rounds the abutment at $Z_c/y=\pm 0.00$, this value appears as 37%. If the collar width decreases from $B_c=10$ cm to $B_c=2.5$ cm, from the trends of the bed profiles of each case it can be concluded that the maximum reduction in scour depth is obtained when the collar is located at $Z_c/y=-0.5$. It should also be noted that, as the width of the collars decreases, the gaps between the bed profiles of Z_c/y values tested get smaller, and eventually they coincide with the one of no collar case as seen in Fig. 4.6.(d). This indicates that the smallest collar width tested, $B_c=2.5$ cm, has almost no influence on the reduction of scour depth around the abutment.



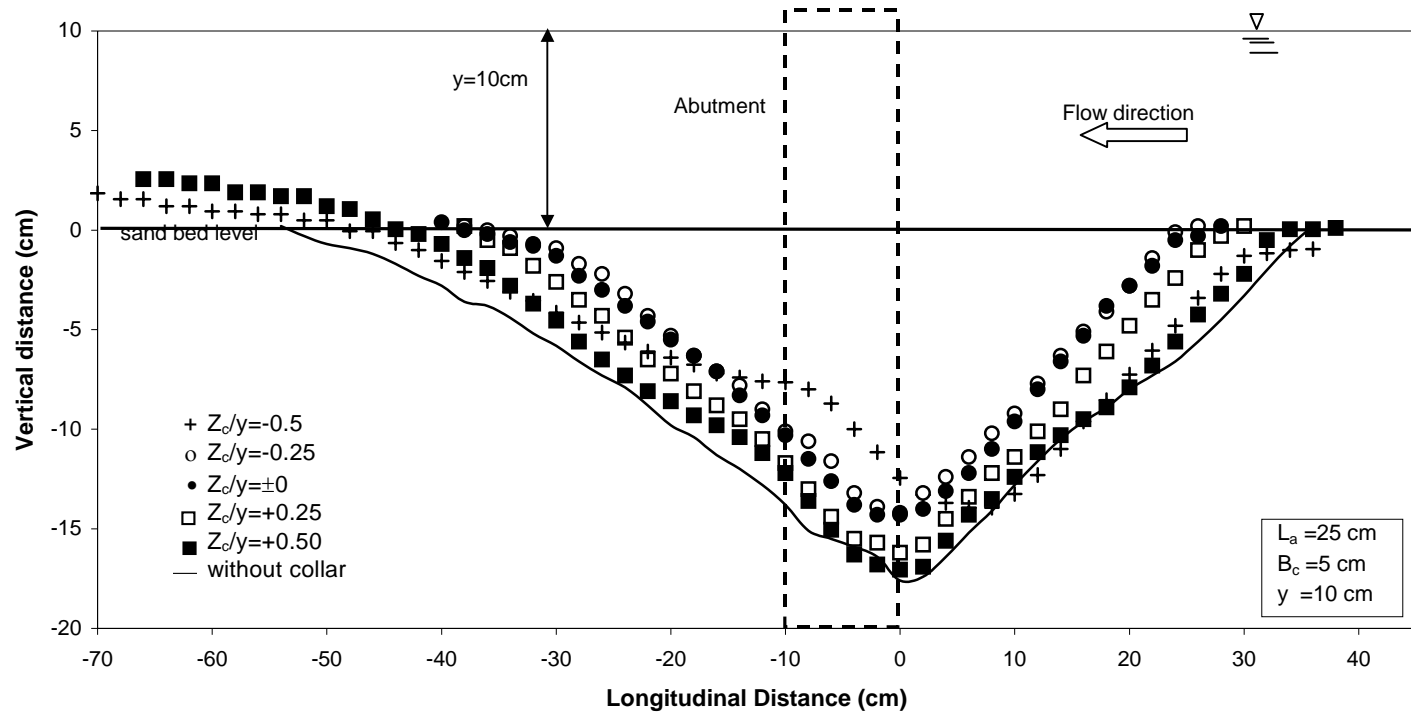
(a) $L_a/B_c=2.5$

Figure 4.6. Bed profiles around the bridge abutment of $L_a=25\text{ cm}$ with and without collars



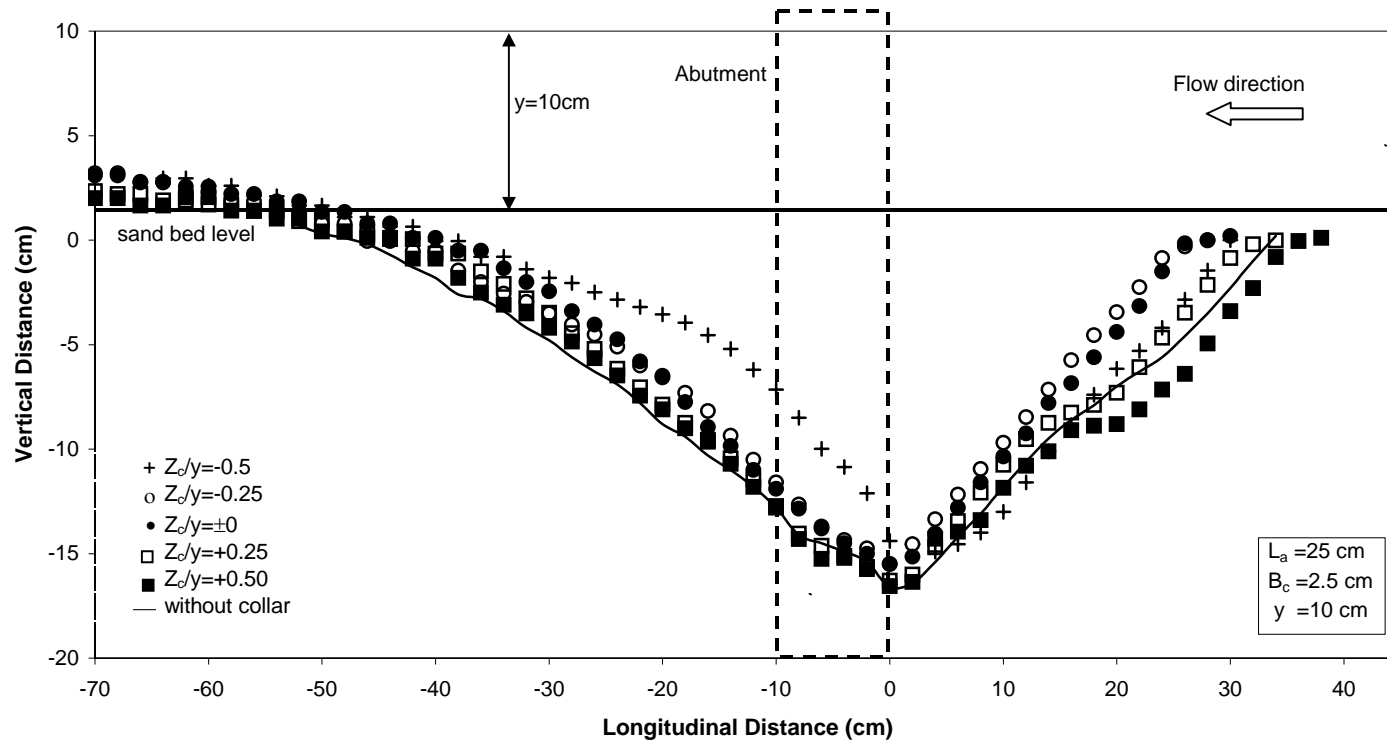
(b) $L_a/B_c=3.33$

Figure 4.6. Bed profiles around the bridge abutment of $L_a=25$ cm with and without collars



(c) $L_a/B_c = 5.0$

Figure 4.6. Bed profiles around the bridge abutment of $L_a = 25 \text{ cm}$ with and without collars

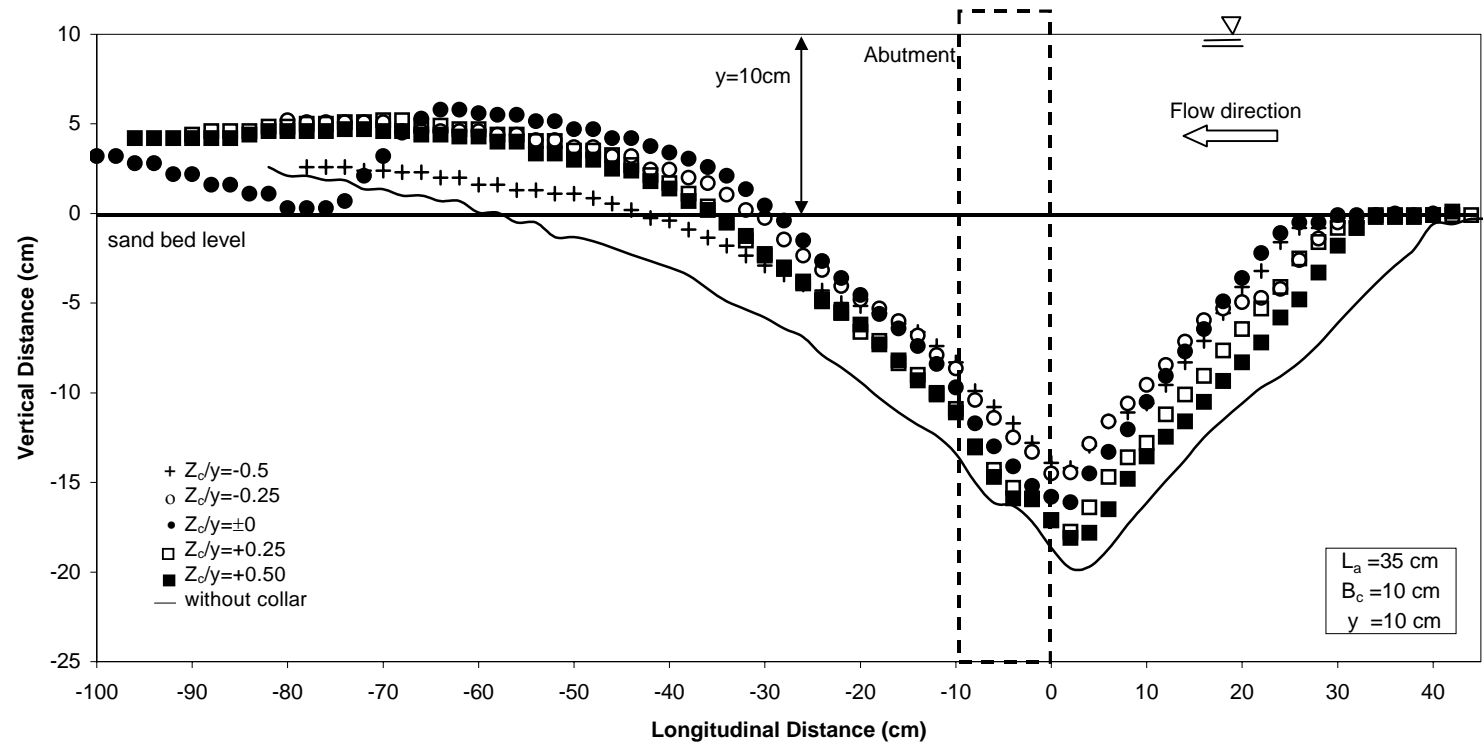


(d) $L_a/B_c=10$

Figure 4.6. Bed profiles around the bridge abutment of $L_a=25\text{ cm}$ with and without collars

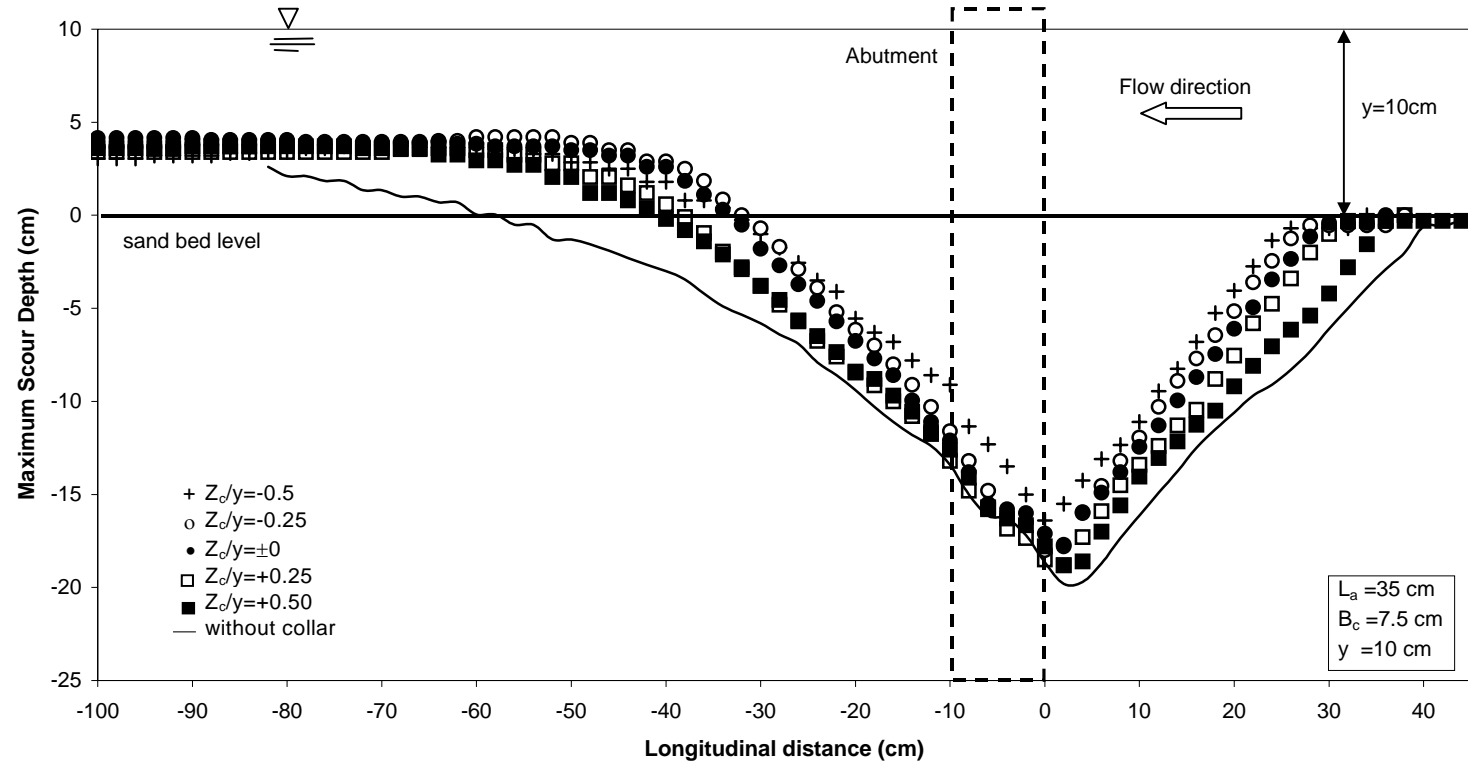
The bed profiles around the longest abutment tested in the experiments, $L_a=35$ cm, are shown in Fig. 4.7. Scour-reducing capacities of the collars for $L_a=35$ cm are not as high as those of smaller abutment lengths. It is obvious that while the ratio of the y/L_a is decreasing for a constant flow depth, degradation around the abutment is increasing due to the increasing contraction ratio of the channel section. Moreover, the efficiency of the collars also decreases as their widths decrease. For each collar tested in this group the one having the value of $Z_c/y=-0.50$ gave their highest scour depth reduction percent; 27.8% for $B_c=10$ cm, 12.4% for $B_c=7.5$ cm, 2.9% for $B_c=5$ cm and 1% for $B_c=2.5$ cm.

Figure 4.8-4.11 show some photographs of the experimental set-ups and bed profiles obtained after the experiments.



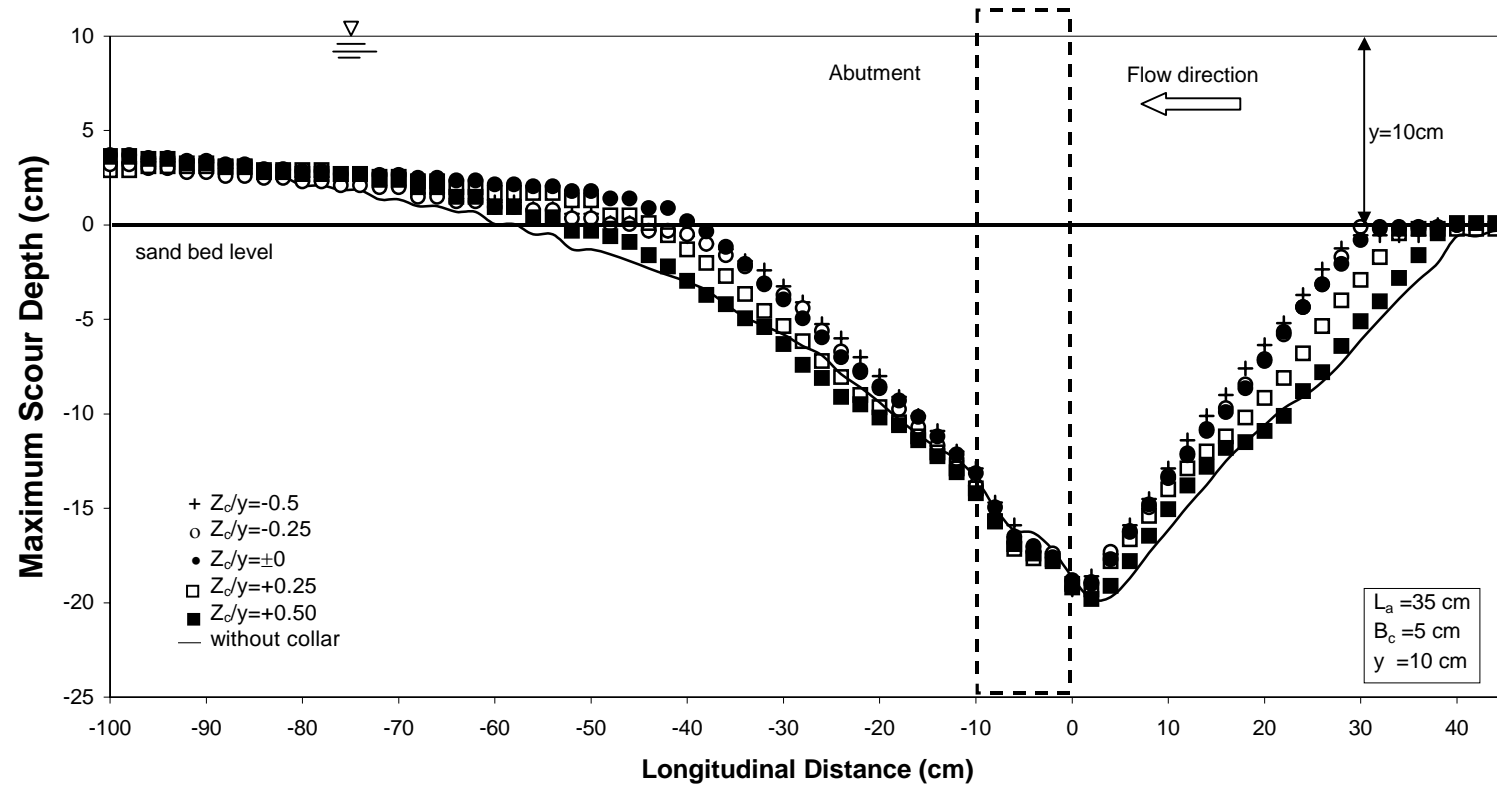
(a) $L_a/B_c=3.5$

Figure 4.7. Bed profiles around the bridge abutment of $L_a=35\text{ cm}$ with and without collars



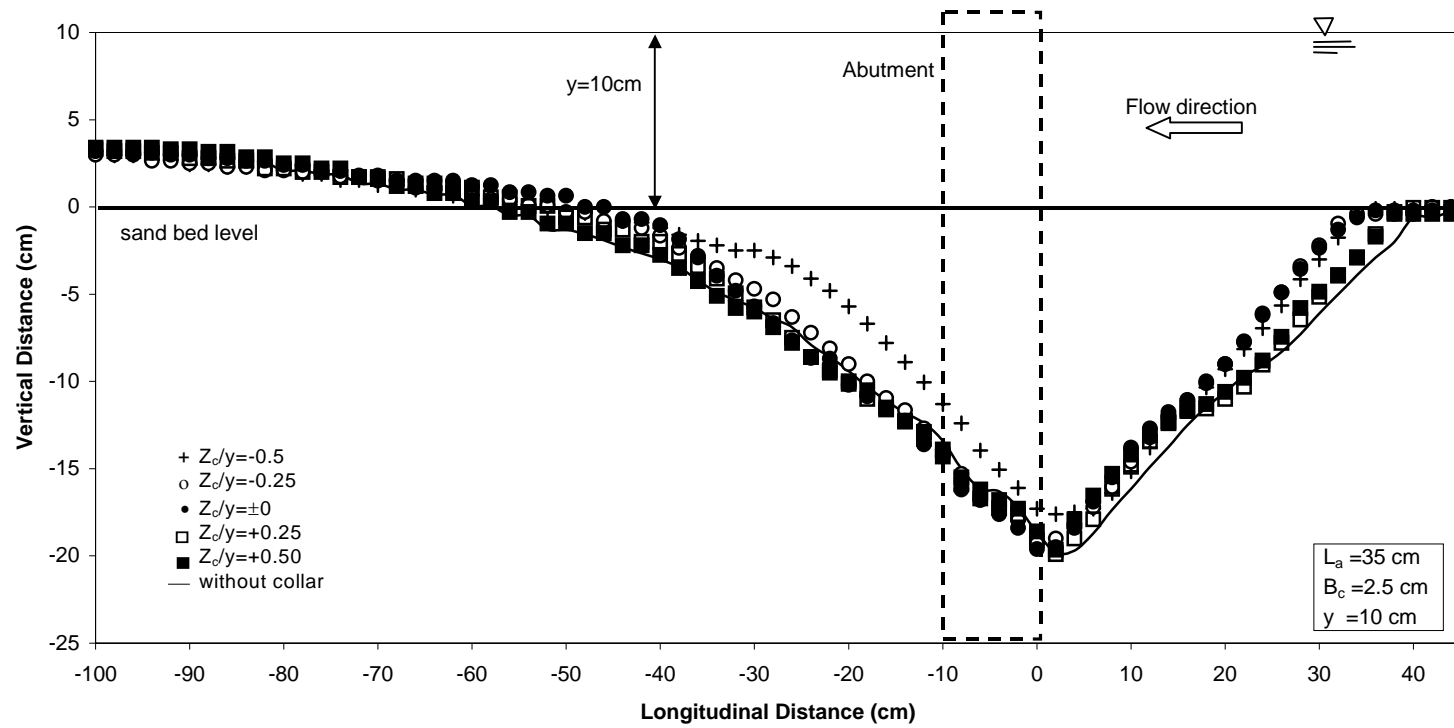
(b) $L_a/B_c=4.67$

Figure 4.7. Bed profiles around the bridge abutment of $L_a=35\text{ cm}$ with and without collars



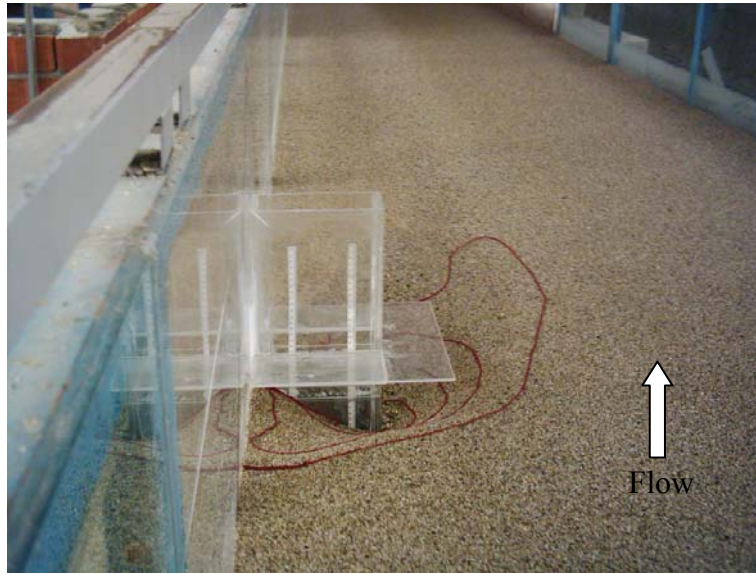
(c) $L_a/B_c=7.0$

Figure 4.7. Bed profiles around the bridge abutment of $L_a=35\text{ cm}$ with and without collars

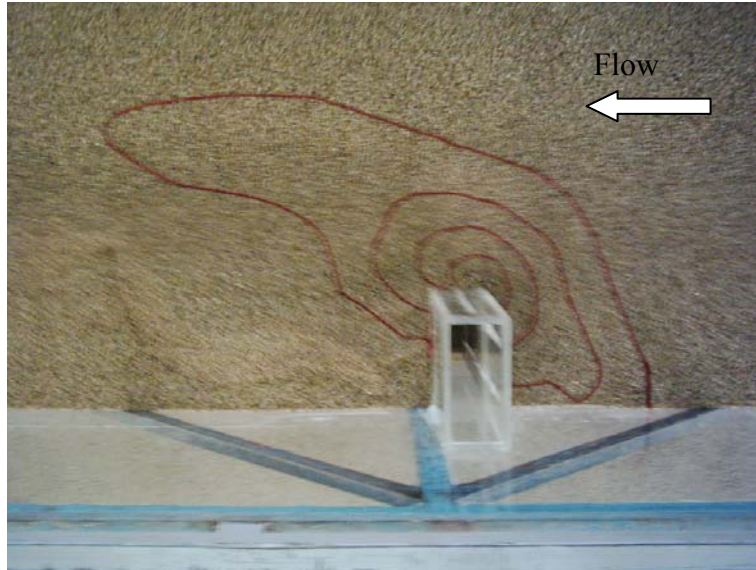


(d) $L_a/B_c=14$

Figure 4.7. Bed profiles around the bridge abutment of $L_a=35\text{ cm}$ with and without collars

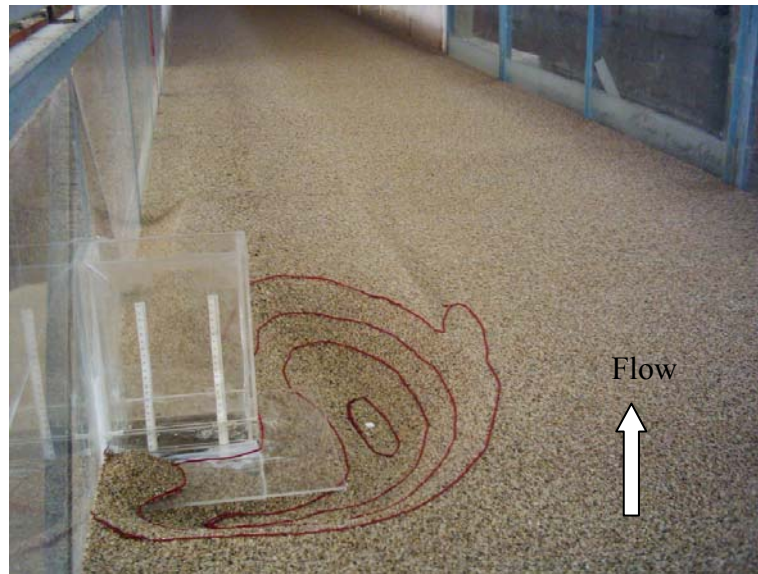


a) Upstream view

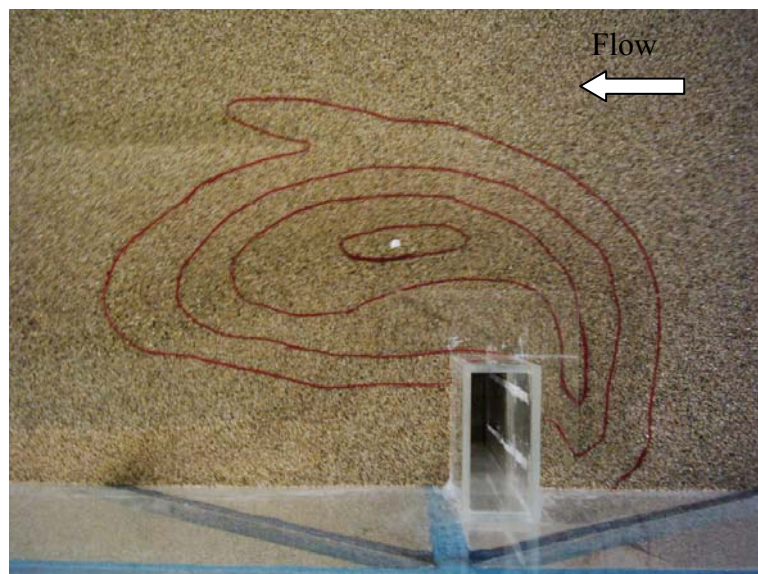


b) Top view

Figure 4.8. Abutment-collar arrangement and scour hole
($L_a=20$ cm, $Z_c=+5$ cm, $B_c=10$ cm)

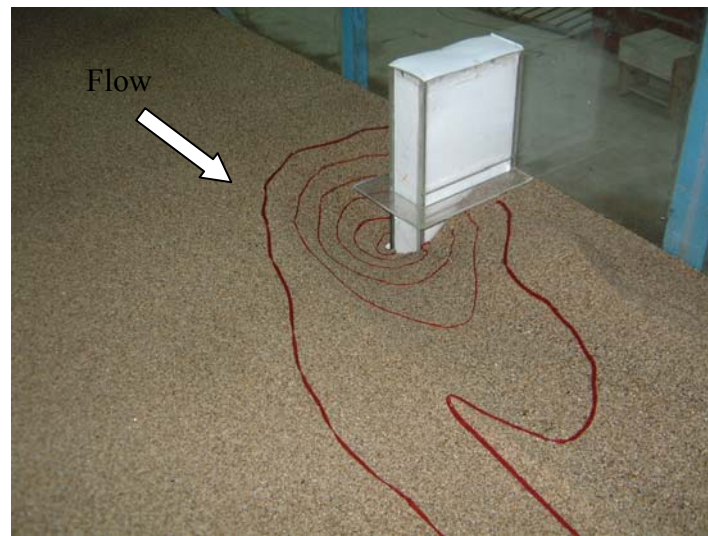


a) Upstream view

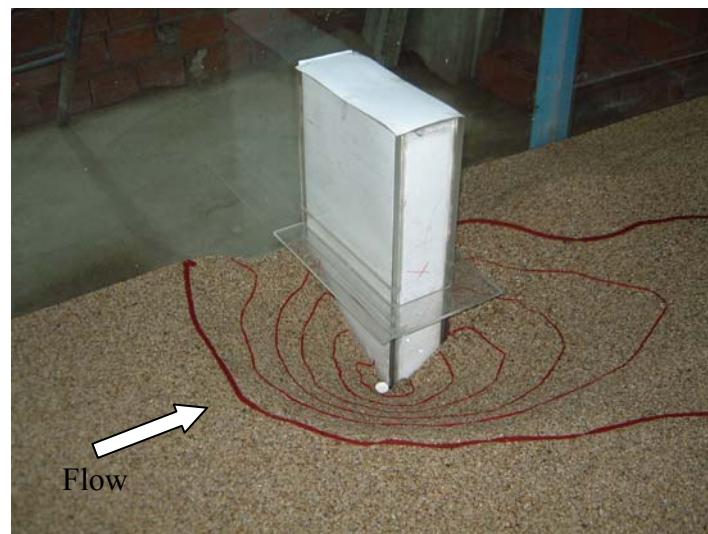


b) Top view

Figure 4.9. Abutment-collar arrangement and scour hole
 ($L_a=20$ cm, $Z_c=-5$ cm, $B_c=10$ cm)

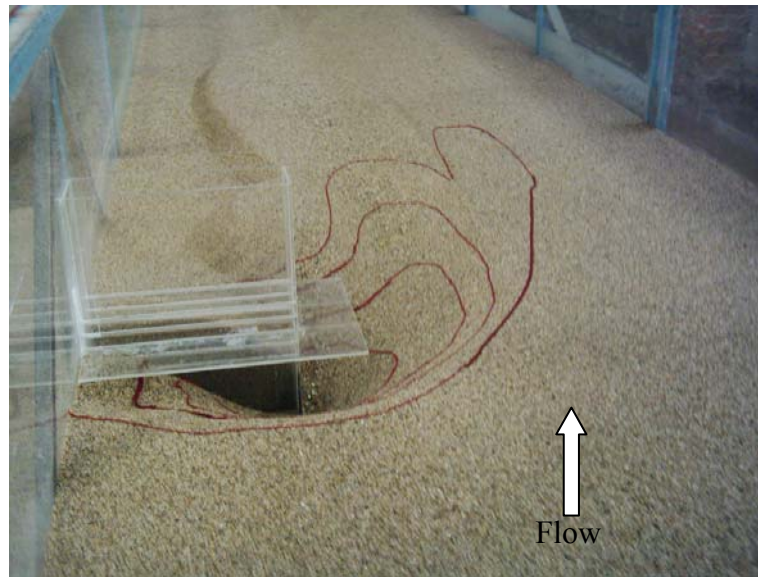


a) Downstream view

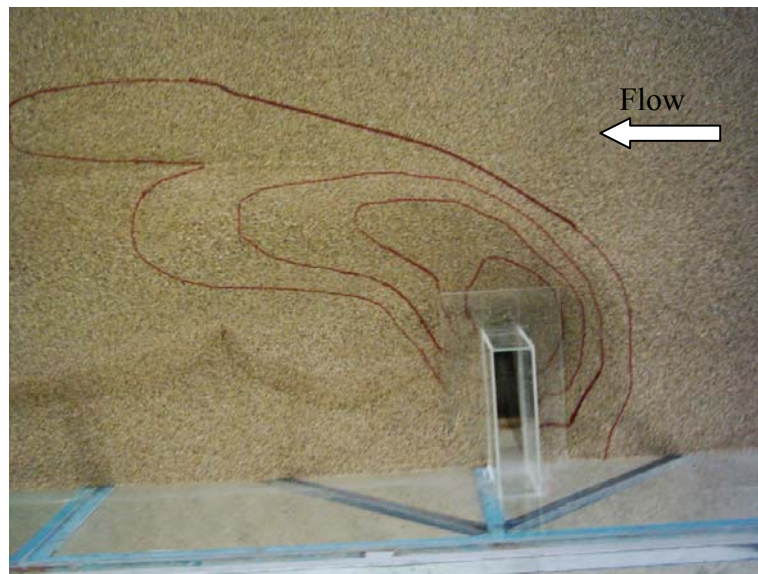


b) Upstream view

Figure 4.10. Abutment-collar arrangement and scour hole
 ($L_a=25$ cm, $Z_c=\pm 0.0$ cm, $B_c=5$ cm)



a) Upstream view



b) Top view

Figure 4.11. Abutment-collar arrangement and scour hole
 ($L_a=35$ cm, $Z_c=\pm 0.0$ cm, $B_c=10$ cm)

4.6.2 Maximum Scour Reductions Around the Abutments with Collars

The total number of the experiments conducted; with abutments of lengths: $L_a=7.5$ cm, 15 cm, 20 cm, 25 cm and 35 cm, collars of widths: $B_c=2.5$ cm, 5.0 cm, 7.5 cm and 10 cm, and finally collar locations of $Z_c=-5$ cm, -2.5 cm, ± 0.0 cm, 2.5 cm and 5.0 cm is 100. Bed profiles obtained at the end of these experiments, each conducted for a period of 6-hours, were given in the previous section. Referring to these bed profiles maximum scour depths around the abutments for each experiment were determined. Table 4.2 lists the experimental data to show the maximum scour depths around the abutments with and without collar conditions. In this table, $(d_s)_{\max}$ depicts the maximum scour depth around the abutment which has no collar around it, and $(d_s)_{\max_c}$ depicts the maximum scour depth around the abutment protected by a collar. The last column of the table shows the percent reduction of the maximum scour depth when the collar is used.

Figure 4.12 summarizes the overall effect of abutment length, collar width and the location of the collar on the reduction of maximum scour depth. Each line given in the figure corresponds to a constant L_a/B_c value. L_a/B_c values are stated on the figures. At small values of L_a/B_c which is less than about 2.0, maximum reductions in scour depths are mainly obtained when the collars are located at the bed level, $Z_c/y=0.0$. For greater values of L_a/B_c , maximum reduction in scour depths are mostly observed when the collars have the value of $Z_c/y=-0.50$. This figure also clearly prevails that scour reduction capacity of a collar increases as the width of the collar increases, and decreases with increasing abutment length. Collars are generally more effective in reducing the scour depth around the abutment when they are located below the sand bed, $-0.50 < Z_c/y < -0.25$, compared to the cases of above the sand

bed, $0.0 < Z_c/y < 0.50$, for the value of $L_a/B_c > 2.0$. Trend lines of data points in Fig. 4.12 also imply that at Z_c/y values less than -0.50 , higher reductions in the maximum scour depths around the abutments can be obtained than those given in the figure for $Z_c/y = -0.50$. For design purposes when the optimum value of Z_c/y is required, the one close to the bed level but having adequate scour reduction capacity should be selected.

From Table 4.2, for each abutment length and collar width tested, the location of the collar which results in the maximum reduction in the scour depth is selected and presented in Table 4.3 along with the corresponding values of $[(d_s)_{max_c} / y]_{opt}$ and $[Z_c / y]_{opt}$. In this table, θ depicts ratio of the total area of the abutment and collar to the abutment area on horizontal plane. That is:

$$\theta = \frac{L_c B_t}{L_a B_a} = \frac{A_{total}}{A_{abutment}} \quad (5)$$

θ , simply shows how big the collar is when compared to the area of the abutment.

Table 4.2. Experimental data for $Q=0.05 \text{ m}^3/\text{s}$, $y=10 \text{ cm}$ and $B_a=10 \text{ cm}$

Run no	L_a (cm)	B_c (cm)	Z_c (cm)	$(d_s)_{\max}$ (cm)	$(d_s)_{\max_c}$ (cm)	% Reduction in max. scour depth
R1	7.5	2.5	-5.0	5.3	5	5.6
R2	7.5	2.5	-2.5	5.3	4	24.5
R3	7.5	2.5	± 0.0	5.3	4.9	7.5
R4	7.5	2.5	2.5	5.3	5.2	1.8
R5	7.5	2.5	5.0	5.3	5.3	0
R6	7.5	5	-5.0	5.3	5	5.6
R7	7.5	5	-2.5	5.3	2.5	52.8
R8	7.5	5	± 0.0	5.3	1.2	77.3
R9	7.5	5	2.5	5.3	4.5	15.0
R10	7.5	5	5.0	5.3	5.2	1.9
R11	7.5	7.5	-5.0	5.3	5	5.6
R12	7.5	7.5	-2.5	5.3	2.5	52.8
R13	7.5	7.5	± 0.0	5.3	0.5	90.5
R14	7.5	7.5	2.5	5.3	4.15	21.7
R15	7.5	7.5	5.0	5.3	5.3	0
R16	7.5	10	-5.0	5.3	5	5.6
R17	7.5	10	-2.5	5.3	2.5	52.8
R18	7.5	10	± 0.0	5.3	0.0	100.0
R19	7.5	10	2.5	5.3	3.2	39.6
R20	7.5	10	5.0	5.3	5.3	0
R21	15	2.5	-5.0	12.6	9.7	23.0
R22	15	2.5	-2.5	12.6	10.6	15.8
R23	15	2.5	± 0.0	12.6	11.3	10.3
R24	15	2.5	2.5	12.6	11.4	9.5
R25	15	2.5	5.0	12.6	11.5	8.7

Table 4.2. Experimental data for $Q=0.05 \text{ m}^3/\text{s}$, $y=10 \text{ cm}$ and $B_a=10 \text{ cm}$ (continued)

Run no	L_a (cm)	B_c (cm)	Z_c (cm)	$(d_s)_{\max}$ (cm)	$(d_s)_{\max_c}$ (cm)	% Reduction in max. scour depth
R26	15	5	-5.0	12.6	5	60.3
R27	15	5	-2.5	12.6	7.5	40.4
R28	15	5	± 0.0	12.6	9.4	25.3
R29	15	5	2.5	12.6	10.8	14.2
R30	15	5	5.0	12.6	11.8	6.3
R31	15	7.5	-5.0	12.6	5	60.3
R32	15	7.5	-2.5	12.6	2.5	80.1
R33	15	7.5	± 0.0	12.6	7.2	42.8
R34	15	7.5	2.5	12.6	9.6	23.8
R35	15	7.5	5.0	12.6	11.1	11.9
R36	15	10	-5.0	12.6	5	60.3
R37	15	10	-2.5	12.6	2.5	80.1
R38	15	10	± 0.0	12.6	1.8	85.7
R39	15	10	2.5	12.6	8.5	32.5
R40	15	10	5.0	12.6	10.6	15.8
R41	20	2.5	-5.0	15.3	12.9	15.6
R42	20	2.5	-2.5	15.3	13.8	9.8
R43	20	2.5	± 0.0	15.3	14	8.4
R44	20	2.5	2.5	15.3	13.8	9.8
R45	20	2.5	5.0	15.3	15.3	0
R46	20	5	-5.0	15.3	9.6	37.2
R47	20	5	-2.5	15.3	12.1	20.9
R48	20	5	± 0.0	15.3	12.8	16.3
R49	20	5	2.5	15.3	13.6	11.1
R50	20	5	5.0	15.3	14.2	7.1

Table 4.2. Experimental data for $Q=0.05 \text{ m}^3/\text{s}$, $y=10 \text{ cm}$ and $B_a=10 \text{ cm}$ (continued)

Run no	L_a (cm)	B_c (cm)	Z_c (cm)	$(d_s)_{\max}$ (cm)	$(d_s)_{\max_c}$ (cm)	% Reduction in max. scour depth
R51	20	7.5	-5.0	15.3	6	61
R52	20	7.5	-2.5	15.3	8.2	46.4
R53	20	7.5	± 0.0	15.3	10.1	33.9
R54	20	7.5	2.5	15.3	12.5	18.3
R55	20	7.5	5.0	15.3	14.3	6.5
R56	20	10	-5.0	15.3	5	67.3
R57	20	10	-2.5	15.3	6.3	58.8
R58	20	10	± 0.0	15.3	8	47.7
R59	20	10	2.5	15.3	12	33.0
R60	20	10	5.0	15.3	13.5	11.7
R61	25	2.5	-5.0	18.3	14.7	19.6
R62	25	2.5	-2.5	18.3	16	12.5
R63	25	2.5	± 0.0	18.3	16.3	10.9
R64	25	2.5	2.5	18.3	17.2	6.0
R65	25	2.5	5.0	18.3	17.5	4.3
R66	25	5	-5.0	18.3	11.9	34.9
R67	25	5	-2.5	18.3	15	18.0
R68	25	5	± 0.0	18.3	15.4	15.8
R69	25	5	2.5	18.3	16.7	8.7
R70	25	5	5.0	18.3	17.3	5.4
R71	25	7.5	-5.0	18.3	9.8	46.4
R72	25	7.5	-2.5	18.3	10.8	40.9
R73	25	7.5	± 0.0	18.3	12.8	30.0
R74	25	7.5	2.5	18.3	14.6	20.2
R75	25	7.5	5.0	18.3	16.4	10.3

Table 4.2. Experimental data for $Q=0.05 \text{ m}^3/\text{s}$, $y=10\text{cm}$ and $B_a=10 \text{ cm}$ (continued)

Run no	L_a (cm)	B_c (cm)	Z_c (cm)	$(d_s)_{\max}$ (cm)	$(d_s)_{\max_c}$ (cm)	% Reduction in max. scour depth
R76	25	10	-5.0	18.3	5	72.7
R77	25	10	-2.5	18.3	8.4	54.0
R78	25	10	± 0.0	18.3	10	45.3
R79	25	10	2.5	18.3	14	23.4
R80	25	10	5.0	18.3	15.4	15.8
R81	35	2.5	-5.0	20.1	19.9	1.0
R82	35	2.5	-2.5	20.1	19.9	1.0
R83	35	2.5	± 0.0	20.1	19.9	1.0
R84	35	2.5	2.5	20.1	20	0.5
R85	35	2.5	5.0	20.1	20	0.5
R86	35	5	-5.0	20.1	19.5	2.9
R87	35	5	-2.5	20.1	19.6	2.4
R88	35	5	± 0.0	20.1	20	0.5
R89	35	5	2.5	20.1	20	0.5
R90	35	5	5.0	20.1	20	0.5
R91	35	7.5	-5.0	20.1	17.6	12.4
R92	35	7.5	-2.5	20.1	19.6	2.4
R93	35	7.5	± 0.0	20.1	19.7	1.9
R94	35	7.5	2.5	20.1	20	0.5
R95	35	7.5	5.0	20.1	20	0.5
R96	35	10	-5.0	20.1	14.5	27.8
R97	35	10	-2.5	20.1	15.1	24.8
R98	35	10	± 0.0	20.1	17	15.4
R99	35	10	2.5	20.1	18.2	9.4
R100	35	10	5.0	20.1	18.5	7.9

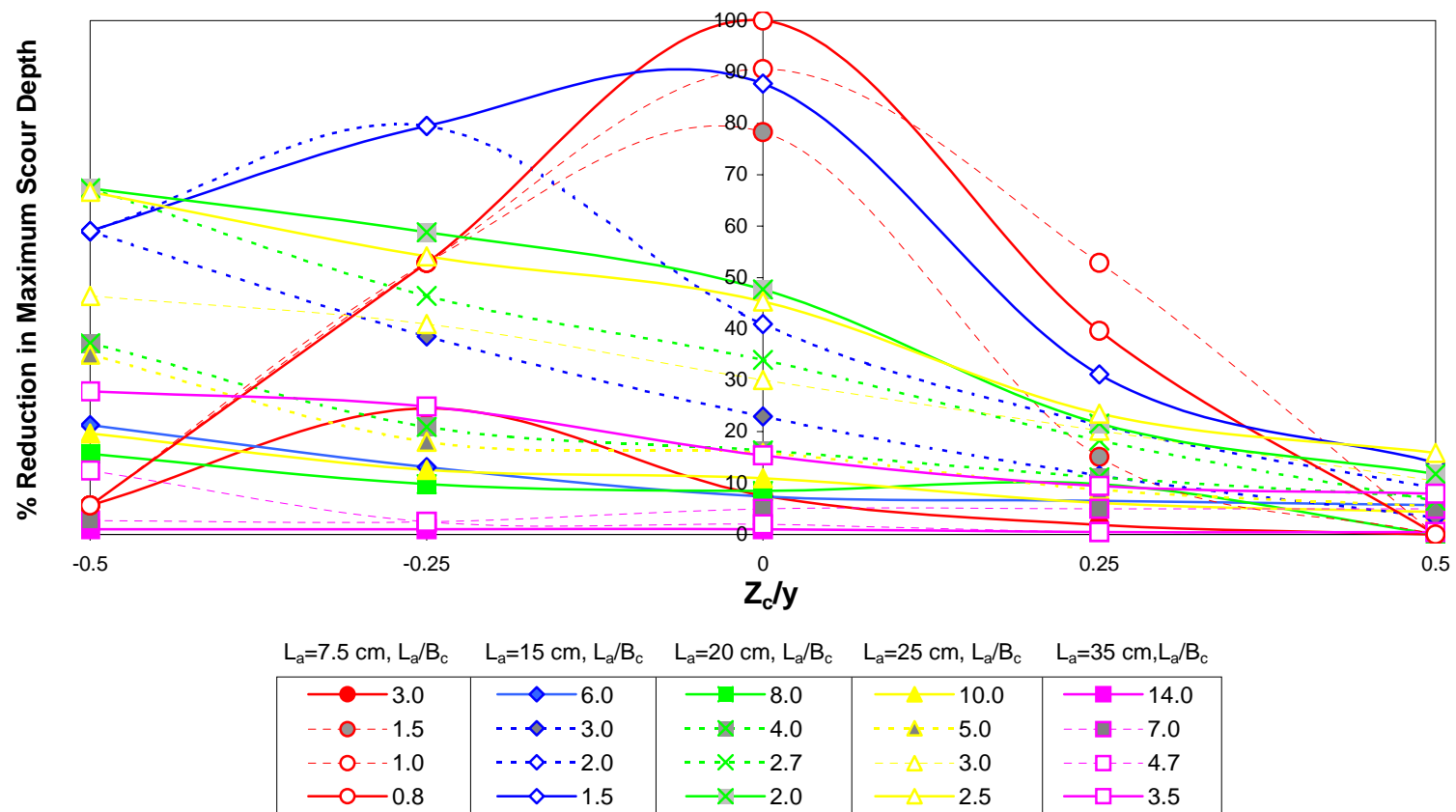


Figure 4.12. Effect of collar size and elevation on the maximum scour depth around the abutments of various lengths ($Q=0.05 \text{ m}^3/\text{s}$, $y=10 \text{ cm}$)

Table 4.3. Optimum design parameters of an abutment-collar arrangement

L_a/B_a	L_a/B_c	θ ($A_{total}/A_{abutment}$)	$[Z_c/y]_{opt}$	$[(d_s)_{max_c}/y]_{opt}$	$[\%Reduction]_{opt}$
0.75	3	2	-0.25	0.40	24.5
	1.5	3.33	0.00	0.12	77.3
	1	5	0.00	0.05	90.5
	0.75	7	0.00	0	100
1.5	6	1.75	-0.50	0.97	23
	3	2.67	-0.50	0.50	60
	2	3.75	-0.25	0.25	80
	1.5	5	0.00	0.18	86
2	8	1.69	-0.50	1.29	16
	4	2.5	-0.50	0.96	37
	2.67	3.44	-0.50	0.60	61
	2	4.5	-0.50	0.50	67
2.5	10	1.65	-0.50	1.47	20
	5	2.4	-0.50	1.19	35
	3.33	3.25	-0.50	0.98	46
	2.5	4.2	-0.50	0.61	67
3.5	14	1.61	-0.50	1.99	1
	7	2.29	-0.50	1.95	2.9
	4.67	3.04	-0.50	1.76	12.4
	3.5	3.86	-0.50	1.45	28

Variation of $[(d_s)_{max_c}/y]_{opt}$ versus θ values are shown in Figure 4.13 with $(L_a/B_a)_{opt}$ as a third parameter. On data points corresponding $(Z_c/y)_{opt}$ values are also given. $[(d_s)_{max_c}/y]_{opt}$ values show a decreasing trend with increasing θ values for a given value of L_a/B_a . For a given abutment and collar size, the optimum location of the collar and the corresponding maximum scour depths can be computed easily from this figure. For instance, if θ value is selected as 7 for an abutment of $L_a/B_a = 0.75$, expected scour depth is determined as zero.

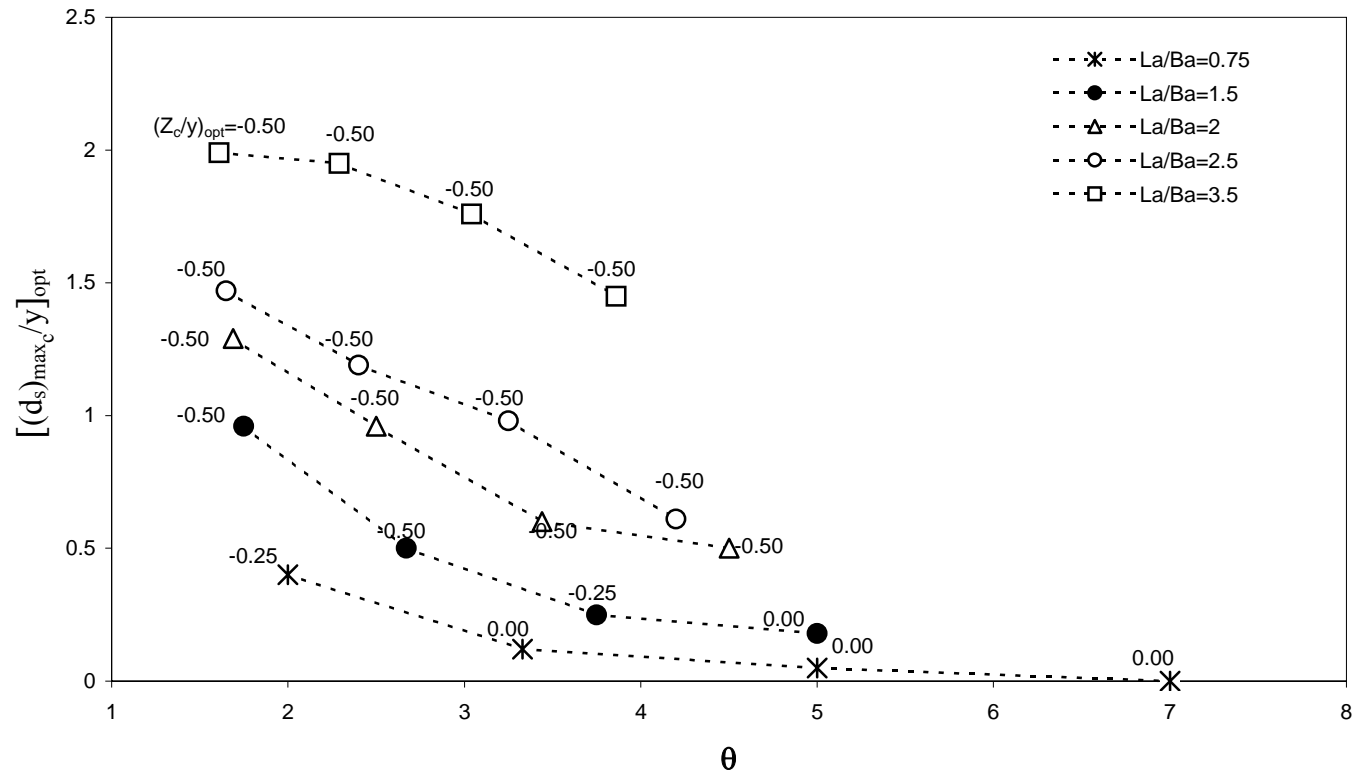


Figure 4.13. Variation of $[(d_s)_{max_c} / y]_{opt}$ with θ ($Q=0.050 \text{ m}^3/\text{s}$, $y=10 \text{ cm}$, $F_r=0.34$, $U/U_c=0.90$)

An alternative figure to Figure 4.13 is Figure 4.14 in which the parameter on the horizontal axis is $\theta^{0.5} (L_a / B_c)^{0.5}$ instead of θ . In this figure, as seen, the data points can be considered as collected around a linear line instead of grouping as a function of L_a/B_a as shown in Figure 4.13. Referring to this figure one can estimate the $[(d_s)_{\max_c}/y]_{\text{opt}}$ value of an abutment of known L_a , B_c and θ within the range of parameters used in this study.

To determine the optimum locations of the collars for known values of L_a/B_c , the data of $[Z_c/y]_{\text{opt}}$ given in Table 4.3 are plotted versus L_a/B_c in Fig. 4.15. From this figure the following classification for L_a/B_c and $[Z_c/y]_{\text{opt}}$ can be proposed.

$$\begin{aligned} [Z_c/y]_{\text{opt}} &= 0 & \text{for } L_a/B_c < 2.0 \\ -0.50 \leq [Z_c/y]_{\text{opt}} &\leq -0.25 & \text{for } 2.0 \leq L_a/B_c \leq 3.0 \\ [Z_c/y]_{\text{opt}} &= -0.50 & \text{for } 3.0 < L_a/B_c \leq 14 \end{aligned}$$

The above relations are valid for the range of L_a/B_c between 0.75 and 14.

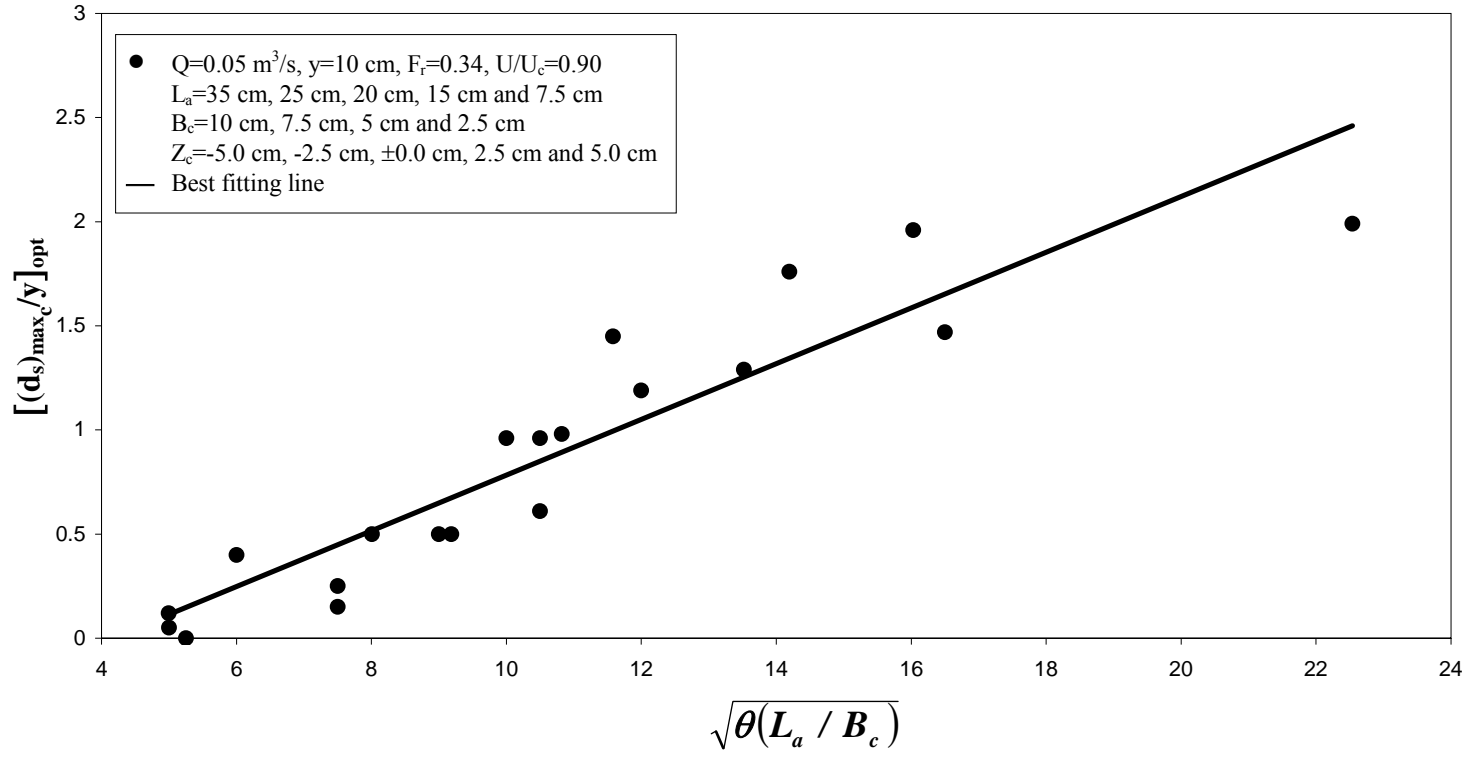


Figure 4.14. Variation of $[(d_s)_{\max_c} / y]_{\text{opt}}$ with $\sqrt{\theta(L_a / B_c)}$

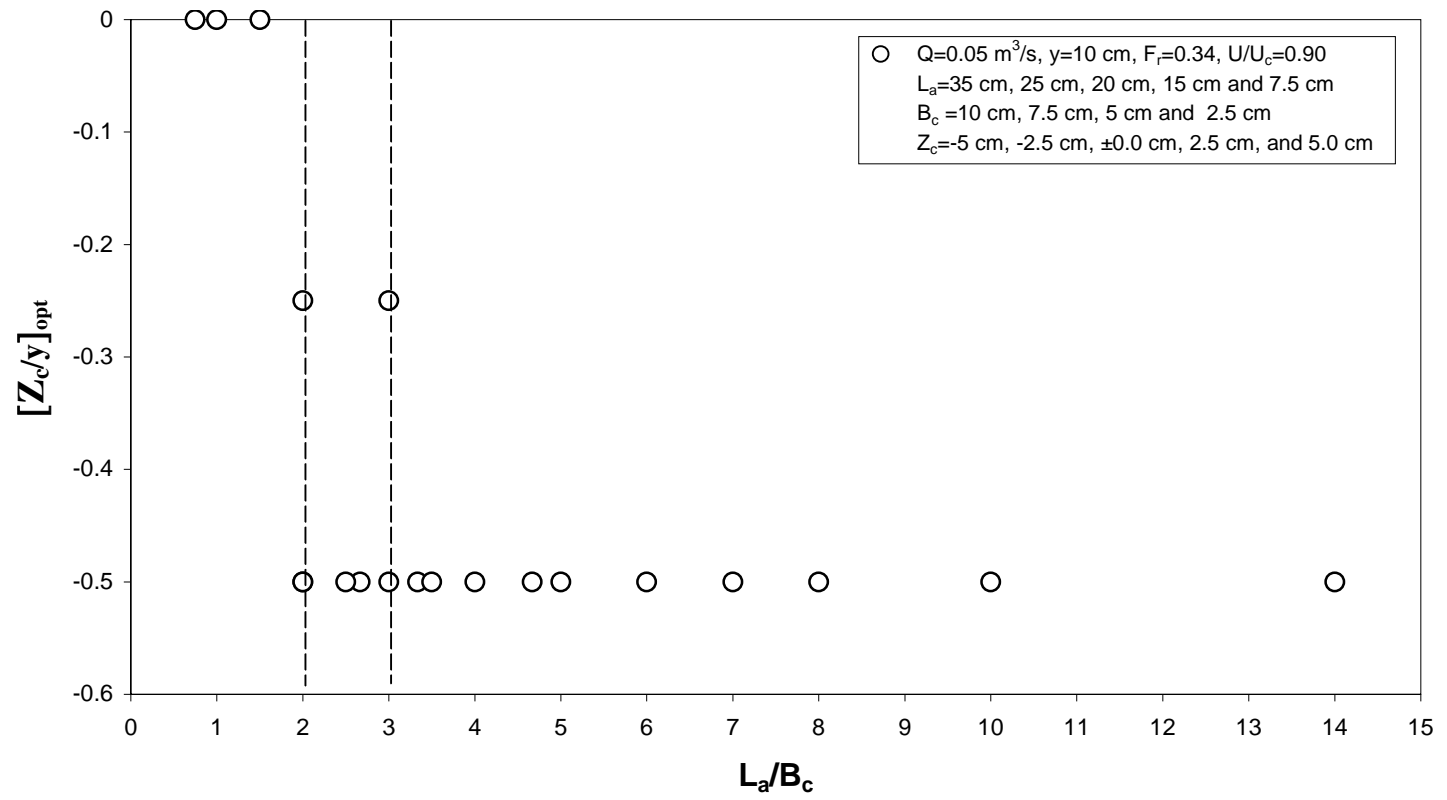


Figure 4.15. Variation of $[Z_c/y]_{\text{opt}}$ with L_a/B_c

Figure 4.16 shows the variation of $[\% \text{Reduction}]_{\text{opt}}$ with L_a/B_c (Table 4.3). Almost all of the data points follow closely the best fitting curve of the data. After determining the optimum location of the collar from Fig. 4.15 for a given L_a/B_c , one can also estimate the corresponding $[\% \text{Reduction}]_{\text{opt}}$ from Fig. 4.16. Consequently, referring to this figure it can be concluded that to have at least 20% reduction in the maximum scour depth around an abutment, the L_a/B_c value of the abutment must be less than 6, while this value would be less than about 2 to have at least 60% reduction.

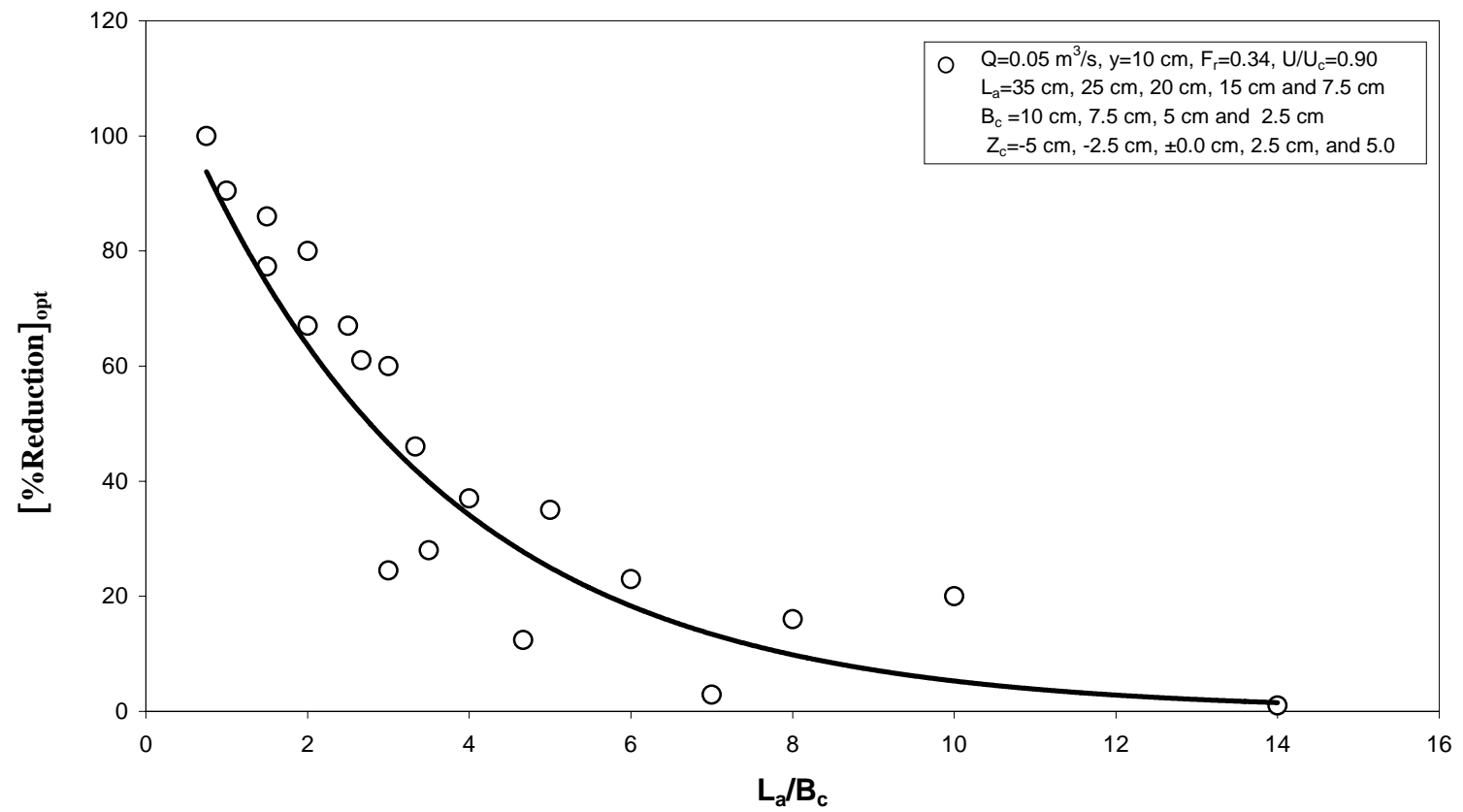


Figure 4.16. Variation of $[\%Reduction]_{opt}$ with L_a/B_c

4.6.3 Effect of Flow Depth on the Maximum Scour Depth at Bridge Abutments

In order to show the effect of flow depth at threshold condition of sediment motion on the maximum scour depth around the abutment some additional experiments with five different flow discharges were conducted. The tested discharges, the corresponding flow depths and U/U_c ratios are as follows, respectively: $Q=0.055 \text{ m}^3/\text{s}$, $0.050 \text{ m}^3/\text{s}$, $0.045 \text{ m}^3/\text{s}$, $0.040 \text{ m}^3/\text{s}$, and $0.035 \text{ m}^3/\text{s}$; $y=9.60 \text{ cm}$, 8.85 cm , 7.95 cm , 7.15 cm and 6.45 cm , and $U/U_c=0.98$, 1.0 , 0.94 , 0.97 and 0.93 . All these values as well as the properties of abutments and collars, and experimental data are presented in Table 4.4. Figure 4.17 shows the variation of percent reductions in the maximum scour depths around the abutments of different lengths at different discharges with collars of $B_c=10 \text{ cm}$ and 5 cm . It is clearly seen from this figure that the data are collected in two groups. As mentioned earlier, when the collar width of $B_c=10 \text{ cm}$ is used the higher reduction in the maximum scour depth is observed when compared to the cases where the collar widths of $B_c=5 \text{ cm}$. Decreasing Z_c/y , increased the collar efficiency. Flow did not penetrate below the collar of $B_c=10 \text{ cm}$ when it was placed at $Z_c=-5 \text{ cm}$ in all experiments. The L_a/B_c values of the data in the upper group vary between 1.5 and 2.5, and their maximum % reductions in maximum scour depths range between 60% and 77% for values of $[Z_c/y]_{\text{opt}}$ greater than about 0.521. As for the data in the lower group, they all have constant L_a/B_c value of 5 with the values of % reduction in maximum scour depths varying between 19 and 38. All these values stated above are consistent with those of Figure 4.12 for which $Q=0.050 \text{ m}^3/\text{s}$, $y=10 \text{ cm}$ and $F_r=0.34$ and $U/U_c=0.90$. As a conclusion it can be stated that whatever the flow depth is, as long as it corresponds to the threshold condition of sediment motion, as the value of Z_c/y decreases, the

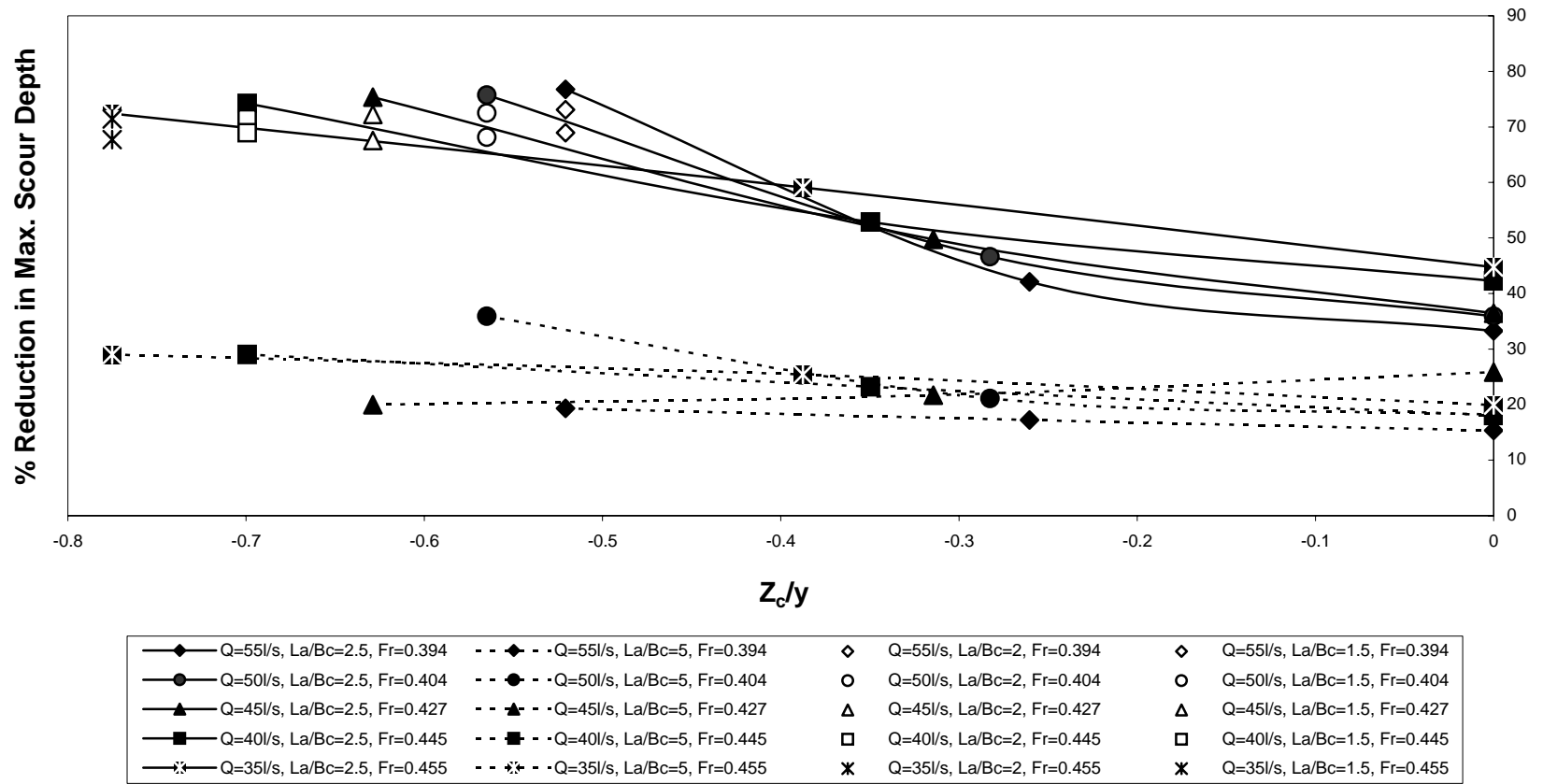


Figure 4.17. Variation of percent reduction in maximum scour depth with Z_c/y for $B_c=10$ cm and $B_c=5$ cm for various discharges

reduction in maximum scour depth increases. At about $Z_c/y=-0.5$, at least 70% reduction in maximum scour depth is obtained under the flow conditions tested in this study.

Figure 4.18 combines all the data given in Figure 4.17 along with the trend lines of data of $L_a/B_c=2, 3$ and 5 presented in Figure 4.12. for Z_c/y values between ± 0.00 and -0.50 . The aim of preparing this figure is to show the effect of flow depth at clear water flow condition on the % reduction in maximum scour depth. As it had been explained the data presented in Figure 4.12 from experiments with a constant flow depth of $y=10$ cm for which $U/U_c=0.90$. As it is marked in Figure 4.18, all the data given here were obtained from experiments of various flow depths and U/U_c values.

Therefore, based on this figure it can be concluded that not only for $y=10$ cm but for all the flow depths corresponding to clear water flow condition, the data of similar L_a/B_c values follow each other closely. That is, for given Z_c/y and L_a/B_c values, one can obtain almost the same % reduction in maximum scour depth regardless of the flow depth.

Table 4.4 Experimental data for various flow depths of threshold condition of sediment motion

Run no	Q (m ³ /s)	y (cm)	U/U _c	F _r	L _a (cm)	B _c (cm)	Z _c (cm)	(d _s) _{max} (cm)	(d _s) _{max,c} (cm)	% Reduction in max. scour depth
S1	0.055	9.60	0.98	0.394	25	-	-	21.5	-	-
S2					25	10	-5		5	77
S3					25	10	-2.5		12.45	42
S4					25	10	0		14.35	33
S5					25	5	-5		17.35	19
S6					25	5	-2.5		17.8	17
S7					25	5	0		18.2	15
S8					20	-	-	18.6	-	-
S9					20	10	-5		5	73
S10					15	-	-	16.1	-	-
S11					15	10	-5		5	69
S12	0.050	8.85	1.00	0.404	25	-	-	20.6	-	-
S13					25	10	-5		5	76
S14					25	10	-2.5		11	47
S15					25	10	0		13.2	36
S16					25	5	-5		16.25	21
S17					25	5	-2.5		16.85	18
S18					25	5	0		17.4	16
S19					20	-	-	18.2	-	-
S20					20	10	-5		5	73
S21					15	-	-	15.7	-	-
S22					15	10	-5		5	68
S23	0.045	7.95	0.94	0.427	25	-	-	20.3	-	-
S24					25	10	-5		5	75
S25					25	10	-2.5		10.2	50
S26					25	10	0		12.9	36
S27					25	5	-5		15.05	26
S28					25	5	-2.5		15.9	22
S29					25	5	0		16.25	20
S30					20	-	-	18	-	-
S31					20	10	-5		5	72
S32					15	-	-	15.4	-	-
33					15	10	-5		5	68

Table 4.4 Experimental data for various flow depths of threshold condition of sediment motion (continued)

Run no	Q (m ³ /s)	y (cm)	U/U _c	F _r	L _a (cm)	B _c (cm)	Z _c (cm)	(d _s) _{max} (cm)	(d _s) _{max_c} (cm)	% Reduction in max. scour depth
S34	0.040	7.15	0.97	0.445	25	-	-	19.4	-	-
S35					25	10	-5		5	74
S36					25	10	-2.5		9.15	53
S37					25	10	0		11.2	42
S38					25	5	-5		13.75	29
S39					25	5	-2.5		14.9	23
S40					25	5	0		15.9	18
S41					20	-	-	17.5	-	-
S42					20	10	-5		5	71
S43					15	-	-	16.1	-	-
S44					15	10	-5		5	69
S45	0.035	6.45	0.93	0.455	25	-	-	18.1	-	-
S46					25	10	-5		5	72
S47					25	10	-2.5		7.7	59
S48					25	10	0		10	45
S49					25	5	-5		12.85	29
S50					25	5	-2.5		13.5	25
S51					25	5	0		14.5	20
S52					20	-	-	17.5	-	-
S53					20	10	-5		5	71
S54					15	-	-	15.5	-	-
S55					15	10	-5		5	68

From Table 4.4, for each abutment length and collar width tested, the location of the collar, which results in maximum reduction in the scour depth is selected and presented in Table 4.5 along with the corresponding values of $[\% \text{ Reduction}]_{\text{opt}}$ and F_r numbers.

Based on the parameters given in Table 4.5, Figure 4.19 was plotted to show the effect of the flow depth or the Froude number at clear water flow condition on the magnitude of $[(d_s)_{\text{max}_c}/y]_{\text{opt}}$. This figure also contains all the data given in Figure 4.13 which is valid only for $y=10$ cm or $F_r=0.34$. The data of $L_a/B_a=2.5$, which have the Froude number between 0.394-0.455, follow a well-ordered trend in terms of the Froude number. As the Froude number increases for a given θ , the corresponding value of $[(d_s)_{\text{max}_c}/y]_{\text{opt}}$ increases. Same conclusion can be made for the data of $L_a/B_a=1.5$ and 2.0 as seen in the figure.

The relevant data presented in Table 4.5 were plotted on Figure 4.15 and renamed as Figure 4.20 to show the effect of different y or F_r values of clear water flows on the variation of $[Z_c/y]_{\text{opt}}$. As it is clearly seen on the figure for a given Fr the value of $[Z_c/y]_{\text{opt}}$ is independent of L_a/B_c . However, $[Z_c/y]_{\text{opt}}$ decreases with increasing Fr .

Table 4.5. Optimum design parameters of an abutment-collar arrangement for various flow depths corresponding to threshold conditions of sediment motion

L_a/B_a	F_r	L_a/B_c	θ ($A_{total}/A_{abutment}$)	$[Z_c/y]_{opt}$	$[(d_s)_{max_c}/y]_{opt}$	$[\%Reduction]_{opt}$
2.5	0.394	2.5	4.2	-0.521	0.521	77
		5.0	2.4	-0.521	1.807	19
	0.404	2.5	4.2	-0.565	0.565	76
		5.0	2.4	-0.565	1.836	21
	0.427	2.5	4.2	-0.629	0.629	75
		5.0	2.4	-0.629	1.893	26
	0.445	2.5	4.2	-0.700	0.700	74
		5.0	2.4	-0.700	1.920	29
	0.455	2.5	4.2	-0.775	0.775	72
		5.0	2.4	-0.775	1.991	29
2.0	0.394	2.0	4.5	-0.521	0.521	73
	0.404	2.0	4.5	-0.565	0.565	73
	0.427	2.0	4.5	-0.629	0.629	72
	0.445	2.0	4.5	-0.700	0.699	71
	0.455	2.0	4.5	-0.775	0.775	71
1.5	0.394	1.5	5.0	-0.521	0.521	69
	0.404	1.5	5.0	-0.565	0.565	68
	0.427	1.5	5.0	-0.629	0.629	68
	0.445	1.5	5.0	-0.700	0.699	69
	0.455	1.5	5.0	-0.775	0.775	68

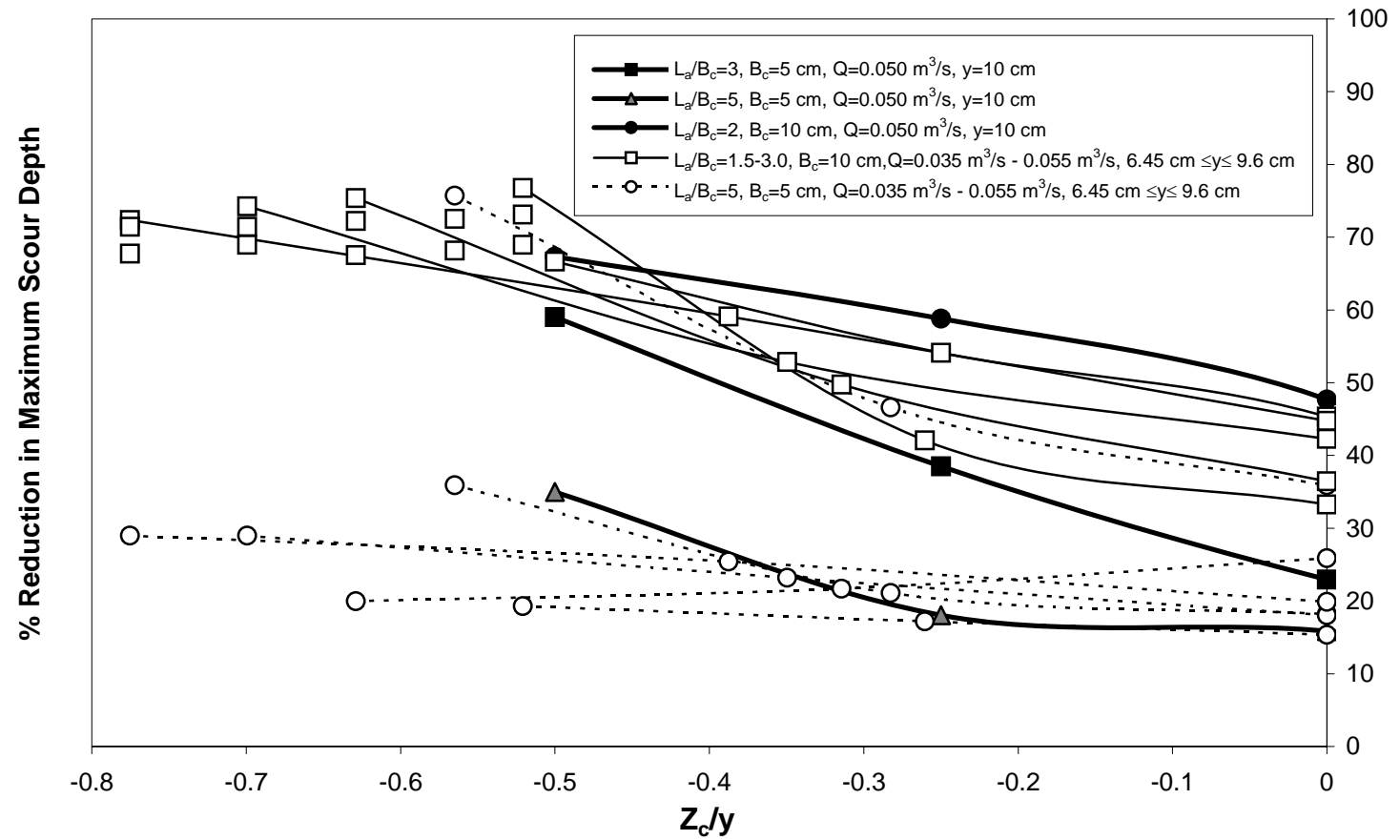


Figure 4.18. Variation of % reduction of maximum scour depth with Z_c/y

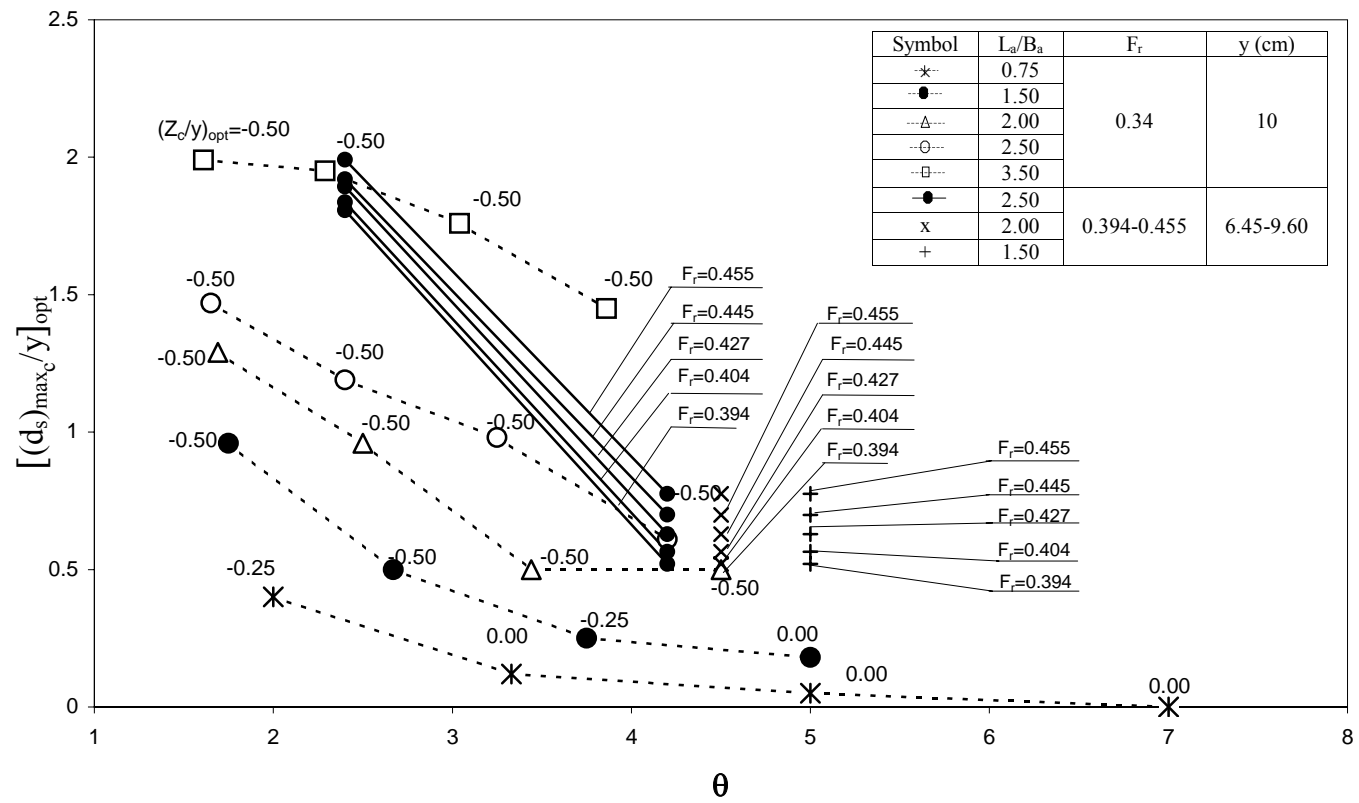


Figure 4.19. Variation of $[(d_s)_{max_c}/y]_{opt}$ with θ for various discharges

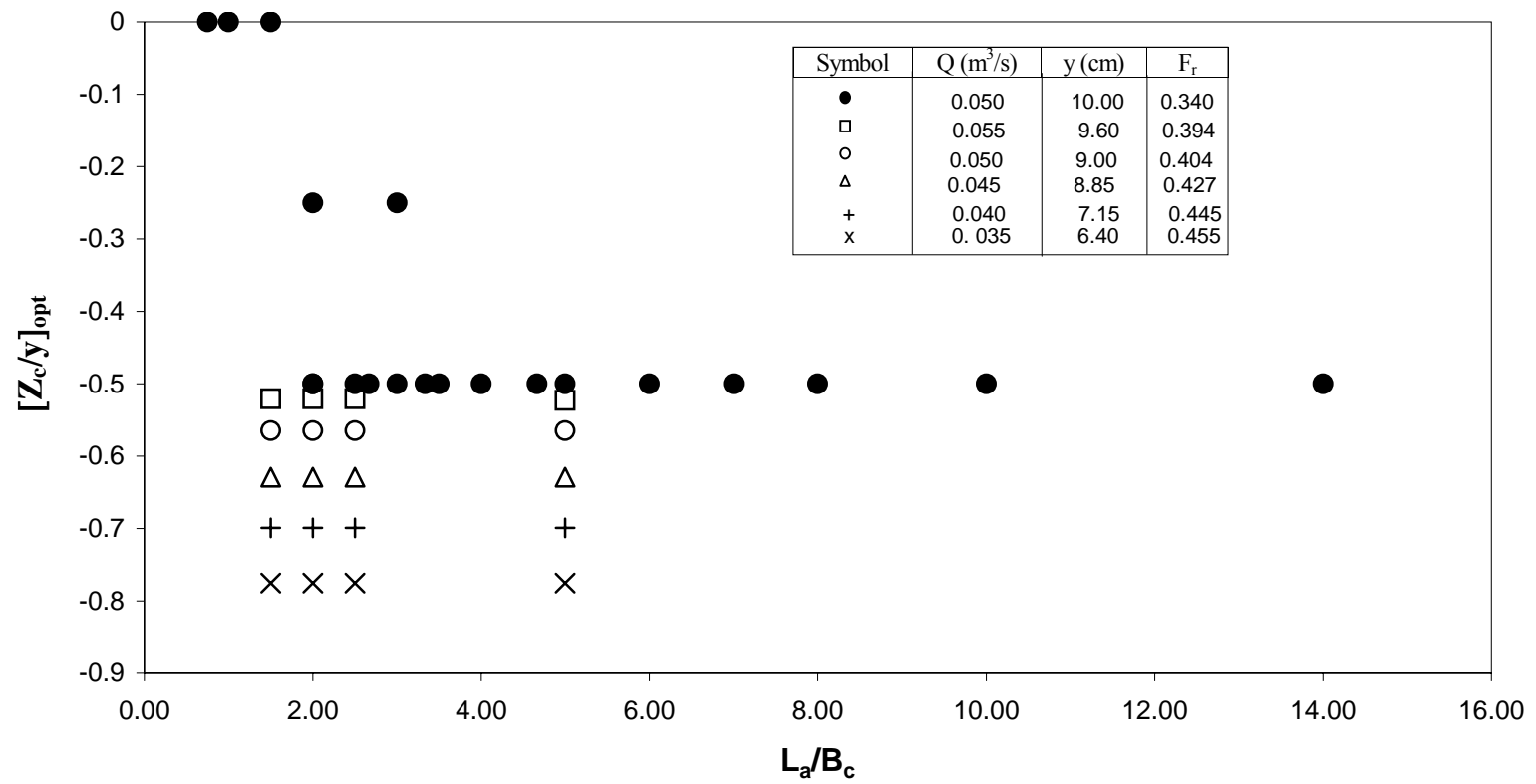


Figure 4.20. Variation of $[(Z_c/y)_{opt}]$ with L_a/B_c for various discharges

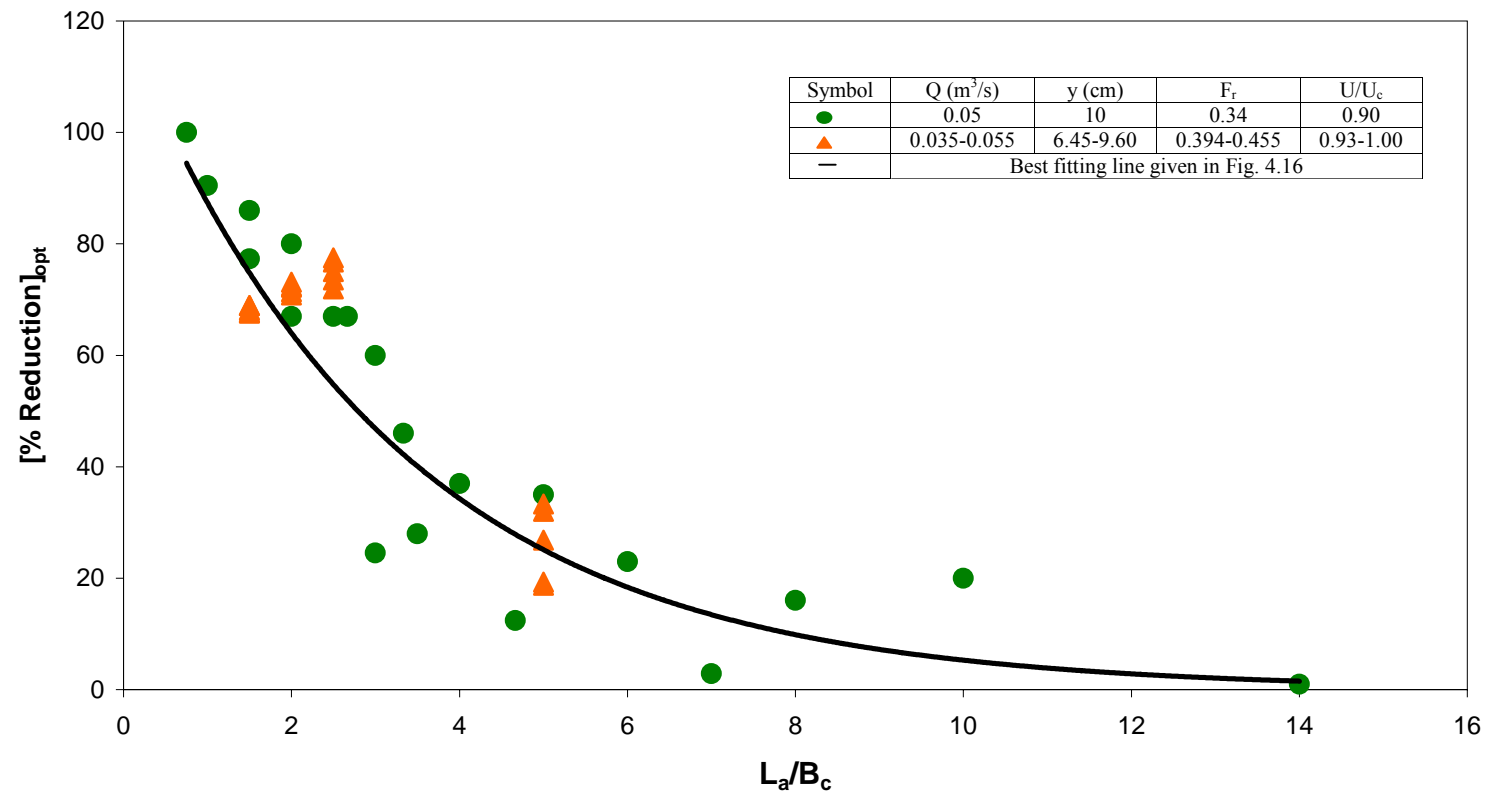


Figure 4.21. Variation of $[\% \text{ Reduction}]_{\text{opt}}$ with L_a/B_c for various discharges

4.6.4 Effect of Flow Depth on the Formation Scour Hole Around the Bridge Abutment

In the earlier experiments carried out with constant discharge, flow depth and velocity ratio, $Q=0.050 \text{ m}^3/\text{s}$, and $y=10 \text{ cm}$ and $U/U_c=0.90$, the scour holes formed at the bottom of all the abutments tested were mainly around P_1 as discussed several times in related sections. Even when the collars were used with abutments, the location of the maximum scour depth and the area over which the scour hole developed did not change in general. Whereas, as the experiments were conducted with collars and various flow depths or U/U_c ratios of clear water cases, it was observed that due to the presence of the collars other scour holes developed at far downstream of the abutments. However, the maximum depths of these scour holes were smaller than those observed at the faces of the abutments when they were tested without collars. To describe the location of these maximum scour depths, the angle, ξ , is defined, as sketched in Fig. 4.22. ξ is the angle between z axis, which coincides with the upstream face of the abutment and perpendicular to the flow, and the line connecting the origin of x - z coordinate system to the point where the maximum scour depth occurs as shown in Fig. 4.22. All the experimental parameters related to the analysis of the shifted scour holes are presented in Table 4.6. Although these scour depths are higher than those recorded at the abutment face when it has a collar around it, they are still lower than the maximum scour depths, which are obtained from without-collar cases. ξ varies between the following values as a function of the abutment length: 20.40° - 27.30° ; 28.10° - 32.50° and 32.8° - 44.10° for the abutment lengths of $L_a=15 \text{ cm}$, 20 cm and 25 cm , respectively. The location of

the maximum scour depths around the abutments and corresponding ξ values are shown in Figure 4.24.

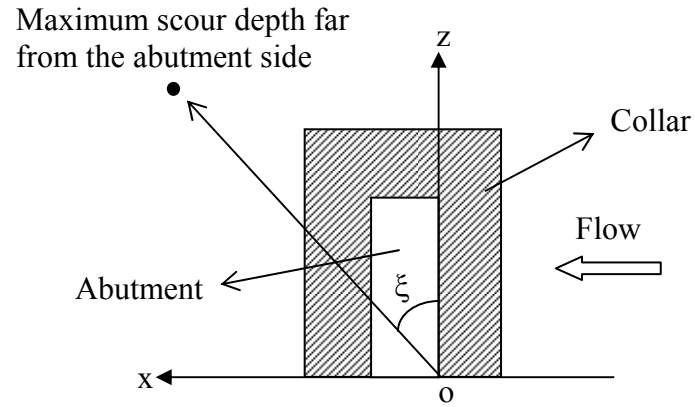


Figure 4.22. Definition sketch for ξ

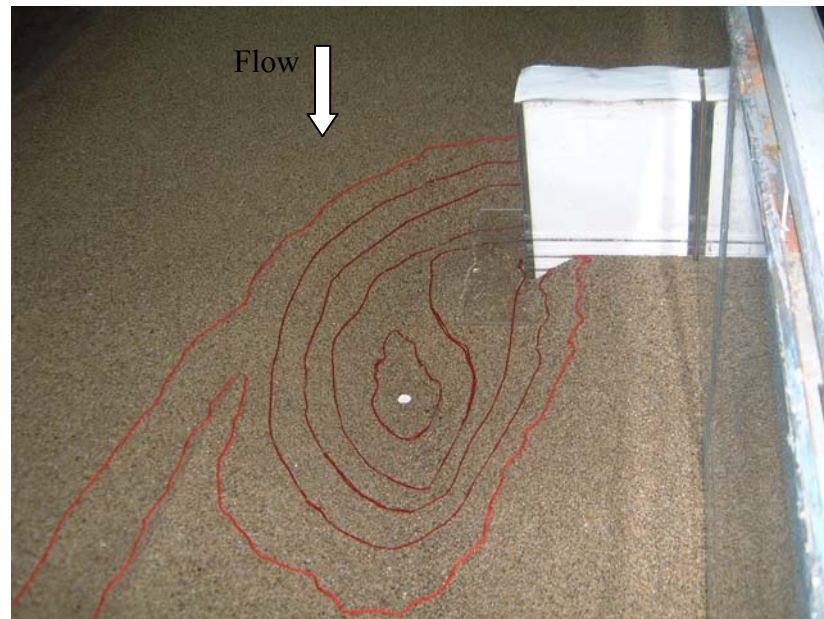


Figure 4.23. Upstream view of the eroded bed around the abutment ($Q=0.055 \text{ m}^3/\text{s}$, $y=9.60 \text{ cm}$, $U/U_c=0.98$, $L_a=25 \text{ cm}$, $Z_c=-5 \text{ cm}$, $B_c=10 \text{ cm}$)

Table 4.6. Experimental data for various Q and L_a values tested

Q (l/s)	L _a (cm)	y (cm)	Z _c (cm)	(d _s) _{max_c} (at the abutment) (cm)	(d _s) _{max} (without collar) (cm)	(d _s) _{max_c} (far from the abutment) (cm)	z (cm)		x (cm)		ξ (°)		
35	15	6.45	5	5	15.5	9.4	8.60-11.1	29.6	29.6 - 31.5	11	11 - 16	20.4	20.4 - 27.3
40	15	7.15			16.1	10.2		30.5		12.5		22.3	
45	15	7.95			15.4	8.6		30		15.5		27.3	
50	15	8.85			15.7	9		31		16		27.3	
55	15	9.60			16.1	11.1		31.5		11.5		20.7	
35	20	6.45			17.5	13	13-13.5	33.5	33 - 36.5	20	19.5 - 22	30.8	28.1 - 32.5
40	20	7.15			17.5	13.5		33		21		32.5	
45	20	7.95			18	13.5		36.5		19.5		28.1	
50	20	8.85			18.2	13		35		22		32.1	
55	20	9.60			18.6	13.4		35		21.6		31.7	
35	25	6.45			18.1	15.1	13.2-15.8	44	44 - 48.5	30	30 - 47	34.3	32.8 - 44.1
40	25	7.15			19.4	15.5		48		31		32.8	
45	25	7.95			20.3	15.8		46.5		36.2		37.0	
50	25	8.85			20.6	14.7		46.5		41		41.4	
55	25	9.60			21.5	13.2		48.5		47		44.1	

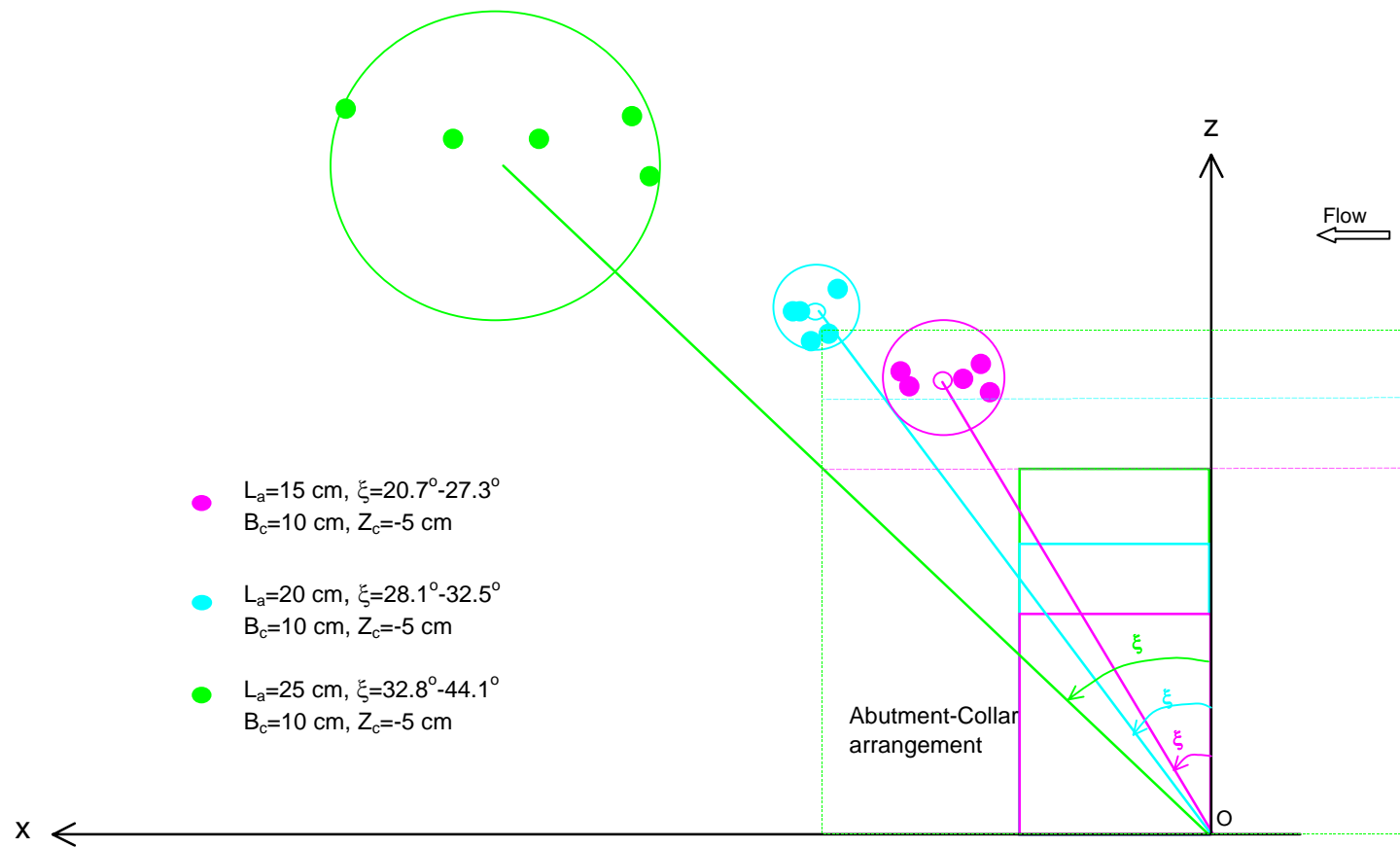


Figure 4.24. Location of $(d_s)_{\max_c}$ far from the abutment face

4.7 PARTIAL –COLLAR ARRANGEMENTS

In addition to full-collar experiments, those partial-collars given in Table 4.7 were tested at the threshold-flow condition for the discharge $Q=0.05 \text{ m}^3/\text{s}$. The tests were performed by placing the collar at elevations of $Z_c=\pm 0 \text{ cm}$ and $Z_c=-5 \text{ cm}$ around the abutment of $L_a=20 \text{ cm}$. Results of the experiments showed that partial–collars of shapes (a) and (b) cause a maximum erosion depth of $(d_s)_{\max}=12.3 \text{ cm}$, and 5 cm as the full-collar for the collar elevations of $Z_c=\pm 0 \text{ cm}$ and -5 cm respectively.

Table 4.7. Optimization of collar shape

Parameters of flow and abutment	$Q=0.050 \text{ m}^3/\text{s}$, $L_a/y=2.5$, $B_a=10\text{cm}$, $L_a/B_c=2$				
Plan views of collar shapes (Flow direction) ←	full	(a)	(b)	(c)	(d)
$(d_s)_{\max}$ at $Z_c/y=\pm 0$	12.3	12.3	12.3	13.3	15
$(d_s)_{\max}$ at $Z_c/y=-0.5$	5	5	5	12.45	13.75

However, collar shapes of (c) and (d) result in higher scour depths of 13.3 cm and 15 cm , respectively at $Z_c/y=\pm 0$. Similar trend is observed when the collar is placed at $Z_c/y=-0.5$ with the scour depths of 12.45 cm and 13.75 cm for the collar shapes of (c) and (d). Therefore, the partial-collar shape of (b) can be considered the optimum from an economical point of view.

4.8 CONCLUSIONS

A collar prevents the sediment particles from erosion by down flow. Efficacy of a collar for preventing scour is a function of its size and its vertical location on the abutment. As the size of the collar increases the scour depth decreases.

If $L_a/y > 1$, the efficiency of the collar increases with decreasing L_a/B_c and the elevation of the collar in downward direction from the bed level, as long as the clear water flow conditions are satisfied, regardless of the flow depth, that is $U/U_c \geq 0.90$.

If $L_a/y < 1$, the collar, which is placed at the bed level ($Z_c/y = \pm 0.00$), gives higher performance than those having other Z_c/y values

Instead of full-collars, partial collars can be used to provide maximum reduction in the scour depth from economical point of view.

CHAPTER 5

TIME DEVELOPMENT OF SCOUR AROUND ABUTMENTS

5.1 GENERAL

As stated earlier the time required to reach the equilibrium scour depth around bridge piers and abutments is very long; it may take days, weeks even months. Since flood times are much shorter than the time necessary to attain the equilibrium state of the scour holes, the study of time variation of the scour depth is quite important.

In this part of the study, time development of scour holes around the abutments of various lengths with and without collars was recorded during 6-hr experimental durations. The effect of the collar widths and their elevations on the reduction of the maximum scour depth was investigated. Studies have shown that collars could protect the abutments from erosion efficiently, so that in some cases they can reduce scouring completely during the test duration.

5.2 LITERATURE REVIEW

Because of failure experiences of bridges many researchers have worked on scour phenomena during the last decades (Rajaratnam and Nwachukwu, 1983; Melville, 1992 and 1997; Lim, 1997; Singh et. al., 1995). Most of the methods stated in the above mentioned papers deal with the determination of design scour depth at bridge

piers and abutments using design discharges for steady flow cases. However, the flow in a river during a flood is unsteady. The time required by the design discharge to scour to its full potential is generally much larger than the time for which it runs. Therefore, for realistic estimation of scour depth in case of flood flows the temporal variation of the scour depth becomes significant for design purposes (Cunha, 1975; Raudkivi and Ettema, 1983; Yanmaz and Altınbilek, 1991; Kothyari et. al., 1992; Melville and Chiew, 1999; Ballio and Orsi, 2000; Kothyari and Ranga Raju, 2001; Radice et. al., 2002; Oliveto and Hager, 2002; Coleman et. al., 2003).

Gill (1972) tested fine and coarse materials around the spur dikes. In the experiments, the range of the water depths was varied between 3.6 cm - 5.2 cm, and 3.6 cm – 5.4 cm for the coarse sand and fine sand, respectively. The maximum test duration for coarse sand was kept about 3 days. Approximately 90% of the scour had occurred in the first 15 hrs. The finer sand was scoured faster than the coarse sand and steady condition was observed nearly 6 hrs to 8 hrs. He derived the equation given below:

$$\frac{d_s}{d_{se}} = A_1 \log(t) + A_2 \quad (5.1)$$

in which the values A_1 and A_2 depend on the properties of the bed material.

Cunha (1975) tested a spur dike with $L_a=20$ cm in a channel of width $B=2$ m. Two different bed materials were used. The median particle sizes were $d_{50}=1.6$ mm and 5.78 mm and corresponding critical velocities of incipient motion for $y=9$ cm were

$U_c=0.38$ m/s and 0.70 m/s, respectively. The test durations were kept about 5 days.

For the time development of the scour, the formula given below was proposed.

$$\frac{d_s}{y} = 325 \left(\frac{u^*}{w} \right)^{3.25} t^{0.16} \quad (5.2)$$

where u^* is the shear velocity, w is the fall velocity of the sediment and t is the scouring time in days.

Cardoso and Bettles (1999) tested six different abutments of $L_a=14.7$ cm, 27 cm, 40 cm, 53 cm, 66.5 cm and 80 cm with a bed material of $d_{50}=0.835$ mm in a compound channel. Test durations were kept between 6 to 120 hours. They derived the relationship given below:

$$\frac{d_s}{d_{se}} = 1 - \left[-1.025 \left(\frac{t}{T} \right)^{0.35} \right] \quad (5.3)$$

where, t is scouring time, T is evaluated for each test as the time where $d_s=0.632d_{se}$.

Kothyari and Ranga Raju (2001) developed a differential model for estimation of the equilibrium scour depth and temporal variation of the scour depth at abutments by using the data reported in the literature. The lengths of the abutments were varying between 10 cm to 140 cm and the range of the channel widths were 0.6 m to 2.4 m. The variation of median sediment sizes were $d_{50}= 0.29$ mm to 10.55 mm and the tested water depths were varying from 3 cm to 60 cm. Their method is derived from

an earlier one, which considered the scour near a circular pile. The equations calibrated on piers can be applied to abutments once the abutment length L_a is adjusted in order to obtain an equivalent dimension of pier width.

Ballio and Orsi (2001) analyzed the abutment of $L_a=10$ cm and 5 cm. In their tests while the channel width was varying from 0.20 m to 1 m, the median sediment size was kept constant as $d_{50}=5$ mm. The results of the long duration (1.5 to 6 weeks) experiments were presented with the relationship given below.

$$\frac{d_s}{d_{se}} = 1 - e^{-0.028 \left(\frac{tU}{\sqrt{L_a y}} \right)^{0.33}} \quad (5.4)$$

Radice et. al. (2002) conducted a series of experiments to predict the time development of scour depth around the abutments. They used three different abutment lengths of $L_a=5$ cm, 10 cm and 20.2 m. The range of the channel widths were varying from 0.5 m to 0.193 m. Median sizes of sediments were $d_{50}=5$ mm and 1.9 mm. They derived the equations given below by running all the experiments at incipient motion condition.

$$\frac{d_s}{a} = 0.53 \log \left(\frac{t}{T} \right) + 0.69 \quad \text{for } \frac{t}{T} < 30 \quad (5.5)$$

$$\frac{d_s}{a} = \log \left(\frac{t}{T} \right) \quad \text{for } \frac{t}{T} > 30 \quad (5.6)$$

where, a and T were expressed as functions of the control parameters :

$$\frac{a}{\sqrt{L_a y}} = 2.1 \left(\frac{L_a}{y} \right)^{0.17} \left(\frac{\sqrt{L_a y}}{d_{50}} \right)^{0.17} \left(\frac{B_a}{L_a} \right)^{0.07} \Phi^{0.63} \quad (5.7)$$

where, Φ is some combination of the non-dimensional shear stress.

$$\frac{TU}{\sqrt{L_a y}} = 538.11 \left(\frac{L_a}{y} \right)^{0.77} \left(\frac{B_a}{L_a} \right)^{-0.46} \quad (5.8)$$

Oliveto and Hager (2002) used six different sediment sizes of $d_{50}=0.55$ mm, 3.3 mm and 4.8 mm as uniform and 5.3 mm, 1.2 mm and 3.1 mm as mixture in two channels having widths of $B=1$ m and 0.50 m. They tested abutments of $L_a=5$ cm, 10 cm, 20 cm, 40 cm and 60 cm, and derived the below equation after experiments, which took several days:

$$\frac{d_s}{L_a^{2/3} y^{1/3}} = 0.085 \sigma^{-1/2} \left\{ \frac{U}{\sqrt{d_{50}}} \sqrt{\frac{\rho}{(\rho_s - \rho)g}} \right\}^{1.5} \log \left\{ \frac{\left[\left(\frac{\rho_s - \rho}{\rho} \right) g d_{50} \right]^{0.5}}{L_a^{2/3} y^{1/3}} \right\} t \quad (5.9)$$

where $\sigma = (d_{84}/d_{16})^{0.5}$, sediment nonuniformity.

Coleman et. al. (2003) presented an equation to describe the time development of scour around the vertical abutments with sediment of median particle sizes varying between $d_{50}=0.80$ -1.02 mm and relative flow velocities $U/U_c=0.46$ -0.99, respectively. y/L_a varied from 0.17 to 4.

$$\frac{d_s}{d_{se}} = \exp \left[-0.07 \left(\frac{U}{U_c} \right)^{-1} \left| \ln \left(\frac{t}{t_e} \right) \right|^{1.5} \right] \quad (5.10)$$

5.3 EXPERIMENTAL SET-UP

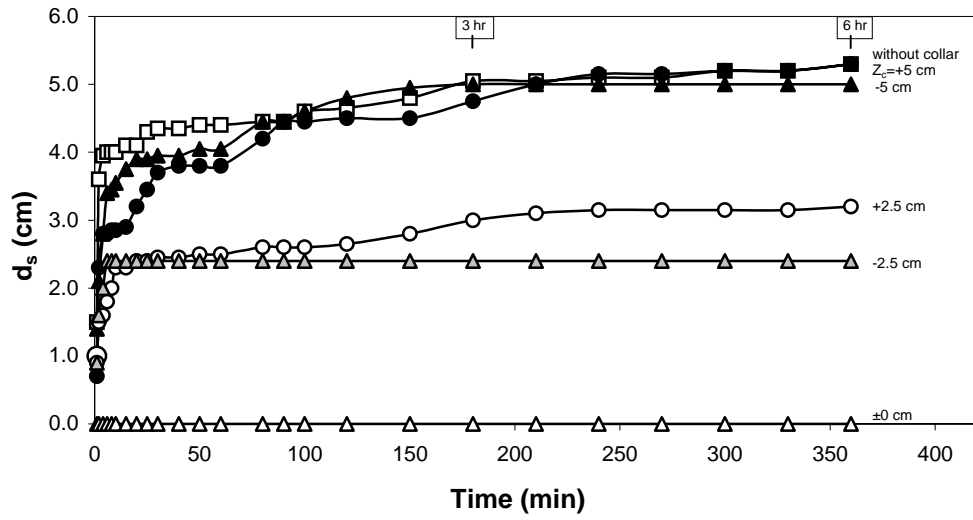
In these tests, the same set-up described in the previous section was used. The scour hole was obtained by performing a 6-hours continuous run under clear-water condition with the flow depth of $y=10$ cm corresponding to the discharge of $Q=0.05$ m³/s, without collar and then with collars. During the experiments at various time intervals ($t=1, 2, 4, 6, 8, 10, 15, 20$ and 30 minutes up to 6 hours) the maximum scour depths were recorded by using a vertical scale attached to the interior wall of Plexiglas abutment with a stick having a small inclined mirror at its end (adapted from Yanmaz, 1991). At the end of the tests profiles of the scour holes at the abutment site were investigated.

Four different collar widths $B_c=2.5$ cm, 5 cm, 7.5 cm and 10 cm were tested. Since the effectiveness of the collar on the development of the scour hole is also a function of its vertical location on the abutment, all collar types were tested at various elevations; at the bed level, 2.5 cm and 5 cm above the bed level and 2.5 cm and 5 cm below the bed level. Abutment lengths are varied as $L_a=35$ cm, 20 cm, 15 cm and 7.5 cm.

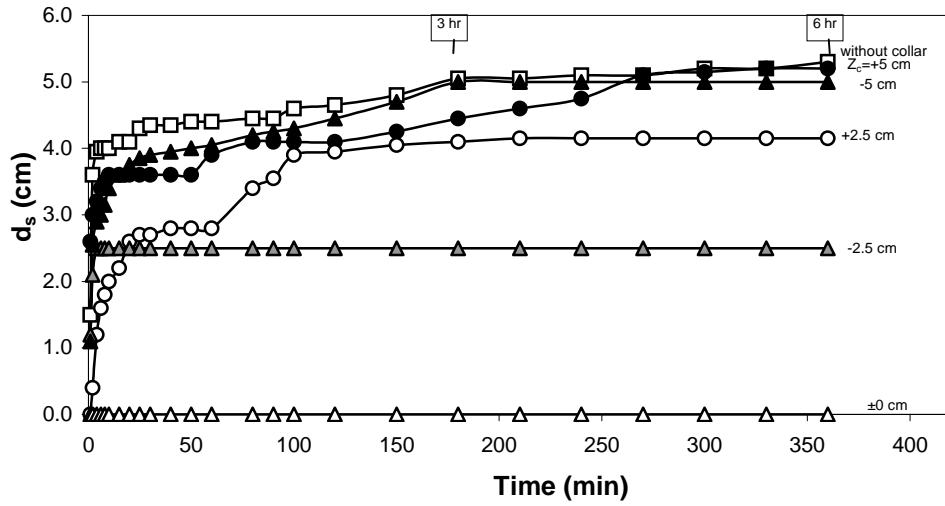
5.4 ANALYSIS OF THE RESULTS

In this study, the maximum scour depths around the abutment –with and without collar- were measured and time development of the scour hole was followed during the scouring process. The effectiveness of the collar widths and elevations in reducing scour depth was investigated. Studies have shown that, not only the collar width but also the elevation of the collar are very effective on the development of the scour hole around the abutments.

If the collars of widths $B_c=10$ cm and 7.5 cm are placed at bed the level around the abutment of $L_a=7.5$ cm, no scour phenomena is seen around the abutment during the test period (Fig. 5.1 (a) and (b)). Whereas, for $Z_c=-2.5$ cm, over a very short time period the bed level is eroded down to the level of the collar, but after that until the end of the experiment no scour is observed below the collars. At other collar elevations, that is $Z_c=+2.5$ cm, +5 cm and -5 cm, maximum scour depth deepens rapidly and then following the trend of the case of without collar progressively increases. When the collar of width $B_c=5$ cm is placed at $Z_c=\pm 0$ cm, no scour depth is measured up to 250 minutes [Fig. 5.1.(c)]. After that, scouring begins and scour depth reaches about 1 cm at the end of the experiment. The maximum scour depth during the whole test period is 2.5 cm when $Z_c=-2.5$ cm for the collar of $B_c=5$ cm. When the collar width becomes 2.5 cm, the scourless time duration gets smaller, from 250 minutes to 42 minutes for $Z_c=\pm 0.0$ cm, and from 360 minutes to 290 minutes for $Z_c=-2.5$ cm [Fig. 5.1 (d)].

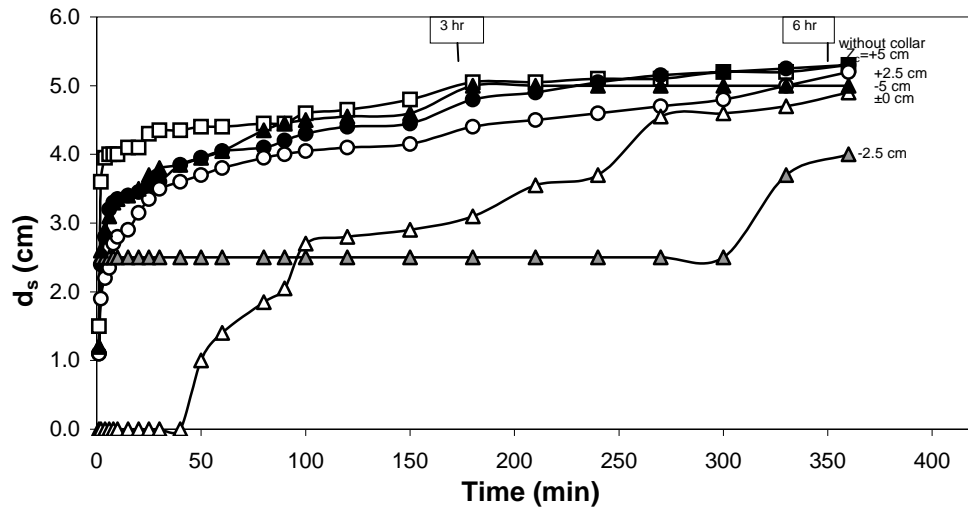


(a) $L_a=7.5$ cm and $B_c=10$ cm

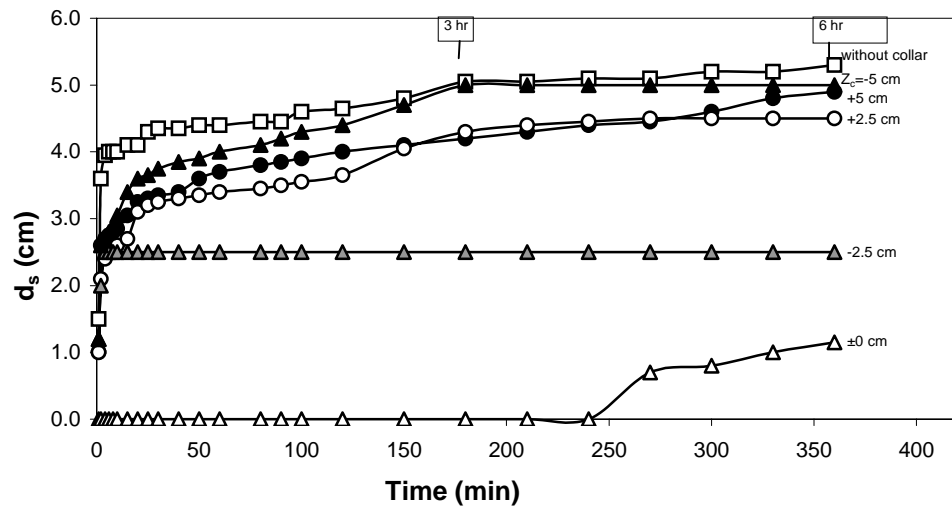


(b) $L_a=7.5$ cm and $B_c=7.5$ cm

Figure 5.1. Time development of maximum scour depth around the abutment for various values of Z_c



(c) $L_a=7.5$ cm and $B_c=5$ cm



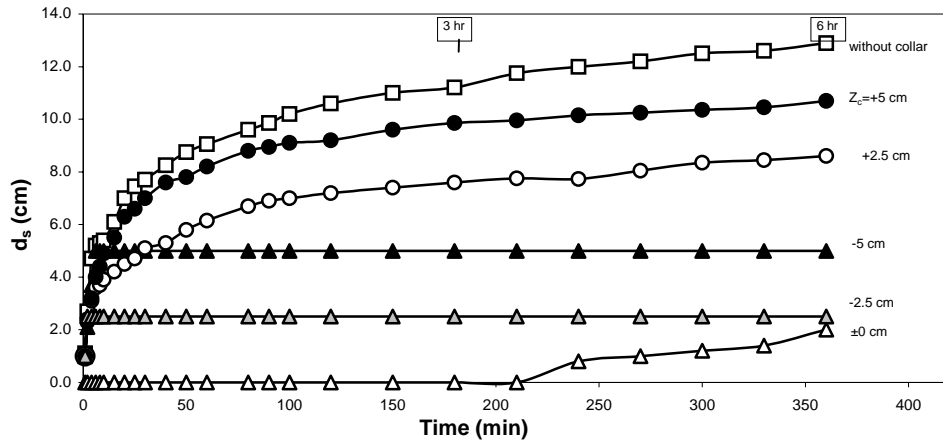
(d) $L_a=7.5$ cm and $B_c=2.5$ cm

Figure 5.1. Time development of maximum scour depth around the abutment for various values of Z_c (continued)

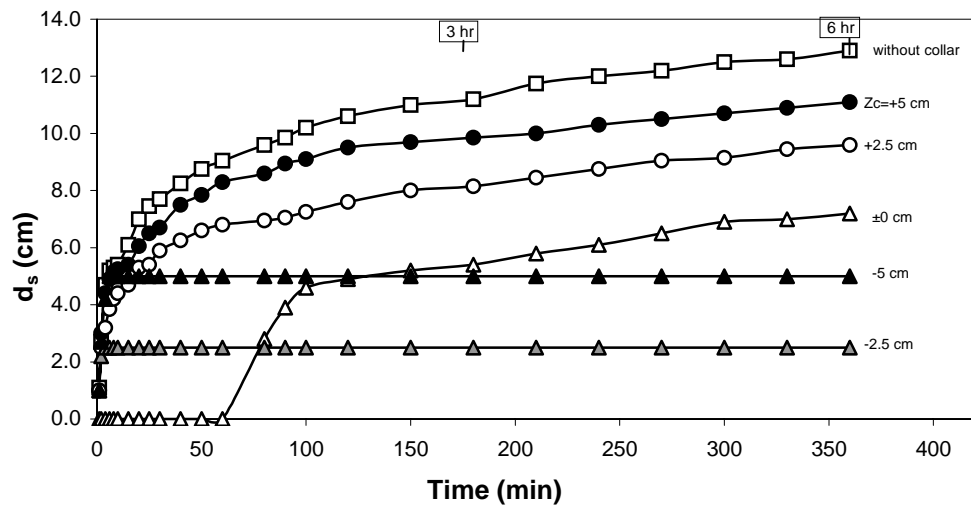
The variation of maximum scour depth with time for the abutment of $L_a=15$ cm having; no collar, collar of widths of 2.5 cm, 5 cm, 7.5 cm and 10 cm, and collar elevations of +5 cm, +2.5 cm, ± 0 cm, -2.5 cm, and -5 cm is shown in Figures 5.2.(a), (b), (c) and (d). From these figures it can be stated that, while the collar width is decreasing from $B_c=10$ cm to 2.5 cm, the lines of various Z_c values are getting closer to each other. As the vertical distance between the collar and the bed level, Z_c , increases in upward direction, the scour depths for a given time approaches towards the scour depth values of the abutment that has no collar.

The effectiveness of the collars above the bed level on the reduction of the scour depth is not as much as the collars placed at or below the bed level. When the collar of $B_c=10$ cm is placed at the bed level, for a certain time period, about 200 minutes, no scour is observed around the abutment. While the ratio of collar width to abutment length, B_c/L_a , is getting smaller, because of the reduction in the shielding capacity of the collar, this time period during which no scour occurs becomes shorter. The no-scour time period is reduced from 200 to about 65 minutes, 25 minutes and 1 minutes, while the collar widths are decreasing from $B_c=10$ cm to $B_c=7.5$ cm, 5 cm and 2.5 cm, respectively for the collar elevation of $Z_c=\pm 0$ cm. After these durations, scour hole develops rapidly and then it deepens at a slower rate and almost in a parallel form follows the curve of the collar of $Z_c=+2.5$ cm. When the collars of $B_c=10$ cm and 7.5 cm are placed below the bed level, the bed material above the collar is washed away immediately, but then the maximum scour value is recorded as the collar level because of the erosion capacity of the flow is not high enough for scouring the bed material below the collars during the test duration. When the collar of $B_c=5$ cm is placed at $Z_c=-2.5$ cm, scour phenomena starts below

the collar after $t=100$ minutes while no scour is observed below the same collar after that time period when it is placed at $Z_c=-5$ cm. When the width of the collar is decreased to $B_c=2.5$ cm, scouring occurs below the collar even when it is placed at $Z_c=-5$ cm after 100 minutes from the beginning of the test. From the general trends of the data points given in Fig. 5.2 it is clearly seen that as the width of the collar increases, and it is located further down from the bed level, the value of the time period over which no scour is observed below the collar increases. For a time period of 6 hours, the maximum scour depth for the abutment of $L_a=15$ cm with the collar of $B_c=10$ cm or 7.5 cm, when they are located at $Z_c=-2.5$ cm, doesn't exceed the value of 2.5 cm. Whereas the corresponding maximum scour depth for the abutment of $L_a=15$ cm with the collar of $B_c=5$ cm located at $Z_c=-5$ cm is 5 cm.

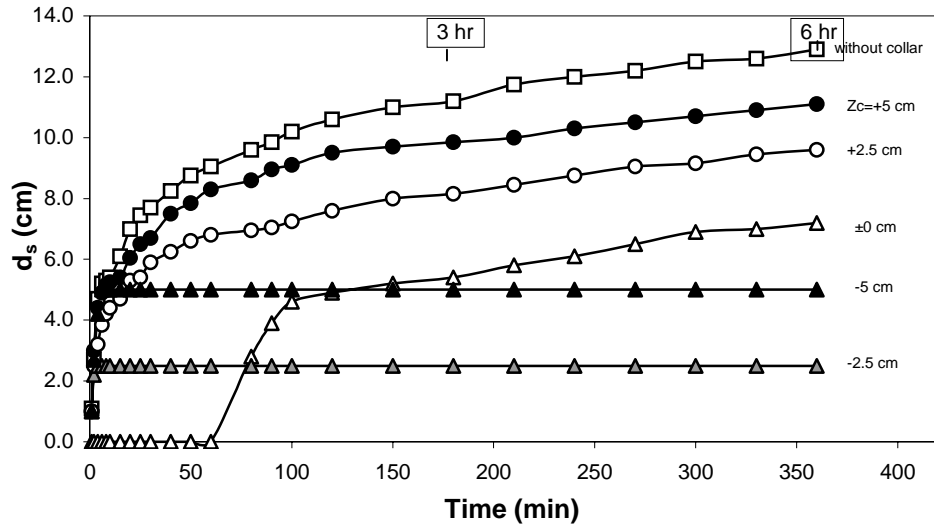


(a) $L_a=15$ cm and $B_c=10$ cm

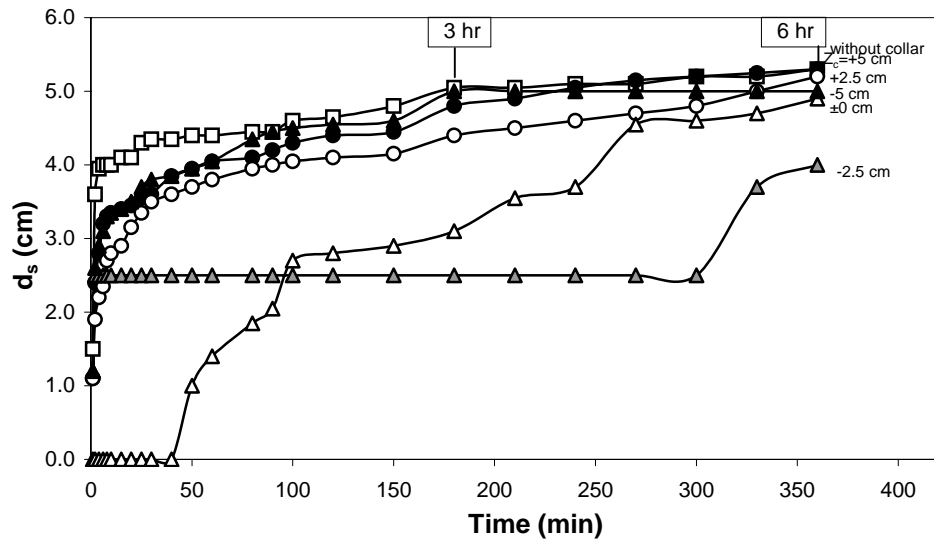


(b) $L_a=15$ cm and $B_c=7.5$ cm

Figure 5.2. Time development of maximum scour depth around the abutment for various values of Z_c



(c) $L_a=15$ cm and $B_c=5$ cm

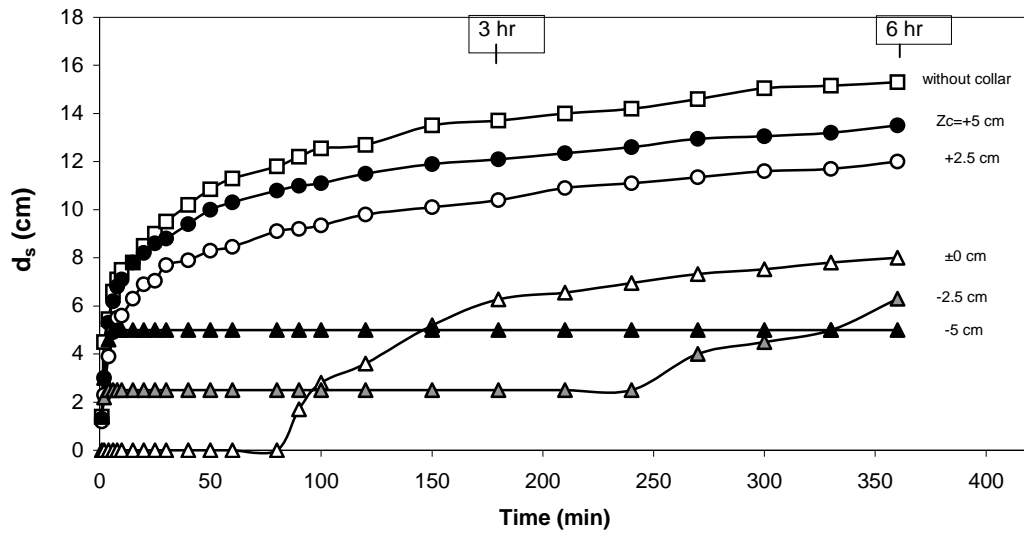


(d) $L_a=15$ cm and $B_c=2.5$ cm

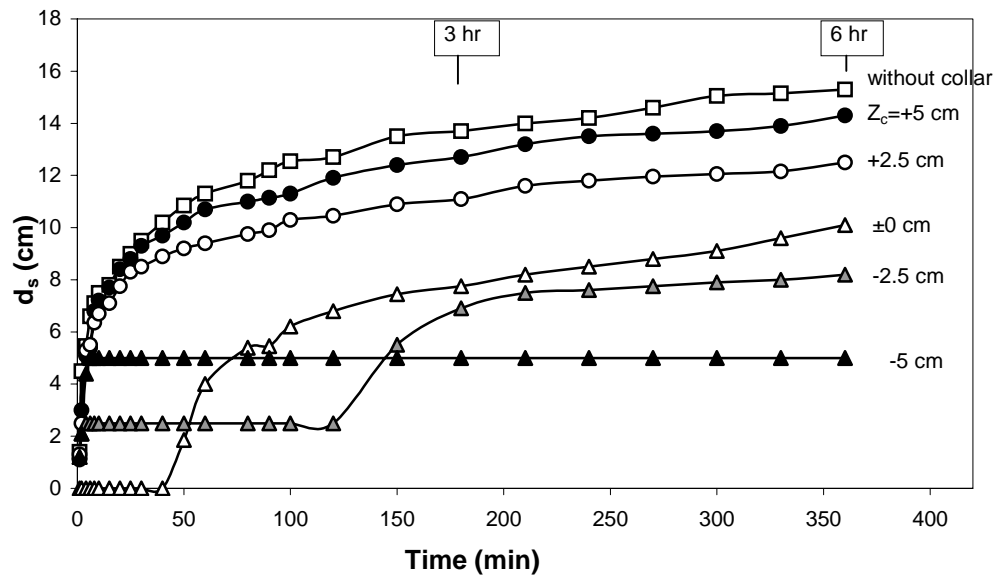
Figure 5.2. Time development of maximum scour depth around the abutment for various values of Z_c (continued)

The time variation of maximum scour depths for the third set of experiments conducted in this study is presented in Figures. 5.3. (a), (b), (c) and (d). All of the experimental parameters used here are the same as those given in Fig. 5.2 except L_a , which is 20 cm. If one analyses the trends of the data points given in these figures it is seen that for a selected set of experiment, that is for $L_a=20$ cm and any of B_c tested, as the location of the collar goes up, from -5 cm to $+5$ cm, the development of scour profile approaches to the one of no collar case. The collar of $Z_c=\pm 0.0$ cm gives no scour depth for a certain time as a function of collar width and then results in scour depths at further times greater than those of collars at $Z_c=-2.5$ cm and -5 cm.

When the collar is placed at bed level, in Figure 5.3. (a), for a certain time period, about 85 minutes, no scour is observed around the abutment. After this time period the scour hole develops rapidly and then it continues deepening at a slower rate in such a way that the data points follow almost the same trend of those of abutment having the collar at elevations above the bed level. If the collar is placed below the bed level, the flow sweeps away all the bed material over the collar down to the collar level immediately. After that, because of the weaker down flow and lower erosion capacity of the flow, no scour is observed around the abutment during the time periods of 250 minutes and 360 minutes for the collars of $Z_c=-2.5$ cm and -5 cm, respectively. At the end of these time periods the scouring process starts around the abutment of $Z_c=-2.5$ cm following a trend similar to that of $Z_c=\pm 0$ cm, while the collar of $Z_c=-5$ cm doesn't cause any further erosion by the end of the experiment. However, from the general trends of the experimental data of various Z_c values, which are given in Fig. 5.3 (a), one can conclude that, if the experiments had been conducted longer than 6 hours, deeper scour holes might have been observed around

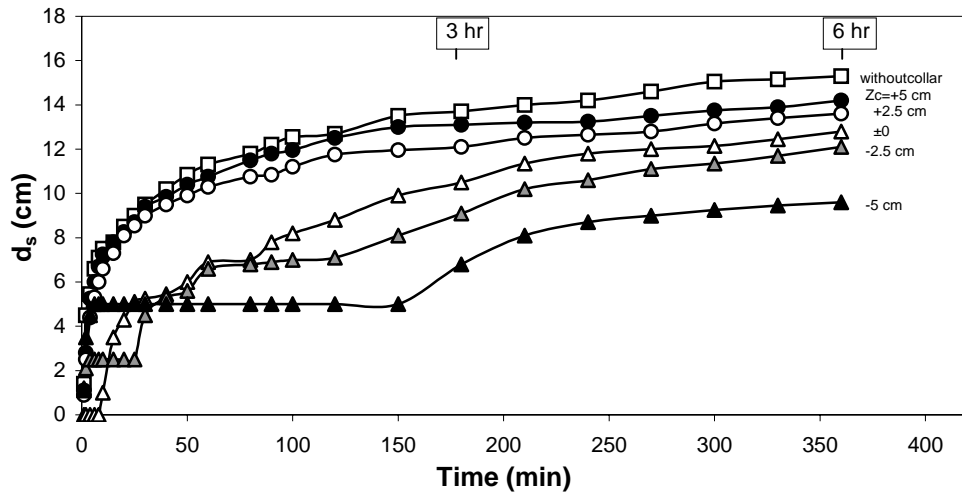


(a) $L_a=20$ cm and $B_c=10$ cm

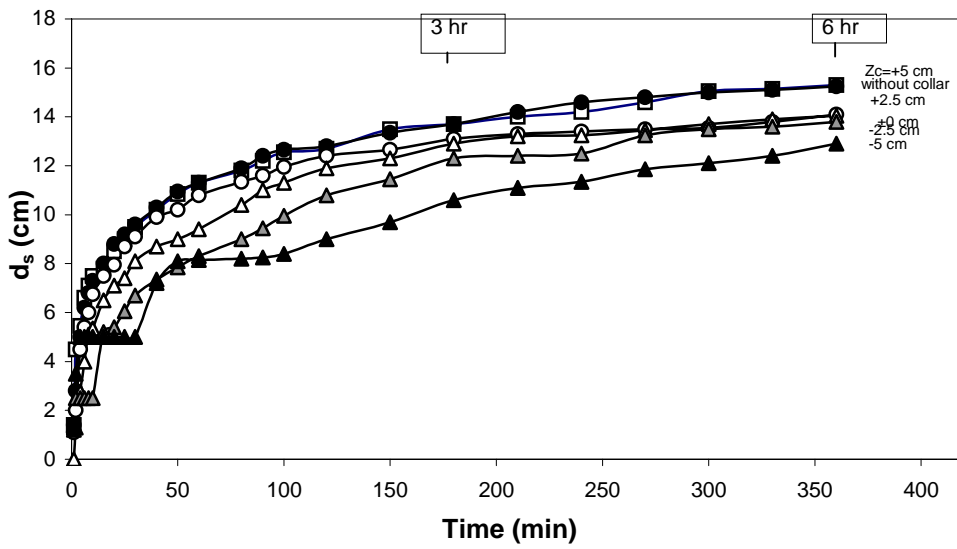


(b) $L_a=20$ cm and $B_c=7.5$ cm

Figure 5.3. Time development of maximum scour depth around the abutment for various values of Z_c



(c) $L_a=20$ cm and $B_c=5$ cm



(d) $L_a=20$ cm and $B_c=2.5$ cm

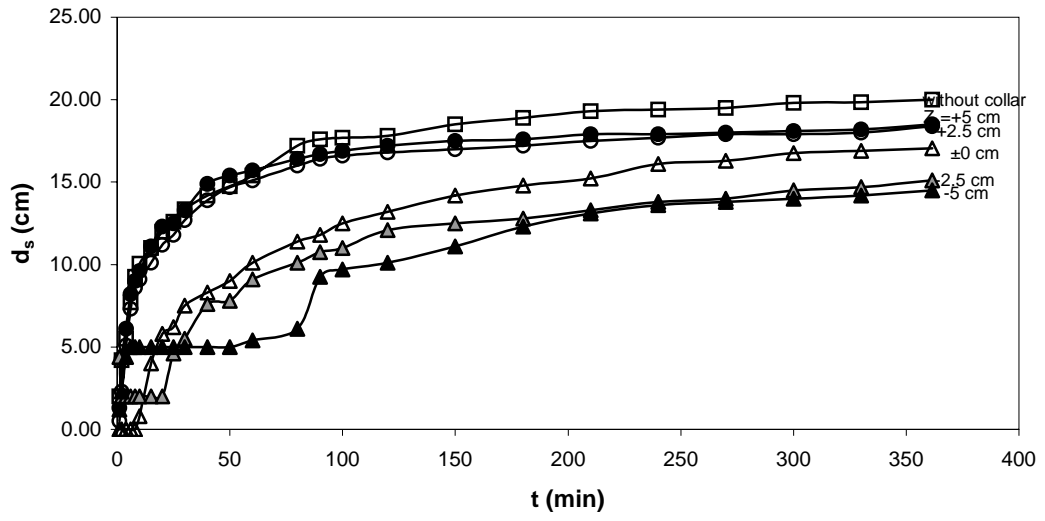
Figure 5.3. Time development of maximum scour depth around the abutment for various values of Z_c (continued)

the abutment of $Z_c = -5$ cm. However, it might be stated that the maximum scour depth to be obtained at the end of the extended time period would be much smaller than that of $Z_c = -2.5$ cm. Fig. 5.3. (a), (b), (c) and (d) show that, when the collar width is reduced from $B_c = 10$ cm to 2.5 cm, scourless time periods decrease from 360 minutes, 250 minutes and 85 minutes to 35 minutes, 15 minutes and 0.08 minutes for collar elevations of $Z_c = -5$ cm, -2.5 cm and ± 0 cm, respectively. The lines representing the scouring follow the parallel trend to each other and it is seen that, installing the collar at elevations lower than the bed level gives better results concerning the maximum scour depth. The best location of the collar of $B_c = 10$ cm for the total period of experiment is observed to be 5 cm below the bed level, which results in 67% reduction in the scour depth, compared to the case of abutment having no collar. The collars of $Z_c = -2.5$ cm and $Z_c = \pm 0$ cm reduce the maximum scour depths %59 and %48, respectively with compared to the case of abutment having no collar for the total period of the experiment.

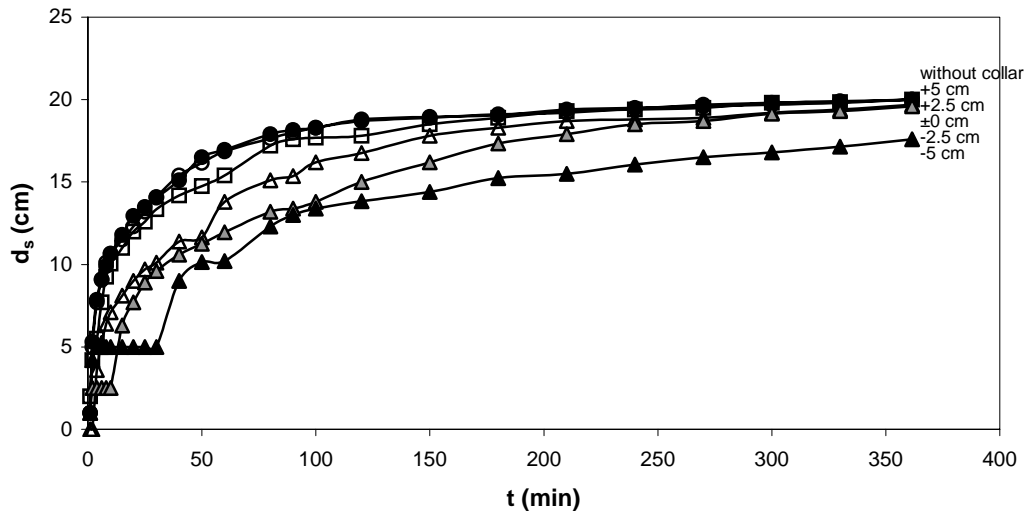
It is noticed from Figures 5.2.(a) and 5.3.(a) that; if the collar width is kept constant as $B_c = 10$ cm, the scouring begins at $t = 210$ minutes for the abutment of $L_a = 15$ cm, while at the same collar elevation it begins at $t = 85$ minutes for $L_a = 20$ cm at bed level. Similarly, when the scouring below the collar starts at $t = 250$ minutes in Fig. 5.3.(a) for $L_a = 20$ cm, $B_c = 10$ cm and $Z_c = -2.5$ cm, although the collar width is reduced from $B_c = 10$ cm to 7.5 cm, there is no scouring below the collar in Fig. 5.2.(b) for $L_a = 15$ cm at $Z_c = -2.5$ cm yet. That is, if the collar width is kept constant, its effectiveness in reducing the scour depth increases as the abutment length decreases.

In Figs. 5.4.(a), (b), (c) and (d) time development of maximum scour depth around

the abutment length of $L_a=35$ cm is shown. The effect of the collars on reducing the scour depth are not seen so much with compared to the cases of abutment lengths of $L_a=15$ cm and 20 cm. When the collar width decreases from $B_c=10$ cm to 2.5 cm, its scour reduction capacity decreases very rapidly. It loses its shielding effect almost completely at the end of the test duration. When $B_c=10$ cm is installed around the abutment, percent reduction of the maximum scour depth values are %7.5, 8.0, 15, 25, and 28 for $Z_c=+5$ cm, +2.5 cm, ± 0 cm, -2.5 cm and -5 cm, respectively. The effect of the collar elevation on reducing the scour depth becomes insignificant as the collar width decreases from 10 cm to 2.5 cm for the abutment length of $L_a=35$ cm. For the abutment of $L_a=35$ cm and $B_c=2.5$ cm the scour data of all the Z_c values tested almost overlap in Fig. 5.4.(d).

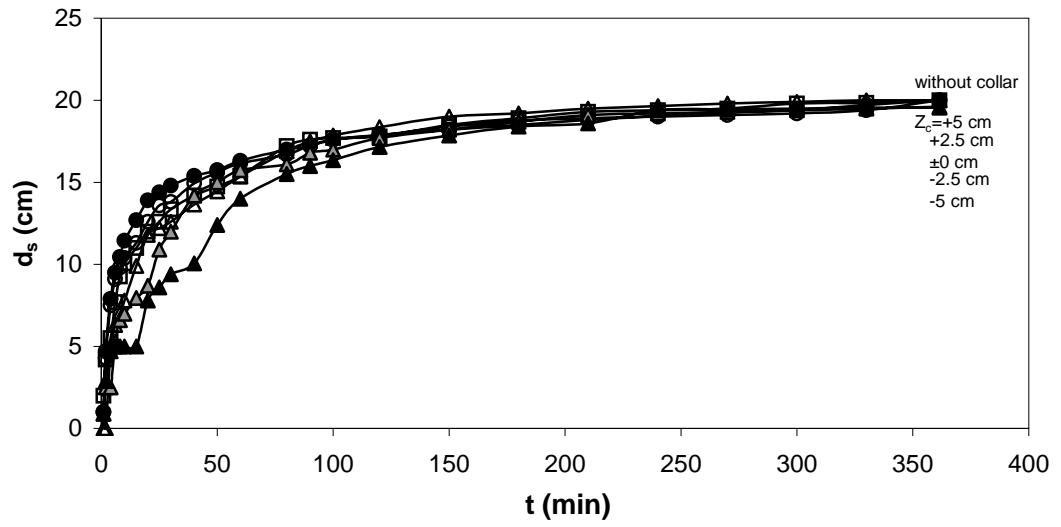


(a) $L_a=35$ cm and $B_c=10$ cm

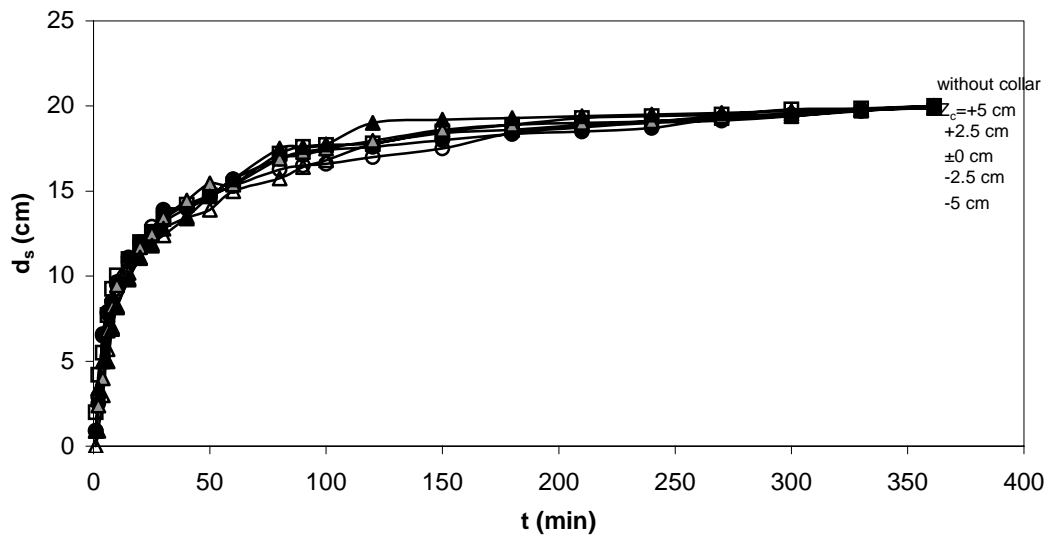


(b) $L_a=35$ cm and $B_c=7.5$ cm

Figure 5.4. Time development of maximum scour depth around the abutment for various values of Z_c



(c) $L_a=35$ cm and $B_c=5$ cm



(d) $L_a=35$ cm and $B_c=2.5$ cm

Figure 5.4. Time development of maximum scour depth around the abutment for various values of Z_c (continued)

5.5 TIME DEVELOPMENT OF d_s FOR LONG DURATION (12-HOURS) TESTS

In this part of the study, 6 runs were made each having 12-hours test duration to see if the time development of the maximum scour depths of the abutments, with or without collar cases, shows any differences. Abutment length of $L_a=20$ cm and the widest collar of $B_c=10$ cm were tested in these experiments. Firstly, time development of maximum scour depth around the abutment, which has no collar around it, was recorded during 12 hours. This procedure was repeated for the same abutment when the collar was placed at $Z_c/y=-0.50, -0.25, \pm 0.00, +0.25$ and $+0.50$. Results of the experimental data are presented in Fig. 5.5. The general trends of the d_s versus time curves of the collars placed above the bed level are very similar to that of the abutment having no collar. The only difference between these curves is the d_s values corresponding to the same time period. The d_s value of the abutment having no collar is always higher than the other ones. And they both require many hours to reach the equilibrium scour depth. When the collar is placed on the bed level, for a certain time period no scour is observed around the abutment (about 50 minutes), and then the trend of the data points follow a similar trend as those having collars at higher elevations on the abutment. If the collars are placed below the bed level, such as $Z_c=-2.5$ cm and -5 cm, after a very short time the material between the bed level and the collar is washed away and the scour depths do not exceed the levels of the collars for a certain time period; 250 minutes for $Z_c=-2.5$ cm, and 720 minutes for $Z_c=-5$ cm. The time periods required to have the following maximum scour depths around the abutment; $d_s=0.0$ cm, 2.5 cm and 5 cm are 50 minutes, 100 minutes and 160 minutes, respectively, if the collar is placed at the bed level.

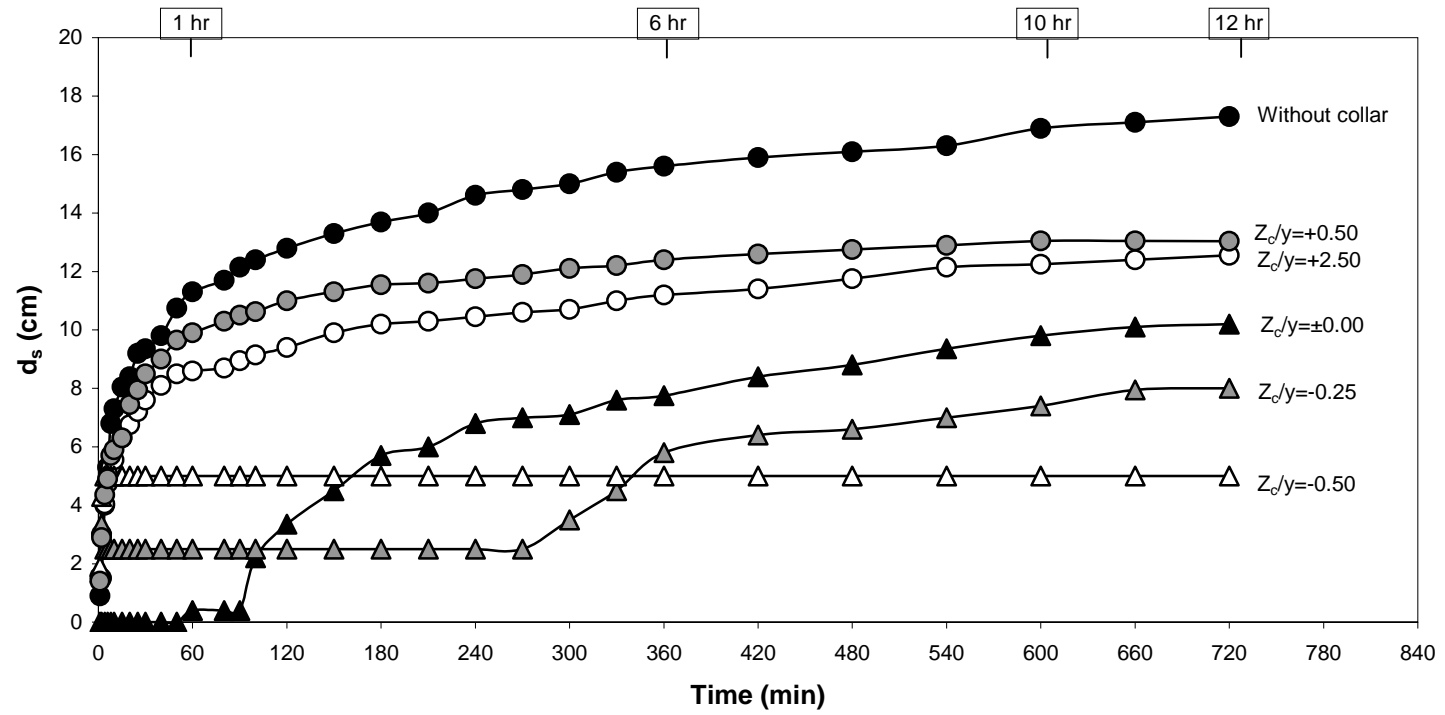


Figure 5.5 Time development of scouring around the abutment for $L_a=20$ cm and $B_c=10$ cm, for various values of Z_c ($T=12$ hours)

When the collar is placed at $Z_c = -2.5$ cm, the maximum scour depth becomes $d_s = 2.5$ cm until $t = 300$ minutes, and then it becomes $d_s = 5$ cm at $t = 445$ minutes. If the collar is at $Z_c = -5$ cm, until the end of the experiments d_s value becomes constant as 5 cm. Probably this d_s value will exceed 5 cm at the end of the test durations longer than 12 hours, but it can be concluded that its equilibrium scour depth will be much smaller than the one of the abutment having no collar.

Therefore, for design purpose when the location of the collar is to be selected, the expected time period of the design discharge becomes an important parameter.

5.6 STUDIES ON EQUILIBRIUM SCOUR DEPTH AROUND THE ABUTMENTS

Due to limitations in the laboratory conditions, duration of the experiments was kept constant as 6 hours. Therefore, all comparisons of scour depths presented here for the cases with or without collar are the results of experiments having 6-hours time period. However, it is very well known that the time necessary for the equilibrium scour cases, especially for cases without collar, is longer than 6 hours (Melville, 1992; Lim, 1997). In order to see how the scouring process develops after 6 hours, a few tests were repeated for 12 hours as discussed in the previous sections. From the results of these experiments it was seen that for both cases, namely with or without collar cases, the equilibrium scour conditions were not reached. When the results of 12 hours long and 6 hours long experiments are compared, it is observed that although scouring process continues after 6 hours, the rate of scouring decreases with time.

5.6.1 Comparison of Experimental Results with the equation of Coleman et. al. (2003)

Coleman et. al. (2003) derived an equation for the variation of scour depth d_s with time, with both parameters normalized by their equilibrium values (d_{se} and t_e , respectively).

$$\frac{d_s}{d_{se}} = \exp \left[-0.07 \left(\frac{U}{U_c} \right)^{-1} \left| \ln \left(\frac{t}{t_e} \right) \right|^{1.5} \right] \quad (5.9)$$

where; t_e is the time required to reach the equilibrium scour depth and nondimensionalised as:

$$t^* = \frac{t_e U}{L_a} \quad (5.10)$$

and based on the data of $U/U_c=0.46-0.99$;

$$t^* = 10^6 \left(\frac{U}{U_c} \right)^3 \left(\frac{y}{L_a} \right) \left\{ 3 - \left[1.2 \left(\frac{y}{L_a} \right) \right] \right\} \quad \text{for } y/L_a < 1 \text{ and } L_a/d_{50} > 60 \quad (5.11)$$

$$t^* = 1.8 \times 10^6 \left(\frac{U}{U_c} \right)^3 \quad \text{for } y/L_a \geq 1 \text{ and } L_a/d_{50} > 60 \quad (5.12)$$

Assuming that the equations given above are applicable to tests conducted in this study due to some common experimental conditions, an attempt was made to determine the corresponding d_s/d_{se} values. Table 5.1 presents all the related data of this study. This table shows that, at the end of the 6-hours test duration maximum scour depths reach 63-69 % of the equilibrium scour depth. Test results of the experiment conducted for a test period of 12 hours for the abutment of $L_a=20$ cm is also given in Table 5.5 at the last row. For this case the d_s/d_{se} value is about 73 %. An increase of 100 % in test period results in small amount of increase in the value of d_s/d_{se} , from 63 % to 73 %.

Table 5.1 Parameters used in calculation of the equilibrium scour depth

L_a (cm)	y (cm)	U (m/s)	y/L_a	L_a/d_{50}	U/U_c	d_s (cm)	t^*	t_e (min)	t (min)	t/t_e	d_{se} (cm)	d_s/d_{se}
15	10.00	0.33	0.67	101.35	0.90	12.60	1069200	8100	360	0.044	19.33	0.652
20	10.00	0.33	0.50	135.14	0.90	15.30	874800	8836	360	0.041	23.87	0.641
25	10.00	0.33	0.40	168.92	0.90	18.30	734832	9278	360	0.039	28.86	0.634
35	10.00	0.33	0.29	236.49	0.90	20.10	553445	9783	360	0.037	32.06	0.627
25	9.60	0.38	0.38	168.92	0.98	21.50	917712	10063	360	0.036	33.18	0.648
20	9.60	0.38	0.48	135.14	0.98	18.60	1095096	9606	360	0.037	28.44	0.654
15	9.60	0.38	0.64	101.35	0.98	16.10	1344474	8845	360	0.041	24.25	0.664
25	8.85	0.37	0.35	168.92	1.00	22.20	911621	10266	360	0.035	34.10	0.651
20	8.85	0.37	0.44	135.14	1.00	18.15	1092533	9843	360	0.037	27.67	0.656
15	8.85	0.37	0.59	101.35	1.00	15.70	1352280	9137	360	0.039	23.57	0.666
25	7.95	0.38	0.32	168.92	0.98	20.00	783685	8661	360	0.042	29.99	0.667
20	7.95	0.38	0.40	135.14	0.98	18.00	943914	8346	360	0.043	26.79	0.672
15	7.95	0.38	0.53	101.35	0.98	15.40	1179238	7820	360	0.046	22.65	0.680
25	7.15	0.37	0.29	168.92	0.97	18.90	693490	7810	360	0.046	27.92	0.677
20	7.15	0.37	0.36	135.14	0.98	17.50	865080	7794	360	0.046	25.74	0.680
15	7.15	0.37	0.48	101.35	0.98	16.10	1089285	7360	360	0.049	23.40	0.688
25	6.45	0.36	0.26	168.92	0.98	17.80	653303	7561	360	0.048	26.02	0.684
20	6.45	0.36	0.32	135.14	0.98	17.15	793135	7344	360	0.049	24.93	0.688
15	6.45	0.36	0.43	101.35	0.98	15.50	1005306	6981	360	0.052	22.33	0.694
20	10.00	0.33	0.50	135.14	0.90	17.30	874800	8836	720	0.081	23.57	0.734

5.6.2 Comparison of Experimental Results with Oliveto and Hager's (2002)

Equation

Oliveto and Hager (2002) proposed Eqn. (5.13), which is the same as Eqn. (5.7) described in Section 5.2, for the development of scour equation by conducting a series of experiments and tested this equation with the available literature data.

$$Z = 0.068 N \sigma^{-1/2} F_d^{1.5} \log(T) \quad (5.13)$$

where; Z=dimensionless scour depth and

$$Z = d_s / L_R \quad (5.14)$$

$$L_R = L_a^{2/3} y^{1/3} \quad (5.15)$$

N=shape number equal to N=1 for circular piers and N=1.25 for rectangular abutments, F_d =densimetric Froude number :

$$F_d = \frac{U}{(g' d_{50})^{1/2}} \quad (5.16)$$

g' is reduced gravitational acceleration and ;

$$g' = \{(\rho_s - \rho) / \rho\} g \quad (5.17)$$

T is the dimensionless time of scour and given the equation below;

$$T' = \{(g' d_{50})^{1/2} / L_R\} t \quad (5.18)$$

Figure 5.6 presents the experimental data of this study in the form of Eqn. (5.13) proposed by Oliveto and Hager (2002). This figure shows that the general trends of the experimental data are quite consistent with Eqn. (5.13) especially for values of T greater than about 5000.

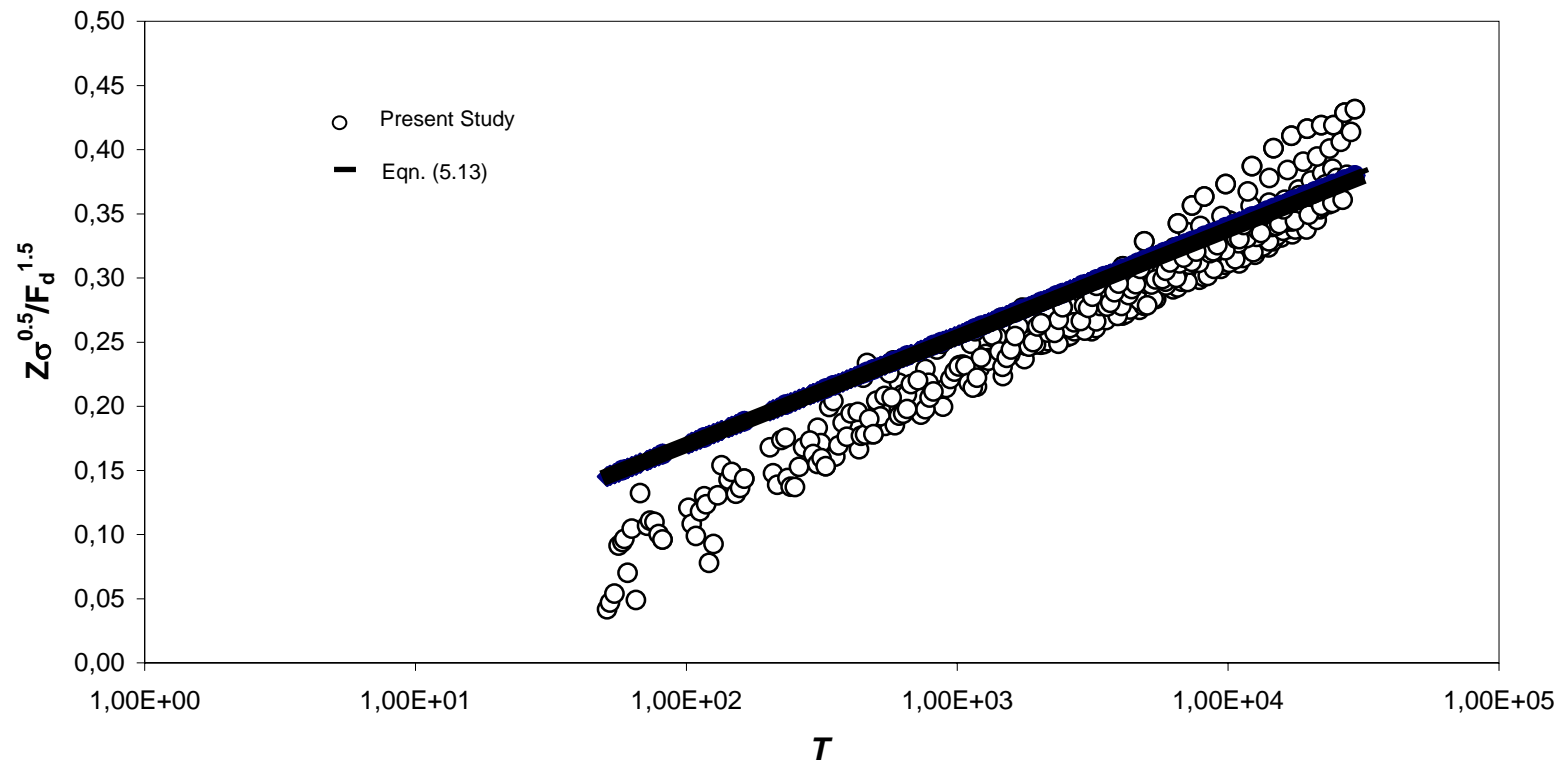


Figure 5.6. Comparison of present data with Oliveto and Hager's (2002) Equation

5.7 CONCLUSIONS

In this study time development of the local scour around the abutment with and without collars of various sizes and installed at different elevations was studied. It is observed that, while the elevation of the collars decreases below the bed material, the local scour depth decreases. When the collar is placed above the bed level, it has also reducing scour depth effect but not as much as those to be installed below the bed level.

Increasing the width of the collar also affects the maximum scour depth around the abutment. If the collar width is kept constant, it protects the abutment, which is shorter with compared to the others, more efficiently.

Using collar at abutments is very effective in slowing down the development of scouring. As floods often last much shorter than the equilibrium durations, this property of collars becomes important in practice to prevent the abutments against scouring.

At the end of the 6-hours test duration maximum scour depth reaches 63-69 % of the equilibrium scour depth. Based on the results of a specific test of duration of 12 hours it was seen that, this percentage increased up to 73%.

CHAPTER 6

INTERACTION BETWEEN THE ABUTMENT AND THE PIER

6.1 GENERAL

Local scouring process that occurs in a river or stream in the presence of bridge piers or abutments is a problem that received a lot of attention in the past (Raudkivi and Ettema, 1983; Meville and Shutherland, 1989; Breusers and Roudkivi, 1991; Johnson 1995; Melville, 1997; Ettema et. al., 1998; Ahmed and Rajaratnam, 1998; Johnson and Dock, 1998; Fischenich and Landers, 2000; Sturm and Janjua, 1994; Kuhnle et. al., 2002; Chang et. al., 2004; Sheppard et. al., 2004). Among the great number of experimental and field studies, scouring due to a single pier or an abutment usually has been studied separately. However, there have been a little study about interaction between piers in the scour process, a pier and an abutment have not been investigated together. In this part of the study, the problem of the interaction between an abutment and a pier is studied. The collar effect on the interaction cases is also tested and the results are illustrated.

6.2 LITERATURE REVIEW

Luigi et. al. (2001) conducted experiments with three piers (round-nosed with a length and width of 8 cm and 2 cm, respectively) which are aligned to each other and spaced 40 cm apart. The angle between the flow direction and pier axis were varying as 15°, 35°, 45°, 60°, and 80°. They observed that as the angle increases the

points of maximum scour depth moves along the exposed side of the pier. In some cases the maximum scour depth for one pier can be 30% over the maximum depth for another pier. They reported that the flow field becomes more complex and piers have a stronger influence over the other.

Choi and Ahn (2001) performed a series of experiments by the successive bridge piers along the flow direction. They used five semi-circular piers, having width and length of 1.24 cm and 1.73 cm, respectively. Four of the piers were placed in a straight line through the flow direction while one of them was installed with the distortion between the centerline of the pier with the maximum length of 8 times of the pier width. It was indicated that the local scour depth are severely affected by the interaction between bridge piers. In the low flow, which can be characterized low Froude number; the maximum scour depth was observed when the piers were installed in straight line in the flow direction. However, in the high flow, which can be characterized high Froude number, the maximum scour is obtained when the piers were installed with some distortion from the flow direction.

6.3 DIMENSIONAL ANALYSIS

For clear-water approach flow conditions, if there is interaction between the abutment and the pier, which are rounded with or without a collar, the maximum scour depth, $(d_s)_{\max}$, at an abutment is a function of:

$$\left[(d_s)_{\max} \right]_{\text{int}} = f \left\{ \begin{matrix} L_a, B_a, B_c, Z_c, T_c, U, y, S, g, \\ \rho_s, \rho, \mu, d_{50}, \sigma_g, t, B, D, \lambda \end{matrix} \right\} \quad (6.1)$$

where, D =pier diameter; λ is the distance between the abutment and the periphery of the pier on a straight line perpendicular to the flow direction; $[(d_s)_{\max}]_{\text{int.}}$ is the maximum scour depth around the abutment or pier, interacting each other; $(d_s)_{\max}$ is the maximum scour depth around the pier or abutment in separated cases. The definitions of the other parameters are the same as given in Chapter 2 and 3.

Considering that the experiments are conducted under clear-water flow conditions with one sediment size and constant; bed slope, collar width, channel width, collar thickness, abutment width, duration of the experiment, and discharge, the relationship given above can be put into the dimensionless form:

$$\frac{[(d_s)_{\max}]_{\text{int.}}}{[(d_s)_{\max}]_{\text{or.}}} = f\left(\frac{L_a}{B_a}, \frac{L_a}{B_c}, \frac{Z_c}{y}, \frac{L_a}{D}, \frac{D}{y}, \frac{\lambda}{L_a}\right) \quad (6.2)$$

For no-collar-case:

$$\frac{[(d_s)_{\max}]_{\text{or.}} - [(d_s)_{\max}]_{\text{int.}}}{[(d_s)_{\max}]_{\text{or.}}} = f\left(\frac{L_a}{B_a}, \frac{L_a}{D}, \frac{D}{y}, \frac{\lambda}{L_a}\right) \quad (6.3)$$

6.4 EXPERIMENTAL PROCEDURE

All tests were performed near the threshold flow condition at $Q=0.055 \text{ m}^3/\text{s}$ and $y=9.60 \text{ cm}$. The abutment lengths and the pier diameters are $L_a=25 \text{ cm}$ and 15 cm ; and $D=10 \text{ cm}$ and 5 cm , respectively. Firstly, the abutment, which was placed to the sidewall of the channel and the pier, which was placed to the center of the channel width, were tested separately in the recess section of the channel. After that, the

abutment and the pier have been tested together. For the experiments on interaction cases, the longitudinal distance, λ , between the abutment and the pier is varied as, $\lambda/L_a=1, 1.5, 2$ and 2.5 for $L_a=25$ cm and $1.5, 2, 2.5$ and 3 for $L_a=15$ cm. Then, the abutment and the pier were tested separately with collars of $B_c=10$ cm for the abutments and $B_{cp}=D$ (B_{cp} =the width of the collar around the pier) for the pier. From the previous studies, it is known that the efficiency of the collar installed on the abutment increases when it is placed below the bed level. But, according to the studies given in the literature it is said that the scour reducing capacity of the collar installed on the pier is the maximum when the collar is placed at the bed level. So, while the depth of the collar was kept constant $Z_c=-5$ cm for the abutments, it was varied as $Z_c=-5$ cm and ± 0 cm for the piers. Therefore, the interaction cases were arranged as below:

- 1) Both the abutment and the pier have no collar around them,
- 2) The abutment has the collar but the pier doesn't have collar around it,
- 3) The abutment has a collar around it at $Z_c=-5$ cm and the pier has rounded by a collar at $Z_c= \pm 0$ cm,
- 4) Both the abutment and the pier have collars around them at $Z_c=-5$ cm.

6.5 DISCUSSION OF RESULTS

6.5.1. Interaction Cases

The presence of the abutment and the pier together can generate a complex flow field between them and this leads to the occurrence and development of a scour process that can be quite different from the ones of an abutment and a pier which will occur when they are tested separately. For this reason, a series of experiments were performed to investigate the characteristics of the maximum scour depths around the abutment and the pier various spacing, λ , between them as 25 cm, 37.5 cm, 50 cm, and 62.5 cm for the experiments performed for $L_a=25$ cm, and 22.5 cm, 35 cm, 45 cm and 62.5 cm for $L_a=15$ cm. Two different pier diameters, $D=10$ cm and 5 cm, were tested.

In these experiments, the selected abutments, the piers and their combinations were tested without and with collars located at various elevations on both abutments and piers. The collar width was $B_c=10$ cm for all the abutments while it was selected for the piers as equal to the pier diameter, $B_{cp}=D$.

After collecting the data for all interaction cases tested, the comparisons between them were done and how the abutment and the pier affect each other for all cases were investigated.

6.5.2. Comparisons of Interaction Cases 1, 2, 3 and 4

Tables 6.1 to 6.4 present the characteristic parameters of the abutments and the piers, and flow as well as maximum scour depths occurred around the abutments at point P_1 , and around the piers at points P_2 , P_3 , P_4 corresponding to the experiments

conducted with only abutment, pier, and combination of them without collar around them.

Table 6.1 reveals that the presence of the bridge pier in the flow medium reduces the maximum scour depth around the abutment as the value of λ increases. However, same thing can not be said for the abutment. The abutment results in small increases on the scour depth around the pier.

All the parameters of Case 2 are the same as those of Case 1 except D, which is 5 cm (Table 6.2). When the pier diameter is reduced to D=5 cm, half of the one given in Table 6.1, the scour depths around this pier, when there is no abutment in the channel, become almost half of those of the pier of D=10 cm. In this case, the presence of the pier in the flow medium does not affect the maximum scour depths around the abutment for each value of λ tested. The maximum scour depths at P₂, P₃ and P₄ increase with increasing λ and then become maximum for $\lambda=37.5$ cm. For the remaining λ values, $(d_s)_{\max}$ values at P₂, P₃ and P₄ decrease as λ increases. One can say that at further values of λ , $(d_s)_{\max}$ values at P₂, P₃ and P₄ approach to those given in the table for only pier case.

Table 6.3 presents the maximum scour depths for L_a=15 cm and D=10 cm. The main difference between this table and Table 6.1 is only the reduction in the length of the abutment from 25 cm to 15 cm. As the value of λ increases, $(d_s)_{\max}$ value at P₁ value slightly increases while those at P₂, P₃ and P₄ decrease and approach almost their initial values.

Table 6.1. Schematic view and the results of the interaction **Case1**

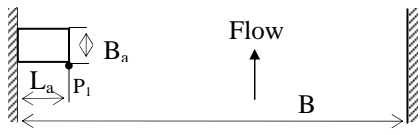
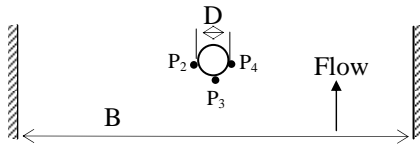
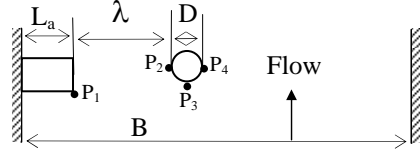
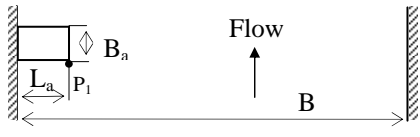
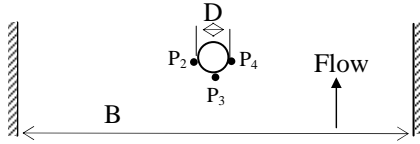
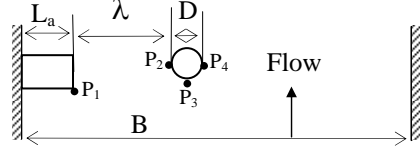
$L_a=25$ cm, $B_a=10$ cm, $D=10$ cm, $B=1.5$ m, $Q=0.055\text{m}^3/\text{s}$, $y=9.6$ cm <i>*There is no collar around the Pier</i> <i>*There is no collar around the Abutment</i>					
Positions of the Circular Pier and the Abutment	λ (cm)	Maximum Scour Depth (cm)			
		P ₁	P ₂	P ₃	P ₄
	-	21.5	-	-	-
	-	-	12.3	13	12.6
	25.0	20.45	14.1	15.4	14.1
	37.5	16	16.3	15.9	15.7
	50.0	15.35	15.35	15.6	14.9
	62.5	14.3	14.3	14.4	13.35

Table 6.2. Schematic view and the results of the interaction **Case 2**

$L_a=25$ cm, $B_a=10$ cm, $D=5$ cm, $B=1.5$ m, $Q=0.055\text{m}^3/\text{s}$, $y=9.6$ cm <i>*There is no collar around the Pier</i> <i>*There is no collar around the Abutment</i>					
Positions of the Circular Pier and the Abutment	λ (cm)	Maximum Scour Depth (cm)			
		P ₁	P ₂	P ₃	P ₄
	-	21.5	-	-	-
	-	-	6.8	6.5	7
	25.0	21.1	8.5	8.8	7.7
	37.5	21.2	11	11.1	10.8
	50.0	21.1	10	10.6	9.7
	62.5	21	8.5	8.7	8.25

The effect of pier diameter, $D=5$ cm, on the scour depth at the abutment is negligible in Case 4 (Table 6.4) similar to Case 2. Whereas, due to the presence of the abutment, maximum scour depths around the pier first remains almost constant at values of $\lambda=22.5$ cm and 30.0 cm, but later on decrease as λ increases.

Variation of λ/L_a with $[(d_s)_{\max}]_{\text{int.}}/[(d_s)_{\max}]_{\text{or.}}$ ratios for the interaction cases of 1, 2, 3 and 4 are given in Figure 6.1. Here $[(d_s)_{\max}]_{\text{int.}}$ designates the maximum scour depth around the pier or the abutment in interaction cases, $[(d_s)_{\max}]_{\text{or.}}$ depicts the maximum scour depth at the pier and the abutment corresponding to the experiments conducted with only pier or abutment. In Figure 6.1 the data points of abutment fall below $[(d_s)_{\max}]_{\text{int.}}/[(d_s)_{\max}]_{\text{or.}}=1$ while those of pier fall above $[(d_s)_{\max}]_{\text{int.}}/[(d_s)_{\max}]_{\text{or.}}=1$ for varying λ/L_a values. This situation clearly implies that there is positive influence of the pier on the abutment concerning the maximum scour depth at P_1 . For values of λ/L_a varying between 1.0 and 2.5 the $[(d_s)_{\max}]_{\text{int.}}/[(d_s)_{\max}]_{\text{or.}}$ values of piers vary between about 1.40 and 1.70 which means that the abutments result in 40%-70% deeper scour holes around the piers. For λ/L_a greater than about 2.5, $[(d_s)_{\max}]_{\text{int.}}/[(d_s)_{\max}]_{\text{or.}}$ becomes only function of L_a/D and is almost independent of λ/L_a .

Table 6.3. Schematic view and the results of the interaction **Case 3**

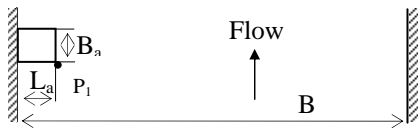
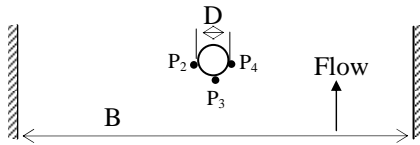
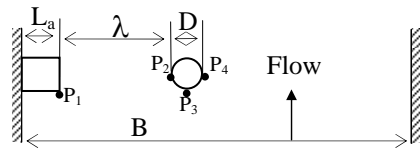
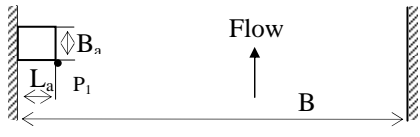
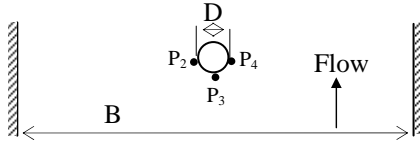
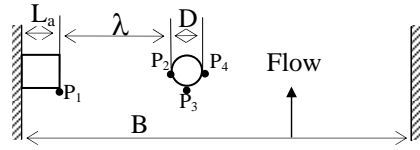
$L_a=15$ cm, $B_a=10$ cm, $D=10$ cm, $B=1.5$ m, $Q=0.055\text{m}^3/\text{s}$, $y=9.6$ cm <i>*There is no collar around the Pier</i> <i>*There is no collar around the Abutment</i>					
Positions of the Circular Pier and the Abutment	λ (cm)	Maximum Scour Depth (cm)			
		P_1	P_2	P_3	P_4
	-	16.1	-	-	-
	-	-	12.3	13.0	12.6
	22.5	13.9	14.4	15.51	14.5
	30.0	14.9	14.2	14.4	14.5
	37.5	14.65	11.8	13.7	12
	45.0	15.05	12.5	13.3	11.9

Table 6.4. Schematic view and the results of the interaction **Case 4**

$L_a=15$ cm, $B_a=10$ cm, $D=5$ cm, $B=1.5$ m, $Q=0.055\text{m}^3/\text{s}$, $y=9.6$ cm <i>*There is no collar around the Pier</i> <i>*There is no collar around the Abutment</i>					
Positions of the Circular Pier and the Abutment	λ (cm)	Maximum Scour Depth (cm)			
		P_1	P_2	P_3	P_4
	-	16.1	-	-	-
	-	-	6.8	6.5	7
	22.5	15.9	10	9.7	9.7
	30.0	15.4	9.9	9.9	9.7
	37.5	16.4	9.2	8.6	8.2
	45.0	16.25	7.9	8.5	7.7

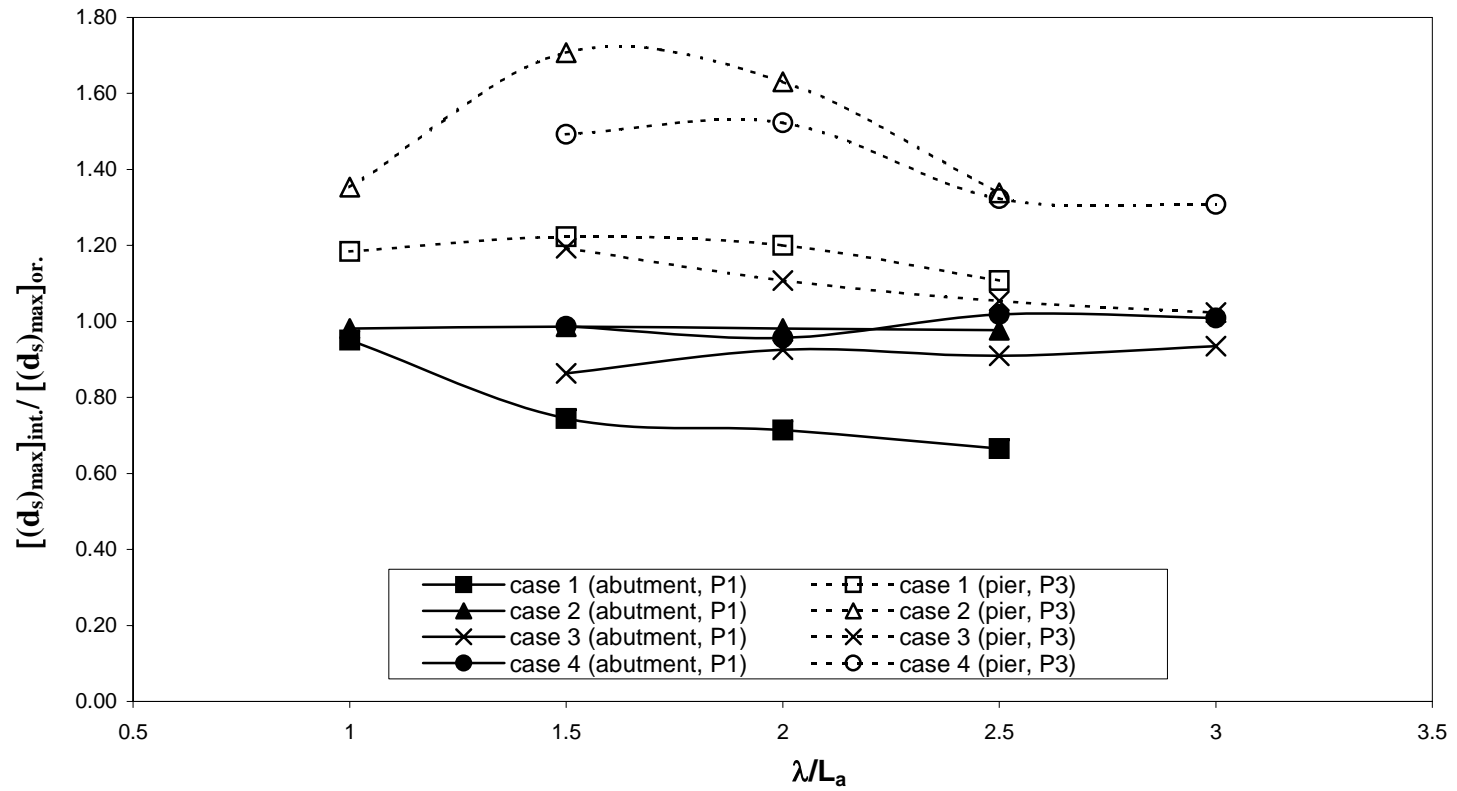


Figure 6.1. Variation of maximum scour depths around the abutment and the pier in the interaction
Cases of 1, 2, 3 and 4.

6.5.3. Comparisons of Interaction Cases 5, 6, 7 and 8

From earlier experiments it had been observed that as a protective device a collar could be used around an abutment at about -5 cm below the bed level to have a scour hole of minimum depth. For this reason, in interaction cases 5, 6, 7 and 8 a collar was used around the abutment at -5 cm below the bed level while the pier to be tested with it had no collar. Schematic views of the cases tested and their results are presented in Tables 6.5-6.8.

When only an abutment of $L_a=15$ cm and $B_a=10$ cm is tested in the channel with a collar of $B_c=10$ cm located at $Z_c=-5$ cm, the $(d_s)_{\max}$ at P_1 value is determined as 5.0 cm, (Table 6.5) which was 16.1 cm when the collar was not used (Table 6.3).

As it is seen, a reduction of about 69 % in maximum scour depth at point P_1 is achieved due to the presence of the collar on the abutments. When a pier of $D=10$ cm is introduced into the flow medium across the abutment at a distance of λ which varies between 25.0 cm to 62.5 cm, the maximum scour depth at point P_1 penetrates below the collar and varies between 9.05 cm and 9.9 cm. The presence of the pier into the flow medium makes the scour depth at point P_1 almost double. Even though λ increases from 25.0 cm to 62.5 cm, the magnitude of the scour depth does not almost change. It means that at λ values greater than 62.5 cm, the effect of the pier on the scour depth at point P_1 may decrease and eventually at much higher values of λ the scour depth may approach to the original one of 5 cm. At values of λ less than 25.0 cm, scour depths greater than 10.0 cm at point P_2 may be observed.

On the other hand, scour depths at points P_2 , P_3 , and P_4 around the pier decrease as λ increases and approach to the initial values, which are 12.3 cm, 13 cm and 12.6 cm, respectively.

Similar situation is observed in Tables 6.6 where the diameter of the pier is $D=5$ cm, while all the other parameters are the same as those given in Table 6.5. The presence of the abutment affects the scour depths around the pier in a negative direction as λ value decreases.

Table 6.5. Schematic view and the results of the interaction **Case 5**

$L_a=25$ cm, $B_a=10$ cm, $D=10$ cm, $B=1.5$ m, $Q=0.055\text{m}^3/\text{s}$, $y=9.6$ cm <i>*There is no collar around the Pier</i> <i>*There is a collar around the Abutment at $Z_c=-5$ cm, $B_c=10$ cm</i>					
Positions of the Circular Pier and the Abutment	λ (cm)	Maximum Scour Depth (cm)			
		P ₁	P ₂	P ₃	P ₄
	-	5.0	-	-	-
	-	-	12.3	13	12.6
	25.0	9.6	16.4	16.5	15.35
	37.5	9.9	15.4	15.85	15.85
	50.0	9.2	14.5	14.8	13.5
	62.5	9.05	13.5	14.5	13.5

Table 6.6. Schematic view and the results of the interaction **Case 6**

$L_a=25$ cm, $B_a=10$ cm, $D=5$ cm, $B=1.5$ m, $Q=0.055\text{m}^3/\text{s}$, $y=9.6$ cm <i>*There is no collar around the Pier</i> <i>*There is a collar around the Abutment at $Z_c=-5$ cm, $B_c=10$ cm</i>					
Positions of the Circular Pier and the Abutment	λ (cm)	Maximum Scour Depth (cm)			
		P ₁	P ₂	P ₃	P ₄
	-	5.0	-	-	-
	-	-	6.8	6.5	7
	25.0	10.3	13.6	13.6	13.35
	37.5	10.6	11.35	10.4	10.75
	50.0	10.6	8.2	8.6	8.6
	62.5	10.9	8.1	8.2	8.2

In Tables 6.7 and 6.8 the major parameters are $L_a=15$ cm, and $D=10$ cm, and $L_a=15$ cm, and $D=5$ cm, respectively. 10 cm reduction in the abutment length compared to the previous cases, results in a major reduction in the scour depth at point P_1 around the abutment even in interaction cases for any value of λ tested regardless of what the pier diameter is; 10 cm or 5.0 cm. The original scour depth of 5.0 cm at point P_1 corresponding to single-abutment experiment, remains constant even after the use of the pier in the experiments. It means that at λ values greater than 22.5 cm, the scour depth at point P_1 will not be greater than 5.0 cm. Whereas, the scour depths at points P_2 , P_3 and P_4 around the pier first increase compared to single-pier experiments at $\lambda=22.5$ cm, and then decrease and approach to the original values as λ gets greater than 22.5 cm.

Figure 6.2 gives the relationship between $[(d_s)_{\max}]_{\text{int.}} / [(d_s)_{\max}]_{\text{or.}}$ and λ/L_a for both piers and abutments tested in interaction cases 5-8. Here, the data of small L_a/D ratios, similar to Figure 6.1, give minimum values of $[(d_s)_{\max}]_{\text{int.}} / [(d_s)_{\max}]_{\text{or.}}$ with increasing λ/L_a . $[(d_s)_{\max}]_{\text{int.}} / [(d_s)_{\max}]_{\text{or.}}$ is almost independent of λ/L_a for λ/L_a greater than about 2.

Table 6.7. Schematic view and the results of the interaction **Case 7**

$L_a=15$ cm, $B_a=10$ cm, $D=10$ cm, $B=1.5$ m, $Q=0.055\text{m}^3/\text{s}$, $y=9.6$ cm <i>*There is no collar around the Pier</i> <i>*There is a collar around the Abutment at $Z_c=-5$ cm, $B_c=10$ cm</i>					
Positions of the Circular Pier and the Abutment	λ (cm)	Maximum Scour Depth (cm)			
		P ₁	P ₂	P ₃	P ₄
	-	5.0	-	-	-
	-	-	12.3	13	12.6
	22.5	5.0	15.3	16.3	15.7
	30.0	5.0	14.5	15.5	15
	37.5	5.0	13.2	14.6	12.8
	45.0	5.0	14.3	13.2	12.8

Table 6.8. Schematic view and the results of the interaction **Case 8**

$L_a=15$ cm, $B_a=10$ cm, $D=5$ cm, $B=1.5$ m, $Q=0.055\text{m}^3/\text{s}$, $y=9.6$ cm <i>*There is no collar around the Pier</i> <i>*There is a collar around the Abutment at $Z_c=-5$ cm, $B_c=10$ cm</i>					
Positions of the Circular Pier and the Abutment	λ (cm)	Maximum Scour Depth (cm)			
		P ₁	P ₂	P ₃	P ₄
	-	5.0	-	-	-
	-	-	6.8	6.5	7
	22.5	5.0	9.4	8.9	7.85
	30.0	5.0	9.15	8.7	8.8
	37.5	5.0	8.2	8.8	8.4
	45.0	5.0	7.8	8.10	7.6

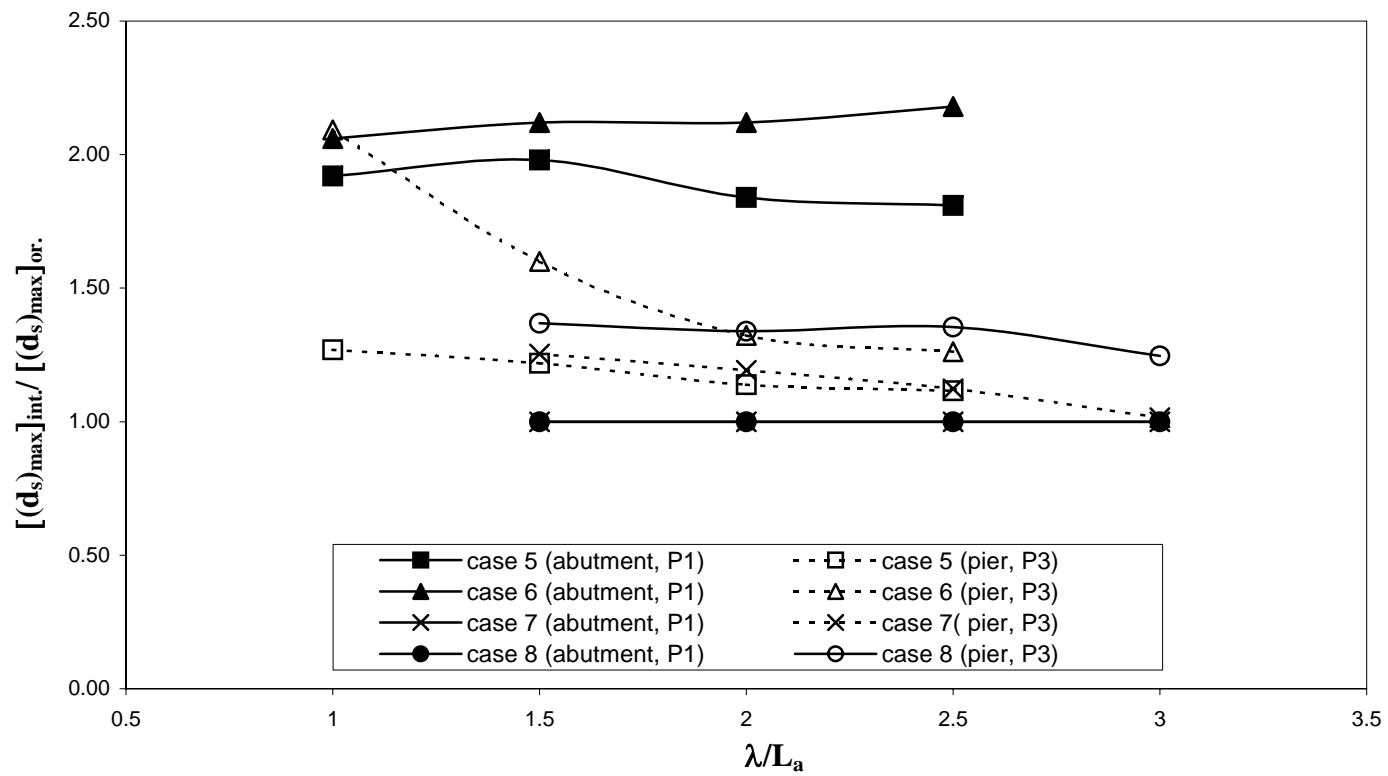


Figure 6.2. Variation of maximum scour depths around the abutment and the pier in the interaction Cases of 5, 6, 7 and 8.

6.5.4. Comparisons of Interaction Cases 9, 10, 11 and 12

In this part of the study, both the abutment and the pier have collars; the one of the abutment is located at $Z_c = -5.0$ cm, and the one of the pier is placed at the bed level, $Z_c = \pm 0.0$ cm.

In Tables 6.9 and 6.10 the results of the experiments conducted with the abutment of $L_a = 25$ cm, and the piers of $D = 10$ cm and $D = 5$ cm are presented. When only an abutment or a pier is tested with collars located at above mentioned levels, the maximum scour depths at points P_1 for the abutments and P_2 , P_3 and P_4 for the pier are named as the original scour depth values. These are quite small in magnitude compared to the corresponding values in Table 6.1 for the cases where there are no collars around them. However when both of them are introduced into the flow medium, these values rapidly increase; at P_1 becomes 11.7 cm from 5 cm, and at P_3 becomes 11.3 cm from 0.85 cm for $\lambda = 25$ cm.

Within the range of λ values tested, the effect of the pier on the scour depth at point P_1 is almost negligible. Whereas, as λ changes from 25.0 cm to 62.5 cm, at P_3 the scour depth changes from 11.3 cm to 5.2 cm, which means that as λ increases the effect of the abutment on the scour depths around the pier decreases about 100%.

Similar observations can be made from the results of experiments conducted with the same abutment used in “interaction case 9” with a pier of $D = 5$ cm, “interaction case 10” of which results are given in Table 6.10.

Table 6.9. Schematic view and the results of the interaction **Case 9**

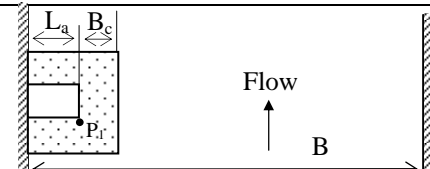
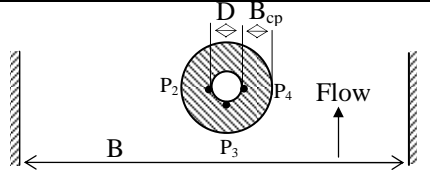
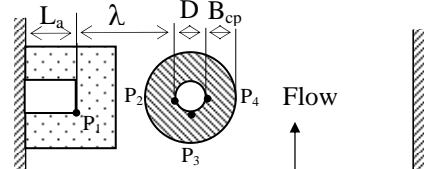
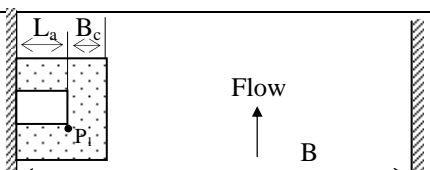
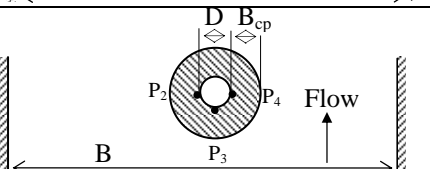
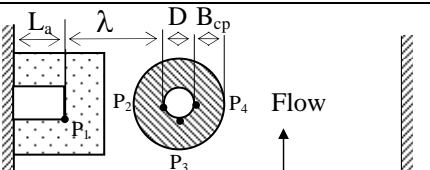
$L_a=25$ cm, $B_a=10$ cm, $D=10$ cm, $B=1.5$ m, $Q=0.055\text{m}^3/\text{s}$, $y=9.6$ cm <i>*There is a collar around the Pier at $Z_{cp}=\pm 0$ cm, $B_{cp}=10$ cm</i> <i>*There is a collar around the Abutment at $Z_c=-5$ cm, $B_c=10$ cm</i>					
Positions of the Circular Pier and the Abutment	λ (cm)	Maximum Scour Depth (cm)			
		P_1	P_2	P_3	P_4
	-	5.0	-	-	-
	-	-	0.9	0.85	1
	25.0	11.7	8.4	11.3	12.25
	37.5	10.6	7	7.22	6.3
	50.0	10.4	6.8	6.3	5.95
	62.5	10.3	4.5	5.2	3.6

Table 6.10. Schematic view and the results of the interaction **Case 10**

$L_a=25$ cm, $B_a=10$ cm, $D=5$ cm, $B=1.5$ m, $Q=0.055\text{m}^3/\text{s}$, $y=9.6$ cm <i>*There is a collar around the Pier at $Z_{cp}=\pm 0$ cm, $B_{cp}=10$ cm</i> <i>*There is a collar around the Abutment at $Z_c=-5$ cm, $B_c=10$ cm</i>					
Positions of the Circular Pier and the Abutment	λ (cm)	Maximum Scour Depth (cm)			
		P_1	P_2	P_3	P_4
	-	5.0	-	-	-
	-	-	0.4	1.1	0.65
	25.0	9.7	13	13.3	13.25
	37.5	11	6	5.9	5.65
	50.0	10.6	4.4	4.6	4.4
	62.5	11.2	3.5	3.4	3.2

The results of the experiments conducted with an abutment of $L_a=15$ cm and pier diameters of $D=10$ cm and 5 cm are given in Tables 6.11 and 6.12, respectively. Due to the reduced length of the abutment, from 25 cm to 15 cm, all of the scour depths at P_1 obtained from the experiments of single abutment and abutment-pier combinations for various values of λ are the same as 5 cm. This means that there is no effect of the pier on the magnitude of the maximum scour depth at point P_1 of the abutments within the ranges of λ values tested. On the other hand, the presence of the abutment into the flow medium strongly affects the scour depths around the pier. While the scour depth at point P_3 is 0.85 cm for the original case, it becomes 5.1 cm for $\lambda=22.5$ cm and 3.7 cm for $\lambda=45.0$ cm. Similar situation is observed from Table 6.12 where $D=5$ cm.

The variation of $\left[(d_s)_{\max} \right]_{\text{int.}} / \left[(d_s)_{\max} \right]_{\text{or.}}$ with λ/L_a is presented in Figure 6.3, for both abutments and piers tested in “interaction cases 9-12”. The curves of small L_a/D ratios for piers first rapidly decrease with increasing λ/L_a , and then at a smaller rate continue decreasing. The curves of the abutments are almost horizontal, which means the parameter on the vertical axis is independent of λ/L_a .

Table 6.11. Schematic view and the results of the interaction **Case 11**

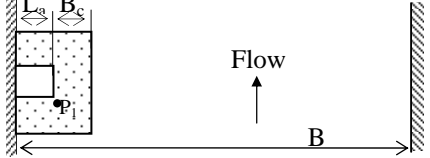
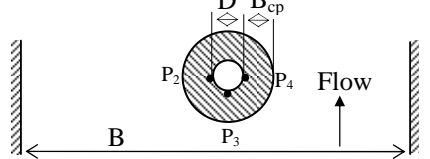
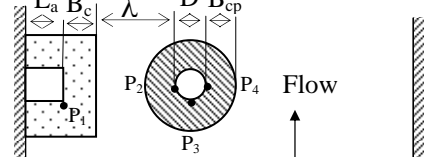
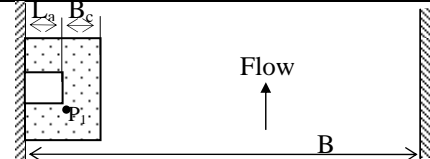
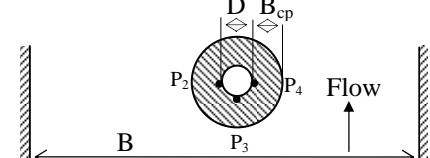
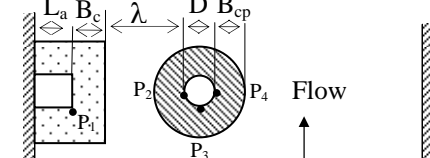
$L_a=15$ cm, $B_a=10$ cm, $D=10$ cm, $B=1.5$ m, $Q=0.055\text{m}^3/\text{s}$, $y=9.6$ cm <i>*There is a collar around the Pier at $Z_{cp}=\pm 0$ cm, $B_{cp}=10$ cm</i> <i>*There is a collar around the Abutment at $Z_c=-5$ cm, $B_c=10$ cm</i>					
Positions of the Circular Pier and the Abutment	λ (cm)	Maximum Scour Depth (cm)			
		P ₁	P ₂	P ₃	P ₄
	-	5.0	-	-	-
	-	-	0.9	0.85	1
	22.5	5.0	7.8	6.5	7.0
	30.0	5.0	5	5.5	4.6
	37.5	5.0	4	3.9	4
	45.0	5.0	3.7	3.7	3.9

Table 6.12. Schematic view and the results of the interaction **Case 12**

$L_a=15$ cm, $B_a=10$ cm, $D=5$ cm, $B=1.5$ m, $Q=0.055\text{m}^3/\text{s}$, $y=9.6$ cm <i>*There is a collar around the Pier at $Z_{cp}=\pm 0$ cm, $B_{cp}=5$ cm</i> <i>*There is a collar around the Abutment at $Z_c=-5$ cm, $B_c=10$ cm</i>					
Positions of the Circular Pier and the Abutment	λ (cm)	Maximum Scour Depth (cm)			
		P ₁	P ₂	P ₃	P ₄
	-	5.0	-	-	-
	-	-	0.4	0.7	0.6
	22.5	5.0	7.9	7.4	5.4
	30.0	5.0	4.7	4.9	4.6
	37.5	5.0	3.6	3.6	3.2
	45.0	5.0	3.1	3.1	3

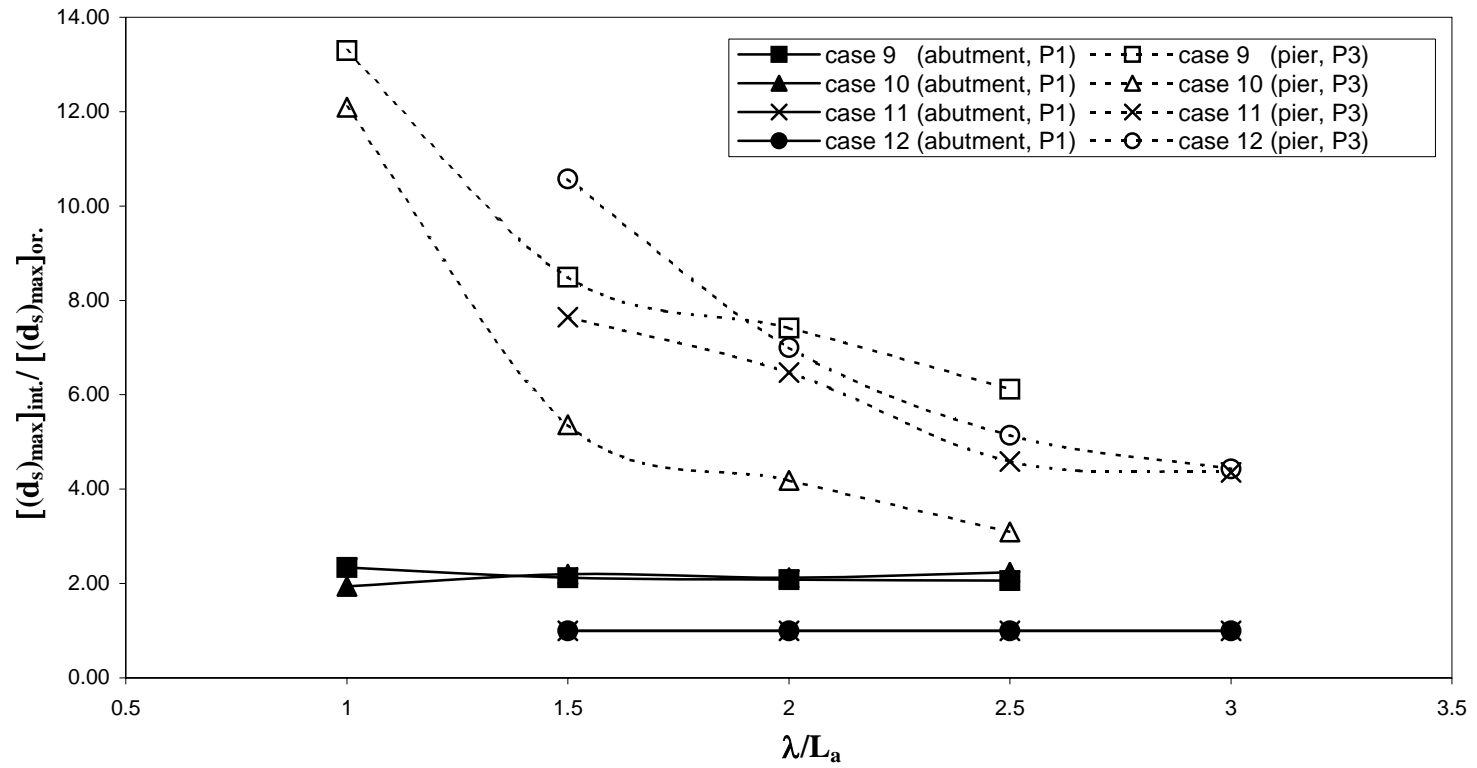


Figure 6.3. Variation of maximum scour depths around the abutment and the pier in the interaction
Cases of 9, 10, 11 and 12.

6.5.5. Comparisons of Interaction Cases 13, 14, 15 and 16

The arrangements of the abutments and piers described under the titles of “interaction cases 13-16” and their experimental results are summarised in Tables 6.13-6.16. The main difference of the arrangements applied here from the previous ones, which had been given in Tables 6.9-6.12, is the location of the collar on the pier, $Z_c = -5.0$ cm. In this case, whatever the abutment length and pier diameter, the original scour depths at points P_1 , P_2 , P_3 and P_4 are 5 cm. Under given flow conditions the scour hole can not penetrate below the collars for both the abutment and the pier when they are tested alone. When the abutment-collar combination is tested together at various λ values it is observed that scour depths at P_1 values do not almost change while those at P_2 , P_3 and P_4 first increase for $\lambda = 25.0$ cm and then become 5.0 cm for other λ values in Tables 6.13 and 6.14.

In Tables 6.15 and 6.16 it is seen that all the scour depths at points P_1 , P_2 , P_3 and P_4 are 5.0 cm. This situation clearly implies that, the reduction in the abutment length, from $L_a = 25$ cm to 15 cm is very effective on reducing the scour depths around both the abutment and pier. λ values greater than 22.5 cm do not also show any change on the maximum scour depths. If λ values less than 22.5 cm are tested, varying scour depths around the abutment and pier may be observed.

The explanations given above can also be stated from Fig. 6.4. The value of

$\left[(d_s)_{\max} \right]_{\text{int.}} / \left[(d_s)_{\max} \right]_{\text{or.}}$ is almost independent of λ/L_a beyond 1.5.

Table 6.13. Schematic view and the results of the interaction **Case 13**

$L_a=25$ cm, $B_a=10$ cm, $D=10$ cm, $B=1.5$ m, $Q=0.055$ m ³ /s, $y=9.6$ cm <i>*There is a collar around the Pier at $Z_{cp}=-5$ cm, $B_{cp}=10$ cm</i> <i>*There is a collar around the Abutment at $Z_c=-5$ cm, $B_c=10$ cm</i>					
Positions of the Circular Pier and the Abutment	λ (cm)	Maximum Scour Depth (cm)			
		P ₁	P ₂	P ₃	P ₄
	-	5.0	-	-	-
	-	-	5.0	5.0	5.0
	25.0	9.2	7.4	7.0	7.2
	37.5	10.3	5.0	5.0	5.0
	50.0	10.1	5.0	5.0	5.0
	62.5	10.1	5.0	5.0	5.0

Table 6.14. Schematic view and the results of the interaction **Case 14**

$L_a=25$ cm, $B_a=10$ cm, $D=5$ cm, $B=1.5$ m, $Q=0.055$ m ³ /s, $y=9.6$ cm <i>*There is a collar around the Pier at $Z_{cp}=-5$ cm, $B_{cp}=10$ cm</i> <i>*There is a collar around the Abutment at $Z_c=-5$ cm, $B_c=10$ cm</i>					
Positions of the Circular Pier and the Abutment	λ (cm)	Maximum Scour Depth (cm)			
		P ₁	P ₂	P ₃	P ₄
	-	5.0	-	-	-
	-	-	5.0	5.0	5.0
	25.0	10.3	10.5	10.2	9.6
	37.5	10.8	5.5	5.5	5.5
	50.0	10.8	5.0	5.0	5.0
	62.5	10.8	5.0	5.0	5.0

Table 6.15. Schematic view and the results of the interaction **Case 15**

$L_a=15$ cm, $B_a=10$ cm, $D=10$ cm, $B=1.5$ m, $Q=0.055\text{m}^3/\text{s}$, $y=9.6$ cm <i>*There is a collar around the Pier at $Z_{cp}=-5$ cm, $B_{cp}=10$ cm</i> <i>*There is a collar around the Abutment at $Z_c=-5$ cm, $B_c=10$ cm</i>					
Positions of the Circular Pier and the Abutment	λ (cm)	Maximum Scour Depth (cm)			
		P ₁	P ₂	P ₃	P ₄
	-	5.0			
	-	-	5.0	5.0	5.0
	22.5	5.0	5.0	5.0	5.0
	30.0	5.0	5.0	5.0	5.0
	37.5	5.0	5.0	5.0	5.0
	45.0	5.0	5.0	5.0	5.0

Table 6.16. Schematic view and the results of the interaction **Case 16**

$L_a=15$ cm, $B_a=10$ cm, $D=50$ cm, $B=1.5$ m, $Q=0.055\text{m}^3/\text{s}$, $y=9.6$ cm <i>*There is a collar around the Pier at $Z_{cp}=-5$ cm, $B_{cp}=5$ cm</i> <i>*There is a collar around the Abutment at $Z_c=-5$ cm, $B_c=10$ cm</i>					
Positions of the Circular Pier and the Abutment	λ (cm)	Maximum Scour Depth (cm)			
		P ₁	P ₂	P ₃	P ₄
	-	5.0			
	-	-	5.0	5.0	5
	22.5	5.0	5.0	5.0	5.0
	30.0	5.0	5.0	5.0	5.0
	37.5	5.0	5.0	5.0	5.0
	45.0	5.0	5.0	5.0	5.0

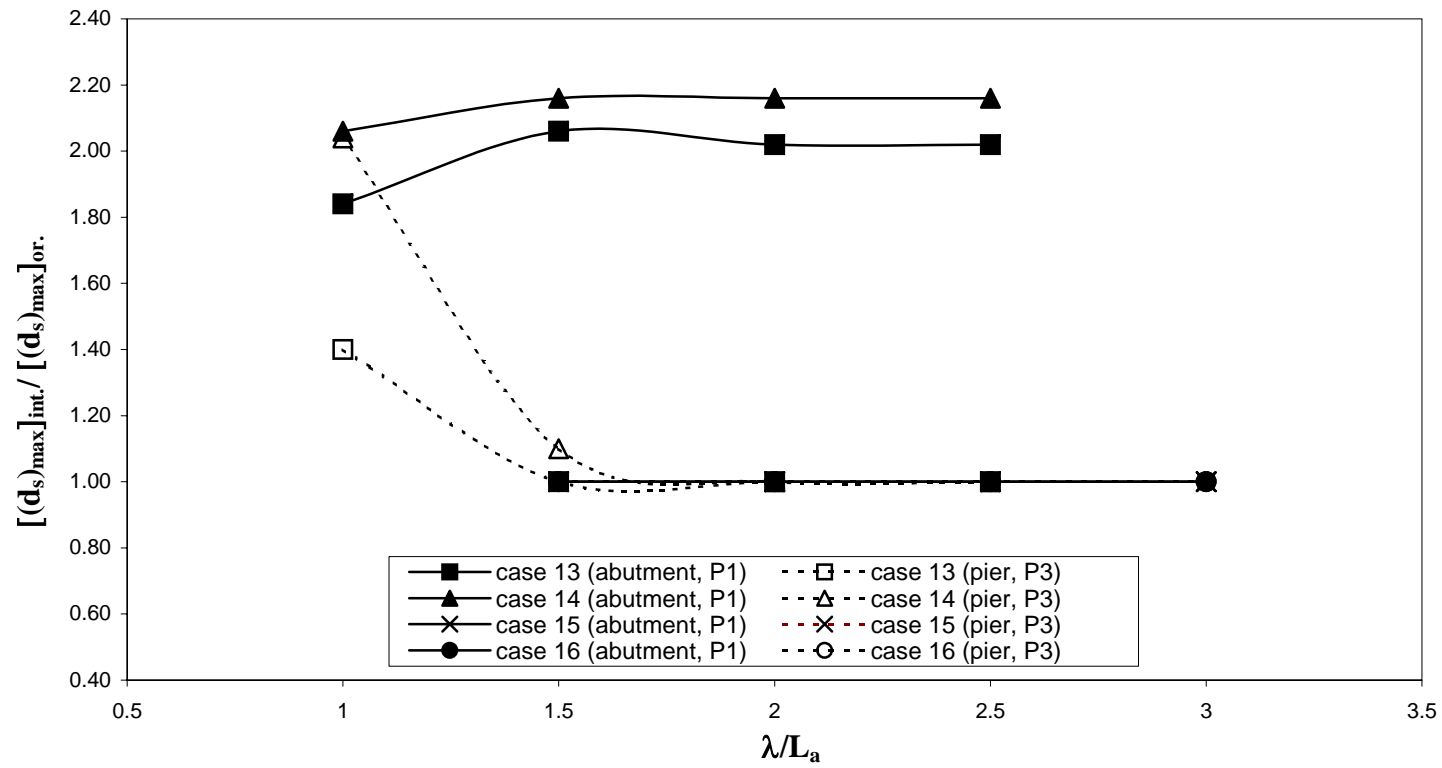


Figure 6.4. Variation of maximum scour depths around the abutment and the pier in the interaction
Cases of 13, 14, 15 and 16.

6.5.6. Comparisons of Interaction Case 17

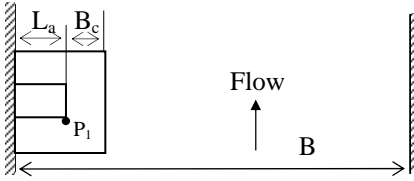
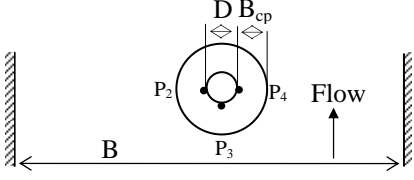
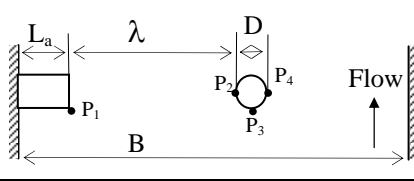
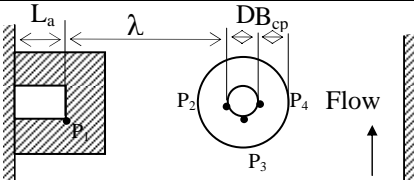
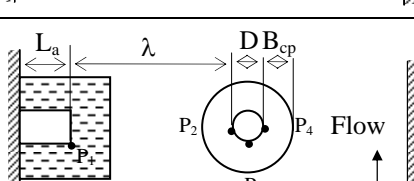
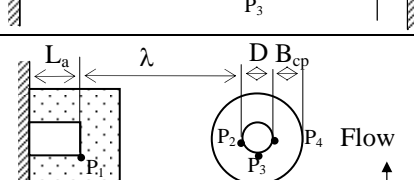
Finally, a series of experiments were conducted with the abutment-pier combination keeping the distance between them as constant, $\lambda=62.5$ cm, under the title of “interaction case 17”. Plan views of the abutment-pier combinations tested and all the other parameters and results of the experiments are presented in Table 6.17. The reason of conducting these specific experiments is to see the effect of location of the collar to be placed on both the abutment and the pier rather than ± 0.0 cm and -5 cm on the scour depths around the abutment and pier. For this reason in Table 6.17 first the results of the single experiments of the abutment and pier without and with collars at elevations of ± 0.0 cm, -2.5 cm and -5 cm were given as reference values. Then, the abutment-pier combination without collar was presented as the original values to be used in comparison analysis. Finally, the abutment-pier combinations were listed in such a way that first, the collar of the abutment was located at bed level, $Z_c=\pm 0.0$ cm, and the collar of the pier was tested at $Z_c=\pm 0.0$ cm, -2.5 cm and -5 cm. Later on the collar of the abutment was placed to -2.5 cm and -5 cm, and for each case the location of the collar of the pier was changed as $Z_c=\pm 0.0$ cm, -2.5 cm and -5 cm, and the experiments were repeated.

If attention is given on Table 6.17 it is seen that in each group of the abutment-pier arrangement where Z_c is equal to ± 0.0 cm, -2.5 cm, and -5 cm, the maximum scour depths at point P_1 do not vary significantly whatever the collar elevation is on the pier. Whereas, in each group the maximum scour depths at points P_2 , P_3 and P_4 significantly changed as a function of the location of the collar on the pier. They were always 2.5 cm for $Z_{cp}=-2.5$ cm and 5 cm for $Z_{cp}=-5$ cm. Among the last three

groups, the collar combinations of $Z_c=\pm 0.0$ cm and $Z_{cp}=-2.5$ cm; $Z_c=-2.5$ cm and $Z_{cp}=-2.5$ cm; and $Z_c=-5$ cm and $Z_{cp}=-2.5$ cm produce the minimum scour depths at points P_1 , P_2 , P_3 and P_4 . For the whole set up, the last combination of collars; $Z_c=-5$ cm and $Z_{cp}=-2.5$ cm gives the optimum collar locations on the abutment and pier which will result in minimum scour depths at points P_1 , P_2 , P_3 and P_4 compared to the original case where the abutment and the pier have no collar.

The variations of $\{[(d_s)_{max}]_{or.} - [(d_s)_{max}]_{int.}\} / [(d_s)_{max}]_{or.}$, % reduction in maximum scour depth, with dimensionless collar location for abutment and pier are given in Figures 6.5 and 6.6.

Table 6.17. Schematic view and the results of the interaction **Case 17**

$L_a=25$ cm, $B_a=10$ cm, $D=5$ cm, $B=1.5$ m, $Q=0.055$ m ³ /s, $y=9.6$ cm, $\lambda=62.5$ cm <i>*There is a collar around the Pier with $B_{cp}=5$ cm and</i> $Z_{cp}= \pm 0.0$ cm, -2.5 cm, and -5 cm <i>*There is a collar around the Abutment with $B_c=10$ cm</i> $Z_{cp}= \pm 0.0$ cm, -2.5 cm, and -5 cm						
Positions of the Circular Pier and the Abutment	Z_c (cm)	Z_{cp} (cm)	Maximum Scour Depth (cm)			
			P ₁	P ₂	P ₃	P ₄
	No collar	-	21.5	-		
	± 0.0		14.35			
	-2.5		12.45			
	-5.0		5.0			
	-	No collar	-	6.8	6.5	7.0
		± 0.0		0.4	1.1	0.65
		-2.5		2.5	2.5	2.5
		-5.0		5.0	5.0	5.0
	-	-	21	8.5	6.5	7.0
	± 0.0	± 0.0	14.8	3.80	4.0	3.80
	± 0.0	-2.5	15	2.50	2.50	2.50
	± 0.0	-5.0	14.98	5.0	5.0	5.0
	-2.5	± 0.0	13.2	3.50	3.40	3.0
	-2.5	-2.5	12.6	2.50	2.50	2.50
	-2.5	-5.0	12.35	5.0	5.0	5.0
	-5	± 0.0	11.2	3.5	3.4	3.2
	-5	-2.5	11.05	2.50	2.50	2.50
	-5	-5.0	10.8	5.0	5.0	5.0

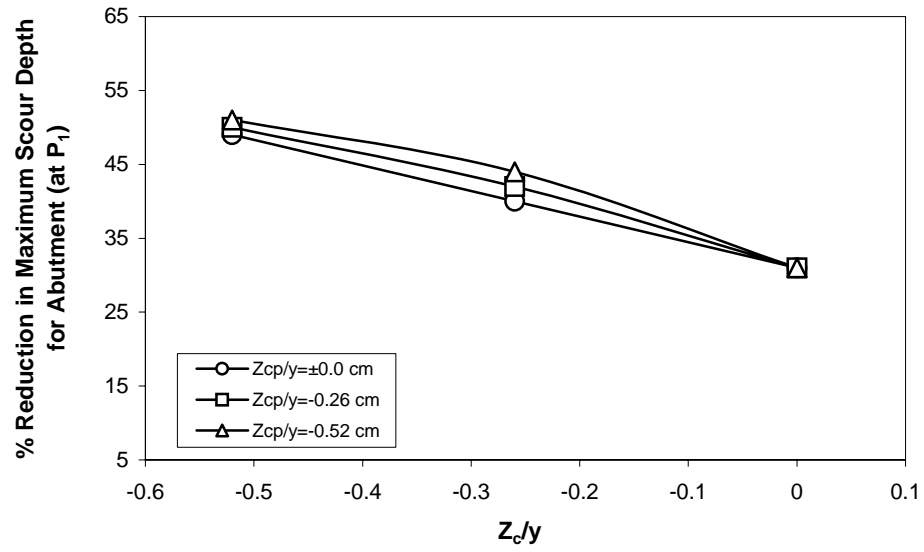


Figure 6.5. Variation of % Reduction in maximum scour depth with dimensionless collar location for pier in Case 17

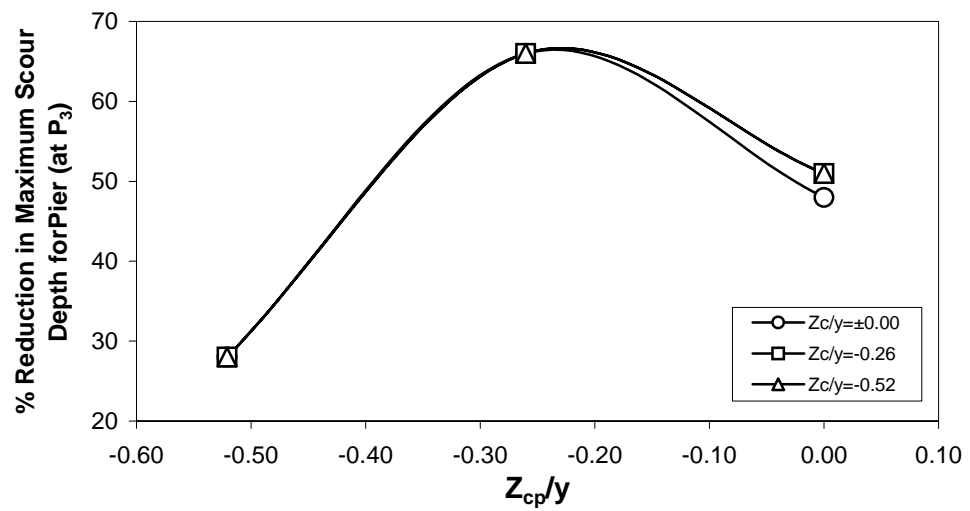


Figure 6.6. Variation of % Reduction in maximum scour depth with dimensionless collar location for abutment in Case 17

6.6. CONCLUSIONS AND RECOMMENDATIONS FOR FUTURE STUDIES

The distance between a bridge abutment and a pier is a very important parameter, which influences the flow conditions and the scour depths around these structures. For this reason, abutment-pier combinations of various sizes were tested without and with collars located at different elevations on both structures. The effect of the pier on the abutment and the effect of the abutment on the pier regarding the scour depths were investigated. The variations on the scour depths compared to the original cases, where there is only abutment and pier without collar, were plotted with respect to the dimensionless distance between the abutment and pier, λ/L_a . From these studies it was observed that even though the scour depth around abutments and piers can be reduced by means of collars used on them at certain elevations when they are tested one by one in the flow medium, these collars do not show same performance in reducing the scour depths around the structures when piers and abutments are tested together. Therefore, it can be stated that there is a strong interaction between abutments and piers. For practical purposes, to determine the combined effects of abutments and piers on the development of scour profiles around these structures, their model studies should be conducted together.

In order to give further conclusions regarding this topic, in future studies abutments and piers of various sizes should be tested together at several λ values with varying the locations of the collars on both structures. Use of more than one type sediment as bed material is also suggested.

CHAPTER 7

SUMMARY AND CONCLUSIONS

In this study, scour around the vertical abutments of various sizes, the effectiveness of the collars, which are used to reduce the maximum scour depth around the abutment, and time development of scouring around the abutment with or without collar have been investigated. The interaction between the abutment and the pier was also studied. More than 150 experiments were performed for various arrangements.

It is observed that, the collar can protect the abutment efficiently. Even in some cases, no scour depths are recorded. Moreover, even if a collar can not stop the formation of the scour hole around the abutment, it slows down the scouring depth considerably. It is obvious that, the larger the collar width, the higher performance the collar gives.

It has also been shown that the abutments having collars around them have equilibrium scour depths much smaller than those have no collars.

Instead of full-collars, partial collars around the abutments can be used to provide maximum reduction in scour depth from economical point of view.

The results of the interaction studies between abutments and piers are considerably different than those of single abutment and single pier for both cases where the structures are tested with or without collars.

In practice if a bridge is to be protected against local scour, abutments and piers of the bridge cannot be treated, as they will be in the flow medium only by themselves. Therefore, the collar size and location, which are proper for one abutment or pier to protect it from severe erosion, should not be directly applied to the problem stated above. Sizes and locations of the collars to be applied on the abutments and piers should be determined after proper model studies.

REFERENCES

- Ahmed, F. and Rajaratnam, N. (1998). Flow Around Bridge Piers. J. of Hydr. Engrg, Vol. 124, No. 3, 288-300.
- Ballio, F., and Orsi, E., (2000). Time Evolution of Scour Around Bridge Abutments. IV International Conference on Hydro-Science and Hydro-Engineering, Seoul, Korea.
- Ballio, F., and Orsi, E., (2001). Time Evolution of Scour Around Bridge Abutments. Water Engr. Research, Vol. 2, No. 4, 243-259.
- Balachandar, R., and Kells, J. A., (1997). Local Channel Scour in Uniformly Graded Sediments: The Time Scale Problem. Canadian J. of Civ. Engr., Vol. 24, 799-807.
- Breusers, H. N. C., Nicollet, G., and Shen, H. W., (1977). Local Scour Around Cylindrical Piers. J. of Hydr. Research, Vol. 15, No. 3, 211-252.
- Breusers, H. N. C., and Raudkivi, A. J., (1991). Scouring. A.A. Balkema, Rotterdam, Brookfield.

Cardoso, A. H., and Bettess, R., (1999). Effects of Time and Channel Geometry on Scour at Bridge Abutments. J. of Hydr. Engrg, Vol. 125, No. 4, 388-398.

Chang, W. Y., Lai, J. S., and Yen, C. L., (2004). Evolution of Scour Depth at Circular Bridge Piers. J. of Hydr. Engrg, Vol. 130, No. 9, 905-913.

Chaurasia, E. S. R., and Lal, P. B. B., (2002). Local Scour Around Bridge Abutments. Int. J. of Sed. Reseach, Vol. 17, No. 1, 48-74.

Chiew, Y.M., (1992). Scour Protection at Bridge Piers. J. of Hydr. Engrg, Vol. 118, No. 9, 1260-1269.

Chiew, Y. M., (1995). Mechanics of Riprap Failure at Bridge Piers. J. of Hydr. Engrg, Vol. 121, No. 9, 635-643.

Chiew, Y. M., (2004). Local Scour and Riprap Stability at Bridge Piers in a Degrading Channel. J. of Hydr. Engrg, Vol. 130, No. 3, 218-226.

Choi, G. W., and Ahn, S. J., (2001). Maximum Local Scour Depth Variation at Bridge Piers. XXIX IAHR Congress Proceedings, Theme D, Vol. 2, Beijing, China.

Coleman, S. E., Lauchlan, C. S., and Melville, B.W., (2003). Clear-Water Scour Development at Bridge Abutments. J. of Hydr. Research, Vol. 41, No. 5, 521-531.

Cunha, L.V., (1975). Time Evolution of Local scour. XVI IAHR Congress Proceedings, Vol. 2, Sao Paulo, Brasil.

Dargahi, B., (1990). Controlling Mechanism of Local scouring. J. of Hydr. Engrg, Vol. 116, No. 10, 1197-1214.

Dey, S. (1997). Local Scour at Piers, Part I: A Review of Developments of Research. International Journal of Sediment Research. Vol. 12, No.2, 23-45.

Duarte, C. A., and Sainz, J. A. (1999). Riprap at Bridge Piers. J. of Hydr. Research, Vol. 37, No. 3, 291-302.

Ettema, R., Mostafa, E. A., Melville B. W., and Yassin A. A., (1998). Local Scour at Skewed Piers. J. of Hydr. Research, Vol. 124, No. 7, 756-760.

Federal Highway Administration, (2001). Evaluating Scour At Bridges. National Highway Institute, Publication No. FHWA NHI 01-001, HEC No. 18, U. S.

Fischenich, C., and Landers, M. (2000). Computing Scour. U. S. Army Engineer Research and Development Center, ERDC TN-EMRRP-SR-05, Vicksburg, MS.

Garde, R. J., Subramanya, K., and Nambudripad, K. D., (1961). Study of Scour Around Spur-Dikes. J. of the Hydr. Division Proceedings of the American Society of Civil Engineers, Volume 87, No. 6, 23-37.

Gill, M. A., (1972). Erosion of Sand Beds Around Spur-Dikes. J. of the Hydr. Division Proceedings of the American Society of Civil Engineers, Vol. 98, No. 9, 1587-1602.

Graf, W. H., (1971). Hydraulics of Sediment Transport, McGraw-Hill Book Company, N.Y.

Graf, W. H., (1996). Fluvial Hydraulics, John Wiley & Sons, N.Y.

Jansen P. Ph., (1979). Principles of River Engineering. Delftse U. M., Delft.

Johnson, P. A., (1995). Comparison of Pier-Scour Equations Using Field Data. J. of Hydr. Eng., Vol. 121, No. 8, 626-629.

Johnson, P. A., and Dock, D. A., (1998). Probabilistic Bridge Scour Estimates. J. of Hydr. Eng., Vol. 124, No. 7, 750-754.

Kandasamy, J. K., and Melville, B. W., (1998). Maximum Local Scour Depth at Bridge Piers and Abutments. J. of Hydr. Eng., Vol. 36, No. 2, 183-198.

Kothyari, U. C., Garde, R. J., and Ranga Raju, K. G., (1992). Live-Bed Scour Around Cylindrical Bridge Piers. J. of Hydr. Research, Vol. 30, No. 5, 701-715.

Kothyari, U. C. and Ranga Raju, K. G., (2001). Scour Around Spur Dikes and Bridge Abutments. J. of Hydr. Research, Vol. 39, No. 4, 367-374.

Kothyari, U. C., and Ranga Raju, K. G., (2001). Scour Around Spur Dikes and Bridge Abutments.” J. of Hydr. Research, Vol. 39, No. 4, 367-374.

Kouchakzadeh, S., and Townsend, R. D., (1997). Maximum Scour Depth at Bridge Abutments Terminating in the Floodplain Zone. Canadian. J. of Civ. Engr., Vol. 24, 996-1006.

Kuhnle, R. A., Alonso, C. V., and Shields Jr, F. D., (2002). Local Scour Associated with Angled Spur Dikes. J. of Hydr. Engr., Vol. 41, No. 5, 521-531 Vol. 128, No. 12, 1087-1093.

Kumar, V., Raju, K. G. R., and Vittal, N., (1997). Reduction of local scour around bridge piers using slots and collars. J. of Hydr. Eng., Vol. 125, No. 12, 1302-1305.

Kwan, R. T. F., and Melville, B. W., (1994). Local Scour and Flow Measurements at Bridge Abutments. J. of Hydr. Eng., Vol. 32, No. 5, 661-673.

Laursen, E. M., (1962). Scour at Bridge Crossings. American Society of Civil Engineers Transactions, Vol. 127, Part 1, 166-209.

Lim, S. Y., (1997). Equilibrium Clear-Water Scour Around an Abutment. J. of Hydr. Engrg, Vol. 123, No.3, 237-243.

Lim, S. Y., and Cheng, N. S., (1998). Prediction of Live-Bed Scour at Abutments. J. of Hydr. Engrg, Vol. 124, No. 6, 635-638.

Luigi, B., Revelli, R., and Ridolfi, L., (2001). Experimental Evidence of the Interaction Between Piers in the Scour Process. XXIX IAHR Congress Proceedings, Beijing, China, Vol. 2, 607-612.

Mashahir, M. B. and Zarrati, A. R., (2002). Effect of Collar on Time Development of Scouring around Rectangular Bridge Piers. The 5th International Conference on Hydro Science and Engineering, Warsaw, Poland.

Melville, B. W., (1992). Local Scour at Bridge Abutments. J. of Hydr. Eng., Vol. 118, No. 4, 615-631.

Melville, B. W. (1997). Pier and Abutment Scour: Integrated Approach. J. of Hydr. Engrg, Vol. 123, No. 2, 125-136.

Melville, B. W. and Chiew, Y. M., (1999). Time Scale for Local Scour at Bridge Piers. J. Hydr. Engrg, Vol. 125, No. 1, 59-65.

Melville, B. W. and Raudkivi, A. J., (1977). Flow Characteristics in Local Scour at Bridge Piers. J. Hydr. Research, Vol. 15, No. 4, 373-381.

Melville, B. W., and Shutherland, J. (1989). Design Method for Local Scour at Bridge Piers. J. of Hydr. Eng., Vol. 116, No. 10, 1290-1292.

Miller, C. A., Johnson, D., and Steinhart, R. (1992). Bridge Scour Prediction Methods Applicable to Streams in Pennsylvania. Department of Transportation., Research Project 89-03.

Oliveto, G., and Hager, W. H., (2002). Temporal Evolution of clear-water pier and abutments scour. J. of Hydr. Eng., Vol. 128, No. 9, 811-820.

Radice, A., Franzetti, S., and Ballio, F., (2002). Local Scour at Bridge Abutments. River Flow 2002, International Conference on Fluvial Hydraulics, Louvain-la-Neuve, Vol. 2, 1059-1068.

Rajaratnam, N. and Nwachukwu, B. A., (1983). Flow Near Groin-like Structures. J. of Hydr. Engrg., Vol. 109, No. 3, 463–480.

Raudkivi, A. J., (1967). Loose Boundary Hydraulics. Pergamon Press. N.Y.

Raudkivi, A. J. and Ettema, R., (1983). Clear-Water Scour at Cylindrical Piers. J. of Hydr. Eng., Vol. 109, No. 3, 338-350.

Sheppard, D. M., Odeh, M., and Glasser, T., (2004). Large Scale Clear-Water Local Pier Scour Experiments. J. of Hydr. Eng., Vol. 130, No. 10, 957-963.

Simons, D. B., and Şentürk, F., (1992). Sediment Transport Technology. Water Resources Publications, Colorado.

Singh, K. K., Verma, D. V. S., and Tiwari, N. K., (1995). Scour Protection at Circular Bridge Pier. Sixth International Symposium on River Sedimentation, New Delhi, India, 1057-1068.

Singh, C. P., Setia, B. and Verma, D. V. S., (2001). Collar-Sleeve Combination as a Scour Protection Device Around a Circular Pier. XXIX IAHR Congress Proceedings, Beijing, China, Vol. 2, 202-210.

Sturm, T. W., and Janjua, N. S., (1994). Clear-Water Scour Around Abutments in Floodplains. J. of Hydr. Engr, Vol. 120, No. 8, 956-971.

Yanmaz, A. M., (2002). Köprü Hidroliği. METU Press., Ankara.

Yanmaz, A. M. and Altınbilek, H. D., (1991). Study of Time-Dependent Local Scour Around Bridge Piers. J. Hydr. Engrg, Vol. 117, No. 10, 1247-1268.

Zarrati, A. R., Gholami, H. and Mashahir, M. B., (2004). Application of Collar to Control Scouring Around Rectangular Bridge Piers. J. Hydr. Research, Vol. 42, No. 1, 97-103.

APPENDIX A

Table A.1. Cross-sections of the scour holes for $L_a=7.5$ cm

Scour Depth for $L_a=7.5$ cm (cm)											
X (cm)	Without Collar	$B_c=10$ (cm)					$B_c=7.5$ (cm)				
		Z_c (cm)									
		-5	-2.5	0	2.5	5	-5	-2.5	0	2.5	5
-72	0.0	0.1		0.0				0.6			
-70	0.0	0.1	0.4	0.0				0.6	-0.1		
-68	0.0	0.1	0.4	0.0				0.5	-0.1		
-66	0.0	0.1	0.4	0.0				0.5	0.4		
-64	0.0	0.1	0.4	1.1				0.2	0.4		
-62	0.1	-0.1	0.4	2.3				0.2	2.8		
-60	0.1	-0.1	0.4	3.2		0.1	0.0	-0.2	2.8		
-58	0.3	0.1	0.4	3.5		0.1	0.0	-0.2	3.1		
-56	0.3	0.1	0.4	3.5		0.1	0.0	-0.1	3.1		
-54	0.5	0.3	0.4	3.5		0.1	0.3	-0.1	3.1		
-52	0.5	1.2	1.4	3.1		0.1	0.7	0.2	3.1		
-50	0.7	2.0	3.2	3.1		0.5	1.4	1.1	2.8		
-48	0.7	2.0	3.5	2.8		0.5	1.5	2.2	2.8		
-46	1.0	2.0	3.3	2.8		0.6	1.6	3.1	2.7		
-44	1.3	1.5	3.3	2.5		1.0	1.3	3.1	2.7		
-42	1.1	1.5	3.1	2.3		1.5	1.3	3.0	2.3		
-40	1.1	0.9	2.9	1.8		1.4	1.0	2.7	2.1		
-38	0.8	0.9	2.5	1.3	0.1	1.4	1.0	2.4	1.7		
-36	0.8	0.5	1.9	0.9	0.0	1.1	0.5	2.0	1.4		
-34	0.4	0.5	1.3	0.4	0.0	1.1	0.5	1.4	0.8		
-32	0.4	-0.3	0.6	-0.1	0.0	0.5	-1.1	0.9	0.2		
-30	0.1	-0.3	-0.4	-0.6	-0.1	0.5	-1.1	0.5	0.0		
-28	0.1	-0.4	-0.8	-0.9	-0.1	0.1	-0.7	-0.2	0.0		
-26	-0.4	-0.4	-1.2	-1.1	0.0	0.1	-0.7	-0.6	-0.3	0.0	
-24	-0.4	-0.8	-1.8	-0.9	0.0	-0.2	-0.7	-1.1	-0.2	0.0	
-22	-0.6	-0.8	-2.1	-0.6	0.7	-0.2	-0.7	-1.6	0.1	0.2	
-20	-0.6	-0.6	-1.8	-0.3	1.0	-0.3	-0.8	-1.9	-0.1	0.5	
-18	-0.6	-0.6	-1.8	0.2	1.3	-0.3	-0.8	-2.0	-0.1	1.0	-0.3
-16	-0.5	-0.6	-1.8	0.2	1.3	0.0	-0.5	-1.8	-0.1	1.5	-0.3
-14	-0.3	-0.4	-1.8	0.2	1.2	0.0	-0.5	-1.8	-0.1	1.4	-0.3
-12	-0.1	-0.1	-1.8	0.2	1.0	-0.1	-0.6	-1.8	-0.1	1.2	-0.1
-10	-0.8	-0.3	-1.8	0.2	0.8	-0.6	-0.9	-1.8	-0.1	0.7	-0.5
-8	-1.4	-1.3	-1.8	0.2	0.5	-1.3	-1.6	-1.8	-0.1	0.2	-1.0
-6	-2.2	-2.0	-1.8	0.2	-0.3	-1.8	-2.3	-1.8	-0.1	-0.4	-1.8
-4	-3.4	-2.9	-1.8	0.2	-1.3	-2.6	-3.1	-1.8	-0.1	-1.7	-2.7
-2	-3.8	-3.3	-1.8	0.2	-2.2	-3.7	-3.7	-1.8	-0.1	-2.4	-3.6
0	-4.4	-4.2	-1.8	0.2	-2.8	-4.3	-4.3	-1.8	-0.1	-3.2	-4.1
2	-4.7	-4.2	-1.8	0.2	-2.2	-4.6	-4.3	-1.8	-0.1	-2.3	-3.8
4	-3.3	-3.7	-1.8	0.2	-0.8	-3.7	-4.3	-1.8	-0.1	-1.3	-2.8
6	-2.3	-2.5	-1.8	0.2	-0.1	-2.3	-2.5	-1.8	-0.4	-0.2	-1.3
8	-1.0	-1.3	-1.8	0.2	-0.1	-2.0	-0.8	-1.8	0.5	0.2	-0.1
10	-0.5	-0.1	-1.6	0.2	-0.1	0.0	0.0	-0.6	0.5	0.6	0.3

Table A.1. Cross-sections of the scour holes for $L_a=7.5$ cm (continued)

Scour Depth for $L_a=7.5$ cm (cm)											
X (cm)	Without Collar	$B_c=5$ (cm)					$B_c=2.5$ (cm)				
		Z_c (cm)									
		-5	-2.5	0	2.5	5	-5	-2.5	0	2.5	5
-70	0.0	0.1			0.0						
-68	0.0	0.1			0.7						0.2
-66	0.0	0.1			1.1						0.2
-64	0.0	0.1			2.8						0.2
-62	0.1	-0.1		0.1	3.3						0.2
-60	0.1	-0.1	0.2	0.3	3.2		-0.1		0.1		0.2
-58	0.3	0.1	0.1	0.3	3.2		-0.1		0.3		0.2
-56	0.3	0.1	0.1	0.5	2.9		-0.1		0.3		0.6
-54	0.5	0.3	0.2	0.5	2.9		0.3		0.3		0.6
-52	0.5	1.2	0.7	0.6	2.9		0.3	0.1	0.3		0.6
-50	0.7	2.0	1.0	0.6	2.8		0.4	0.1	0.5		0.6
-48	0.7	2.0	1.5	0.9	2.3		0.8	0.4	2.5		0.6
-46	1.0	2.0	0.7	1.8	2.1		1.2	0.4	3.1		0.5
-44	1.3	1.5	0.7	2.9	1.7		1.5	0.5	2.9		0.5
-42	1.1	1.5	1.6	2.9	1.6	0.0	1.5	0.5	2.6		0.5
-40	1.1	0.9	1.6	2.7	1.2	0.0	1.5	1.8	2.6	0.2	0.5
-38	0.8	0.9	1.2	2.4	0.8	0.0	1.5	2.7	2.5	0.0	0.5
-36	0.8	0.5	1.2	2.1	0.3	-0.1	1.3	2.7	2.2	0.0	0.0
-34	0.4	0.5	1.0	1.6	-0.2	-0.1	1.3	2.4	1.9	0.0	0.0
-32	0.4	-0.3	0.8	1.0	-0.8	-0.2	0.7	2.0	1.4	0.0	0.0
-30	0.1	-0.3	0.4	0.5	-1.1	-0.2	0.7	1.7	1.0	0.0	0.0
-28	0.1	-0.4	0.0	-0.3	-1.3	0.1	0.1	1.2	0.6	0.0	0.0
-26	-0.4	-0.4	-0.2	-1.1	-1.3	0.1	0.1	0.7	0.1	0.4	0.3
-24	-0.4	-0.8	-0.6	-1.5	-1.0	0.1	-0.4	-0.1	-0.4	0.8	0.3
-22	-0.6	-0.8	-0.7	-1.7	-0.9	0.1	-0.4	-0.8	-0.6	1.2	0.3
-20	-0.6	-0.6	-0.6	-2.1	-0.3	0.5	-0.6	-1.3	-0.8	1.3	0.3
-18	-0.6	-0.6	-0.5	-2.1	-0.2	1.5	-0.6	-1.8	-0.9	1.7	0.3
-16	-0.5	-0.6	-0.7	-1.8	-0.2	2.0	-0.8	-2.1	-0.9	1.6	0.7
-14	-0.3	-0.4	-0.9	-1.8	-0.2	1.7	-0.8	-2.2	-0.7	1.3	0.4
-12	-0.1	-0.1	-1.1	-1.8	-0.2	1.3	-0.6	-2.5	-0.3	0.8	0.0
-10	-0.8	-0.3	-1.6	-1.8	-0.2	0.9	-0.6	-2.5	-0.3	0.4	-0.8
-8	-1.4	-1.3	-2.1	-1.8	-0.2	0.2	-0.1	-2.5	-0.3	-0.4	-1.3
-6	-2.2	-2.0	-2.5	-1.8	-0.2	-0.8	-0.1	-2.5	-1.2	-1.6	-1.8
-4	-3.4	-2.9	-3.0	-1.8	-0.2	-1.8	-0.5	-2.5	-2.4	-2.5	-2.8
-2	-3.8	-3.3	-3.8	-1.8	-0.2	-2.8	-1.5	-2.5	-3.5	-3.2	-3.2
0	-4.4	-4.2	-4.3	-1.8	-0.8	-3.6	-2.4	-3.0	-4.2	-4.2	-4.6
2	-4.7	-4.2	-4.3	-1.8	-1.5	-2.9	-2.8	-3.7	-3.6	-3.6	-4.0
4	-3.3	-3.7	-3.5	-1.8	-1.8	-1.6	-3.4	-4.2	-2.8	-1.9	-2.8
6	-2.3	-2.5	-2.2	-1.7	-1.1	-0.5	-4.5	-3.0	-1.3	-0.4	-1.2
8	-1.0	-1.3	-0.8	-0.8	-0.3	0.1	-4.5	-1.8	-0.3	0.0	-0.1
10	-0.5	-0.1	0.1	0.1	0.1	0.1	-3.0	-0.3	0.0	0.0	0.1
14	-0.5	-0.1	0.1	0.1	0.1	0.1	-2.1	-0.3	0.0	0.0	0.1
16	-0.3	0.1	0.1	0.1	0.1	0.1	-0.6	-0.3	0.0	0.0	0.1
20	-0.3	0.1	0.1	0.1			0.1	-0.3	0.0		0.1

Table A.2. Cross-sections of the scour holes for $L_a=15$ cm

Scour Depth for $L_a=15$ cm (cm)											
X (cm)	Without Collar	$B_c=10$ (cm)					$B_c=7.5$ (cm)				
		Z_c (cm)									
		-5	-2.5	0	2.5	5	-5	-2.5	0	2.5	5
-56							2.8	2.7	3.2		2.4
-54							2.8	2.2	2.7	0.1	4
-52							2.15	2.2	2.7	1.1	4.6
-50	2.3	1.2	2.1	2.4	0.05	4.6	2.15	1.55	2	2.2	4.5
-48	1.75	0.95	2	1.9	0.7	4.75	1.6	1.55	2	3.1	4.35
-46	1.75	0.2	2	1.9	1.2	4.75	1.6	1.2	1.3	3.8	4.35
-44	1.2	-0.35	1.9	1.25	1.65	4.5	1.2	0.6	1.3	4.2	3.8
-42	1.2	-0.85	1.9	1.25	2	4.3	0.85	0	0.55	4.05	3.8
-40	0.8	-1.3	1.5	0.4	2.4	4.2	0.6	-0.4	0.55	4.05	3.4
-38	0.4	-1.6	1.2	0.4	2.6	3.95	0	-0.95	0.1	3.7	3.4
-36	0	-1.95	0.7	0	2.85	3.6	-0.5	-1.5	0.1	3.7	2.6
-34	-0.2	-2.3	0.3	0	3.3	3.4	-1	-2.1	-0.2	2.9	2.6
-32	-1.1	-2.7	-0.3	-0.25	3.45	2.65	-1.6	-2.5	-0.2	2.9	2.3
-30	-1.9	-3.6	-1.35	-0.25	3.2	2.6	-2.25	-3.1	-0.3	2.1	2
-28	-2.4	-4.3	-2	-0.4	2.85	1.75	-2.8	-3.3	-0.6	2.1	1.05
-26	-3.2	-4.8	-2	-0.4	2.2	1	-3.5	-3.3	-1	1.2	0.2
-24	-3.8	-4.8	-2.6	-0.4	1.6	0.6	-3.75	-3.4	-1.2	1.2	-0.05
-22	-4.5	-4.8	-2.6	-0.6	1.1	-0.2	-4.25	-3.4	-1.25	0.5	-0.8
-20	-5.2	-4.8	-2.6	-0.3	0.35	-0.9	-4.6	-3.4	-1	-0.35	-1.5
-18	-5.6	-4.8	-2.6	-0.2	-0.15	-1.8	-4.5	-3.4	-0.45	-0.9	-2.2
-16	-6.1	-4.8	-2.6	-0.2	-0.7	-2.6	-4.8	-3.6	-0.3	-1.8	-2.8
-14	-6.8	-4.8	-2.6	-0.2	-1.2	-3.1	-4.8	-3.45	-0.6	-2.4	-3.45
-12	-7.35	-4.8	-2.6	-0.2	-2	-4.1	-4.8	-2.8	-1.1	-3.25	-4.15
-10	-8.1	-4.8	-2.6	-0.2	-2.8	-5	-4.8	-2.8	-2	-3.8	-5
-8	-8.8	-4.8	-2.6	-0.2	-3.55	-5.9	-4.8	-2.8	-3	-4.6	-5.8
-6	-9.45	-4.8	-2.6	-0.3	-4.8	-6.8	-4.8	-2.8	-3.9	-5.6	-6.8
-4	-10.15	-4.8	-2.6	-0.3	-6	-7.8	-4.8	-2.8	-4.8	-7	-8.1
-2	-10.9	-4.8	-2.6	-1.3	-6.6	-8.7	-4.8	-2.8	-5.65	-7.95	-9.1
0	-11.9	-4.8	-2.6	-2	-7.7	-9.65	-4.8	-3.3	-6.5	-8.8	-9.9
2	-12.2	-4.8	-2.6	-1.8	-7.3	-9.65	-4.8	-3.6	-5.8	-8.1	-10
4	-10.6	-4.8	-2.6	-2.25	-5.9	-8.35	-4.8	-3.9	-4.65	-6.75	-8.5
6	-9.4	-4.8	-2.6	-2.95	-4.9	-7.05	-4.8	-5.2	-4.05	-5.6	-7.45
8	-8.5	-4.8	-2.6	-3.3	-3.25	-5.65	-5.05	-5.65	-3.3	-4	-5.8
10	-7.65	-4.8	-3.35	-3.05	-2.2	-4.25	-5.3	-5.45	-2.8	-2.5	-4.4
12	-6.7	-3.95	-4.25	-2.2	-0.7	-2.9	-4.3	-4.5	-2.7	-1.35	-2.8
14	-5.1	-3.15	-4.15	-1.3	0.1	-1.5	-3.1	-3.25	-1.9	-0.1	-1.55
16	-4	-1.65	-3.15	-0.3	0.1	-0.2	-0.9	-2.1	-0.45	-0.1	-0.5
18	-2.8	-0.35	-2	0	0.1	-0.2	-0.05	-0.9	0	-0.1	0.1
20	-1.2	-0.35	-0.8		0.1	-0.2	-0.05	-0.35	0	-0.1	0.1
22	-0.5	0.05	0.1		0.1	-0.2	-0.05	-0.35	0	0.1	0.1
24	-0.5	0.05	0.1		0.1	0	-0.05	-0.35	0.1	-39.8	0.1
26	-0.5	0.05	0.1				-0.05	-0.35			

Table A.2. Cross-sections of the scour holes for $L_a=15$ cm
(continued)

Scour Depth for $L_a=15$ cm (cm)											
X (cm)	Without Collar	$B_c=5$ (cm)					$B_c=2.5$ (cm)				
		Z_c (cm)									
		-5	-2.5	0	2.5	5	-5	-2.5	0	2.5	5
-106			-0.6								
-104			-0.6								
-102			-0.6								
-100			0								
-98			1.7								
-96		-0.8	2.9	0							
-94		-0.8	2.9	-0.3					-0.3		
-92		-0.8	2.9	0.35			-0.5		0.2		
-90		-0.4	2.9	2.7			-0.5		0.2		
-88		-0.4	2.9	2.7			-0.5		0.2		
-86		1	4	3.8			-0.2		0.6		
-84		2.6	4.1	3.8			-0.2		0.8		
-82		3.9	4.1	3.85			1.6		1.1		
-80		4.7	4.1	3.85			2.9		1.3		
-78		4.7	4.1	4.15		-0.3	4.5		2.2	-0.3	-0.25
-76		4.7	3.9	4.15		-0.2	4.6	-0.3	3.4	-0.3	-0.1
-74		4.4	3.9	4.2		-0.2	4.55	-0.3	4.05	-0.3	-0.1
-72		4.4	3.85	4.2		0.5	4.55	-0.3	4.2	-0.05	0.95
-70		4.1	3.85	4.1		2.1	4.3	0.6	4.2	-0.05	2.5
-68		4.1	3.45	4.1		3.5	4.3	1.9	4.1	1.5	3.75
-66		4	3.45	4		3.8	4.1	3.6	4.1	2.9	4
-64		4	3.15	4	-0.4	3.8	4.1	3.9	3.5	3.7	3.9
-62		3.8	3.15	3.95	-0.3	3.7	3.8	4.2	3.5	3.9	3.9
-60		3.8	2.9	3.95	-0.3	3.7	3.8	4.2	3.35	3.7	3.65
-58		3.5	2.9	3.7	-0.2	3.55	3.6	4	3.35	3.7	3.65
-56		3.5	2.35	3.7	-0.2	3.55	3.6	4	3.05	3.55	3.45
-54		3.2	2.35	3.4	0.85	3.2	3.3	3.8	3.05	3.55	3.45
-52		3.2	2.05	3.4	1.8	3.2	3.3	3.8	2.7	3.25	3.25
-50	2.3	2.7	2.05	3.3	2.75	3	2.9	3.3	2.7	3.25	3.25
-48	1.75	2.7	1.8	3.3	3.7	3	2.9	3.3	2.3	3.25	2.9
-46	1.75	2.2	1.55	2.9	4.2	2.7	2.2	3	2.3	3.25	2.9
-44	1.2	2.2	1.1	2.9	4.1	2.7	2.2	3	1.85	3.1	2.5
-42	1.2	1.35	0.9	2.5	4.1	2.25	1.95	2.5	1.85	3.1	2.5
-40	0.8	1.35	0.65	2.5	3.7	2.25	1.35	2.5	1.45	3	2
-38	0.4	0.4	0.1	2	3.7	2.05	1	2.2	1.45	3	2
-36	0	0.4	-0.6	2	3.4	1.65	0.5	2.2	1.2	2.3	1.75
-34	-0.2	-0.9	-0.6	1.85	3	1.25	-0.15	1.7	1.2	2.3	1.3
-32	-1.1	-0.9	-1.1	1.65	2.6	0.95	-0.8	1.7	0.7	1.9	0.7
-30	-1.9	-1.9	-1.1	1.25	2.2	0.45	-1.3	1.3	0.4	1.5	0.1
-28	-2.4	-1.9	-1.35	0.9	1.4	-0.2	-2.05	1.1	-0.1	0.85	-0.3
-26	-3.2	-2.15	-1.65	0.6	1	-0.8	-2.55	0.7	-0.3	0.4	-0.95
-24	-3.8	-2.65	-2.6	0.1	0.45	-1.4	-3.25	0.2	-0.85	-0.55	-1.5
-22	-4.5	-3.25	-2.9	-0.4	-0.4	-2.15	-4.1	-0.5	-1.55	-1.15	-2.15
-20	-5.2	-3.6	-3.2	-0.85	-1.1	-2.55	-4.5	-1.15	-2.2	-1.95	-2.8
-18	-5.6	-4.3	-3.35	-1.3	-1.8	-3.1	-5	-1.9	-2.7	-2.45	-3.4
-16	-6.1	-5.2	-3	-1.95	-2.5	-3.65	-5	-2.3	-3.55	-3.35	-4.1
-14	-6.8	-5.2	-2.6	-2.5	-3.8	-4.5	-5	-2.8	-4.25	-3.8	-5.1

Table A.2. Cross-sections of the scour holes for $L_a=15$ cm
(continued)

-12	-7.35	-5.2	-2.6	-3.1	-4.7	-5.2	-5	-3.2	-5	-4.4	-5.6
-10	-8.1	-5.2	-2.6	-3.8	-5.25	-5.8	-5	-4.1	-5.9	-5.2	-6.3
-8	-8.8	-5.2	-3.1	-4.5	-5.7	-6.4	-5.2	-5.3	-6.4	-6.1	-6.7
-6	-9.45	-5.2	-3.95	-5.25	-6.5	-7.45	-5.8	-6.4	-7.3	-7.7	-7.9
-4	-10.15	-5.2	-5.2	-6.6	-7.7	-8.8	-6.65	-7.5	-8.2	-8.7	-8.5
-2	-10.9	-5.2	-5.9	-7.65	-8.55	-9.95	-7.3	-8.5	-9.5	-9.85	-9.6
0	-11.9	-5.2	-6.8	-8.6	-10	-11	-8.5	-9.6	-10.7	-10.6	-10.7
2	-12.2	-5.8	-7.2	-8.1	-9.45	-10.85	-9.9	-9.5	-10.5	-10.35	-10.6
4	-10.6	-6.85	-7.35	-6.75	-8.15	-9.6	-10.15	-8.6	-8.45	-9.1	-9.1
6	-9.4	-7.6	-7	-5.5	-6.8	-8.1	-9.25	-7.45	-7.1	-7.6	-7.6
8	-8.5	-6.3	-6.15	-3.9	-5.15	-6.7	-7.55	-6.15	-5.65	-6.1	-7
10	-7.65	-5.3	-4.6	-2.35	-3.65	-5.45	-6.25	-4.7	-4.5	-4.6	-5.7
12	-6.7	-4.1	-3.55	-1.1	-2.25	-4.05	-5.15	-3.35	-3	-3.55	-4.5
14	-5.1	-2.9	-2.65	-0.5	-1.05	-2.8	-3.9	-2.25	-1.5	-1.95	-3.25
16	-4	-1.5	-1.25	0	-0.25	-1.2	-2.65	-1	-0.5	-1	-2.05
18	-2.8	-0.3	-0.35	0	-0.25	-0.4	-1.3	-0.15	-0.1	-0.1	-0.6
20	-1.2	-0.3	-0.35	0	-0.25	-0.1	-0.3	-0.15	-0.1	-0.1	0
22	-0.5	-0.3	-0.35		-0.25	-0.1	-0.3	-0.15	-0.1	-0.1	0
24	-0.5	-0.3	-0.35		0	-0.1	-0.3	-0.15	-0.1	-0.1	0
26	-0.5	-0.3	0			0.1	0	0	0	0.1	0
28	0.1	0									0
30											0

Table A.3. Cross-sections of the scour holes for $L_a=20$ cm

Scour Depth for $L_a=20$ cm (cm)											
X (cm)	Without Collar	$B_c=10$ (cm)					$B_c=7.5$ (cm)				
		Z_c (cm)									
		-5	-2.5	0	2.5	5	-5	-2.5	0	2.5	5
-116	3.8	4.2	4.5	1.0			4.8	4.3	1.0		
-114	4.5	4.2	4.5	1.1			4.8	4.2	1.0		
-112	4.7	4.2	4.5	1.5			4.8	4.2	1.7		
-110	4.7	4.2	4.5	1.7			4.8	4.0	1.7		
-108	4.7	4.2	4.2	2.2			4.7	4.0	4.0		
-106	4.7	4.2	4.2	2.5			4.7	3.9	4.0		
-104	4.7	4.2	4.0	3.2			4.7	3.9	2.3		
-102	4.7	4.2	4.0	3.7			4.7	3.8	2.3		
-100	4.7	4.2	3.7	4.3			4.4	3.8	2.4		
-98	4.7	4.2	3.7	4.9			4.4	3.7	2.4		0.0
-96	4.7	4.2	3.6	4.9			4.4	3.7	2.4		0.1
-94	4.7	4.1	3.6	4.9			4.4	3.7	2.4		0.1
-92	4.7	4.1	3.2	4.9			4.3	3.7	2.4		0.1
-90	4.7	3.7	3.2	4.7			4.3	3.3	2.3		0.1
-88	4.6	3.7	3.1	4.7			4.3	3.3	2.3		0.6
-86	4.8	3.7	3.1	4.4			4.3	3.1	2.4		2.0
-84	4.6	3.5	2.9	4.4		-0.3	4.1	3.1	2.9		3.6
-82	4.4	3.5	2.9	4.0		-0.3	4.1	2.8	2.4		5.2
-80	4.4	3.2	2.7	4.0	-0.1	-0.3	3.9	2.8	4.1		4.7
-78	4.2	3.2	2.7	3.8	-0.1	0.0	3.9	2.6	4.4		4.7
-76	3.9	2.8	2.2	3.8	-0.1	0.0	3.9	2.6	4.4		4.7
-74	3.8	2.8	2.2	3.5	-0.1	1.5	3.9	2.2	3.9		4.7
-72	3.4	2.8	2.1	3.5	-0.1	2.9	3.2	2.2	3.9		4.7
-70	3.4	2.4	2.1	3.1	-0.3	4.4	3.2	1.9	3.9	-0.3	4.8
-68	3.2	2.4	1.8	3.1	-0.3	5.0	2.9	1.9	3.8	-0.3	4.8
-66	3.2	2.4	1.8	2.6	-0.3	4.7	2.9	1.6	3.8	-0.3	4.8
-64	2.9	2.4	1.2	2.6	0.2	4.7	2.7	1.6	3.3	-0.3	4.4
-62	2.9	2.4	1.2	2.3	1.6	4.7	2.7	1.2	3.3	0.0	4.4
-60	2.4	2.4	0.9	2.3	3.2	4.7	2.5	1.2	2.6	1.7	4.3
-58	2.4	2.4	0.9	2.1	4.6	4.3	2.5	0.7	2.6	3.2	4.3
-56	2.4	2.4	0.5	2.1	5.4	4.3	2.1	0.7	2.6	4.8	4.1
-54	2.0	2.4	0.5	2.0	5.3	4.1	2.1	0.3	2.6	5.2	4.1
-52	2.0	2.4	0.2	2.0	5.3	4.1	1.6	0.3	2.4	5.2	3.7
-50	1.6	2.4	0.2	1.8	4.9	3.7	1.6	-0.3	2.4	4.7	3.7
-48	1.6	2.4	-0.2	1.8	4.9	3.7	1.3	-0.3	2.2	4.7	3.2
-46	1.4	2.2	-0.2	1.1	4.5	3.6	0.9	-1.1	2.2	4.2	3.2
-44	1.1	1.9	-0.3	1.1	4.5	3.2	0.6	-1.1	2.2	4.2	3.0
-42	1.0	1.4	-0.4	0.4	4.2	2.9	-0.4	-1.9	2.2	3.8	2.7
-40	0.5	0.7	-0.6	0.4	4.2	2.6	-0.4	-1.9	1.9	3.4	2.2
-38	0.1	0.0	-1.0	0.1	3.8	1.9	-0.9	-2.6	1.9	3.1	1.8
-36	-0.3	-0.9	-1.4	0.1	3.5	1.6	-1.2	-2.6	1.7	2.8	1.1
-34	-1.0	-1.7	-1.8	-0.5	3.2	1.1	-1.8	-2.8	1.7	2.3	0.7
-32	-1.8	-2.2	-2.4	-0.5	2.5	0.5	-2.3	-2.8	1.4	1.9	0.2
-30	-2.3	-2.6	-2.4	-0.5	2.0	0.0	-2.8	-2.8	1.4	1.1	-0.5
-28	-3.3	-2.9	-2.7	-0.5	1.1	-0.6	-3.4	-2.8	0.9	0.4	-1.2

Table A.3. Cross-sections of the scour holes for $L_a=20$ cm
(continued)

-26	-3.9	-3.5	-2.7	-0.4	0.5	-1.3	-4.1	-3.0	0.9	-0.4	-2.1
-24	-5.1	-4.3	-2.6	-0.4	-0.3	-2.2	-4.7	-3.2	0.5	-1.2	-2.6
-22	-5.8	-4.8	-2.6	-0.2	-1.1	-3.2	-5.4	-3.6	0.1	-1.9	-3.3
-20	-6.8	-5.2	-3.2	-0.2	-1.8	-3.6	-6.4	-3.6	-0.8	-2.6	-4.4
-18	-7.7	-5.2	-3.2	-0.4	-2.6	-4.5	-6.0	-2.9	-1.4	-3.6	-4.9
-16	-8.3	-5.2	-3.0	-0.4	-3.6	-5.1	-6.3	-2.9	-2.1	-4.0	-5.7
-14	-8.8	-5.2	-3.0	-0.4	-4.2	-5.6	-6.2	-2.6	-2.6	-5.0	-6.4
-12	-9.8	-5.2	-2.5	-0.9	-4.8	-6.7	-6.4	-2.6	-3.2	-5.8	-7.2
-10	-10.8	-5.2	-2.5	-1.8	-5.5	-7.5	-5.8	-2.8	-4.0	-6.5	-8.2
-8	-12.1	-5.2	-2.6	-2.8	-6.8	-8.5	-5.3	-3.6	-5.2	-7.2	-8.8
-6	-13.1	-5.2	-2.6	-3.7	-8.1	-10.0	-5.2	-4.3	-6.3	-8.3	-10.3
-4	-13.5	-5.2	-3.2	-5.0	-9.2	-10.8	-5.2	-5.3	-7.1	-9.9	-11.6
-2	-13.5	-5.2	-4.3	-6.0	-10.0	-11.3	-5.2	-6.2	-7.8	-10.6	-12.2
0	-14.5	-5.2	-5.8	-7.1	-10.8	-12.5	-5.2	-7.2	-9.0	-11.4	-13.1
2	-14.7	-5.2	-4.4	-6.6	-10.5	-12.6	-5.2	-6.1	-8.6	-11.3	-13.1
4	-13.4	-5.2	-4.6	-5.5	-9.0	-10.9	-5.7	-6.0	-7.4	-10.0	-11.5
6	-12.1	-5.2	-5.7	-4.4	-7.9	-9.9	-6.1	-6.5	-6.1	-8.7	-10.3
8	-10.7	-5.2	-6.0	-4.1	-6.5	-8.6	-7.1	-6.7	-5.0	-7.3	-9.3
10	-9.5	-5.9	-6.0	-3.7	-5.3	-7.4	-7.8	-6.2	-4.9	-5.7	-7.9
12	-8.6	-6.6	-5.2	-3.0	-4.1	-5.8	-8.0	-5.0	-3.1	-4.5	-6.7
14	-8.0	-6.1	-4.1	-1.8	-2.7	-4.7	-7.5	-3.8	-2.5	-3.3	-5.3
16	-7.4	-5.1	-2.8	-0.8	-1.7	-3.2	-6.5	-2.3	-1.4	-1.8	-4.2
18	-6.5	-4.1	-1.8	-0.6	-0.7	-2.2	-5.2	-1.2	-0.3	-0.4	-3.1
20	-5.3	-2.9	-0.6	-0.6	-0.2	-0.8	-3.7	-0.2	-0.1	0.1	-1.7
22	-4.0	-1.4	-0.1	-0.1	-0.2	-0.2	-2.5	-0.2	-0.1	0.1	-0.7
24	-2.7	-0.8	-0.1	-0.1	-0.2	-0.2	-1.5	0.1	-0.1	0.1	-0.1
26	-1.4	-0.1	-0.1	-0.1	-0.2	-0.2	-0.4		0.1	0.1	-0.1
28	-0.6	-0.1	-0.1	-0.1	-0.2	-0.2	-0.4			0.1	-0.1
30	-0.6	-0.1	0.1	0.1	0.0	0.0	-0.2				-0.1
32	-0.3	-0.1					-0.2				-0.1
34	-0.3	-0.1					-0.2				0.1
36	-0.3	0.0					0.0				
38	-0.3						0.0				
40	-0.1						0.0				
42	-0.1										
44	-0.1										
46	-0.1										

Table A.3. Cross-sections of the scour holes for $L_a=20$ cm

Scour Depth for $L_a=20$ cm (continued) (cm)											
X (cm)	Without Collar	$B_c=5$ (cm)					$B_c=2.5$ (cm)				
		Z_c (cm)									
		-5	-2.5	0	2.5	5	-5	-2.5	0	2.5	5
-116	3.8	0.0	-1.0	3.6		0.0		-0.4	0.8		4.4
-114	4.5	1.7	-0.6	3.7		0.0		-0.4	4.1		4.4
-112	4.7	2.9	0.8	3.7		0.7	-0.4	-0.4	4.1		4.4
-110	4.7	4.2	2.0	3.7		2.1	-0.4	-0.3	4.7		4.4
-108	4.7	4.4	3.4	3.7		3.1	-0.4	-0.3	4.7		4.3
-106	4.7	4.4	3.9	3.7		4.0	0.6	-0.3	4.7		4.3
-104	4.7	4.4	4.1	3.6		4.5	2.1	3.1	4.7	-0.3	4.3
-102	4.7	4.4	4.1	3.6		4.5	3.4	4.3	4.7	-0.3	4.3
-100	4.7	4.2	4.1	3.6		4.5	4.0	4.7	4.7	-0.3	4.3
-98	4.7	4.2	3.9	3.6		4.5	4.2	4.6	4.7	0.9	4.3
-96	4.7	4.2	3.9	3.6	-1.0	4.5	4.2	4.6	4.7	2.5	4.3
-94	4.7	4.2	3.9	3.5	-1.2	4.5	4.2	4.6	4.5	4.0	4.3
-92	4.7	4.2	3.9	3.5	-1.2	4.5	4.2	4.6	4.5	4.2	4.2
-90	4.7	4.2	3.9	3.5	-0.4	4.4	4.2	4.6	4.3	4.2	4.2
-88	4.6	4.0	3.7	3.5	0.7	4.4	4.2	4.2	4.3	4.2	4.2
-86	4.8	4.0	3.7	3.5	2.2	4.4	4.2	4.2	4.3	4.2	4.2
-84	4.6	3.9	3.7	3.1	3.7	4.3	4.2	4.2	4.3	3.9	4.0
-82	4.4	3.9	3.7	3.1	3.9	4.3	4.2	4.2	4.0	3.9	4.0
-80	4.4	3.9	3.7	3.1	3.8	4.2	4.2	4.2	3.7	3.8	3.9
-78	4.2	3.9	3.7	3.1	3.8	4.2	4.2	3.7	3.7	3.8	3.9
-76	3.9	3.7	3.7	3.1	3.6	4.0	4.1	3.7	3.4	3.6	3.5
-74	3.8	3.7	3.7	3.0	3.6	4.0	4.1	3.7	3.4	3.6	3.5
-72	3.4	3.4	3.7	3.0	3.6	4.0	4.1	3.7	3.4	3.5	3.2
-70	3.4	3.4	3.6	3.0	3.3	3.9	4.1	3.7	3.4	3.5	3.2
-68	3.2	3.2	3.6	3.0	3.3	3.5	3.8	3.3	3.4	3.4	3.2
-66	3.2	3.2	3.5	2.9	3.2	3.5	3.8	3.3	3.1	3.4	2.9
-64	2.9	2.7	3.5	2.9	3.2	3.3	3.5	3.3	3.1	3.4	2.9
-62	2.9	2.7	3.4	2.8	3.1	3.3	3.5	3.3	2.7	3.4	2.5
-60	2.4	2.3	3.4	2.8	3.1	3.2	3.2	2.9	2.7	3.0	2.5
-58	2.4	2.3	3.4	2.6	3.0	3.2	3.2	2.9	2.3	3.0	2.1
-56	2.4	2.2	3.4	2.6	3.0	2.9	2.8	2.5	2.3	2.9	2.1
-54	2.0	1.9	3.3	2.2	3.0	2.9	2.8	2.5	1.9	2.9	1.9
-52	2.0	1.6	3.3	2.2	3.0	2.4	2.4	2.1	1.9	2.8	1.9
-50	1.6	1.2	3.0	2.1	2.7	2.4	2.4	2.1	1.4	2.8	1.8
-48	1.6	0.9	3.0	2.1	2.7	2.1	2.2	1.5	1.4	2.5	1.8
-46	1.4	0.7	2.7	2.6	2.3	2.1	1.9	1.5	1.4	2.5	1.2
-44	1.1	0.5	2.7	2.6	2.3	1.8	1.6	1.4	1.2	2.0	1.2
-42	1.0	0.2	2.2	2.9	2.0	1.3	1.3	1.1	0.8	2.0	1.0
-40	0.5	-0.3	2.2	2.9	2.0	0.9	1.0	0.7	0.2	1.5	0.7
-38	0.1	-0.8	1.8	2.7	1.7	0.4	0.6	0.1	-0.3	1.2	0.3
-36	-0.3	-1.1	1.8	2.5	1.3	-0.3	0.1	-0.4	-0.7	0.5	-0.2
-34	-1.0	-1.7	0.9	2.2	0.9	-0.9	-0.3	-1.0	-1.2	0.0	-0.6
-32	-1.8	-2.1	0.5	1.6	0.3	-1.6	-0.9	-1.5	-2.0	0.1	-1.0
-30	-2.3	-2.6	0.0	0.7	-0.3	-2.3	-1.5	-1.8	-2.6	-1.3	-1.4
-28	-3.3	-3.1	-0.5	0.0	-1.0	-2.9	-1.9	-2.1	-3.3	-2.2	-2.1

Table A.3. Cross-sections of the scour holes for $L_a=20$ cm (continued)

-20	-6.8	-5.4	-2.9	-2.8	-4.3	-6.0	-4.3	-3.8	-6.0	-5.2	-5.1
-18	-7.7	-5.6	-3.4	-3.8	-5.1	-6.9	-4.8	-4.4	-6.9	-5.8	-5.8
-16	-8.3	-5.3	-3.8	-4.5	-5.8	-7.6	-5.1	-5.3	-7.2	-6.7	-6.7
-14	-8.8	-5.1	-4.5	-5.2	-6.4	-8.4	-5.2	-6.1	-7.9	-7.1	-7.5
-12	-9.8	-5.1	-5.1	-6.1	-7.1	-9.3	-5.0	-7.4	-8.7	-8.0	-8.5
-10	-10.8	-5.1	-5.6	-6.9	-7.6	-10.5	-5.6	-8.8	-9.3	-8.8	-9.1
-8	-12.1	-5.3	-6.6	-7.8	-8.4	-10.5	-6.7	-10.0	-9.8	-9.7	-10.5
-6	-13.1	-5.8	-7.8	-8.8	-9.4	-10.7	-7.8	-10.8	-10.5	-10.7	-11.8
-4	-13.5	-6.0	-8.9	-9.8	-10.2	-10.3	-9.2	-11.3	-11.3	-11.6	-13.3
-2	-13.5	-7.2	-10.0	-11.0	-11.1	-11.8	-10.3	-14.7	-11.6	-11.9	-14.0
0	-14.5	-8.5	-11.2	-12.2	-12.6	-12.9	-12.1	-12.7	-12.8	-12.8	-15.1
2	-14.7	-8.6	-10.5	-11.2	-12.3	-13.5	-12.3	-12.5	-12.6	-13.3	-14.0
4	-13.4	-9.7	-9.8	-9.7	-11.0	-12.0	-12.8	-11.5	-11.5	-12.0	-12.6
6	-12.1	-10.5	-9.1	-8.6	-9.7	-10.8	-12.2	-10.4	-10.2	-10.7	-11.0
8	-10.7	-10.6	-8.4	-7.1	-8.5	-9.8	-11.2	-9.2	-8.9	-9.6	-10.0
10	-9.5	-10.1	-6.9	-6.0	-7.2	-8.9	-9.8	-7.9	-7.7	-8.7	-9.3
12	-8.6	-9.1	-5.5	-4.7	-5.8	-8.1	-8.4	-6.6	-6.5	-7.3	-8.7
14	-8.0	-7.8	-3.8	-3.7	-4.5	-7.1	-7.2	-5.2	-5.0	-5.7	-7.9
16	-7.4	-6.3	-2.8	-2.5	-3.1	-5.8	-5.9	-4.1	-3.8	-4.7	-6.7
18	-6.5	-5.3	-1.6	-1.2	-2.0	-4.6	-4.7	-2.7	-1.3	-3.3	-5.6
20	-5.3	-4.0	-0.8	-0.1	-0.5	-3.2	-3.7	-1.3	-0.1	-2.2	-4.3
22	-4.0	-2.7	-0.8	-0.1	-0.5	-1.6	-2.4	-0.4	0.2	-0.9	-3.1
24	-2.7	-1.5	-0.1	0.0	-0.3	-0.6	-1.0	-0.4	0.2	0.2	-1.8
26	-1.4	-0.6	-0.1	0.0	-0.3	-0.1	-0.4	-0.4		0.2	-0.8
28	-0.6	-0.6	-0.1	0.0	-0.3	-0.1	-0.4	-0.4		0.2	-0.4
30	-0.6	0.0	0.1		0.0	0.1	-0.1	0.0		0.0	-0.4
32	-0.3	0.0				0.1	-0.1				-0.4
34	-0.3	0.0				0.1	-0.1				-0.4
36	-0.3	0.0					0.0				0.0
38	-0.3	0.1									
40	-0.1										
42	-0.1										
44	-0.1										
46	-0.1										

Table A.4. Cross-sections of the scour holes for $L_a=25$ cm

Scour Depth for $L_a=25$ cm (cm)											
X (cm)	Without Collar	$B_c=10$ (cm)					$B_c=7.5$ (cm)				
		Z_c (cm)									
		-5	-2.5	0	2.5	5	-5	-2.5	0	2.5	5
-74		0.9					0.7				
-72		0.4					0.7		1.3	3.1	
-70		0.4					0.3	2.2	1.3	3.1	2.4
-68		0.3					0.3	2.2	0.7	2.9	2.4
-66		0.3					-0.1	2.3	0.7	2.9	2.4
-64		-0.3					-0.1	2.3	0.2	2.7	2.4
-62		-0.3					-0.6	1.8	0.2	2.7	2.3
-60		-0.9	0.0			4.0	-0.6	1.8	0.3	2.7	2.3
-58		-0.9	-0.2			4.0	-1.3	1.6	0.3	2.7	2.3
-56		-1.9	-1.8			3.7	-1.3	1.6	1.8	2.8	2.3
-54	0.0	-1.9	-1.8			3.7	-2.0	1.1	1.8	2.8	2.1
-52	-0.5	-2.7	-1.6			3.0	-2.0	1.1	3.1	2.8	2.1
-50	-0.9	-2.7	-2.0			2.5	-2.5	0.8	3.1	2.8	1.8
-48	-1.1	-3.5	-2.5		3.5	2.5	-2.5	0.8	2.7	2.7	1.8
-46	-1.4	-3.6	-3.0		3.3	2.1	-3.0	0.2	2.7	2.7	1.3
-44	-1.9	-4.4	-3.6		3.1	1.8	-3.2	0.2	2.3	2.4	1.3
-42	-2.5	-4.7	-4.2		2.5	1.3	-3.8	-0.5	2.3	2.4	0.3
-40	-3.0	-5.2	-4.2		2.1	0.9	-4.2	-0.5	1.7	1.7	0.3
-38	-3.8	-5.5	-5.5		1.5	0.3	-4.6	-1.4	1.7	1.7	-0.8
-36	-4.0	-5.8	-6.0		1.0	-0.4	-5.0	-1.4	0.7	0.8	-1.4
-34	-4.6	-6.1	-6.8		0.4	-1.1	-5.4	-2.0	0.7	0.8	-2.8
-32	-5.4	-6.2	-6.8		-0.5	-1.8	-5.8	-2.0	0.1	-0.5	-2.9
-30	-6.0	-6.5	-6.9	0.2	-1.2	-2.6	-6.0	-3.0	-0.6	-1.6	-3.7
-28	-6.8	-6.7	-6.9	-0.5	-1.9	-3.1	-6.3	-3.4	-1.5	-2.3	-4.8
-26	-7.5	-6.7	-7.0	-1.0	-2.6	-3.8	-6.6	-3.9	-2.3	-3.6	-5.6
-24	-8.1	-7.0	-7.1	-1.6	-3.6	-4.4	-6.9	-4.3	-3.2	-4.4	-6.4
-22	-9.0	-7.3	-7.2	-2.5	-4.4	-5.4	-7.0	-4.5	-3.9	-5.3	-7.2
-20	-10.0	-7.8	-7.4	-3.0	-5.2	-6.2	-6.9	-4.9	-4.6	-6.0	-7.9
-18	-10.6	-7.4	-7.5	-3.7	-5.9	-6.9	-6.7	-5.5	-5.5	-6.9	-8.8
-16	-11.5	-6.9	-7.5	-4.2	-6.4	-7.8	-6.8	-5.9	-6.5	-7.9	-9.7
-14	-12.2	-6.6	-8.0	-4.9	-7.4	-8.3	-6.6	-6.2	-7.2	-8.9	-10.6
-12	-13.0	-6.4	-8.2	-5.7	-8.4	-9.0	-6.9	-6.8	-8.2	-10.0	-11.8
-10	-14.0	-6.5	-8.1	-6.3	-9.5	-10.3	-6.9	-7.1	-9.3	-11.2	-13.1
-8	-15.3	-6.5	-8.2	-7.4	-10.7	-11.2	-7.8	-7.7	-10.5	-12.4	-13.7
-6	-15.7	-6.5	-8.5	-8.5	-12.2	-12.8	-8.5	-8.8	-11.3	-13.3	-15.3
-4	-16.1	-6.5	-9.0	-9.6	-13.1	-13.5	-9.3	-10.2	-12.4	-13.9	-15.8
-2	-16.6	-6.7	-8.5	-10.5	-13.6	-14.5	-10.1	-11.2	-13.0	-13.8	-16.3
0	-17.8	-7.3	-9.0	-11.0	-15.0	-14.7	-10.5	-11.2	-13.1	-14.5	-16.8
2	-17.6	-7.4	-9.0	-10.4	-13.9	-13.8	-9.0	-10.9	-12.3	-14.3	-16.4
4	-16.6	-8.0	-9.0	-9.2	-12.7	-12.2	-9.9	-10.1	-11.3	-12.9	-15.3
6	-15.4	-8.8	-9.5	-8.2	-11.4	-11.4	-10.7	-9.8	-10.2	-11.8	-14.1
8	-14.3	-9.8	-10.0	-7.3	-10.2	-10.4	-10.5	-9.3	-9.1	-11.1	-13.0
10	-13.0	-10.0	-11.0	-6.5	-8.8	-9.2	-10.5	-8.5	-8.2	-9.4	-12.0
12	-11.8	-9.8	-11.2	-5.8	-7.1	-7.9	-9.7	-7.0	-6.1	-8.5	-10.7
14	-10.7	-8.9	-10.0	-4.9	-6.0	-6.6	-8.8	-5.5	-4.4	-7.3	-10.0
16	-9.8	-7.9	-9.0	-4.0	-4.4	-5.5	-7.3	-4.3	-3.7	-5.8	-8.7
18	-9.1	-6.8	-8.5	-4.0	-3.0	-4.2	-6.2	-3.0	-2.6	-4.9	-7.3

Table A.4. Cross-sections of the scour holes for $L_a=25$ cm
(continued)

24	-6.8	-4.2	-7.2	-1.5	-0.3	-0.7	-2.6		-1.1	-1.5	-3.9
26	-5.8	-2.8	-7.0	-0.3	-0.3	-0.3	-1.7			-1.2	-2.8
28	-4.7	-1.8	-6.7	-0.1		-0.1	-1.2				-1.6
30	-3.5	-1.4	-6.2			-0.1	-1.2				-1.2
32	-2.2	-1.4	-5.5			-0.1					
34	-1.0	-1.2	-4.9								
36	0.0	-1.2	-4.5								
38			-3.8								
40			-2.8								
42			-1.3								
44			-0.4								
46			0.0								

Table A.4. Cross-sections of the scour holes for $L_a=25$ cm
(continued)

Scour Depth for $L_a=25$ cm (cm)											
X (cm)	Without Collar	$B_c=5$ (cm)					$B_c=2.5$ (cm)				
		Z_c (cm)									
		-5	-2.5	0	2.5	5	-5	-2.5	0	2.5	5
-70		1.7						2.0	1.9	1.2	0.8
-68		1.4						2.0	1.9	1.0	0.8
-66		1.4				2.4		1.6	1.6	1.0	0.4
-64		1.0				2.4	1.8	1.6	1.6	0.7	0.4
-62		1.0				2.2	1.8	1.1	1.4	0.7	0.9
-60		0.8				2.2	1.4	1.1	1.4	0.5	0.9
-58		0.8				1.7	1.4	0.6	1.0	0.5	0.2
-56		0.6				1.7	0.9	0.6	1.0	0.2	0.2
-54	0.0	0.6				1.5	0.9	0.2	0.6	0.2	-0.2
-52	-0.5	0.3				1.5	0.4	0.2	0.6	-0.3	-0.2
-50	-0.9	0.3				1.0	0.4	-0.4	0.1	-0.3	-0.8
-48	-1.1	-0.3				0.9	-0.1	-0.4	0.1	-0.8	-0.8
-46	-1.4	-0.3				0.4	-0.1	-1.3	-0.4	-0.8	-1.1
-44	-1.9	-0.9				-0.1	-0.6	-1.3	-0.4	-1.2	-1.1
-42	-2.5	-1.2				-0.4	-0.6	-1.7	-1.1	-1.2	-2.1
-40	-3.0	-1.8		0.2	-30.0	-0.9	-1.3	-1.7	-1.1	-1.9	-2.1
-38	-3.8	-2.3	0.0	-0.2	0.0	-1.6	-1.3	-2.7	-1.7	-1.9	-3.0
-36	-4.0	-2.8	-0.2	-0.4	-0.7	-2.1	-2.0	-3.2	-1.7	-2.7	-3.7
-34	-4.6	-3.3	-0.5	-0.8	-1.1	-3.0	-2.0	-3.8	-2.6	-3.3	-4.3
-32	-5.4	-3.8	-0.9	-1.0	-2.0	-3.9	-2.6	-4.2	-3.2	-4.0	-4.7
-30	-6.0	-4.4	-1.1	-1.5	-2.8	-4.8	-3.0	-4.7	-3.7	-4.7	-5.4
-28	-6.8	-4.9	-1.9	-2.5	-3.7	-5.8	-3.3	-5.3	-4.6	-5.7	-6.1
-26	-7.5	-5.4	-2.4	-3.2	-4.5	-6.7	-3.7	-5.7	-5.3	-6.4	-6.9
-24	-8.1	-5.9	-3.4	-4.0	-5.6	-7.5	-4.1	-6.3	-6.0	-7.4	-7.7
-22	-9.0	-6.3	-4.5	-4.8	-6.7	-8.3	-4.4	-7.2	-7.0	-8.3	-8.7
-20	-10.0	-6.6	-5.5	-5.7	-7.4	-8.8	-4.8	-7.8	-7.7	-9.1	-9.3
-18	-10.6	-7.0	-6.5	-6.5	-8.3	-9.5	-5.2	-8.5	-9.0	-10.0	-10.2
-16	-11.5	-7.4	-7.3	-7.3	-9.0	-10.0	-5.8	-9.4	-10.2	-10.8	-10.9
-14	-12.2	-7.6	-8.0	-8.5	-9.7	-10.6	-6.4	-10.6	-11.1	-11.7	-11.9
-12	-13.0	-7.8	-9.2	-9.5	-10.7	-11.4	-7.4	-11.7	-12.2	-12.7	-13.0
-10	-14.0	-7.9	-10.3	-10.5	-11.9	-12.4	-8.4	-12.8	-13.1	-14.0	-13.9
-8	-15.3	-8.2	-10.8	-11.7	-13.2	-13.8	-9.7	-13.9	-14.1	-15.3	-15.5
-6	-15.7	-8.9	-11.8	-12.8	-14.6	-15.3	-11.2	-15.0	-14.9	-15.8	-16.5
-4	-16.1	-10.2	-13.4	-14.0	-15.7	-16.5	-12.1	-15.6	-15.7	-16.3	-16.4
-2	-16.6	-11.4	-14.1	-14.5	-15.9	-17.0	-13.3	-16.0	-16.2	-16.8	-17.0
0	-17.8	-12.7	-14.4	-14.5	-16.4	-17.3	-15.6	-16.7	-16.7	-17.5	-17.8
2	-17.6	-13.5	-13.4	-14.2	-16.0	-17.1	-15.8	-15.8	-16.4	-17.2	-17.6
4	-16.6	-13.9	-12.6	-13.3	-14.7	-15.8	-16.1	-14.6	-15.3	-15.9	-15.5
6	-15.4	-14.2	-11.6	-12.4	-13.6	-14.5	-15.8	-13.4	-14.0	-14.7	-15.2
8	-14.3	-14.2	-10.4	-11.2	-12.4	-13.7	-15.2	-12.2	-12.8	-13.3	-14.6
10	-13.0	-13.5	-9.4	-9.8	-11.6	-12.6	-14.2	-10.9	-11.6	-12.0	-13.1
12	-11.8	-12.5	-7.9	-8.2	-10.3	-11.4	-12.8	-9.7	-10.5	-10.7	-12.0
14	-10.7	-11.2	-6.5	-6.8	-9.2	-10.5	-11.3	-8.4	-9.0	-10.0	-11.3
16	-9.8	-9.8	-5.3	-5.5	-7.5	-9.7	-10.1	-7.0	-8.1	-9.5	-10.3
18	-9.1	-8.8	-4.3	-4.0	-6.3	-9.1	-8.6	-5.8	-6.8	-9.1	-10.1
20	-8.2	-7.5	-3.0	-3.0	-5.0	-8.1	-7.4	-4.7	-5.6	-8.5	-10.0

Table A.4. Cross-sections of the scour holes for $L_a=25$ cm
(continued)

22	-7.5	-6.3	-1.6	-2.0	-3.7	-7.0	-6.5	-3.5	-4.4	-7.3	-9.3
24	-6.0	-4.0	-1.0	-1.0	-2.5	-5.2	-5.0	-2.0	-3.0	-5.5	-8.2
26	-5.8	-3.6	0.0	-0.5	-1.2	-4.5	-4.1	-1.5	-1.4	-4.7	-7.6
28	-4.7	-2.4		0.0	-0.5	-3.4	-2.7	-1.2	-1.2	-3.4	-6.2
30	-3.5	-1.5			0.0	-2.4	-1.2	-30.0	-1.0	-2.1	-4.6
32	-2.2	-1.4				-0.7					
34	-1.0	-1.2				-0.1					
36	0.0	-1.2				-0.1					
38						-0.1					
40						-0.1					
42						-0.1					
44						-0.1					
46						-0.1					

Table A.5. Cross-sections of the scour holes for $L_a=35$ cm

Scour Depth for $L_a=35$ cm (cm)											
X (cm)	Without Collar	$B_c=10$ (cm)					$B_c=7.5$ (cm)				
		Z_c (cm)									
		-5	-2.5	0	2.5	5	-5	-2.5	0	2.5	5
-118							3.4	3.75	4.2	3.85	3.7
-116							3.4	3.75	4.2	3.85	3.7
-114							3.4	3.75	4.2	3.6	3.7
-112							3.3	3.75	4.2	3.6	3.7
-110				3.9			3.3	3.75	4.2	3.6	3.6
-108				3.7			3.05	3.75	4.15	3.6	3.6
-106				3.45			3.05	3.75	4.15	3.6	3.6
-104				3.45			3.05	3.75	4.15	3.4	3.6
-102				3.45			3.05	3.75	4.15	3.4	3.6
-100				3.2			3.05	3.65	4.15	3.4	3.6
-98				3.2			3.05	3.65	4.15	3.4	3.6
-96				2.8		4.2	3.05	3.65	4.15	3.4	3.6
-94				2.8		4.2	3.2	3.65	4.15	3.4	3.6
-92				2.2		4.2	3.2	3.65	4.15	3.4	3.6
-90				2.2	4.4	4.2	3.2	3.8	4.15	3.4	3.7
-88				1.6	4.6	4.2	3.2	3.8	4.05	3.4	3.7
-86				1.6	4.6	4.2	3.35	3.8	4.05	3.4	3.7
-84				1.1	4.6	4.4	3.35	3.8	4.05	3.4	3.7
-82	2.6			1.1	4.85	4.6	3.4	3.8	4.05	3.4	3.7
-80	2.1		5.2	0.3	4.85	4.6	3.4	3.8	4.05	3.4	3.7
-78	2.1	2.6	5.1	0.3	5	4.6	3.6	3.8	3.95	3.4	3.7
-76	1.85	2.6	5.1	0.3	5	4.6	3.6	3.8	3.95	3.4	3.7
-74	1.85	2.6	5.1	0.7	5.1	4.7	3.7	3.8	3.95	3.4	3.7
-72	1.35	2.4	5.1	2.1	5.1	4.7	3.7	3.85	3.95	3.4	3.6
-70	1.35	2.4	5.1	3.2	5.2	4.6	3.7	3.85	3.95	3.4	3.6
-68	1	2.3	4.6	4.5	5.2	4.6	3.7	3.85	3.95	3.6	3.55
-66	1	2.3	4.6	5.3	4.9	4.4	3.65	3.85	3.95	3.6	3.55
-64	0.7	2	4.6	5.8	4.9	4.4	3.65	4	3.95	3.6	3.25
-62	0.7	2	4.6	5.8	4.7	4.3	3.65	4	3.85	3.6	3.25
-60	0.05	1.6	4.6	5.6	4.7	4.3	3.65	4.2	3.85	3.5	2.95
-58	0.05	1.6	4.4	5.5	4.4	4	3.55	4.2	3.7	3.5	2.95
-56	-0.5	1.3	4.4	5.5	4.4	4	3.55	4.2	3.7	3.25	2.7
-54	-0.5	1.3	4.1	5.15	4.05	3.35	3.3	4.2	3.7	3.25	2.7
-52	-1.3	1.1	4.1	5.15	4.05	3.35	3.3	4.2	3.7	2.8	2.05
-50	-1.3	1.1	3.7	4.7	3.5	3	2.85	3.9	3.5	2.8	2.05
-48	-1.55	0.85	3.7	4.7	3.5	3	2.85	3.9	3.5	2.05	1.2
-46	-1.9	0.55	3.2	4.2	3.25	2.5	2.5	3.5	3.2	2.05	1.2
-44	-2.3	0.2	3.2	4.2	2.7	2.4	2.5	3.5	3.2	1.6	0.8
-42	-2.65	-0.25	2.45	3.75	2.15	1.8	1.8	2.9	2.6	1.2	0.35
-40	-3	-0.4	2.45	3.4	1.7	1.4	1.8	2.9	2.6	0.6	-0.2
-38	-3.45	-0.9	2	3.05	1.1	0.7	0.8	2.5	1.85	-0.1	-0.8
-36	-4.2	-1.35	1.7	2.6	0.4	0.2	0.8	1.85	1.1	-0.95	-1.4
-34	-4.9	-1.8	1.05	2.1	-0.5	-0.5	0.4	0.85	0.3	-1.95	-2.1
-32	-5.35	-2.35	0.2	1.35	-1.5	-1.25	-0.25	0	-0.5	-2.9	-2.8
-30	-5.8	-2.9	-0.25	0.45	-2.35	-2.25	-1	-0.7	-1.8	-3.8	-3.8
-28	-6.4	-3.4	-1.45	-0.4	-3.1	-3	-1.75	-1.7	-2.7	-4.8	-4.55

Table A.5. Cross-sections of the scour holes for $L_a=35$ cm
(continued)

-26	-6.9	-3.95	-2.35	-1.5	-3.9	-3.8	-2.55	-2.9	-3.7	-5.65	-5.7
-24	-7.90	-4.30	-3.15	-2.65	-4.80	-4.90	-3.50	-3.90	-4.60	-6.75	-6.50
-22	-8.60	-5.00	-4.05	-3.60	-5.55	-5.50	-4.10	-5.20	-5.70	-7.60	-7.35
-20	-9.4	-5.2	-4.8	-4.6	-6.6	-6.2	-5.6	-6.2	-6.8	-8.4	-8.5
-18	-10.3	-5.6	-5.3	-5.6	-7.1	-7.3	-6.3	-7.0	-7.7	-9.2	-8.8
-16	-11.1	-6.2	-6.0	-6.4	-8.4	-8.2	-6.8	-8.0	-8.6	-10.0	-9.7
-14	-11.8	-6.6	-6.8	-7.4	-9.0	-9.3	-7.8	-9.1	-10.0	-10.8	-10.6
-12	-12.4	-7.4	-7.9	-8.4	-10.0	-10.1	-8.6	-10.3	-11.1	-11.8	-11.7
-10	-13.4	-8.3	-8.7	-9.7	-10.9	-11.1	-9.1	-11.6	-12.1	-13.2	-12.6
-8	-15.0	-9.9	-10.4	-11.7	-13.1	-13.0	-11.4	-13.2	-13.8	-14.8	-14.1
-6	-16.2	-10.8	-11.4	-13.0	-14.3	-14.7	-12.3	-14.8	-15.5	-15.8	-15.7
-4	-16.3	-11.7	-12.5	-14.1	-15.3	-15.9	-13.5	-16.2	-15.8	-16.9	-16.3
-2	-17.2	-12.8	-13.3	-15.2	-16.0	-15.9	-15.0	-16.5	-16.0	-17.4	-16.7
0	-18.7	-13.9	-14.5	-15.8	-17.1	-17.1	-16.4	-18.0	-17.1	-18.5	-17.8
2	-19.8	-14.2	-14.5	-16.1	-17.8	-18.1	-15.5	-17.7	-17.8	-18.8	-18.8
4	-19.7	-13.0	-12.9	-14.5	-16.4	-17.8	-14.3	-16.0	-16.0	-17.3	-18.6
6	-18.7	-11.6	-11.6	-13.3	-14.7	-16.5	-13.1	-14.6	-14.9	-15.9	-17.0
8	-17.4	-11.1	-10.6	-12.1	-13.6	-14.8	-12.4	-13.2	-13.8	-14.5	-15.6
10	-16.2	-10.6	-9.6	-10.5	-12.8	-13.6	-11.1	-12.0	-12.5	-13.4	-14.1
12	-14.9	-9.6	-8.5	-9.1	-11.2	-12.5	-9.5	-10.3	-11.3	-12.4	-13.1
14	-13.8	-8.3	-7.2	-7.7	-10.1	-11.6	-8.3	-8.9	-10.0	-11.3	-12.2
16	-12.5	-7.1	-6.0	-6.5	-9.1	-10.5	-6.8	-7.7	-8.7	-10.5	-11.3
18	-11.5	-5.6	-5.3	-4.9	-7.7	-9.4	-5.3	-6.5	-7.5	-8.8	-10.5
20	-10.6	-4.1	-5.0	-3.6	-6.5	-8.3	-4.1	-5.2	-6.1	-7.6	-9.2
22	-9.7	-3.2	-4.7	-2.2	-5.3	-7.2	-2.8	-3.6	-5.0	-5.8	-8.1
24	-9.1	-1.6	-4.2	-1.1	-4.1	-5.8	-1.3	-2.5	-3.5	-4.8	-7.1
26	-8.3	-0.8	-2.6	-0.5	-2.5	-4.8	-0.7	-1.3	-2.3	-3.4	-6.2
28	-7.3	-0.8	-1.4	-0.5	-1.6	-3.3	-0.7	-0.5	-1.2	-2.0	-5.4
30	-6.1	-0.3	-0.5	-0.1	-0.8	-1.8	-0.7	-0.5	-0.4	-1.0	-4.2
32	-5.0	-0.3	-0.5	-0.1	-0.8	-0.8	-0.7	-0.5	-0.4	-0.3	-2.8
34	-3.9	-0.1	-0.1	-0.1	-0.2	-0.1	0.0	-0.5	-0.4	-0.3	-1.6
36	-2.9	-0.1	0.0	-0.1	-0.2	-0.1		-0.5	0.0	-0.3	-0.3
38	-2.0	-0.1		-0.1	-0.2	-0.1		0.0		0.0	-0.3
40	-0.6	0.0		0.0	-0.1	-0.1					-0.3
42	-0.6				-0.1	0.1					-0.3
44	-0.3				-0.1						-0.3
46	-0.3				0.0						0.0
48	-0.3										
50	0.0										

Table A.5. Cross-sections of the scour holes for $L_a=35$ cm (continued)

Scour Depth for $L_a=35$ cm (cm)											
X (cm)	Without Collar	$B_c=5$ (cm)					$B_c=2.5$ (cm)				
		Z_c (cm)									
		-5	-2.5	0	2.5	5	-5	-2.5	0	2.5	5
-116		3.75	3.8	3.9	3.1	3.65	3.6	3.7	3.7		
-114		3.6	3.8	3.9	3.1	3.65	3.6	3.6	3.7		3.7
-112		3.6	3.7	3.9	3.1	3.65	3.6	3.6	3.7	3.8	4
-110		3.6	3.7	3.9	3.1	3.65	3.3	3.6	3.7	3.7	4
-108		3.6	3.5	3.9	3.1	3.65	3.3	3.6	3.6	3.7	3.8
-106		3.6	3.5	3.9	3.1	3.65	3.35	3	3.6	3.45	3.8
-104		3.5	3.35	3.85	3.1	3.65	3.35	3	3.5	3.45	4.1
-102		3.5	3.35	3.85	3.1	3.65	3.2	3	3.5	3.3	4.1
-100		3.35	3.2	3.7	2.9	3.65	3.2	3	3.2	3.3	3.4
-98		3.35	3.2	3.7	2.9	3.65	2.95	3	3.2	3.2	3.4
-96		3.35	3	3.55	3.1	3.5	2.95	3	3.1	3.2	3.4
-94		3.35	3	3.55	3.1	3.5	2.7	2.65	3.1	3.1	3.4
-92		3.3	2.8	3.4	3.1	3.25	2.7	2.65	3	3.1	3.3
-90		3.3	2.8	3.4	3.1	3.25	2.45	2.5	3	2.8	3.3
-88		3	2.6	3.2	3.05	3.1	2.45	2.5	2.8	2.8	3.15
-86		3	2.6	3.2	3.05	3.1	2.3	2.3	2.8	2.65	3.15
-84		2.9	2.5	2.95	2.9	2.8	2.3	2.3	2.65	2.65	2.85
-82	2.6	2.9	2.5	2.95	2.9	2.8	2.2	2.1	2.65	2.2	2.85
-80	2.1	2.55	2.3	2.85	2.9	2.7	2.2	2.1	2.4	2.2	2.5
-78	2.1	2.55	2.3	2.85	2.9	2.7	1.9	2	2.4	2	2.5
-76	1.85	2.3	2.1	2.7	2.7	2.7	1.9	2	2.05	2	2.2
-74	1.85	2.3	2.1	2.7	2.7	2.7	1.55	1.75	2.05	1.7	2.2
-72	1.35	2.1	2	2.65	2.55	2.4	1.55	1.75	1.8	1.7	1.7
-70	1.35	2.1	2	2.65	2.55	2.4	1.25	1.5	1.8	1.6	1.7
-68	1	1.7	1.5	2.5	2.3	2	1.25	1.5	1.5	1.6	1.2
-66	1	1.7	1.5	2.5	2.3	2	1	1.1	1.5	1.35	1.2
-64	0.7	1.4	1.25	2.35	2	1.5	1	1.1	1.5	1.35	0.8
-62	0.7	1.4	1.25	2.35	2	1.5	0.65	1.1	1.5	1.1	0.8
-60	0.05	1.2	0.95	2.15	1.7	0.95	0.65	1.1	1.25	1.1	0.3
-58	0.05	1.2	0.95	2.15	1.7	0.95	0.3	0.45	1.25	0.55	0.3
-56	-0.5	0.85	0.8	2.05	1.7	0.4	0.3	0.45	0.85	0.55	-0.3
-54	-0.5	0.85	0.8	2.05	1.7	0.4	-0.1	0.1	0.85	0.05	-0.3
-52	-1.3	0.6	0.35	1.8	1.3	-0.3	-0.1	0.1	0.65	0.05	-0.95
-50	-1.3	0.6	0.35	1.8	1.3	-0.3	-0.35	-0.3	0.65	-0.6	-0.95
-48	-1.55	0.1	0.05	1.4	0.5	-0.6	-0.35	-0.3	0	-0.6	-1.5
-46	-1.9	0.1	0.05	1.4	0.5	-0.9	-0.8	-0.8	0	-1.3	-1.5
-44	-2.3	-0.3	-0.3	0.9	0.1	-1.6	-0.8	-0.8	-0.7	-1.3	-2.2
-42	-2.65	-0.3	-0.3	0.9	-0.55	-2.2	-0.9	-1.2	-0.7	-2	-2.2
-40	-3	-0.6	-0.5	0.2	-1.3	-2.95	-1.2	-1.65	-1.05	-2	-2.75
-38	-3.45	-1	-1	-0.35	-2	-3.7	-1.6	-2.35	-1.85	-2.7	-3.5
-36	-4.2	-1.3	-1.6	-1.15	-2.7	-4.2	-1.95	-2.8	-2.9	-3.4	-4.25
-34	-4.9	-1.9	-2.2	-2.05	-3.65	-4.95	-2.2	-3.5	-3.95	-4.1	-5.1
-32	-5.35	-2.4	-3.1	-3.15	-4.55	-5.4	-2.5	-4.2	-4.8	-4.95	-5.8
-30	-5.8	-3.25	-3.7	-3.95	-5.35	-6.3	-2.5	-4.7	-5.7	-5.75	-6
-28	-6.4	-4.1	-4.4	-4.95	-6.15	-7.4	-2.9	-5.3	-6.65	-6.5	-6.9
-26	-6.9	-5.25	-5.6	-5.95	-7.2	-8.1	-3.4	-6.3	-7.65	-7.5	-7.8
-24	-7.9	-6	-6.7	-7	-8.05	-9.1	-4.1	-7.2	-8.65	-8.6	-8.6

Table A.5. Cross-sections of the scour holes for $L_a=35$ cm (continued)

-22	-8.6	-7	-7.7	-7.8	-9	-9.5	-4.8	-8.1	-8.7	-9.35	-9.5
-20	-9.4	-8	-8.55	-8.65	-9.65	-10.2	-5.7	-9	-10.2	-10.15	-10
-18	-10	-9	-9.2	-9.15	-10	-10.5	-6.4	-9.4	-10.45	-10	-10.2
-16	-11.1	-10.1	-10.7	-10.15	-11.2	-11.4	-7.8	-10.95	-11.55	-11.6	-11.5
-14	-11.8	-10.9	-11.65	-11.2	-12.05	-12.25	-8.9	-11.65	-12.25	-12.25	-12.3
-12	-12.4	-12	-12.4	-12.15	-12.9	-13.1	-10.05	-12.7	-13.6	-13.3	-12.9
-10	-13.4	-12.9	-13.8	-13.15	-13.95	-14.2	-11.3	-13.9	-14.3	-14.3	-13.9
-8	-15	-14.7	-15.5	-14.95	-15.7	-15.7	-12.4	-15.3	-16.2	-15.9	-15.5
-6	-16.15	-15.9	-16.8	-16.5	-17.15	-16.9	-13.95	-16.7	-16.8	-16.7	-16.2
-4	-16.3	-17.3	-17.3	-17	-17.65	-17.4	-15.05	-17.35	-17.6	-17.25	-16.8
-2	-17.2	-17.6	-17.4	-17.6	-17.8	-17.7	-16.1	-17.95	-18.4	-17.6	-17.3
0	-18.65	-19.3	-19.2	-18.8	-19	-19.2	-17.3	-19.3	-19.6	-19.1	-18.6
2	-19.8	-18.6	-18.9	-19	-19.3	-19.8	-17.6	-19	-19.5	-19.9	-19.65
4	-19.7	-17.45	-17.3	-17.7	-17.8	-19.1	-17.5	-18.2	-18.4	-19	-18
6	-18.7	-15.9	-16.2	-16.25	-16.65	-17.8	-17.3	-17.2	-16.9	-17.9	-16.55
8	-17.35	-14.5	-14.95	-14.8	-15.4	-16.45	-16.4	-16.05	-15.5	-16.15	-15.3
10	-16.15	-12.9	-13.3	-13.4	-14	-15.05	-15.15	-14.6	-13.8	-14.9	-14.2
12	-14.9	-11.4	-12.2	-12.1	-12.9	-13.8	-13.8	-13.2	-12.7	-13.45	-13.1
14	-13.75	-10.1	-10.9	-10.8	-12	-12.8	-12.15	-12	-11.75	-12.4	-12.3
16	-12.5	-9	-9.7	-9.9	-11.2	-11.8	-11.15	-11.05	-11.1	-11.6	-11.7
18	-11.5	-7.6	-8.45	-8.65	-10.2	-11.5	-10.35	-10	-10.1	-11.55	-11.3
20	-10.6	-6.35	-7.1	-7.2	-9.15	-10.9	-9.3	-9	-9	-11	-10.6
22	-9.7	-5.2	-5.8	-5.65	-8.1	-10.1	-8.15	-7.7	-7.75	-10.3	-9.8
24	-9.1	-3.7	-4.35	-4.35	-6.8	-8.8	-6.95	-6.2	-6.1	-9.05	-8.8
26	-8.3	-2.35	-3.15	-3.15	-5.35	-7.8	-5.65	-4.9	-4.9	-7.8	-7.45
28	-7.3	-1.25	-1.7	-2.05	-4	-6.4	-4.15	-3.4	-3.55	-6.45	-5.8
30	-6.1	-0.55	-0.1	-0.8	-2.9	-5.1	-3	-2.2	-2.35	-5.15	-4.85
32	-5	-0.55	-0.1	-0.2	-1.7	-4.05	-1.75	-0.95	-1.3	-3.9	-3.95
34	-3.9	-0.55	-0.1	-0.2	-0.45	-2.8	-0.55	-0.4	-0.6	-2.9	-2.9
36	-2.9	-0.55	-0.1	-0.2	-0.2	-1.6	-0.1	-0.4	-0.2	-1.55	-1.7
38	-2	0	-0.1	-0.2	-0.2	-0.45	-0.1	-0.4	-0.2	-0.3	-0.4
40	-0.6		0	0	-0.2	0.1	-0.1	-0.4	-0.2	-0.05	-0.4
42	-0.6				-0.2	0.1	-0.1	0	-0.2	-0.05	-0.4
44	-0.3				-0.2	0.1	0		0	-0.05	-0.4
46	-0.3				0	0.1				0	0
48	-0.3					0.1					
50	0										

APPENDIX B

Table B.1. Time variation of scour depth around the abutments for $L_a=7.5$ cm

$L_a=7.5$ cm, $B_a=10$ cm							
Time (min)	B_c (cm)	Scour depth (d_s) (cm)					
		Z_c (cm)					
		Without collar	5	2.5	0	-2.5	-5
1	10.00	1.50	0.70	0.90	0.00	0.90	1.40
2	10.00	3.60	2.30	1.50	0.00	1.60	2.10
4	10.00	3.95	2.80	1.60	0.00	2.00	2.80
6	10.00	4.00	2.80	1.80	0.00	2.40	3.40
8	10.00	4.00	2.85	2.00	0.00	2.40	3.45
10	10.00	4.00	2.85	2.30	0.00	2.40	3.55
15	10.00	4.10	2.90	2.30	0.00	2.40	3.75
20	10.00	4.10	3.20	2.40	0.00	2.40	3.90
25	10.00	4.30	3.45	2.40	0.00	2.40	3.90
30	10.00	4.35	3.70	2.45	0.00	2.40	3.95
40	10.00	4.35	3.80	2.45	0.00	2.40	3.95
50	10.00	4.40	3.80	2.50	0.00	2.40	4.05
60	10.00	4.40	3.80	2.50	0.00	2.40	4.05
80	10.00	4.45	4.20	2.60	0.00	2.40	4.45
90	10.00	4.45	4.45	2.60	0.00	2.40	4.45
100	10.00	4.60	4.45	2.60	0.00	2.40	4.60
120	10.00	4.65	4.50	2.65	0.00	2.40	4.80
150	10.00	4.80	4.50	2.80	0.00	2.40	4.95
180	10.00	5.05	4.75	3.00	0.00	2.40	5.00
210	10.00	5.05	5.00	3.10	0.00	2.40	5.00
240	10.00	5.10	5.15	3.15	0.00	2.40	5.00
270	10.00	5.10	5.15	3.15	0.00	2.40	5.00
300	10.00	5.20	5.20	3.15	0.00	2.40	5.00
330	10.00	5.20	5.20	3.15	0.00	2.40	5.00
360	10.00	5.30	5.30	3.20	0.00	2.40	5.00

Table B.1. Time variation of scour depth around the abutments for $L_a=7.5$ cm
(continued)

1	7.50	1.50	2.60	0.00	0.00	1.20	1.10
2	7.50	3.60	3.00	0.80	0.00	2.10	2.55
4	7.50	3.95	3.20	1.00	0.00	2.50	2.90
6	7.50	4.00	3.40	1.20	0.00	2.50	3.00
8	7.50	4.00	3.50	1.60	0.00	2.50	3.15
10	7.50	4.00	3.60	1.70	0.00	2.50	3.40
15	7.50	4.10	3.60	1.80	0.00	2.50	3.60
20	7.50	4.10	3.60	2.00	0.00	2.50	3.75
25	7.50	4.30	3.60	2.40	0.00	2.50	3.85
30	7.50	4.35	3.60	2.60	0.00	2.50	3.90
40	7.50	4.35	3.60	2.70	0.00	2.50	3.95
50	7.50	4.40	3.60	2.70	0.00	2.50	4.00
60	7.50	4.40	3.90	2.80	0.00	2.50	4.05
80	7.50	4.45	4.10	2.80	0.00	2.50	4.20
90	7.50	4.45	4.10	3.40	0.00	2.50	4.25
100	7.50	4.60	4.10	3.55	0.00	2.50	4.30
120	7.50	4.65	4.10	3.90	0.00	2.50	4.45
150	7.50	4.80	4.25	3.95	0.00	2.50	4.70
180	7.50	5.05	4.45	4.05	0.00	2.50	5.00
210	7.50	5.05	4.60	4.10	0.00	2.50	5.00
240	7.50	5.10	4.75	4.15	0.00	2.50	5.00
270	7.50	5.10	5.10	4.15	0.00	2.50	5.00
300	7.50	5.20	5.15	4.15	0.00	2.50	5.00
330	7.50	5.20	5.20	4.15	0.00	2.50	5.00
360	7.50	5.30	5.20	4.15	0.00	2.50	5.00

Table B.1. Time variation of scour depth around the abutments for $L_a=7.5$ cm
(continued)

$L_a=7.5$ cm, $B_a=10$ cm							
Time (min)	B_c (cm)	Scour depth (d_s) (cm)					
		Z_c (cm)					
		Without collar	5	2.5	0	-2.5	-5
1	5.00	1.50	1.00	1.00	0.00	1.20	1.20
2	5.00	3.60	2.60	2.10	0.00	2.00	2.60
4	5.00	3.95	2.70	2.40	0.00	2.50	2.70
6	5.00	4.00	2.75	2.50	0.00	2.50	2.80
8	5.00	4.00	2.80	2.55	0.00	2.50	2.90
10	5.00	4.00	2.85	2.60	0.00	2.50	3.05
15	5.00	4.10	3.05	2.70	0.00	2.50	3.40
20	5.00	4.10	3.25	3.10	0.00	2.50	3.60
25	5.00	4.30	3.30	3.20	0.00	2.50	3.65
30	5.00	4.35	3.35	3.25	0.00	2.50	3.75
40	5.00	4.35	3.40	3.30	0.00	2.50	3.85
50	5.00	4.40	3.60	3.35	0.00	2.50	3.90
60	5.00	4.40	3.70	3.40	0.00	2.50	4.00
80	5.00	4.45	3.80	3.45	0.00	2.50	4.10
90	5.00	4.45	3.85	3.50	0.00	2.50	4.20
100	5.00	4.60	3.90	3.55	0.00	2.50	4.30
120	5.00	4.65	4.00	3.65	0.00	2.50	4.40
150	5.00	4.80	4.10	4.05	0.00	2.50	4.70
180	5.00	5.05	4.20	4.30	0.00	2.50	5.00
210	5.00	5.05	4.30	4.40	0.00	2.50	5.00
240	5.00	5.10	4.40	4.45	0.00	2.50	5.00
270	5.00	5.10	4.45	4.50	0.70	2.50	5.00
300	5.00	5.20	4.60	4.50	0.80	2.50	5.00
330	5.00	5.20	4.80	4.50	1.00	2.50	5.00
360	5.00	5.30	4.90	4.50	1.15	2.50	5.00

Table B.1. Time variation of scour depth around the abutments for $L_a=7.5$ cm (continued)

1	2.50	1.50	1.10	1.10	0.00	1.20	1.20
2	2.50	3.60	2.40	1.90	0.00	2.50	2.60
4	2.50	3.95	2.80	2.20	0.00	2.50	2.90
6	2.50	4.00	3.20	2.35	0.00	2.50	3.10
8	2.50	4.00	3.30	2.70	0.00	2.50	3.30
10	2.50	4.00	3.35	2.80	0.00	2.50	3.35
15	2.50	4.10	3.40	2.90	0.00	2.50	3.40
20	2.50	4.10	3.45	3.15	0.00	2.50	3.50
25	2.50	4.30	3.55	3.35	0.00	2.50	3.70
30	2.50	4.35	3.60	3.50	0.00	2.50	3.80
40	2.50	4.35	3.85	3.60	0.00	2.50	3.85
50	2.50	4.40	3.95	3.70	1.00	2.50	3.95
60	2.50	4.40	4.05	3.80	1.40	2.50	4.05
80	2.50	4.45	4.10	3.95	1.85	2.50	4.35
90	2.50	4.45	4.20	4.00	2.05	2.50	4.45
100	2.50	4.60	4.30	4.05	2.70	2.50	4.50
120	2.50	4.65	4.40	4.10	2.80	2.50	4.55
150	2.50	4.80	4.45	4.15	2.90	2.50	4.60
180	2.50	5.05	4.80	4.40	3.10	2.50	5.00
210	2.50	5.05	4.90	4.50	3.55	2.50	5.00
240	2.50	5.10	5.05	4.60	3.70	2.50	5.00
270	2.50	5.10	5.15	4.70	4.55	2.50	5.00
300	2.50	5.20	5.20	4.80	4.60	2.50	5.00
330	2.50	5.20	5.25	5.00	4.70	3.70	5.00
360	2.50	5.30	5.30	5.20	4.90	4.00	5.00

Table B.2. Time variation of scour depth around the abutments for $L_a=15$ cm

$L_a=15$ cm, $B_a=10$ cm							
Time (min)	B_c (cm)	Scour depth (d_s) (cm)					
		Z_c (cm)					
		Without collar	5	2.5	0	-2.5	-5
1	10.00	1.10	1.00	1.00	0.00	1.00	1.00
2	10.00	2.70	2.30	2.40	0.00	2.50	2.10
4	10.00	4.70	3.20	3.10	0.00	2.50	3.70
6	10.00	5.20	4.00	3.60	0.00	2.50	5.00
8	10.00	5.30	4.40	3.70	0.00	2.50	5.00
10	10.00	5.40	4.90	3.90	0.00	2.50	5.00
15	10.00	6.10	5.50	4.20	0.00	2.50	5.00
20	10.00	7.00	6.30	4.50	0.00	2.50	5.00
25	10.00	7.45	6.60	4.70	0.00	2.50	5.00
30	10.00	7.70	7.00	5.10	0.00	2.50	5.00
40	10.00	8.25	7.60	5.30	0.00	2.50	5.00
50	10.00	8.75	7.80	5.80	0.00	2.50	5.00
60	10.00	9.05	8.20	6.15	0.00	2.50	5.00
80	10.00	9.60	8.80	6.70	0.00	2.50	5.00
90	10.00	9.85	8.95	6.90	0.00	2.50	5.00
100	10.00	10.20	9.10	7.00	0.00	2.50	5.00
120	10.00	10.60	9.20	7.20	0.00	2.50	5.00
150	10.00	11.00	9.60	7.40	0.00	2.50	5.00
180	10.00	11.20	9.85	7.60	0.00	2.50	5.00
210	10.00	11.75	9.95	7.75	0.00	2.50	5.00
240	10.00	12.00	10.15	7.73	0.80	2.50	5.00
270	10.00	12.20	10.25	8.05	1.00	2.50	5.00
300	10.00	12.50	10.35	8.35	1.20	2.50	5.00
330	10.00	12.60	10.45	8.45	1.40	2.50	5.00
360	10.00	12.90	10.70	8.60	2.00	2.50	5.00

Table B.2. Time variation of scour depth around the abutments for $L_a=15$ cm (continued)

1	7.50	1.10	1.00	1.00	0.00	1.00	1.00
2	7.50	2.70	3.00	2.50	0.00	2.20	2.70
4	7.50	4.70	4.40	3.20	0.00	2.50	4.20
6	7.50	5.20	4.90	3.85	0.00	2.50	5.00
8	7.50	5.30	5.15	4.20	0.00	2.50	5.00
10	7.50	5.40	5.25	4.40	0.00	2.50	5.00
15	7.50	6.10	5.40	4.70	0.00	2.50	5.00
20	7.50	7.00	6.05	5.30	0.00	2.50	5.00
25	7.50	7.45	6.50	5.40	0.00	2.50	5.00
30	7.50	7.70	6.70	5.90	0.00	2.50	5.00
40	7.50	8.25	7.50	6.25	0.00	2.50	5.00
50	7.50	8.75	7.85	6.60	0.00	2.50	5.00
60	7.50	9.05	8.30	6.80	0.00	2.50	5.00
80	7.50	9.60	8.60	6.95	2.80	2.50	5.00
90	7.50	9.85	8.95	7.05	3.90	2.50	5.00
100	7.50	10.20	9.10	7.25	4.60	2.50	5.00
120	7.50	10.60	9.50	7.60	4.90	2.50	5.00
150	7.50	11.00	9.70	8.00	5.20	2.50	5.00
180	7.50	11.20	9.85	8.15	5.40	2.50	5.00
210	7.50	11.75	10.00	8.45	5.80	2.50	5.00
240	7.50	12.00	10.30	8.75	6.10	2.50	5.00
270	7.50	12.20	10.50	9.05	6.50	2.50	5.00
300	7.50	12.50	10.70	9.15	6.90	2.50	5.00
330	7.50	12.60	10.90	9.45	7.00	2.50	5.00
360	7.50	12.90	11.10	9.60	7.20	2.50	5.00

Table B.2. Time variation of scour depth around the abutments for $L_a=15$ cm (continued)

$L_a=15$ cm, $B_a=10$ cm							
Time (min)	B_c (cm)	Scour depth (d_s) (cm)					
		Z_c (cm)					
		Without collar	5	2.5	0	-2.5	-5
1	5.00	1.10	1.00	1.10	0.00	1.10	1.10
2	5.00	2.70	2.70	3.00	0.00	2.00	2.10
4	5.00	4.70	4.80	4.10	0.00	2.50	3.20
6	5.00	5.20	5.10	4.70	0.00	2.50	4.50
8	5.00	5.30	5.30	5.05	0.00	2.50	4.80
10	5.00	5.40	5.50	5.35	0.00	2.50	5.00
15	5.00	6.10	6.50	5.70	0.00	2.50	5.00
20	5.00	7.00	6.90	6.40	0.00	2.50	5.00
25	5.00	7.45	7.30	6.60	1.00	2.50	5.00
30	5.00	7.70	7.40	6.85	1.80	2.50	5.00
40	5.00	8.25	7.70	7.20	3.60	2.50	5.00
50	5.00	8.75	8.20	7.50	4.60	2.50	5.00
60	5.00	9.05	8.80	7.80	5.15	2.50	5.00
80	5.00	9.60	9.05	8.10	5.35	2.50	5.00
90	5.00	9.85	9.30	8.20	5.50	2.50	5.00
100	5.00	10.20	9.50	8.40	6.30	2.50	5.00
120	5.00	10.60	9.75	8.75	6.45	4.50	5.00
150	5.00	11.00	10.20	9.10	6.70	5.30	5.00
180	5.00	11.20	10.50	9.35	7.40	6.30	5.00
210	5.00	11.75	10.65	9.70	7.80	6.60	5.00
240	5.00	12.00	10.90	10.00	8.00	6.70	5.00
270	5.00	12.20	11.20	10.20	8.20	7.00	5.00
300	5.00	12.50	11.30	10.30	8.70	7.15	5.00
330	5.00	12.60	11.40	10.50	9.20	7.25	5.00
360	5.00	12.90	11.50	10.80	9.40	7.50	5.00

Table B.2. Time variation of scour depth around the abutments for $L_a=15$ cm (continued)

1	2.50	1.10	1.10	1.10	0.00	1.30	1.00
2	2.50	2.70	3.00	2.50	0.00	2.50	2.50
4	2.50	4.70	4.60	4.20	0.00	2.50	4.30
6	2.50	5.20	5.20	4.70	0.00	2.50	5.00
8	2.50	5.30	5.30	5.30	1.35	2.50	5.00
10	2.50	5.40	5.40	5.45	1.90	2.50	5.00
15	2.50	6.10	5.90	5.60	2.40	2.50	5.00
20	2.50	7.00	6.50	6.10	2.80	2.50	5.00
25	2.50	7.45	7.00	6.50	3.50	3.80	5.00
30	2.50	7.70	7.40	6.70	3.90	4.40	5.00
40	2.50	8.25	7.70	7.10	4.30	4.80	5.00
50	2.50	8.75	8.30	7.40	5.00	5.30	5.00
60	2.50	9.05	8.70	7.95	5.50	5.90	5.00
80	2.50	9.60	9.30	8.70	6.70	7.05	5.00
90	2.50	9.85	9.60	8.85	6.85	7.20	5.00
100	2.50	10.20	9.80	9.00	6.95	7.60	5.00
120	2.50	10.60	10.10	9.30	7.70	8.00	6.40
150	2.50	11.00	10.50	9.70	8.50	8.50	6.90
180	2.50	11.20	10.70	10.05	9.40	9.20	7.70
210	2.50	11.75	10.90	10.30	9.80	9.35	7.90
240	2.50	12.00	11.10	10.60	10.00	9.70	8.70
270	2.50	12.20	11.50	10.70	10.30	9.90	8.80
300	2.50	12.50	11.60	10.95	10.60	10.30	9.20
330	2.50	12.60	11.70	11.20	10.90	10.40	9.40
360	2.50	12.90	11.80	11.40	11.30	10.60	9.80

Table B.3. Time variation of scour depth around the abutment for $L_a=20$ cm (continued)

$L_a=20$ cm, $B_a=10$ cm							
Time (min)	B_c (cm)	Scour depth (d_s) (cm)					
		Z_c (cm)					
		Without collar	5	2.5	0	-2.5	-5
1	10.00	1.40	1.30	1.20	0.00	1.40	1.40
2	10.00	4.50	3.00	2.30	0.00	2.20	3.00
4	10.00	5.45	5.30	3.90	0.00	2.50	4.60
6	10.00	6.60	6.20	4.90	0.00	2.50	5.00
8	10.00	7.10	6.80	5.50	0.00	2.50	5.00
10	10.00	7.50	7.10	5.60	0.00	2.50	5.00
15	10.00	7.80	7.80	6.30	0.00	2.50	5.00
20	10.00	8.50	8.20	6.90	0.00	2.50	5.00
25	10.00	9.00	8.60	7.05	0.00	2.50	5.00
30	10.00	9.50	8.80	7.70	0.00	2.50	5.00
40	10.00	10.20	9.40	7.90	0.00	2.50	5.00
50	10.00	10.85	10.00	8.30	0.00	2.50	5.00
60	10.00	11.30	10.30	8.45	0.00	2.50	5.00
80	10.00	11.80	10.80	9.10	0.00	2.50	5.00
90	10.00	12.20	11.00	9.20	1.70	2.50	5.00
100	10.00	12.55	11.10	9.35	2.80	2.50	5.00
120	10.00	12.70	11.50	9.80	3.60	2.50	5.00
150	10.00	13.50	11.90	10.10	5.20	2.50	5.00
180	10.00	13.70	12.10	10.40	6.27	2.50	5.00
210	10.00	14.00	12.35	10.90	6.55	2.50	5.00
240	10.00	14.20	12.60	11.10	6.95	2.50	5.00
270	10.00	14.60	12.95	11.35	7.33	4.00	5.00
300	10.00	15.05	13.05	11.60	7.53	4.50	5.00
330	10.00	15.15	13.20	11.70	7.80	5.00	5.00
360	10.00	15.30	13.50	12.00	8.00	6.30	5.00

Table B.3. Time variation of scour depth around the abutment for $L_a=20$
(continued)

1	7.50	1.40	1.10	1.30	0.00	1.20	1.20
2	7.50	4.50	3.00	2.50	0.00	2.10	2.10
4	7.50	5.45	5.10	5.30	0.00	2.50	4.40
6	7.50	6.60	5.40	5.50	0.00	2.50	5.00
8	7.50	7.10	6.80	6.35	0.00	2.50	5.00
10	7.50	7.50	7.20	6.70	0.00	2.50	5.00
15	7.50	7.80	7.70	7.10	0.00	2.50	5.00
20	7.50	8.50	8.40	7.75	0.00	2.50	5.00
25	7.50	9.00	8.80	8.30	0.00	2.50	5.00
30	7.50	9.50	9.30	8.50	0.00	2.50	5.00
40	7.50	10.20	9.70	8.90	0.00	2.50	5.00
50	7.50	10.85	10.20	9.20	1.85	2.50	5.00
60	7.50	11.30	10.70	9.40	4.00	2.50	5.00
80	7.50	11.80	11.00	9.75	5.40	2.50	5.00
90	7.50	12.20	11.15	9.90	5.45	2.50	5.00
100	7.50	12.55	11.30	10.30	6.20	2.50	5.00
120	7.50	12.70	11.90	10.45	6.80	2.50	5.00
150	7.50	13.50	12.40	10.90	7.45	5.50	5.00
180	7.50	13.70	12.70	11.10	7.75	6.90	5.00
210	7.50	14.00	13.20	11.60	8.20	7.50	5.00
240	7.50	14.20	13.50	11.80	8.50	7.60	5.00
270	7.50	14.60	13.60	11.95	8.80	7.75	5.00
300	7.50	15.05	13.70	12.05	9.10	7.90	5.00
330	7.50	15.15	13.90	12.15	9.60	8.00	5.00
360	7.50	15.30	14.30	12.50	10.10	8.20	5.00

Table B.3. Time variation of scour depth around the abutment for $L_a=20$ cm (continued)

$L_a=20$ cm, $B_a=10$ cm							
Time (min)	B_c (cm)	Scour depth (d_s) (cm)					
		Z_c (cm)					
		Without collar	5	2.5	0	-2.5	-5
1	5.00	1.40	1.10	0.90	0.00	1.10	1.20
2	5.00	4.50	2.80	2.50	0.00	2.10	3.50
4	5.00	5.45	5.25	4.40	0.00	2.50	4.50
6	5.00	6.60	6.00	5.30	0.00	2.50	5.00
8	5.00	7.10	6.70	6.00	0.00	2.50	5.00
10	5.00	7.50	7.25	6.60	1.00	2.50	5.00
15	5.00	7.80	7.80	7.30	3.50	2.50	5.00
20	5.00	8.50	8.25	8.10	4.30	2.50	5.00
25	5.00	9.00	8.70	8.55	5.10	2.50	5.00
30	5.00	9.50	9.40	9.00	5.25	4.50	5.00
40	5.00	10.20	9.85	9.50	5.45	5.30	5.00
50	5.00	10.85	10.40	9.90	6.00	5.60	5.00
60	5.00	11.30	10.75	10.30	6.90	6.60	5.00
80	5.00	11.80	11.50	10.75	7.00	6.80	5.00
90	5.00	12.20	11.80	10.85	7.80	6.90	5.00
100	5.00	12.55	11.95	11.20	8.20	7.00	5.00
120	5.00	12.70	12.50	11.75	8.80	7.10	5.00
150	5.00	13.50	13.00	11.95	9.90	8.10	5.00
180	5.00	13.70	13.10	12.10	10.50	9.10	6.80
210	5.00	14.00	13.20	12.50	11.35	10.20	8.10
240	5.00	14.20	13.25	12.65	11.80	10.60	8.70
270	5.00	14.60	13.50	12.80	12.00	11.10	9.00
300	5.00	15.05	13.75	13.15	12.15	11.35	9.25
330	5.00	15.15	13.90	13.40	12.45	11.70	9.45
360	5.00	15.30	14.20	13.60	12.80	12.10	9.60

Table B.3. Time variation of scour depth around the abutment for $L_a=20$ cm (continued)

1	2.50	1.40	1.40	1.10	0.00	1.30	1.20
2	2.50	4.50	2.80	2.00	1.30	2.50	3.50
4	2.50	5.45	5.00	4.50	2.75	2.50	5.00
6	2.50	6.60	6.20	5.40	4.00	2.50	5.00
8	2.50	7.10	6.80	6.00	5.10	2.50	5.00
10	2.50	7.50	7.30	6.75	5.35	2.50	5.00
15	2.50	7.80	8.00	7.50	6.50	5.20	5.00
20	2.50	8.50	8.80	7.95	7.10	5.40	5.00
25	2.50	9.00	9.20	8.70	7.40	6.05	5.00
30	2.50	9.50	9.60	9.10	8.10	6.70	5.00
40	2.50	10.20	10.30	9.90	8.70	7.35	7.20
50	2.50	10.85	10.95	10.20	9.00	7.85	8.10
60	2.50	11.30	11.30	10.80	9.40	8.30	8.15
80	2.50	11.80	11.90	11.35	10.40	9.00	8.20
90	2.50	12.20	12.40	11.60	11.00	9.45	8.25
100	2.50	12.55	12.65	11.95	11.30	9.95	8.40
120	2.50	12.70	12.80	12.40	11.90	10.80	9.00
150	2.50	13.50	13.35	12.65	12.30	11.45	9.70
180	2.50	13.70	13.70	13.10	12.90	12.30	10.60
210	2.50	14.00	14.20	13.30	13.20	12.40	11.10
240	2.50	14.20	14.60	13.40	13.25	12.50	11.35
270	2.50	14.60	14.80	13.50	13.45	13.25	11.85
300	2.50	15.05	15.00	13.55	13.70	13.50	12.10
330	2.50	15.15	15.10	13.80	13.90	13.60	12.40
360	2.50	15.30	15.25	14.10	14.05	13.80	12.90

Table B.4. Time variation of scour depth around the abutments for $L_a=35$ cm

$L_a=35$ cm, $B_a=10$ cm							
Time (min)	B_c (cm)	Scour depth (d_s) (cm)					
		Z_c (cm)					
		Without collar	5	2.5	0	-2.5	-5
1	10.00	2.00	1.30	0.50	0.00	4.40	1.20
2	10.00	4.20	4.30	2.30	0.00	2.00	2.30
4	10.00	5.50	6.10	5.10	0.00	2.00	4.40
6	10.00	7.70	8.20	7.30	0.00	2.00	5.00
8	10.00	9.25	9.00	8.60	0.00	2.00	5.00
10	10.00	10.05	9.60	9.10	0.80	2.00	5.00
15	10.00	11.00	11.10	10.10	4.00	2.00	5.00
20	10.00	12.00	12.30	11.20	5.80	2.00	5.00
25	10.00	12.60	12.50	11.80	6.20	4.60	5.00
30	10.00	13.35	13.30	12.70	7.50	5.50	5.00
40	10.00	14.20	14.90	13.90	8.30	7.60	5.00
50	10.00	14.75	15.40	14.70	9.00	7.80	5.00
60	10.00	15.40	15.70	15.10	10.10	9.10	5.40
80	10.00	17.20	16.40	16.00	11.40	10.10	6.10
90	10.00	17.60	16.70	16.40	11.80	10.75	9.25
100	10.00	17.70	16.90	16.60	12.50	11.00	9.70
120	10.00	17.80	17.20	16.80	13.20	12.10	10.10
150	10.00	18.50	17.50	17.00	14.20	12.50	11.10
180	10.00	18.90	17.60	17.20	14.80	12.80	12.30
210	10.00	19.30	17.90	17.50	15.22	13.30	13.10
240	10.00	19.40	17.90	17.70	16.10	13.80	13.60
270	10.00	19.50	18.00	17.90	16.30	14.00	13.80
300	10.00	19.80	18.10	17.90	16.75	14.50	14.00
330	10.00	19.85	18.20	18.00	16.90	14.70	14.20
360	10.00	20.00	18.50	18.40	17.05	15.10	14.50

Table B.4. Time variation of scour depth around the abutments for $L_a=35$ cm

1	7.50	2.00	1.00	1.00	0.00	1.00	1.00
2	7.50	4.20	5.30	5.00	0.00	2.50	4.20
4	7.50	5.50	7.85	7.70	3.60	2.50	5.00
6	7.50	7.70	9.10	9.05	5.25	2.50	5.00
8	7.50	9.25	9.90	10.10	6.40	2.50	5.00
10	7.50	10.05	10.65	10.65	7.10	2.50	5.00
15	7.50	11.00	11.80	11.50	8.10	6.30	5.00
20	7.50	12.00	12.95	12.30	9.00	7.70	5.00
25	7.50	12.60	13.50	13.20	9.70	8.90	5.00
30	7.50	13.35	14.05	14.10	10.10	9.60	5.00
40	7.50	14.20	15.10	15.40	11.40	10.60	9.00
50	7.50	14.75	16.50	16.15	11.65	11.25	10.15
60	7.50	15.40	16.95	16.85	13.80	11.95	10.20
80	7.50	17.20	17.90	17.65	15.10	13.20	12.30
90	7.50	17.60	18.15	18.00	15.35	13.40	13.00
100	7.50	17.70	18.30	18.30	16.20	13.80	13.40
120	7.50	17.80	18.80	18.70	16.75	15.00	13.85
150	7.50	18.50	18.95	18.90	17.80	16.20	14.40
180	7.50	18.90	19.05	19.10	18.30	17.35	15.25
210	7.50	19.30	19.40	19.20	18.70	17.90	15.50
240	7.50	19.40	19.50	19.45	18.80	18.50	16.05
270	7.50	19.50	19.60	19.70	18.90	18.70	16.50
300	7.50	19.80	19.70	19.80	19.20	19.15	16.80
330	7.50	19.85	19.80	19.90	19.40	19.30	17.15
360	7.50	20.00	20.00	20.00	19.70	19.60	17.60

Table B.4. Time variation of scour depth around the abutments for $L_a=35$ cm (continued)

$L_a=35$ cm, $B_a=10$ cm							
Time (min)	B_c (cm)	Scour depth (d_s) (cm)					
		Z_c (cm)					
		Without collar	5	2.5	0	-2.5	-5
1	5.00	2.00	1.00	1.00	0.00	0.90	0.90
2	5.00	4.20	4.70	4.30	0.00	2.50	2.90
4	5.00	5.50	7.90	7.50	4.70	2.50	5.00
6	5.00	7.70	9.50	9.10	6.30	5.30	5.00
8	5.00	9.25	10.45	9.80	7.05	6.60	5.00
10	5.00	10.05	11.45	10.40	7.80	7.00	5.00
15	5.00	11.00	12.70	11.30	9.90	7.95	5.00
20	5.00	12.00	13.90	12.60	11.80	8.70	7.80
25	5.00	12.60	14.40	13.60	12.20	10.90	8.60
30	5.00	13.35	14.80	13.80	12.60	12.00	9.40
40	5.00	14.20	15.40	14.95	13.65	14.20	10.05
50	5.00	14.75	15.75	15.60	14.45	15.00	12.40
60	5.00	15.40	16.30	16.15	15.35	15.75	14.00
80	5.00	17.20	17.00	16.70	16.90	16.10	15.50
90	5.00	17.60	17.20	17.25	17.50	16.80	16.00
100	5.00	17.70	17.60	17.60	17.85	17.00	16.35
120	5.00	17.80	17.90	17.85	18.35	17.70	17.15
150	5.00	18.50	18.20	18.40	19.00	18.20	17.85
180	5.00	18.90	18.50	18.75	19.20	18.70	18.40
210	5.00	19.30	18.80	18.90	19.50	19.10	18.60
240	5.00	19.40	19.05	19.00	19.65	19.20	19.40
270	5.00	19.50	19.25	19.10	19.80	19.30	19.45
300	5.00	19.80	19.40	19.20	19.90	19.40	19.50
330	5.00	19.85	19.70	19.40	20.00	19.50	19.55
360	5.00	20.00	20.00	20.00	20.00	19.60	19.55

Table B.4. Time variation of scour depth around the abutments for $L_a=35$ cm (continued)

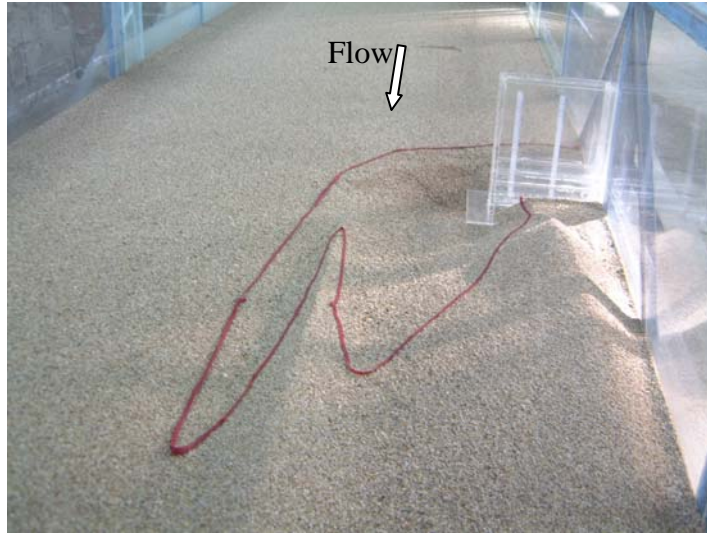
1	2.50	2.00	0.90	0.90	0.00	0.90	0.90
2	2.50	4.20	2.50	2.90	0.90	2.40	3.40
4	2.50	5.50	6.60	6.50	3.00	4.00	5.00
6	2.50	7.70	7.80	7.90	5.70	6.80	5.00
8	2.50	9.25	8.50	8.50	7.00	8.20	6.90
10	2.50	10.05	9.50	9.65	8.15	9.45	8.25
15	2.50	11.00	11.10	10.85	9.80	10.20	9.90
20	2.50	12.00	12.00	11.95	11.05	11.70	11.10
25	2.50	12.60	12.60	12.90	11.90	12.50	11.80
30	2.50	13.35	13.90	13.20	12.40	13.45	12.80
40	2.50	14.20	14.00	14.00	13.40	14.45	13.50
50	2.50	14.75	14.70	14.70	13.90	15.45	14.70
60	2.50	15.40	15.70	15.30	15.00	15.40	15.70
80	2.50	17.20	16.90	16.25	15.75	16.90	17.50
90	2.50	17.60	17.10	16.50	16.40	17.30	17.60
100	2.50	17.70	17.40	16.60	16.80	17.50	17.75
120	2.50	17.80	17.60	17.00	17.75	17.95	19.00
150	2.50	18.50	18.00	17.50	18.40	18.60	19.20
180	2.50	18.90	18.35	18.40	18.60	18.90	19.30
210	2.50	19.30	18.50	18.75	18.90	19.00	19.40
240	2.50	19.40	18.70	19.00	19.10	19.10	19.50
270	2.50	19.50	19.30	19.15	19.30	19.40	19.60
300	2.50	19.80	19.50	19.40	19.40	19.55	19.70
330	2.50	19.85	19.80	19.70	19.75	19.75	19.80
360	2.50	20.00	20.00	20.00	19.90	19.90	19.90

APPENDIX C

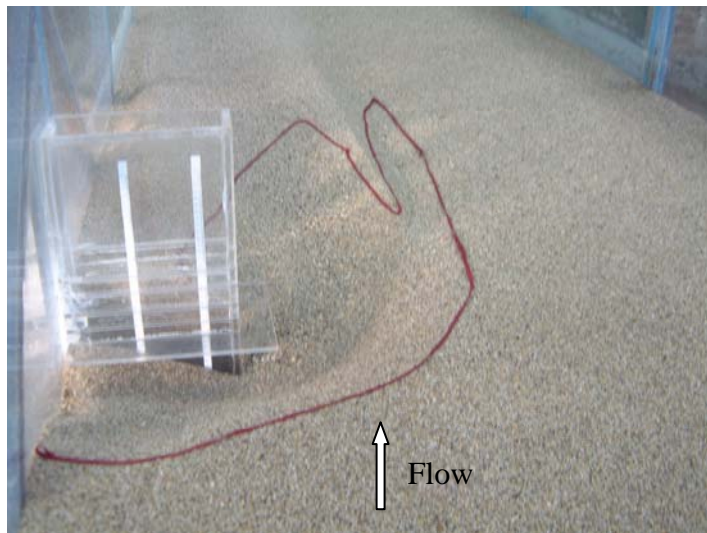
Table C.1. Time development of 12-hours tests for $L_a=20$ cm

$L_a=20$ cm, $B_a=10$ cm							
Time (min)	B_c (cm)	Scour depth (d_s) (cm)					
		Z_c (cm)					
		Without collar	5	2.5	0	-2.5	-5
1	10.00	0.90	1.40	1.56	0.00	1.70	1.90
2	10.00	1.50	2.90	3.00	0.00	2.35	4.30
4	10.00	4.00	4.35	4.05	0.00	2.50	5.00
6	10.00	5.30	4.90	4.75	0.00	2.50	5.00
8	10.00	6.80	5.70	5.30	0.00	2.50	5.00
10	10.00	7.30	5.90	5.55	0.00	2.50	5.00
15	10.00	8.05	6.30	6.30	0.00	2.50	5.00
20	10.00	8.40	7.45	6.75	0.00	2.50	5.00
25	10.00	9.20	7.95	7.20	0.00	2.50	5.00
30	10.00	9.35	8.50	7.60	0.00	2.50	5.00
40	10.00	9.80	9.00	8.10	0.00	2.50	5.00
50	10.00	10.75	9.65	8.50	0.00	2.50	5.00
60	10.00	11.30	9.90	8.60	0.40	2.50	5.00
80	10.00	11.70	10.30	8.70	0.40	2.50	5.00
90	10.00	12.15	10.50	8.95	0.40	2.50	5.00
100	10.00	12.40	10.63	9.15	2.20	2.50	5.00
120	10.00	12.80	11.00	9.40	3.35	2.50	5.00
150	10.00	13.30	11.30	9.90	4.50	2.50	5.00
180	10.00	13.70	11.55	10.20	5.70	2.50	5.00
210	10.00	14.00	11.60	10.30	6.00	2.50	5.00
240	10.00	14.60	11.75	10.45	6.80	2.50	5.00
270	10.00	14.80	11.90	10.60	7.00	2.50	5.00
300	10.00	15.00	12.10	10.70	7.10	3.50	5.00
330	10.00	15.40	12.20	11.00	7.60	4.50	5.00
360	10.00	15.60	12.40	11.20	7.75	5.80	5.00
420	10.00	15.90	12.60	11.40	8.40	6.40	5.00
480	10.00	16.10	12.75	11.75	8.80	6.60	5.00
540	10.00	16.30	12.90	12.15	9.35	7.00	5.00
600	10.00	16.90	13.10	12.25	9.80	7.40	5.00
660	10.00	17.10	13.15	12.40	10.10	7.95	5.00
720	10.00	17.30	13.30	11.55	10.20	8.00	5.00

APPENDIX D

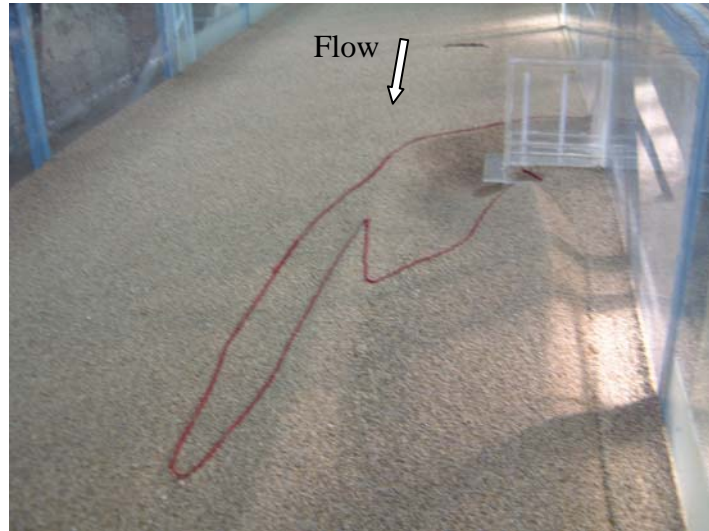


a) Downstream view

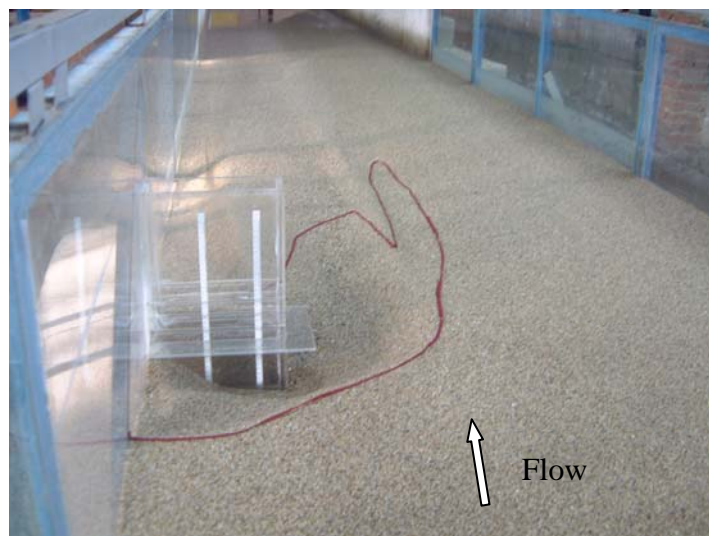


b) Upstream view

Figure D.1. Abutment-collar arrangement and scour hole
($Q=0.035 \text{ m}^3/\text{s}$, $y=6.45 \text{ cm}$, $Z_c=-5 \text{ cm}$, $B_c=5 \text{ cm}$, $L_a=25 \text{ cm}$)



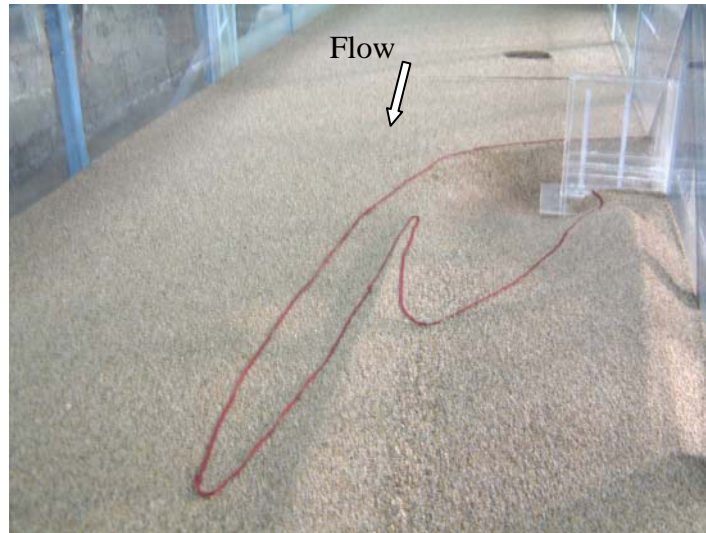
a) Downstream view



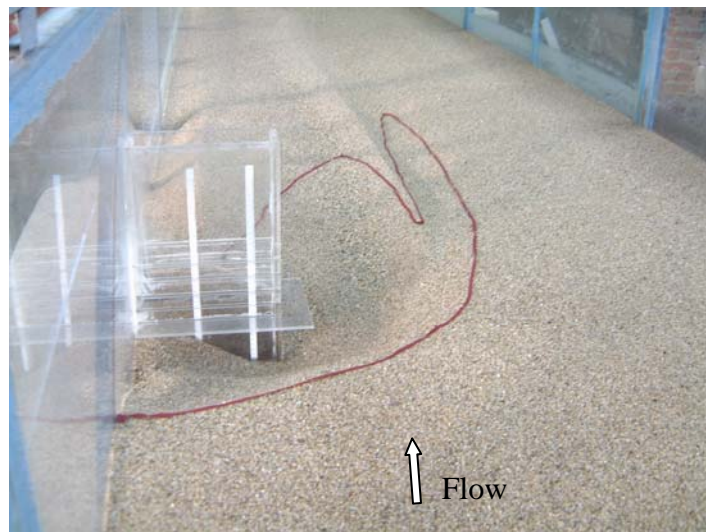
b) Upstream view

Figure D.2. Abutment-collar arrangement and scour hole

($Q=0.040 \text{ m}^3/\text{s}$, $y=7.15 \text{ cm}$, $Z_c=-5 \text{ cm}$, $B_c=5 \text{ cm}$, $L_a=25 \text{ cm}$)



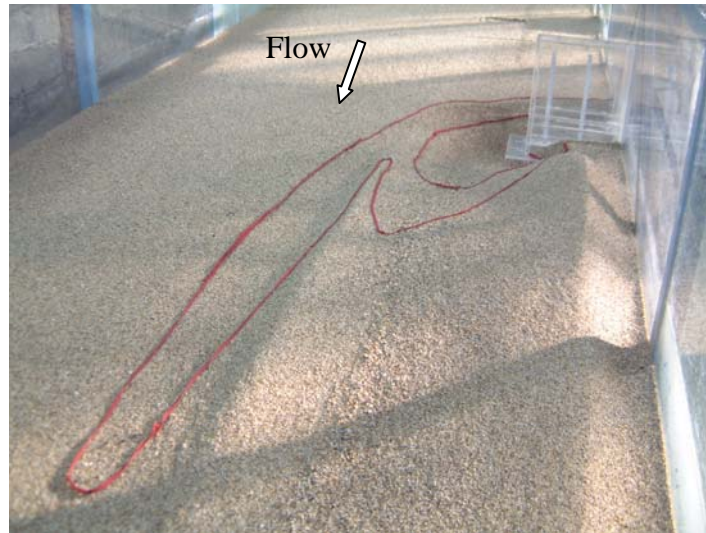
a) Downstream view



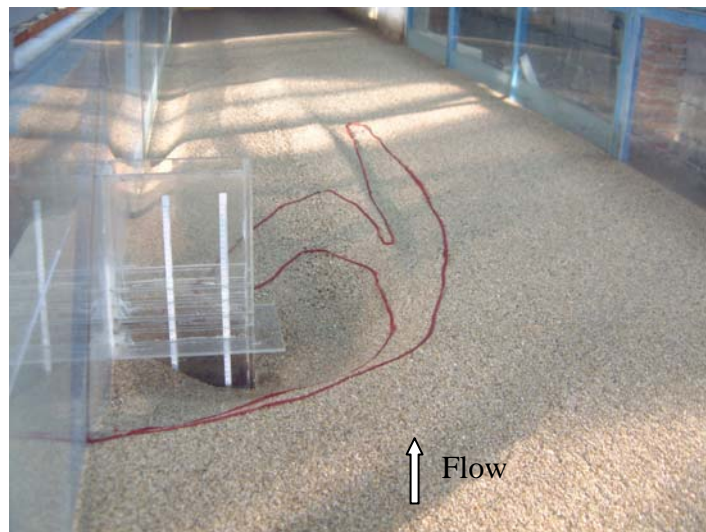
b) Upstream view

Figure D.3. Abutment-collar arrangement and scour hole

($Q=0.045 \text{ m}^3/\text{s}$, $y=7.95 \text{ cm}$, $Z_c=-5 \text{ cm}$, $B_c=5 \text{ cm}$, $L_a=25 \text{ cm}$)



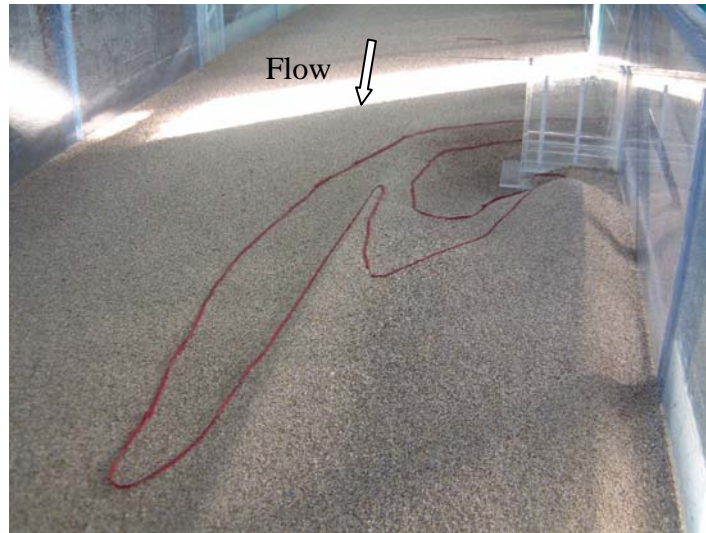
a) Downstream view



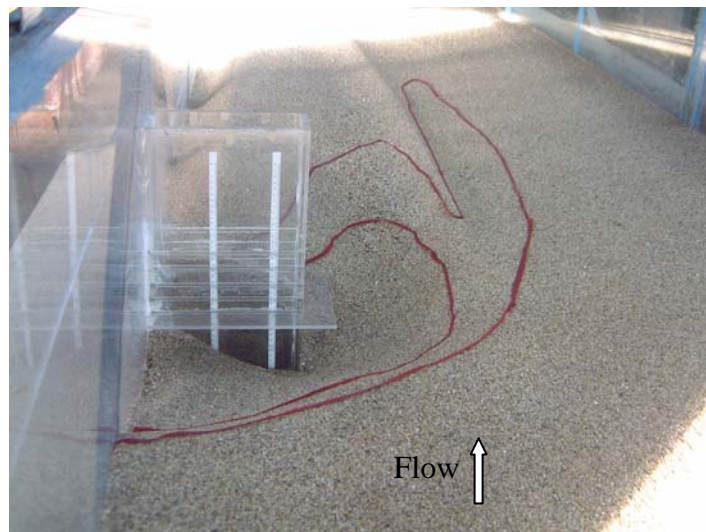
b) Upstream view

Figure D.4. Abutment-collar arrangement and scour hole

($Q=0.050 \text{ m}^3/\text{s}$, $y=8.85 \text{ cm}$, $Z_c=-5 \text{ cm}$, $B_c=5 \text{ cm}$, $L_a=25 \text{ cm}$)



a) Downstream view



b) Upstream view

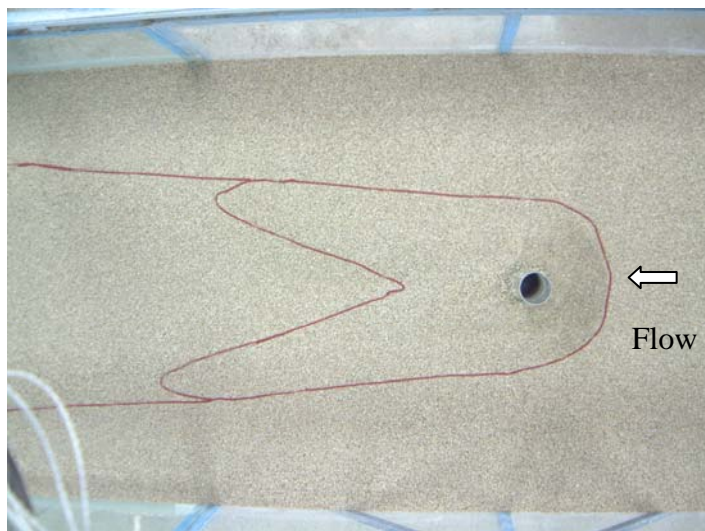
Figure D.5. Abutment-collar arrangement and scour hole

($Q=0.055 \text{ m}^3/\text{s}$, $y=9.60 \text{ cm}$, $Z_c=-5 \text{ cm}$, $B_c=5 \text{ cm}$, $L_a=25 \text{ cm}$)

APPENDIX E

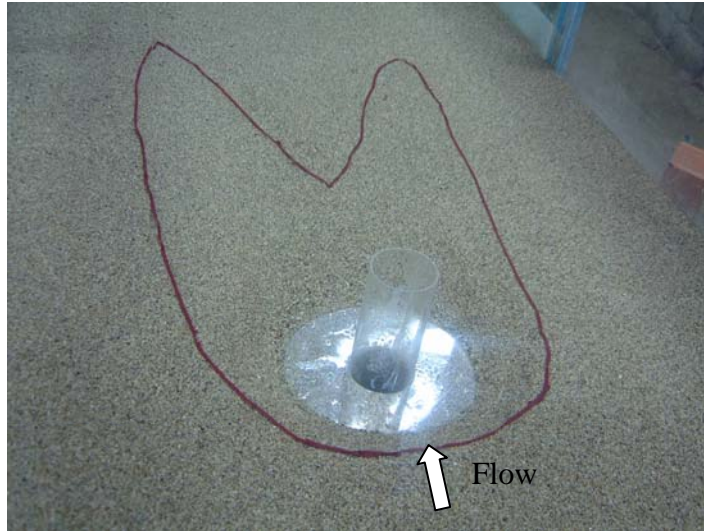


a) Upstream view

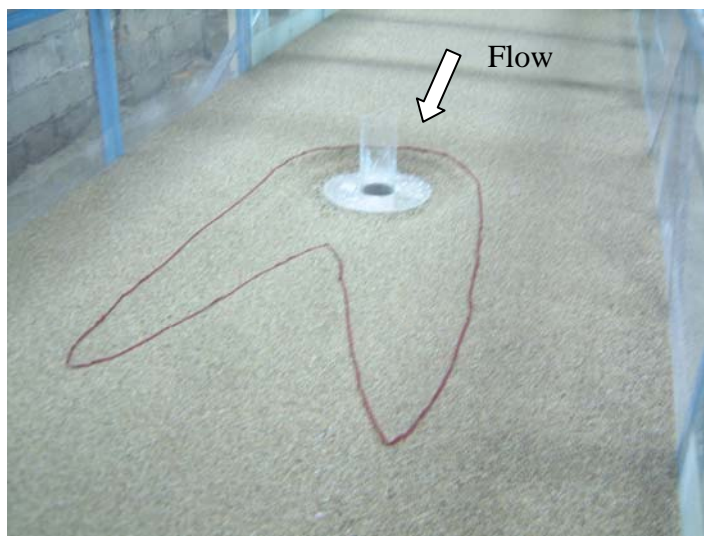


b) Top view

Figure E.1. Scour hole around the pier
($Q=0.055\text{m}^3/\text{s}$, $y=9.60\text{ cm}$, $D=10\text{ cm}$)



a) Upstream view



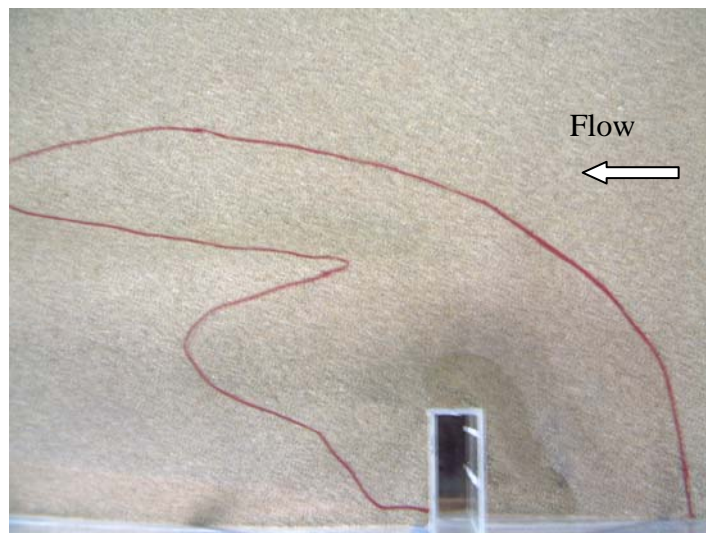
b) Downstream view

Figure E.2. Pier-collar arrangement and scour hole

($Q=0.055\text{m}^3/\text{s}$, $y=9.60\text{ cm}$, $D=10\text{ cm}$, $Z_{cp}=\pm 0.0\text{ cm}$)



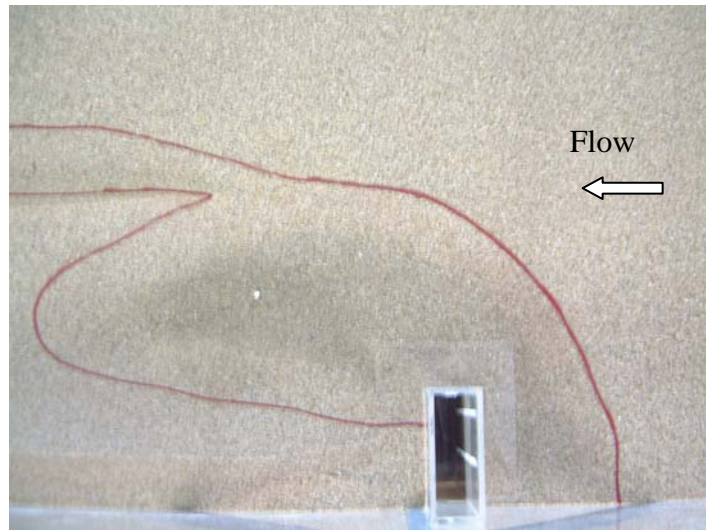
a) Upstream view



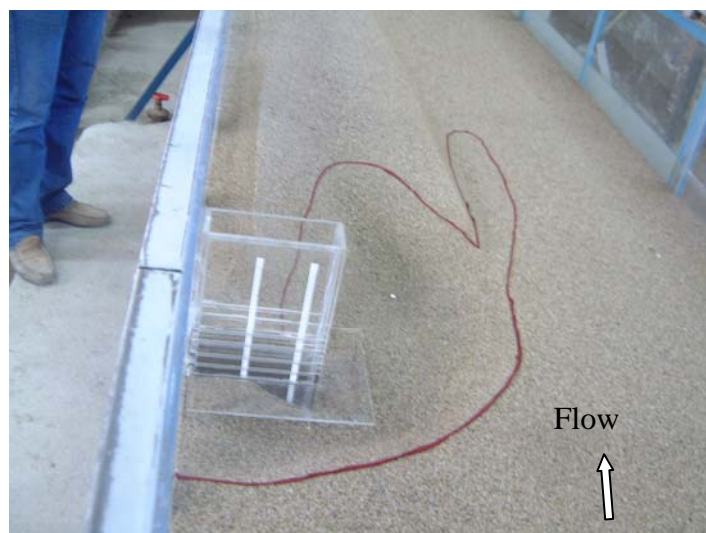
b) Top view

Figure E.3. Scour hole around the abutment

($Q=0.055\text{m}^3/\text{s}$, $y=9.60\text{ cm}$, $L_a=25\text{ cm}$)



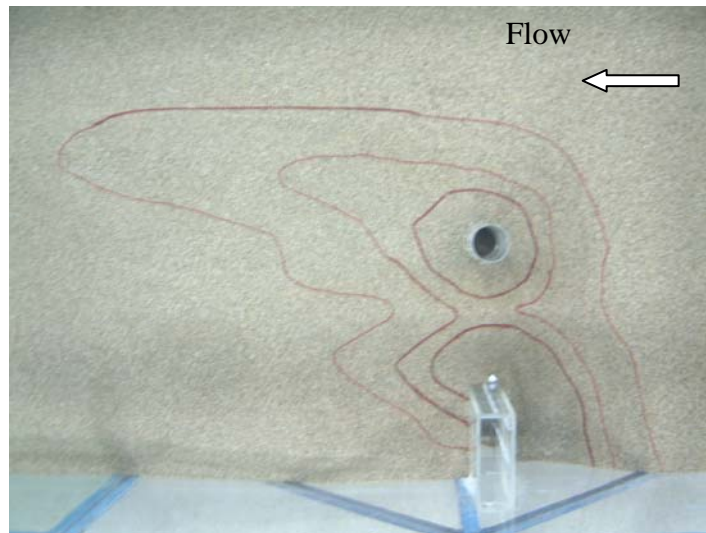
a) Top view



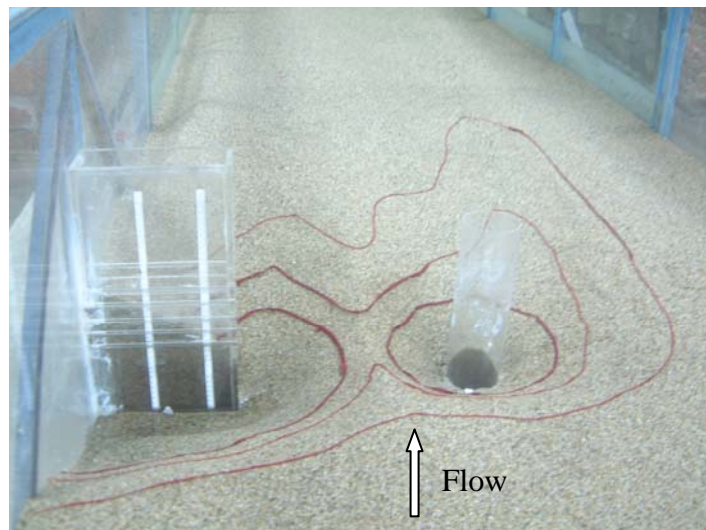
b) Upstream view

E.4. Scour hole around the abutment

($Q=0.055\text{m}^3/\text{s}$, $y=9.60\text{ cm}$, $L_a=25\text{ cm}$, $Z_c=-5\text{ cm}$)



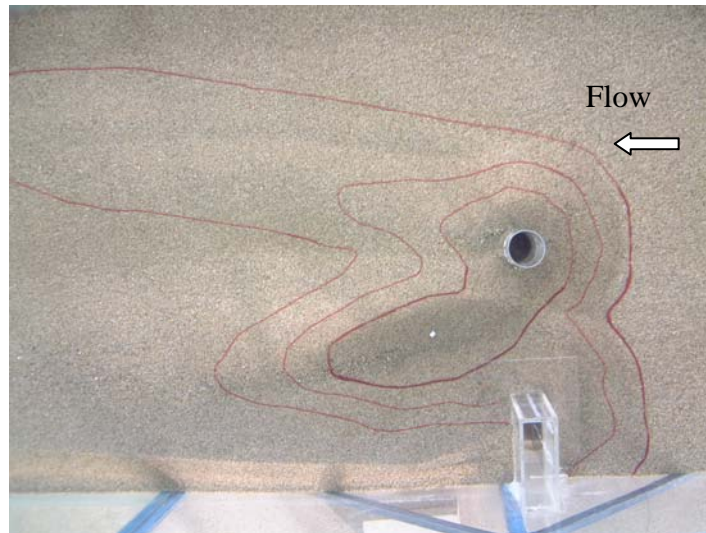
a) Top view



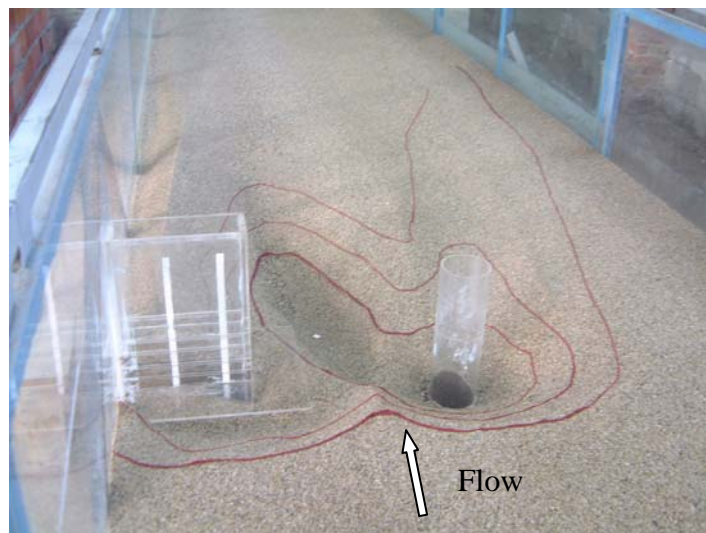
a) Top view

E.5. Interaction between abutment and pier

($Q=0.055\text{m}^3/\text{s}$, $y=9.60\text{ cm}$, $L_a=25\text{ cm}$, $D=10\text{ cm}$, $\lambda=37.5\text{ cm}$)



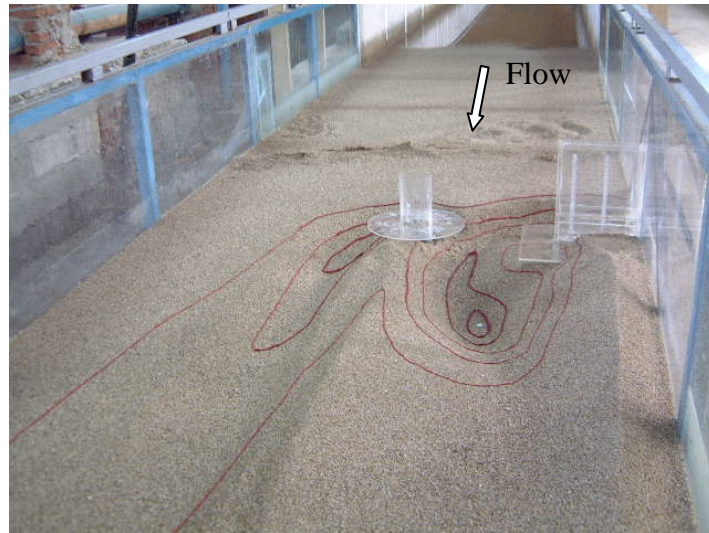
a) Top view



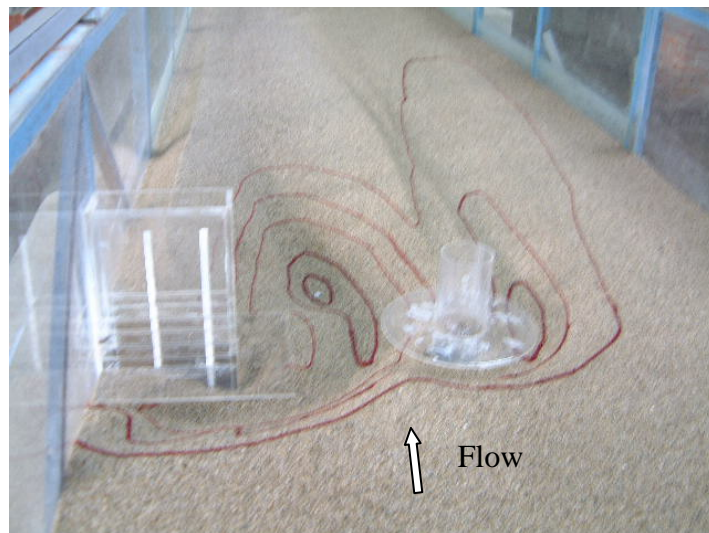
c) Upstream view

E.6. Abutment and pier arrangement for $Q=0.055\text{ m}^3/\text{s}$ and $\lambda=37.5\text{ cm}$

($L_a=25$ cm, $Z_c=-5$ cm for abutment and $D=10$ cm for pier)



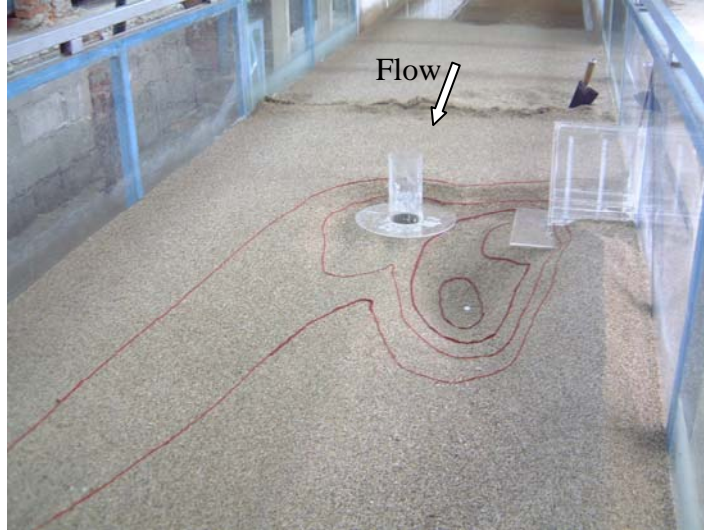
a) Downstream view



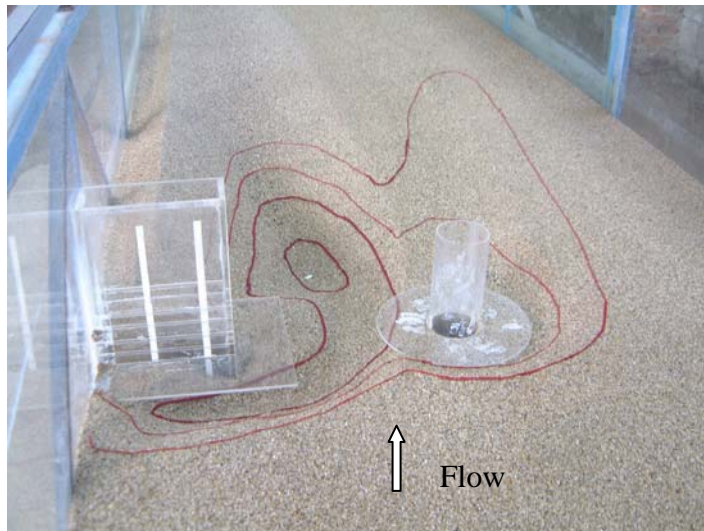
d) Upstream view

E.7. Abutment and pier arrangement for $Q=0.055$ m³/s and $\lambda=37.5$ cm

($L_a=25$ cm, $Z_c=-5$ cm for abutment and $D=10$ cm, $Z_{cp}=\pm 0.0$ cm for pier)



a) Downstream view



b) Upstream view

E.8. Abutment and pier arrangement for $Q=0.055$ m³/s and $\lambda=37.5$ cm
($L_a=25$ cm, $Z_c=-5$ cm for abutment and $D=10$ cm, $Z_{cp}=-5$ cm for pier)

VITA

The author was born in Konya, on the 27th of May 1971. After the completion of her elementary, middle, and high school education in Konya, she started her university education in 1988 at the Selçuk University, Konya. She received her B.S. degree in Civil Engineering department from Selçuk University on 1992. She worked as a research assistant in the Selçuk University from 1993 to 1994. After passing M.S. exam of Middle East Technical University, she was charged in Middle East Technical University during her M.S. study. She has been working in State Hydraulics Works as an engineer since 1998. Her main areas of interest are sediment transport, design of hydraulic structures, and hydraulic modeling and civil engineering structures.